CRUISE REPORT: P14N

Created: Nov 2023, Updated Feb 2024
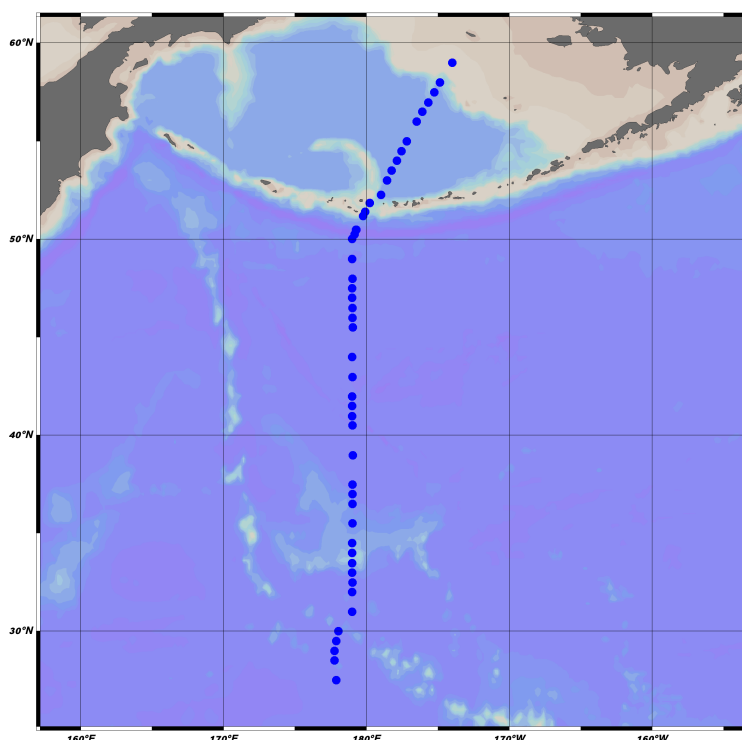
Highlights

Cruise Summary Information

Section Designation	**P14N** (MR23-07)
Expedition Designation (ExpoCode)	**49NZ20231006**
Chief Scientist	**Katsuro Katsumata / RIGC, JAMSTEC**
Dates	6 October - 9 November 2023
Ship	R/V *Mirai*
Ports of Call	Dutch Harbor, USA – Shimizu, JP
Geographic Boundaries	59° 0.24"N 177° 74.99"E 173°99.63"W 27° 50.03"N
Stations	70

Floats and Drifters Deployed	4 Argo Floats
	   3 Core Argo (APEX)
	   1 Deep Argo (DeepNINJA)
	7 GO-BGC Floats

Moorings Deployed and Recovered	0

Contact Information:
Katsuro Katsumata
Research Institute for Global Change • JAMSTEC
k.katsumata@jamstec.go.jp

Report assembled by Savannah Lewis, UCSD/SIO

R/V *Mirai* Cruise Report

MR23-07

GO-SHIP Observation
– P14N –

Bering Sea & North Pacific

6 Oct. 2023 — 9 Nov. 2023

Japan Agency for Marine-Earth Science and Technology
(JAMSTEC)

Contents

The photograph on the title page was shot and kindly provided for this document by Fumine Okada (NME).

1. Cruise Information

Cruise ID	MR23-07
Name of vessel	R/V *Mirai*
Title of cruise	GO-SHIP Observation P14N − quantitative observational experiment in the North Pacific subarctic gyre −
Chief Scientist	Katsuro Katsumata,
	Physical and Chemical Oceanography Research Group, Global Ocean Observation Research Center, Research Institute for Global Change (RIGC), Japan Agency for Marine-Earth Science and Technology (JAMSTEC)
Cruise period	6th October 2023 – 9th November 2023
Ports of departure / call / arrival	Dutch Harbor, United States of America No port calls Shimizu, Japan
Research area	Bering Sea and North Pacific
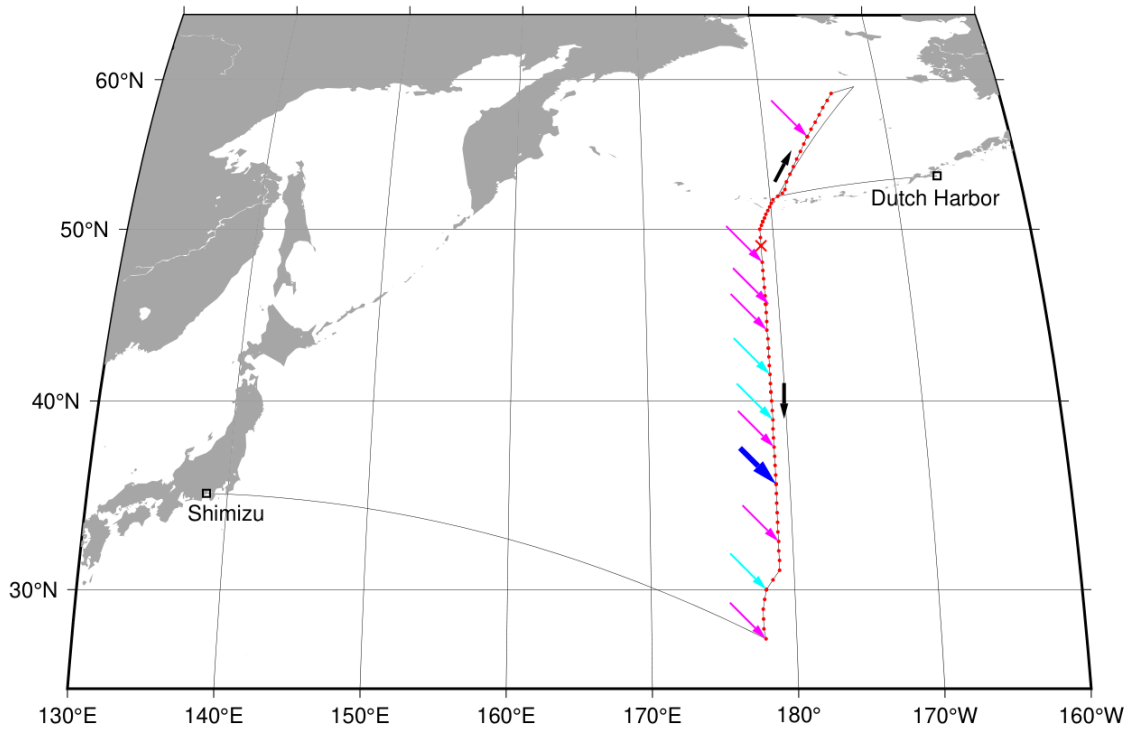
Fig. 1.1 Thin black line shows the cruise track. To avoid rough weather, the station observation was initiated from Station 16, just north of the Amchitka Strait and proceeded northeastword to Station 1. Then after sailing to Station 17, the observation continued southward to Station 70, which is indicated by the two black arrows. The red dots show the CTD stations, the red cross the CTD station where CTD measurement was aborted middepth, magenta arrows deployments of the biogeochemical floats, the cyan arrows deployments of temperature-salinity (core) Argo floats, the blue arrow deployment of a Deep NINJA float.

MR23-07
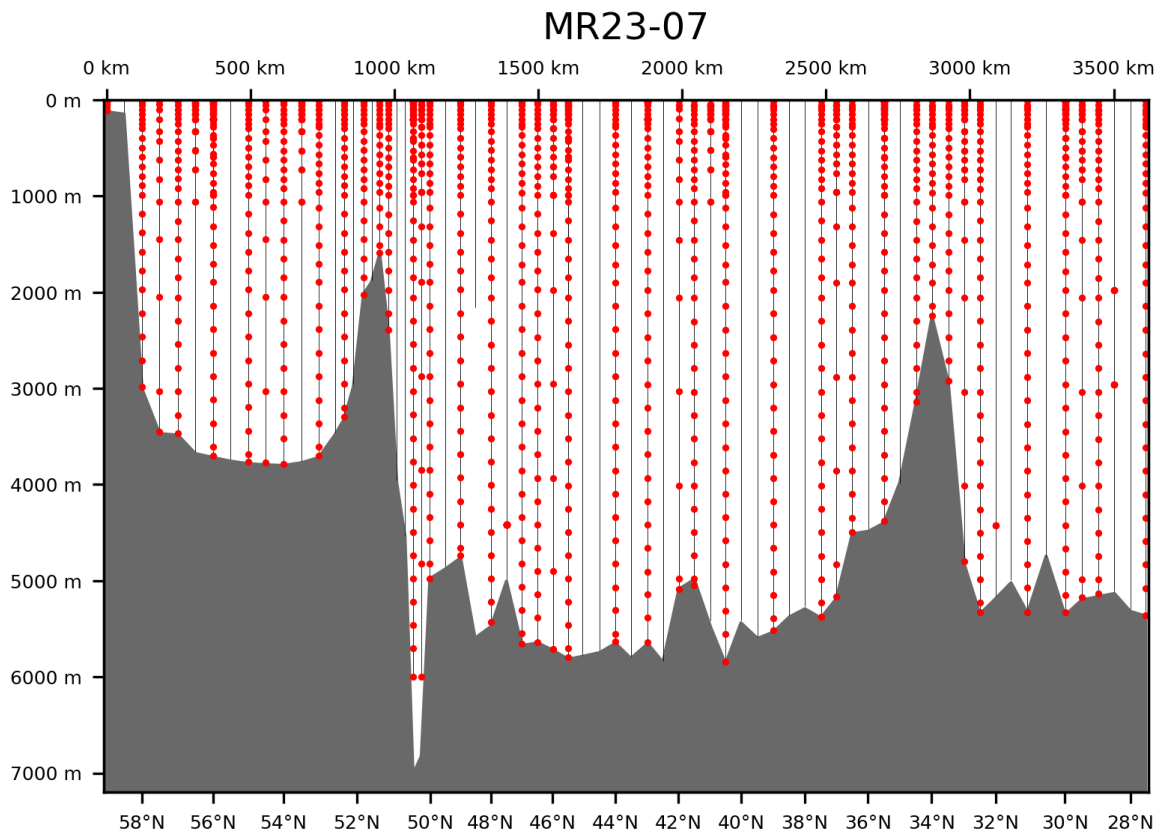
Fig. 1.2. Cross sections showing data sampling positions. Black line shows CTD trace and red dots show Niskin sampling. Gray is ocean bottom bathymetry..
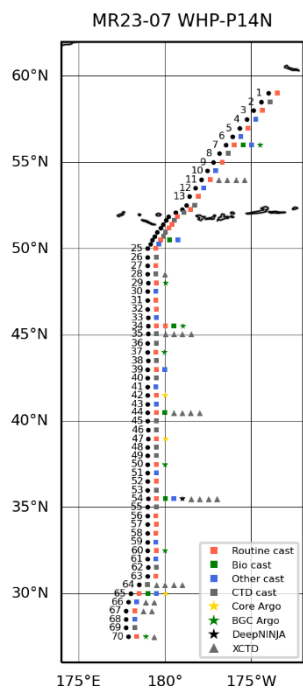
Fig. 1.3. Sampling stations and sampling/deployment performed therein.

Narrative (K. Katsumata)

5th Oct: Embarkation at Dutch Harbor. Health & Safety Course onboard from 1400.

6th Oct: Departure at 0600 morning. Emergency Evacuation Drill completed after a water sampling training session.

7th Oct: The weather forecast predicts a disastrous condition in four days or so. Upon discussion with Captain, we decided to commence our journey from southern Station (but north of the Strait) 16 and work northward.

8th Oct: The condition is very smooth so far. Two patients of motion sickness recovered and resumed their works. First CTD cast went without hiccups.

9th Oct: Another beautiful day.

11th Oct: A low pressure passing south of the Strait. After station 1 (17:00 shiptime), which has been changed to a sampling station, sampling and CTD are suspended.

12th Oct: Wind speed > 20 m/s, Significant waveheight > 4.5 m as of 5AM. Got worse to wind speed > 21 m/s and waveheight > 6 m as of 1PM=UTC0h of 13th Oct
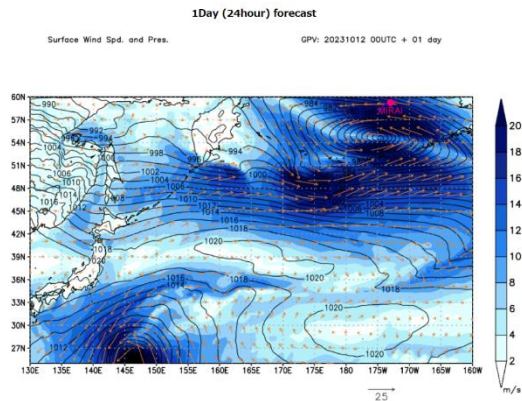
13th Oct: Shifting to Station 17 from around 0500 (morning twilight). Still waveheight > 5m and wind > 15 m/s although atmospheric pressure is increasing for last 30+ hours. Next low pressure on its way.
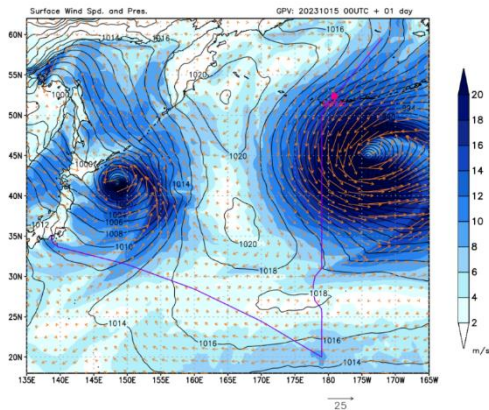
14th Oct: Station 17 at 22:32. Resuming CTD/sampling but the next low is just around the corner.

15th Oct: After station 17, yet another heaving to. At least for 12 hours.

16th Oct: Despite left-over wind and swell, Stations 18 to 22 are done. Enjoyed sunshine after days. A poor bird is found resting in a corner of the ship.

17th, Oct: The birds flocked and there are three of them now. Waiting for the reply from the US to our request to extend our stay within their EEZ for 12 hours. Finally got it 9 hours before expiration.

19th Oct: This is the day after 17th Oct as we are just about to cross the dateline. CTD MOD errors occurred during the downcast of Station 28 around 2000 dbar. We recovered the CTD to change the swivel, During the process, the condition deteriorated quickly and Station 28 was replaced by an XCTD (high resolution type 4A). Shakey wading to Station 29, which is the first station out of the US EEZ. The condition improved drastically as we move southward and we resumed our CTD/sampling. We did not lose shiptime but did not get any datum from Station 28 except for T and S down to 2000 dbar.

20th Oct: Annoyed by yet another low pressure along the Aleutian Islands. Suspend for, at least, 24 hours. Wind speed > 17 m/s, waveheight > 4 m.
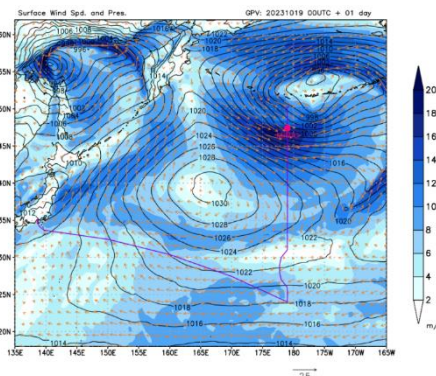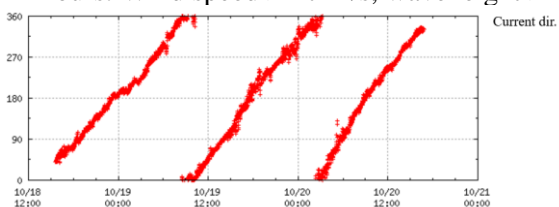
21st Oct: During long waiting, a scientist onboard noticed clockwise rotation of near-surface current. Here at 47° N, the inertial period is about 16.4 hour. Beauty.

22nd, 23rd Oct: Two consecutive days with two consecutive CTD short-circuiting problems. Lost 9+ hours in re-terminating the cable twice.

26th Oct: Station 46 cast 1 came up with an almost 2 m long pink strip around the lower ADCP and optical sensors. Looks (and smells) like jellyfish. Lucky this is a non-sampling station.
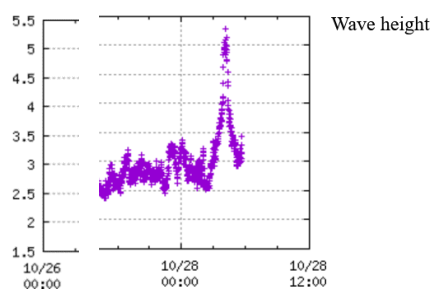
28th: Station 54 cast 3 was postponed due to sudden pickup of wind and swell, which suddenly died and we managed to perform cast 3 (starting at 10/28, 00:45) as well as deployment of Deep NINJA with the A-frame. Once we head to Station 55 the wind and swell were crazy (see around 04:00). After some wading through the 20 m/s > wind and 4 m > swell, both die so quickly that we managed Station 55 after only a 90 minute delay (starting at 10/28 05:38).
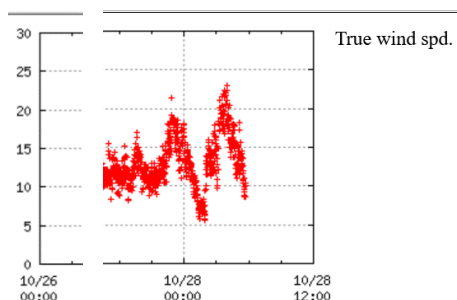
31st Oct: Not much to note as we are going smoothly right on schedule. Stations 64 to 70 have been shifted westward to avoid the newly adopted Marine Reserve (Papahānaumokuākea National Monument), which did not exist in our previous occupation in 2007.

1st Nov: Station 70 completed by the night team. Happy sailing back home to Shimizu.

9th Nov: Disembarkation at Shimizu.

Lost 80+ hours by weather and 10+ hours by CTD maintenance.

2. Science Party

Table 2.1 List of participants for MR23-07

Name	Responsibility	Affiliation
Katsuro Katsumata	Water sampling	RIGC
Shinya Kouketsu	CTD/LADCP/turbulence/Water sampling	RIGC
Yuichiro Kumamoto	DO/Cs/Ra/^{14}C/^{13}C/CFCs/Nutrients	RIGC
Hiroshi Uchida	Salinity/Density/pH/XCTD	RIGC
Kosei Sasaoka	Chl-a/CDOM	RIGC
Masahito Shigemitsu	CFCs/FDOM/DOC	RIGC
Ryohei Yamaguchi	CTD/LADCP/turbulence/Water sampling/density/SUM file	RIGC
Hiroyuki Fujiwara	Water sampling	RIGC
Taichi Yokokawa	CH_4/N_2O/Bacteria/DNA/Water sampling	SUGAR
Akiko Makabe	CH_4/N_2O/Bacteria/DNA/Water sampling	SUGAR
Yusuke Tsukatani	CH_4/N_2O/Bacteria/DNA/Water sampling	SUGAR
Shigeru Kawai	CH_4/N_2O/Bacteria/DNA/Water sampling	SUGAR
Addie Norgaard	GO-BGC floats/Water sampling	UCSD
Adelaide Wink	CDOM/Water sampling	UGI
Siyu Jiang	Plankton	AORI
Yuanzhi Qi	Radio isotopes	MALT
Wakana Sawada	CFCs/Water sampling	RIGC
Yugo Nishimura	FDOM/CDOM/DOC	RIGC
Kaisei Mashita	CFCs	RIGC
Mone Ozawa	FDOM/CDOM/DOC	RIGC
Masanori Murakami	Meteorology/Geophysics/ADCP/XCTD	NME
Fumine Okada	Meteorology/Geophysics/ADCP/XCTD	NME
Haruna Yamanaka	Meteorology/Geophysics/ADCP/XCTD	NME
Yasuhiro Arii	Water sampling/TA	MWJ
Katsunori Sagishima	DO/TSG/Chl-a	MWJ
Rei Ito	CTD/Argo	MWJ
Nobuhiro Fujii	CTD/Argo	MWJ
Shinsuke Toyoda	CTD/Argo	MWJ
Tun Htet Aung	CTD/Argo	MWJ
Riho Fujioka	CTD/Argo	MWJ
Masahiro Orui	DIC/TA/pCO_2	MWJ
Nagisa Fujiki	DIC/TA/pCO_2	MWJ
Misato Kuwahara	DO/TSG/Chl-a	MWJ
Yuko Miyoshi	Nutrients	MWJ
Shiori Ariga	Nutrients	MWJ
Takuya Izutsu	DIC	MWJ
Tomokazu Chiba	DO/Chl-a	MWJ
Nahoko Adachi	Nutrients	MWJ
Takumi Iwai	Water sampling	MWJ
Harua Uno	Water sampling	MWJ
Hibiki Otsuka	Water sampling	MWJ
Aya Takagi	Water sampling	MWJ
Mariko Honda	Water sampling	MWJ

RIGC: Research Institute for Global Change, JAMSTEC; SUGAR: Super-cutting-edge Grand and Advanced Research Program, JAMSTEC; UCSD: University of California, San Diego; UGI: University of Galway Ireland; AORI: Atmosphere Ocean Research Institute, University of Tokyo; MALT: Micro Analysis Laboratory Tandem accelerator, University of Tokyo; NME: Nippon Marine Enterprises; MWJ: Marine Works Japan

3. Underway Measurements

3.1 Navigation

(1)   Personnel

Katsuro Katsumata	JAMSTEC: Principal investigator
Masanori Murakami	Nippon Marine Enterprises, Ltd. (NME)
Fumine Okada	NME
Haruna Yamanaka	NME
Yoichi Inoue	MIRAI crew

(2)   System description

Ship's position and velocity were provided by Navigation System on R/V MIRAI. This system integrates GNSS position, Doppler sonar log speed, Gyro compass heading and other basic data for navigation. This system also distributes ship's standard time synchronized to GPS time server via Network Time Protocol. These data were logged on the network server as "SOJ" data every 5 seconds. Sensors for navigation data are listed below;

i)   GNSS system:

R/V MIRAI has four GNSS systems, all GNSS positions were offset to radar-mast position, datum point. Anytime changeable manually switched as to GNSS receiving state.

a) StarPack-D (version 11.01.02), Differential GNSS system.
    Antenna: Located on compass deck, starboard.

b) StarPack-D (version 11.01.02), Differential GNSS system.
    Antenna: Located on compass deck, portside.

c) Standalone GPS system.
    Receiver: Trimble SPS751
    Antenna: Located on navigation deck, starboard.

d) Standalone GPS system.
    Receiver: Trimble SPS751
    Antenna: Located on navigation deck, portside.

ii)   Doppler sonar log:

FURUNO DS-30, which use three acoustic beams for current measurement under the hull.

iii) Gyro compass:

TOKYO KEIKI TG-8000, Sperry type mechanical gyro compass.

iv) GPS time server:

SEIKO TS-2550 Time Server, synchronizing to GPS satellites every 1 second.

(3)   Data period (Times in UTC)

17:00 06 Oct. 2023 – 23:40 08 Nov. 2023

(4)   Remarks (Times in UTC)

i)   The following periods, sea surface temperature and salinity were available.
00:50:00UTC 07 Oct. 2023 - 23:59:00UTC 07 Oct. 2023

ii)   The following periods, sea surface salinity was invalid due to the maintenance.
1:24:00UTC 18 Oct. 2023 - 2:00:00UTC 18 Oct. 2023

iii) The following two entries are missing, because data acquisition was suspended due to system malfunction.
21:14:25 on 26 Oct. 2023
21:14:40 on 28 Oct. 2023
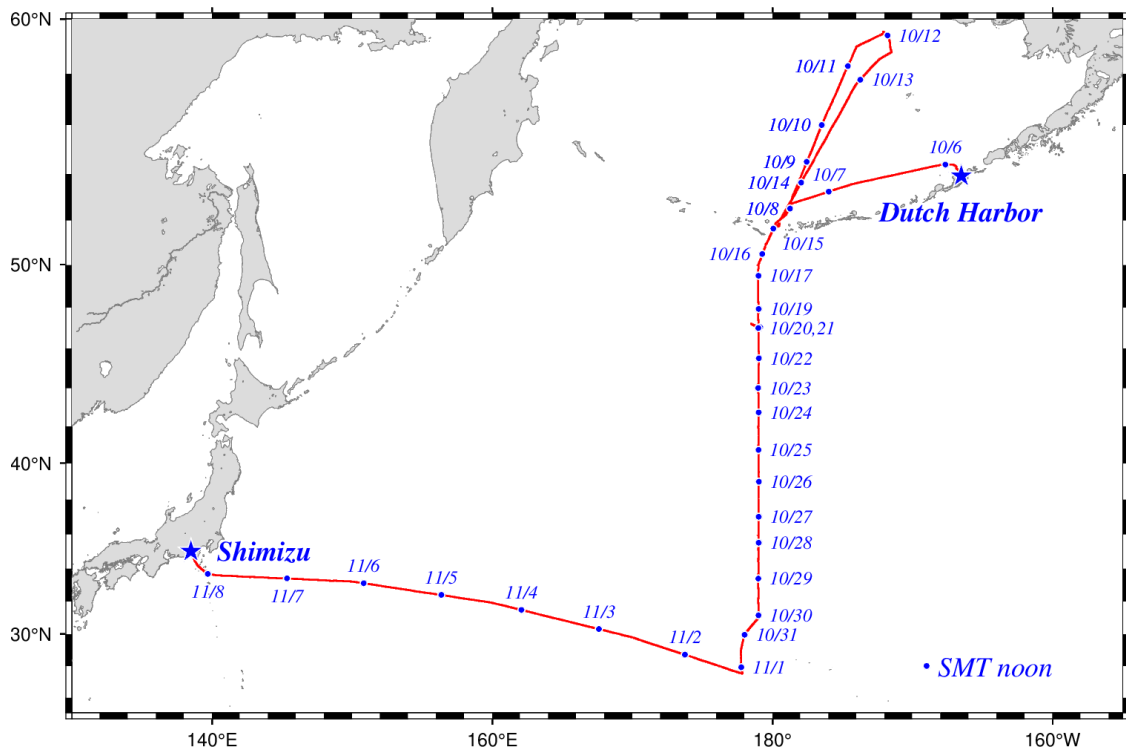
Fig. 3.1 Cruise track of MR23-07

3.2 Swath Bathymetry

(1)   Personnel
　　　　Katsuro Katsumata　　　　JAMSTEC: Principal investigator
　　　　Masanori Murakami　　　　Nippon Marine Enterprises, Ltd（NME）
　　　　Fumine Okada　　　　　　NME
　　　　Haruna Yamanaka　　　　NME
　　　　Yoichi Inoue　　　　　　MIRAI crew

(2)   **Introduction**
　　　　R/V MIRAI is equipped with a Multi narrow Beam Echo Sounding system (MBES), SEABEAM 3012 (L3 Communications, ELAC Nautik). The objective of MBES is collecting continuous bathymetric data along ship's track to make a contribution to geological and geophysical investigations and global datasets.

(3)   **Data Acquisition**
　　　　The "SEABEAM 3012" on R/V MIRAI was used for bathymetry mapping during this cruise.
　　　　To get accurate sound velocity of water column for ray-path correction of acoustic multibeam, we used Surface Sound Velocimeter (SSV) data to get the sea surface sound velocity (at 6.62m), and the deeper depth sound velocity profiles were calculated by temperature and salinity profiles from CTD, XCTD and Argo float data by the equation in Del Grosso (1974) during this cruise.
　　　　Table 3.2-1 shows system configuration and performance of SEABEAM 3012.

Table 3.2-1 SEABEAM 3012 system configuration and performance

----

Frequency:	12 kHz
Transmit beam width:	2.0 degree
Transmit power:	4 kW
Transmit pulse length:	2 to 20 msec.
Receive beam width:	1.6 degree
Depth range:	50 to 11,000 m
Number of beams:	301 beams
Beam spacing:	Equi-angle
Swath width:	60 to 150 degrees
Depth accuracy:	< 1 % of water depth (average across the swath)

(4)   **Data processing**
i)   Sound velocity correction
　　　　Each bathymetry data were corrected with sound velocity profiles calculated from the nearest CTD and XCTD data in the distance. The equation of Del Grosso (1974) was used for calculating sound velocity. The data corrections were carried out using the HIPS software version 11.3 (Teledyne CARIS, Canada)

ii)   Editing and Gridding
　　　　Editing for the bathymetry data were carried out using the HIPS. Firstly, the bathymetry data during ship's turning was basically deleted, and spike noise of each swath data was removed. Then the bathymetry data were checked by "Regular Grid Surface (resolution: 100 m averaged grid)".
　　　　Finally, all accepted data were exported as XYZ ASCII data (longitude [degree], latitude [degree], depth [m]), and converted to 150 m grid data using "nearneighbor" utility of GMT (Generic Mapping Tool) software.

Table 3.2-2 Parameters for gridding on "nearneighbor" in GMT

Gridding mesh size:	150 m
Search radius size:	150 m
Number of sectors around grid point:	16
Minimum number of sectors with data required for averaging: 2	

----

(5)   Data archives

These data obtained in this cruise will be submitted to the Data Management Group of JAMSTEC, and will be opened to the public via "Data Research System for Whole Cruise Information in JAMSTEC (DARWIN)" in JAMSTEC web site.

http://www.godac.jamstec.go.jp/darwin/e

3.3　Surface Meteorological Observation

(1)　Personnel
Katsuro Katsumata　　　JAMSTEC: Principal investigator
Masanori Murakami　　　Nippon Marine Enterprises, Ltd（NME）
Fumine Okada　　　　　NME
Haruna Yamanaka　　　　NME
Yoichi Inoue　　　　　　MIRAI crew

(2)　Objectives
　　　Surface meteorological parameters are observed as a basic dataset of the meteorology. These parameters provide the temporal variation of the meteorological condition surrounding the ship.

(3)　Methods
　　　Surface meteorological parameters were observed during this cruise. In this cruise, the two systems for the observation were used.

i)　MIRAI Surface Meteorological observation (SMet) system
　　　Instruments of SMet system are listed in Table 3.3-1 and measured parameters are listed in Table 3.3-2. Data were collected and processed by KOAC-7800 weather data processor made by Koshin-Denki, Japan. The data set consists of 6 seconds averaged data.

ii)　Shipboard Oceanographic and Atmospheric Radiation (SOAR) measurement system
　　　SOAR system designed by BNL (Brookhaven National Laboratory, USA) consists of major five parts.

a)　Analog meteorological data sampling with CR1000 logger manufactured by Campbell Scientific Inc. Canada – wind, pressure, and rainfall (by a capacitive rain gauge) measurement.
b)　Digital meteorological data sampling from individual sensors - air temperature, relative humidity and precipitation (by optical rain gauge (ORG)) measurement.
c)　Radiation data sampling with CR1000X logger manufactured by Campbell Inc. and radiometers with ventilation unit manufactured by Hukseflux Thermal Sensors B.V. Netherlands – short and long wave downward radiation measurement.
d)　Photosynthetically Available Radiation (PAR) sensor manufactured by Biospherical Instruments Inc. (USA) - PAR measurement.
e)　Scientific Computer System (SCS) developed by NOAA (National Oceanic and Atmospheric Administration, USA) - centralized data acquisition and logging of all data sets.

　　　SCS recorded radiation, air temperature, relative humidity, CR1000 and ORG data. SCS composed Event data (JamMet) from these data and ship's navigation data every 6 seconds. Instruments and their locations are listed in Table 3.3-3 and measured parameters are listed in Table 3.3-4.

　　　For the quality control as post processing, we checked the following sensors, before and after the cruise.
　　i.　Capasitive rain gauge (SMet and SOAR)
　　　　Inspect of the linearity of output value from the rain gauge sensor to change input value by adding fixed quantity of test water.
　　ii.　Barometer (SMet and SOAR)
　　　　Comparison with the portable barometer value, PTB330, VAISALA
　　iii.　Thermometer (air temperature and relative humidity) (SMet and SOAR)
　　　　Comparison with the portable thermometer value, HMP75, VAISALA

(4)   Preliminary results
   Fig. 3.3-1 shows the time series of the following parameters.
   Wind (SMet)
   Air temperature (SMet)
   Relative humidity (SMet)
   Precipitation (SOAR ORG)
   Short/long wave radiation (SMet)
   Pressure (SMet)
   Sea surface temperature (SMet)
   Significant wave height (SMet)

(5)   Data archives
   These data obtained in this cruise will be submitted to the Data Management Group of JAMSTEC, and will be opened to the public via "Data Research System for Whole Cruise Information in JAMSTEC (DARWIN)" in JAMSTEC web site.
   http://www.godac.jamstec.go.jp/darwin/e

(6)   Remarks (Times in UTC)
   i)   SST (Sea Surface Temperature) data were available in the following period.
   00:50UTC 07 Oct. 2023 - 23:59UTC 07 Nov. 2023

   ii)   Wave data were invalid due to system trouble in the following period.
   15:55UTC - 20:55UTC 03 Nov. 2023

   iii)   Position data (longitude and latitude) were invalid due to system trouble in the following period.
   21:14:24UTC - 21:14:30UTC 26 Oct. 2023
   21:14:36UTC - 21:14:42UTC 28 Oct. 2023

   iv)   Capacitive rain gauge data were invalid due to transmitting MF/HF radio in the following time.
   01:18UTC 17 Oct. 2023 - 01:20UTC 17 Oct. 2023
   00:23UTC 21 Oct. 2023
   01:29UTC 29 Oct. 2023 - 01:31UTC 29 Oct. 2023

Table 3.3-1 Instruments and installation locations of MIRAI Surface Meteorological observation system

Sensors	Type	Manufacturer	Location (Altitude from surface)
Anemometer	KS-5900	Koshin Denki, Japan	Foremast (25 m)
Tair/RH	HMP155	Vaisala, Finland	Compass deck (21 m)
with aspirated radiation shield	43408 Gill	R.M. Young, U.S.A.	starboard and port side
Thermometer: SST	RFN2-0	Koshin Denki, Japan	4th deck (-1m, inlet -5m)
Barometer	Model-370	Setra System, U.S.A.	Captain deck (13 m) Weather observation room
Capacitive rain gauge	50202	R. M. Young, U.S.A.	Compass deck (19 m)
Optical rain gauge	ORG-815DS	Osi, USA	Compass deck (19 m)
Radiometer (short wave)	MS-802	Eko Seiki, Japan	Radar mast (28 m)
Radiometer (long wave)	MS-202	Eko Seiki, Japan	Radar mast (28 m)

Wave height meter	WM-2	Tsurumi-seiki, Japan	Bow (10 m) Stern (8m)

Table 3.3-2 Parameters of MIRAI Surface Meteorological observation system

Parameter	Units	Remarks
1 Latitude	degree	
2 Longitude	degree	
3 Ship's speed	knot	MIRAI log
4 Ship's heading	degree	MIRAI gyro
5 Relative wind speed	m/s	6sec./10min. averaged
6 Relative wind direction	degree	6sec./10min. averaged
7 True wind speed	m/s	6sec./10min. averaged
8 True wind direction	degree	6sec./10min. averaged
9 Barometric pressure	hPa	adjusted to sea surface level 6sec. averaged
10 Air temperature (starboard)	degC	6sec. averaged
11 Air temperature (port)	degC	6sec. averaged
12 Dewpoint temperature (starboard)	degC	6sec. averaged
13 Dewpoint temperature (port)	degC	6sec. averaged
14 Relative humidity (starboard)	%	6sec. averaged
15 Relative humidity (port)	%	6sec. averaged
16 Sea surface temperature	degC	6sec. averaged
17 Rain rate (optical rain gauge)	mm/hr	hourly accumulation
18 Rain rate (capacitive rain gauge)	mm/hr	hourly accumulation
19 Downwelling shortwave radiation	W/m^2	6sec. averaged
20 Downwelling infra-red radiation	W/m^2	6sec. averaged
21 Significant wave height (bow)	m	hourly
22 Significant wave height (stern)	m	hourly
23 Significant wave period (bow)	second	hourly
24 Significant wave period (stern)	second	hourly

Table 3.3-3 Instruments and installation locations of SOAR system

Sensors (Meteorological)	Type	Manufacturer	Location (altitude from surface)
Anemometer	05106	R.M. Young, USA	Foremast (25 m)
Barometer with pressure port	PTB210 61002 Gill	Vaisala, Finland R.M. Young, USA	Foremast (23 m)
Rain gauge	50202	R.M. Young, USA	Foremast (24 m)
Tair/RH with aspirated radiation shield	HMP155 43408 Gill	Vaisala, Finland R.M. Young, USA	Foremast (23 m)
Optical rain gauge	ORG-815DR	Osi, USA	Foremast (24 m)

Sensors (PRP)	Type	Manufacturer	Location (altitude from surface)
Radiometer (short wave)	SR20	Hukseflux Thermal Sensors B.V., Netherlands	Foremast (25 m)
Radiometer (long wave)	IR20	Hukseflux Thermal Sensors	Foremast (25 m)

B.V., Netherlands

Sensor (PAR&UV)	Type	Manufacturer	Location (altitude from surface)
PAR&UV sensor	PUV-510	Biospherical Instrum ents Inc., USA	Navigation deck (18m)

Table 3.3-4 Parameters of SOAR system (JamMet)

| Parameter	Units	Remarks
1 Latitude	degree	
2 Longitude	degree	
3 SOG	knot	
4 COG	degree	
5 Relative wind speed	m/s	
6 Relative wind direction	degree	
7 Barometric pressure	hPa	
8 Air temperature	degC	
9 Relative humidity	%	
10 Rain rate (optical rain gauge)	mm/hr	
11 Precipitation (capacitive rain gauge)	mm/hr	reset at 50 mm
12 Down welling shortwave radiation	W/m^2	
13 Down welling infra-red radiation	W/m^2	
14 Defuse irradiance	W/m^2	
15 PAR	$microE/cm^2/sec$	
16 UV 305 nm	$microW/cm^2/nm$	
17 UV 320 nm	$microW/cm^2/nm$	
18 UV 340 nm	$microW/cm^2/nm$	
19 UV 380 nm	$microW/cm^2/nm$	
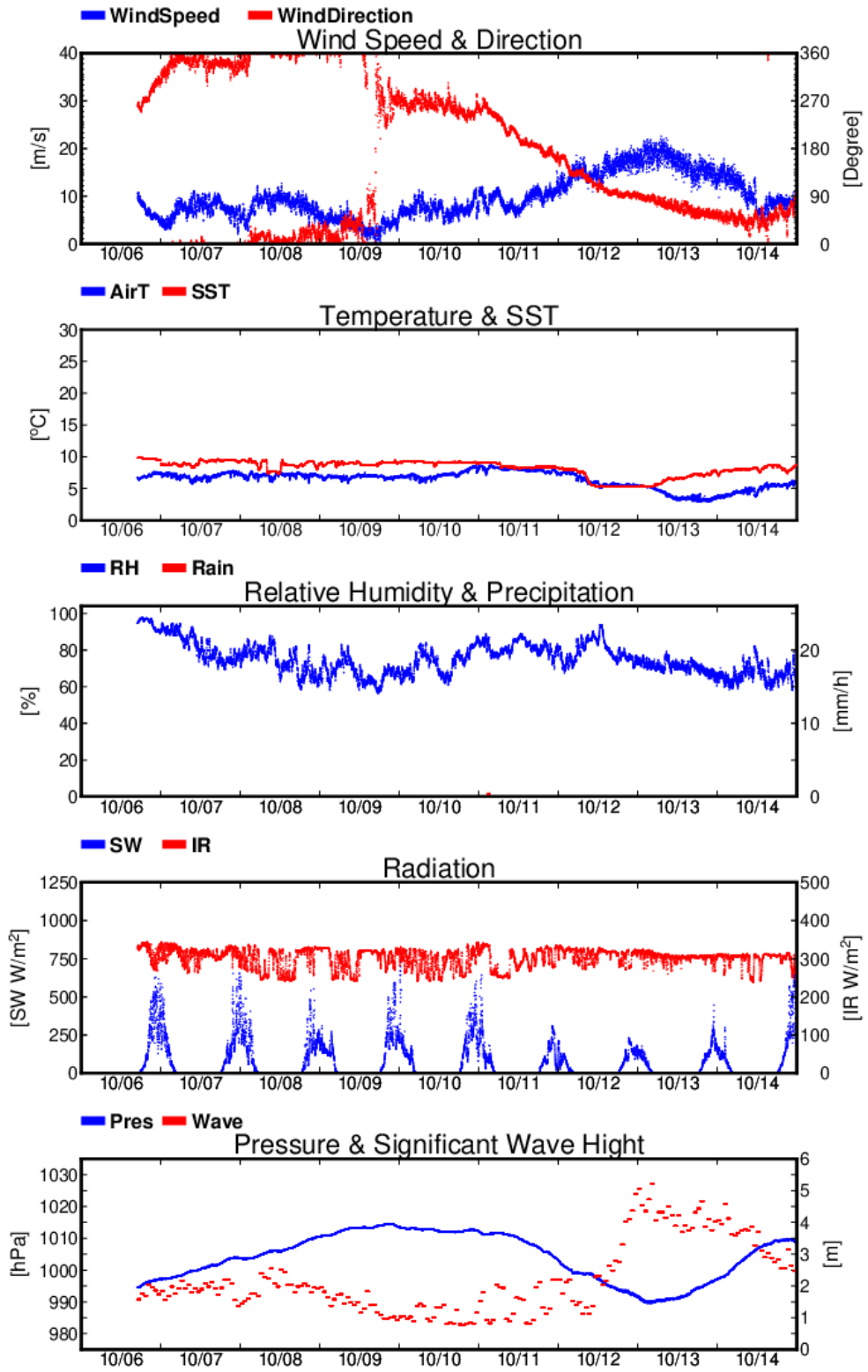
Fig. 3.3-1 Time series of surface meteorological parameters during this cruise
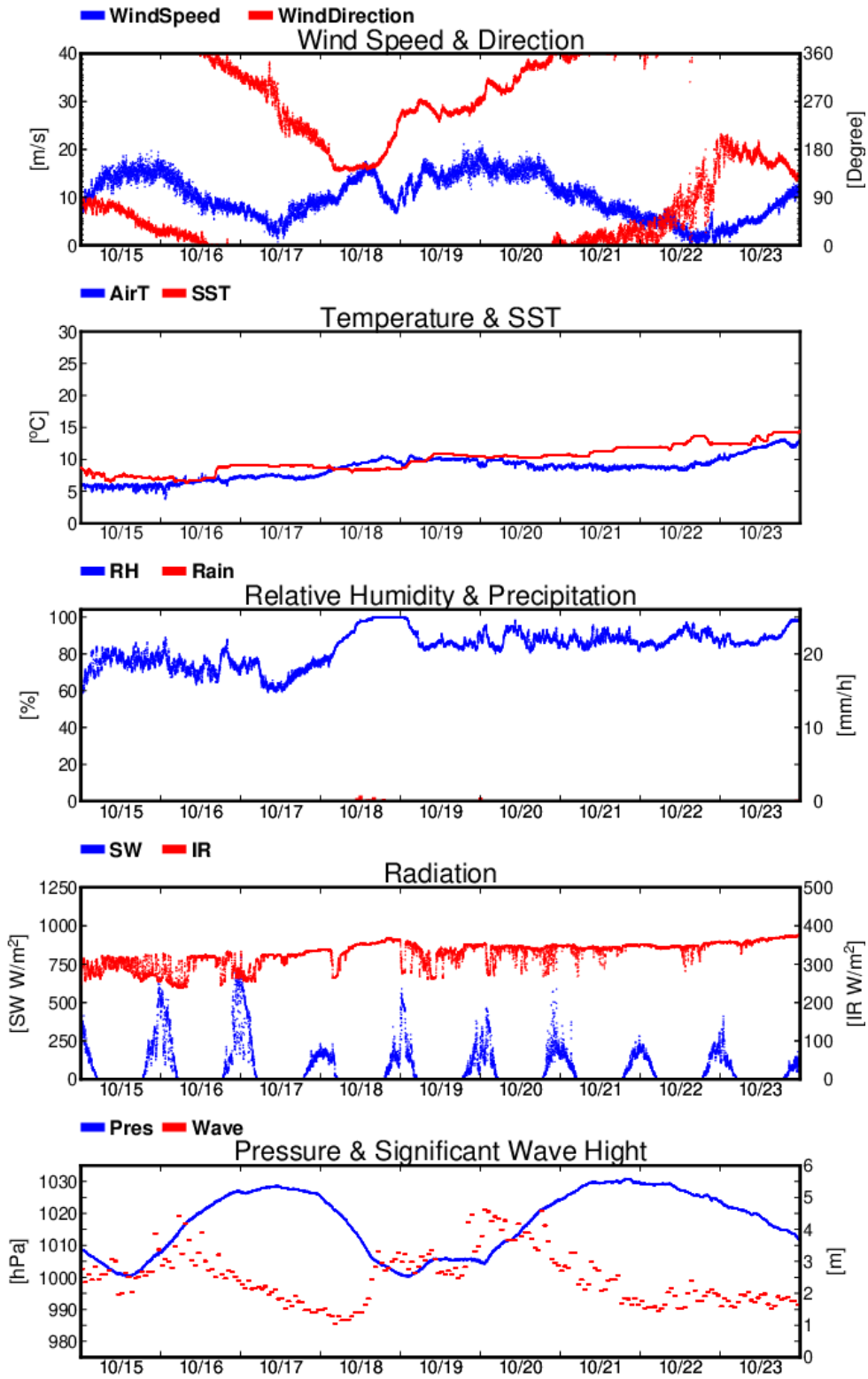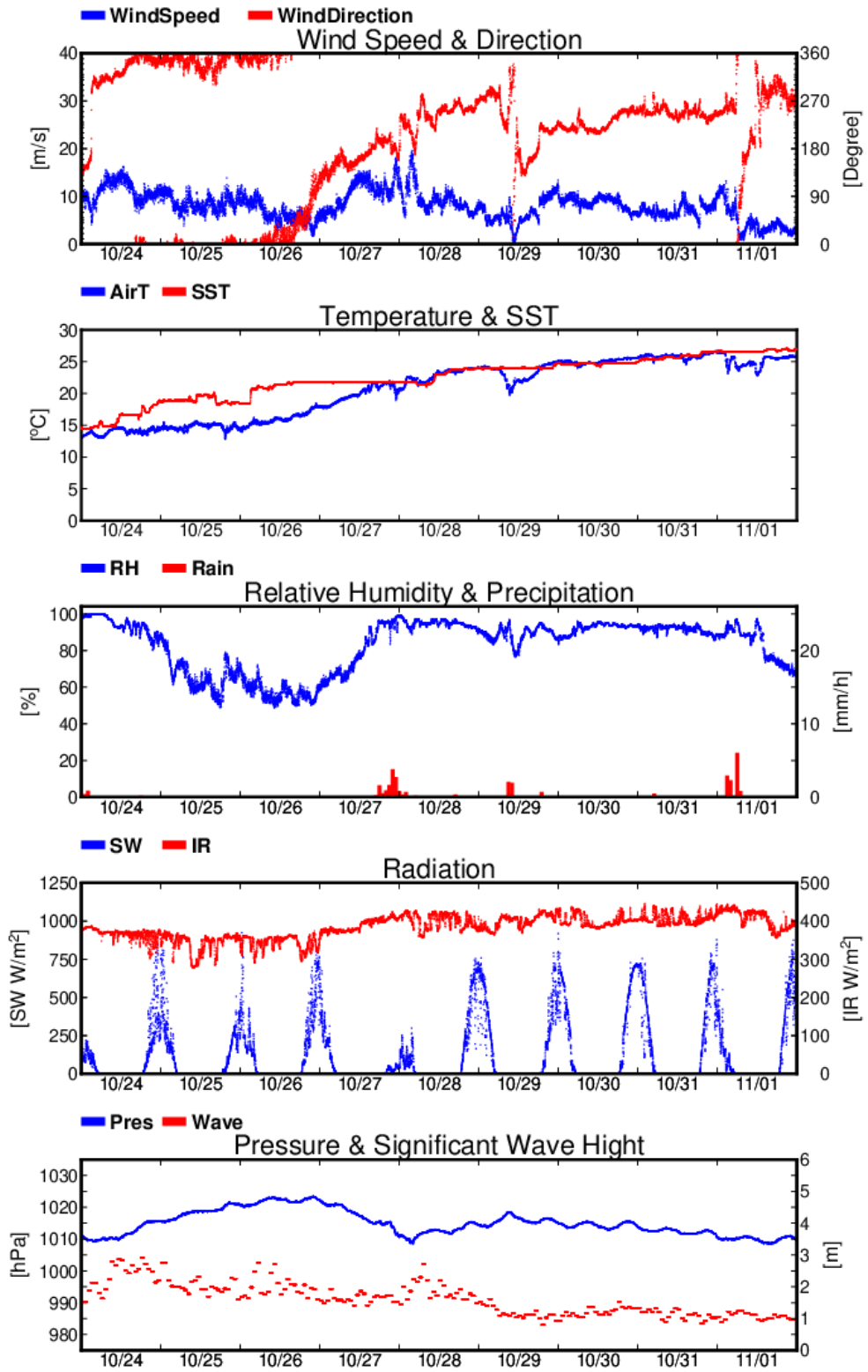
19

Fig. 3.3-1 (Continued)
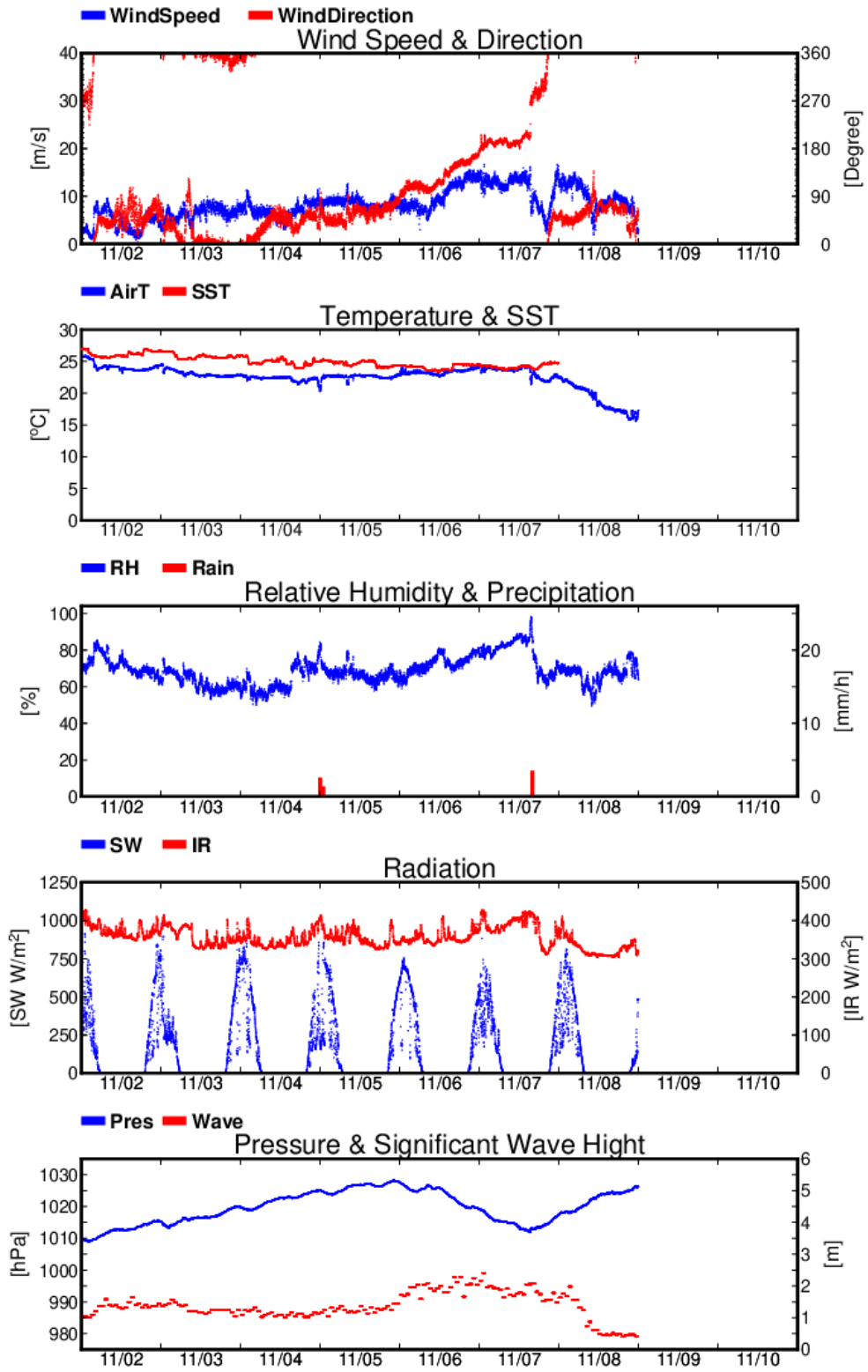
Fig. 3.3-1 (Continued)

Fig. 3.3-1 (Continued)

3.4 Thermo-Salinograph and Related Properties
December 7, 2023

(1) Personnel
Hiroshi UCHIDA (JAMSTEC RIGC)
Katsunori SAGISHIMA (MWJ) (Operation leader)
Misato KUWAHARA (MWJ)
Tomokazu CHIBA (MWJ)

(2) Objective
The objective of this measurements is to collect sea surface salinity, temperature, dissolved oxygen, fluorescence, and turbidity data continuously along the cruise track.

(3) Instruments and method
The Continuous Sea Surface Water Monitoring System (Marine Works Japan Co, Ltd., Yokosuka, Kanagawa, Japan) automatically measures salinity, temperature, dissolved oxygen, fluorescence, turbidity, total dissolved gas pressure in surface seawater at a sampling interval of 1 minute. This system is installed in the sea surface monitoring laboratory and bottom of the ship (only thermometer) and connected to shipboard LAN system. Measured data along with time and position of the ship were displayed on a monitor and stored in a personal computer. Seawater was continuously pumped up to the laboratory from about 5 m water depth and flowed into the system through a vinyl-chloride pipe or a tube. One thermometer is located just before the seawater pump at bottom of the ship. Flow rate in the system was manually adjusted about 1.0 L/min.
Instruments used in this cruise are as follows:

Temperature (bottom of the ship), SBE 38, Sea-Bird Scientific, Inc., Bellevue, Washington, USA
    Serial no. 3857820-0540
Temperature and conductivity, SBE 45, Sea-Bird Scientific, Inc.
    Serial no. 4557888-0264
Dissolved oxygen, RINKO II, JFE Advantech, Co., Ltd., Osaka, Japan
    Serial no. 0035
Chlorophyll fluorometer, C3, Turner Designs, Inc., Sunnwale, California, USA
    Serial no. 2300707 (fluorescence and turbidity)
Data acquisition software, SeaMoni, Marine Works Japan, Co., Ltd.
    Version 1.2.0.0

(4) Pre-cruise calibration
Pre-cruise sensor calibrations for the SBE 38, and SBE 45 were performed by the manufacturer.
Pre-cruise sensor calibration for C3 was performed by Marine Works Japan, Co., Ltd. The C3 chlorophyll fluorometer was calibrated with 100 ppb uranine solution, then the Secondary Solid Standard (SSS) was calibrated using the calibrated chlorophyll fluorometer.
Pre-cruise sensor calibration for RINKO was performed at JAMSTEC. The oxygen sensor was immersed in fresh water in a 1-L semi-closed glass vessel, which was immersed in a temperature-controlled water bath. Temperature of the water bath was set to 1, 10, 20 and 29°C. Temperature of the fresh water in the vessel was measured by a thermistor of the portable dissolved oxygen sensor (expanded uncertainty of smaller than 0.01°C, ARO-PR, JFE Advantech, Co., Ltd.). At each temperature, the fresh water in the vessel was bubbled with standard gases (4, 10, 17, and 25% oxygen consisted of the oxygen-nitrogen mixture, whose relative expanded uncertainty is 1%, Japan Fine Products, Tochigi, Japan). Nitrogen standard gas (0% oxygen) (G1) and air (21% oxygen) were also used. Absolute pressure of the vessel's headspace was measured by a reference quartz crystal barometer (expanded uncertainty of 0.01% of reading, RPM4 BA100Ks, Fluke Co., Phoenix Arizona, USA) and ranged from about 1040 to 1070 hPa. The data were averaged over 5 minutes at each calibration point (a matrix of 24 points). As a reference, oxygen concentration of the fresh water in the calibration vessel was calculated from the oxygen concentration of the gases, temperature, and absolute pressure at the water depth (about 6 cm) of the sensor's sensing foil as follows:

$$O_2 \ (\mu mol/L) = \{1000 \times c(T) \times (A_p - pH_2O)\} \ / \ \{0.20946 \times 22.3916 \times (1013.25 - pH_2O)\}$$

where $c(T)$ is the oxygen solubility, A_p is absolute pressure (in hPa), and pH_2O is the water vapor pressure (in hPa). The RINKO was calibrated by the modified Stern-Volmer equation slightly modified from a method by Uchida et al. (2010):

$$O_2 \ (\mu mol/L) = [(V_0 \ / \ V)^E - 1] \ / \ K_{sv}$$

where V is raw phase difference, V_0 is raw phase difference in the absence of oxygen, K_{sv} is Stern-Volmer constant. The coefficient E corrects nonlinearity of the Stern-Volmer equation. The V_0 and the K_{sv} are assumed to be functions of temperature as follows.

$$K_{sv} = C_0 + C_1 \times T + C_2 \times T^2$$
$$V_0 = 1 + C_3 \times T$$
$$V = C_4 + C_5 \times (N/10000)$$

where T is temperature (°C) and N is raw output.

(5) Data collection

Data from the Continuous Sea Surface Water Monitoring System were obtained at 1-minute intervals. Periods of measurement, maintenance and problems are listed in Table 3.4-1. Seawater samples for salinity, dissolved oxygen and chlorophyll-a analysis were taken from the Continuous Sea Surface Water Monitoring System basically once in a day to calibrate the sensors in situ. Details of these analysis are described in elsewhere of the cruise report.

Table 3.4-1. Events of the Continuous Sea Surface Water Monitoring System operation.

System Date [UTC]	System Time [UTC]	Events	Note
2023/10/07	00:50	Start data logging	
2023/10/18	01:23 – 01:41	Filter and C3 maintenance	Zero flow rate
2023/10/24	09:44	Filter maintenance	Filter exchanged
2023/11/07	23:59	End data logging	

(5) Post-cruise calibration

Data from the Continuous Sea Surface Water Monitoring System were processed as follows. Spikes in the temperature and salinity data were removed using a median filter with a window of 3 scans (3 minutes) when difference between the original data and the median filtered data was larger than 0.1°C for temperature and 0.5 for salinity. Data gaps were linearly interpolated when the gap was ≤ 13 minutes. Fluorometer and turbidity data were low-pass filtered using a median filter with a window of 3 scans (3 minutes) to remove spikes. Raw data from the RINKO oxygen sensor and fluorometer data were low-pass filtered using a Hamming filter with a window of 15 scans (15 minutes). The remaining erroneous data were manually removed.

Salinity (S [PSU]), dissolved oxygen (O [μmol/kg]), and fluorescence (Fl [RFU]) data were corrected using the water sampled data. Corrected salinity (S_{cor}), dissolved oxygen (O_{cor}), and estimated chlorophyll-a (Chl-a) were calculated from following equations

$$S_{cor} \ [PSU] = c_0 + c_1 \, S + c_2 \, t$$
$$O_{cor} \ [\mu mol/kg] = c_0 + c_1 \, O + c_2 \, T + c_3 \, t + c_4 \, T^2$$
$$Chl\text{-}a \ [\mu g/L] = c_0 \, Fl$$

where S is practical salinity, t is days from a reference time (2023/10/07 00:50 [UTC]), T is temperature in °C. The best fit sets of calibration coefficients ($c_0 \sim c_4$) were determined by a least square technique to minimize the deviation from the water sampled data. The calibration coefficients were listed below.

Salinity
$$c_0 = 8.645242259940150e\text{-}02$$
$$c_1 = 0.9983553361651739$$
$$c_2 = 3.537020068939429e\text{-}04$$

Oxygen
$$c_0 = 15.22754596539572$$
$$c_1 = 0.8579856986769557$$
$$c_2 = 0.5859344910121628$$
$$c_3 = -1.491671090377206e\text{-}02$$

$$c_4 = -2.129245504533969e-02$$

Chlorophyll-a

$$c_0 = 0.4199146287972310 \text{ (for T < 7.5 °C)}$$
$$0.1948505383313815 \text{ (for 7.5 °C <= T < 9.5°C)}$$
$$0.1265289676592355 \text{ (for 9.5 °C <= T < 19°C)}$$
$$0.2032149710321389 \text{ (for T >= 19 °C)}$$

Comparisons between the Continuous Sea Surface Water Monitoring System data and water sampled data are shown in Figs. 3.4.1, 3.4.2 and 3.4.3.

(6) Reference

Uchida, H., G. C. Johnson, and K. E. McTaggart (2010): CTD oxygen sensor calibration procedures, The GO-SHIP Repeat Hydrography Manual: A collection of expert reports and guidelines, IOCCP Rep., No. 14, ICPO Pub. Ser. No. 134.

(7) Data archive

These data obtained in this cruise will be submitted to the Data Management Group (DMG) of JAMSTEC, and will open to the public via "Data Research System for Whole Cruise Information in JAMSTEC (DARWIN)" in JAMSTEC web site.

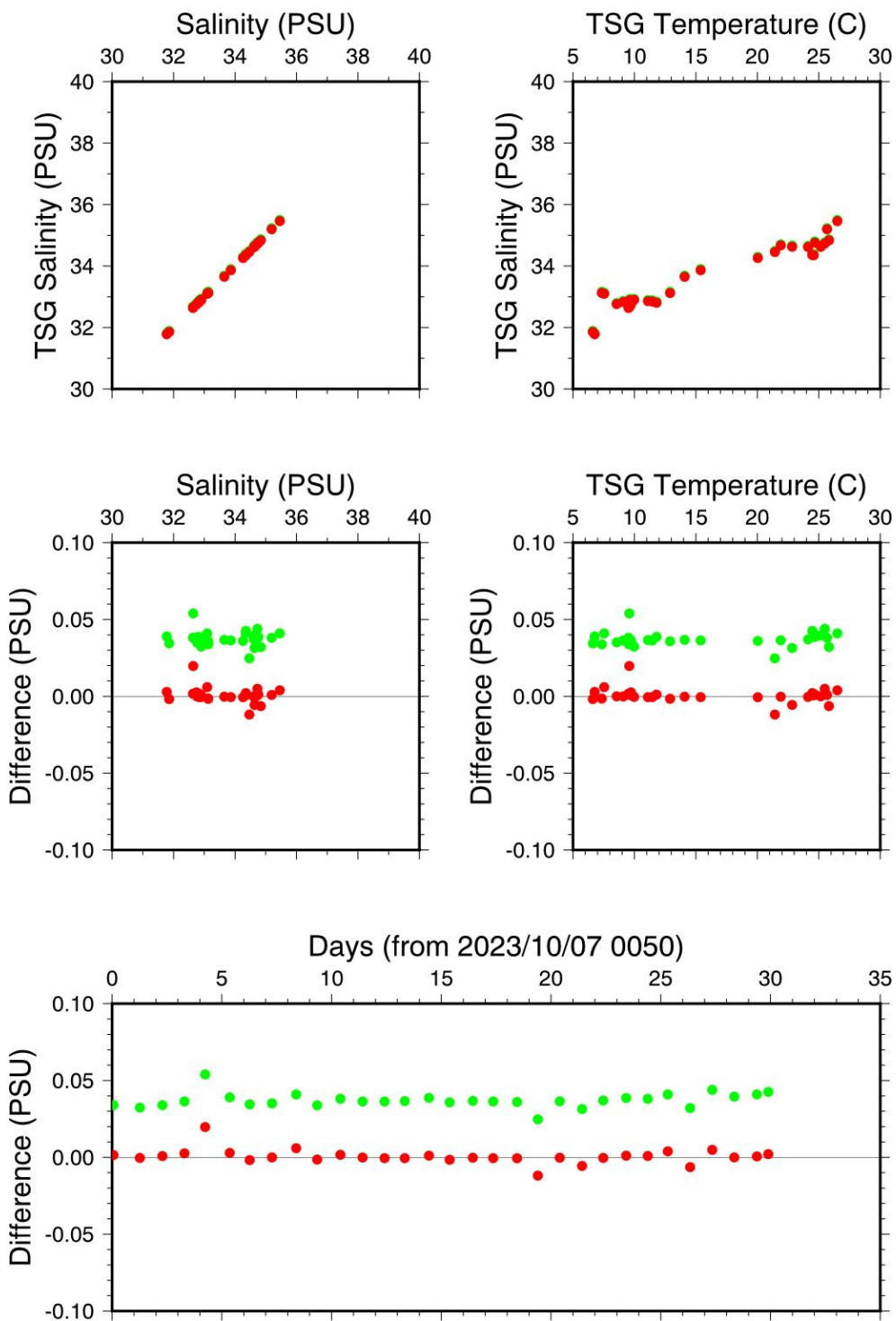<http://www.godac.jamstec.go.jp/darwin/e>

Fig. 3.4-1. Comparison between TSG salinity (red: before correction, green: after correction) and sampled salinity.
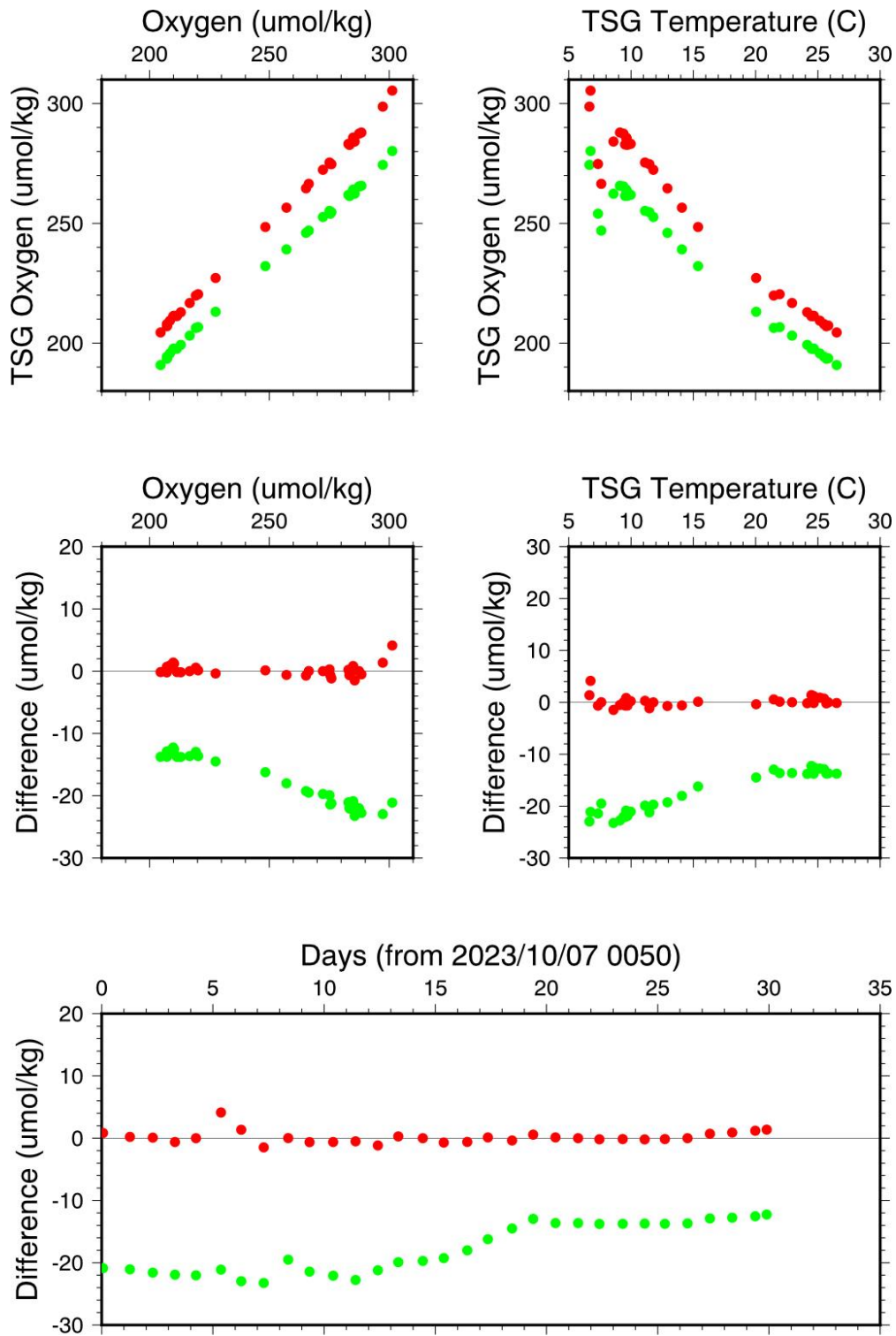
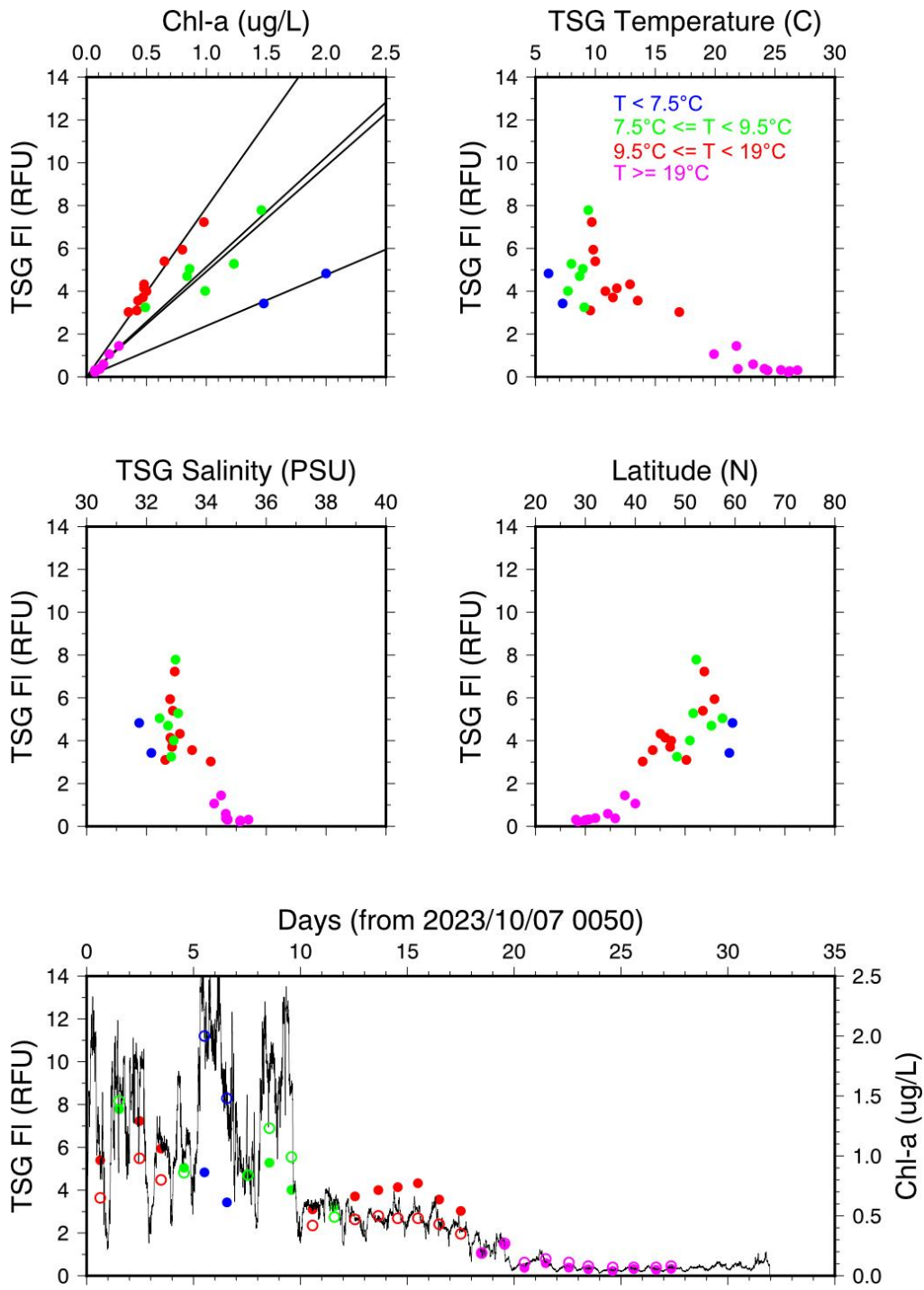Fig. 3.4-2. Same as Fig. 3.4-1, but for dissolved oxygen.

Fig. 3.4-3. Comparison between TSG fluorescence and sampled chlorophyll-a. For the lowest panel, closed circles are TSG fluorescence, and open circles and line are sampled chlorophyll-a and estimated chlorophyll-a from TSG fluorescence, respectively.

3.5. Shipboard ADCP

(1)   Personnel
Shinya Kouketsu   JAMSTEC: Principal investigator
Masanori Murakami   Nippon Marine Enterprises, Ltd. (NME)
Fumine Okada   NME
Haruna Yamanaka   NME
Yoichi Inoue   MIRAI crew

(2)   Objectives
To obtain continuous measurement data of the current profile along the ship's track.

(3)   Instruments and methods
Upper ocean current measurements were made in this cruise, using the hull-mounted Acoustic Doppler Current Profiler (ADCP) system. For most of its operation, the instrument was configured for water-tracking mode. Bottom-tracking mode, interleaved bottom-ping with water-ping, was made to get the calibration data for evaluating transducer misalignment angle in the shallow water. The system consists of following components;

i)   R/V MIRAI has installed the Ocean Surveyor for vessel-mount ADCP (frequency 76.8 kHz; Teledyne RD Instruments, USA). It has a phased-array transducer with single ceramic assembly and creates 4 acoustic beams electronically. We mounted the transducer head rotated to a ship-relative angle of 45 degrees azimuth from the keel.

ii)   For heading source, we use ship's gyro compass (Tokyo Keiki, Japan), continuously providing heading to the ADCP system directory. Additionally, we have Inertial Navigation System (Phins, IXBLUE SAS, France) which provide high-precision heading, attitude information, pitch and roll. They are stored in ".N2R" data files with a time stamp.

iii)   Differential GNSS system (StarPack-D, Fugro, Netherlands) providing precise ship's position

iv)   We used VmDas software version 1.50(TRDI) for data acquisition.

v)   To synchronize time stamp of ping with Computer time, the clock of the logging computer is adjusted to GPS time server continuously by the application software.

vi)   Fresh water is charged in the sea chest to prevent bio fouling at transducer face.

vii)   The sound speed at the transducer does affect the vertical bin mapping and vertical velocity measurement, and that is calculated from temperature, salinity (constant value; 35.0 PSU) and depth (6.5 m; transducer depth) by equation in Medwin (1975).

Data was configured for "8 m" layer intervals starting about 19 m below sea surface and recorded every ping as raw ensemble data (.ENR). Additionally, 30 seconds averaged data were recorded as short-term average (.STA). 300 seconds averaged data were long-term average (.LTA), respectively.

(4)   Parameters
Major parameters for the measurement, Direct Command, are shown in Table 3.5-1.

Table 3.5-1. Major parameters

Environmental Sensor Commands
            EA = 04500   Heading Alignment (1/100 deg)
            ED = 00065   Transducer Depth (0 - 65535 dm)
            EF = +001   Pitch/Roll Divisor/Multiplier (pos/neg) [1/99 - 99]
            EH = 00000   Heading (1/100 deg)
            ES = 35   Salinity (0-40 pp thousand)

```
EX = 00000              Coordinate Transform (Xform: Type; Tilts; 3Bm; Map)
EZ = 10200010           Sensor Source (C; D; H; P; R; S; T; U)
    C (1): Sound velocity calculates using ED, ES, ET (temp.)
    D (0): Manual ED
    H (2): External synchro
    P (0), R (0): Manual EP, ER (0 degree)
    S (0): Manual ES
    T (1): Internal transducer sensor
    U (0): Manual EU
EV = 0              Heading Bias (1/100 deg)
```
Water-Track Commands
```
WA = 255            False Target Threshold (Max) (0-255 count)
WC = 120            Low Correlation Threshold (0-255)
WD = 111 100 000    Data Out (V; C; A; PG; St; Vsum; Vsum^2; #G; P0)
WE = 1000           Error Velocity Threshold (0-5000 mm/s)
WF = 0800           Blank After Transmit (cm)
WN = 100            Number of depth cells (1-128)
WP = 00001          Pings per Ensemble (0-16384)
WS = 800            Depth Cell Size (cm)
WV = 0390           Mode 1 Ambiguity Velocity (cm/s radial)
```

(5)   Preliminary results

Horizontal velocity along the ship's track is presented in Fig.3.5-1.

(6)   Data Process

We plan to do data processing to make corrections for instrument alignment with INU data after the cruise.

(7)   Data archives

These data obtained in this cruise will be submitted to the Data Management Group of JAMSTEC and will be opened to the public via "Data Research System for Whole Cruise Information in JAMSTEC (DARWIN)" in JAMSTEC web site.

http://www.godac.jamstec.go.jp/darwin/e

(8)   Remarks (Times in UTC)

i)   The following time, GNSS and Attitude data input were delayed due to the operation PC trouble.
      10:45:41 – 11:36:07 23 Oct. 2023
      01:15:01 – 01:15:05 02 Nov. 2023

ii)   Ensemble No. was returned to first (#1) in the middle of data file "mr2307007_*", because communication error was occurred. Data files were separated as follow.
      mr2307007_*
      (a) mr2307007a_*
      Ensemble No. : #1 (2023/10/16 08:55:41) → #142561 (2023/10/23 01:46:38)
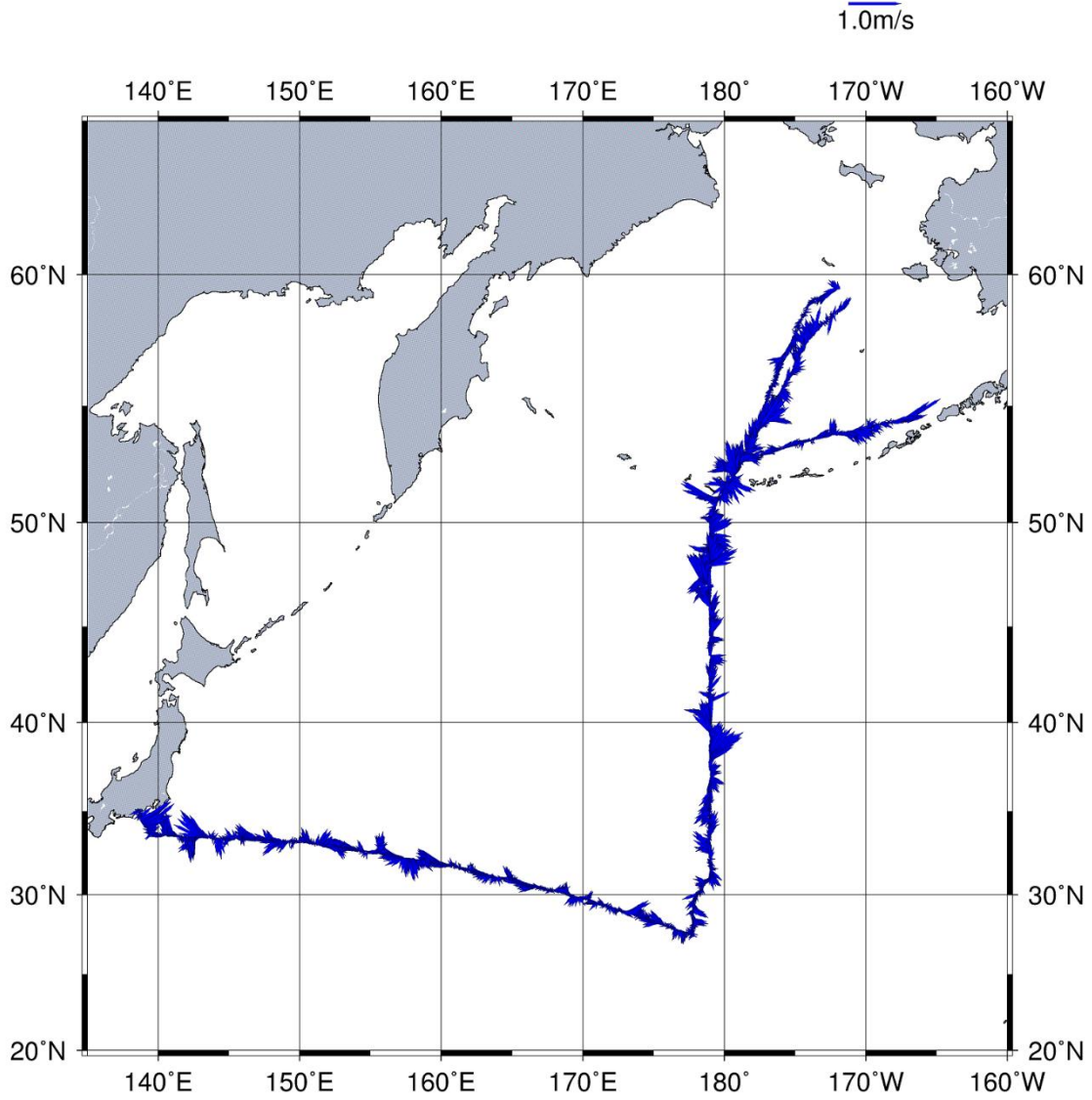   (b) mr2307007b_*
      Ensemble No. : #1 (2023/10/23 01:46:58) → #196531 (2023/11/01 07:37:31)

iii) The following period, ADCP data was invalid due to the system trouble.
      01:46:41 - 01:46:58 23 Oct. 2023

MR23−07 Cruise
10min.Average / Layer : 35−60m

Fig. 3.5-2 Horizontal Velocity along the ship's track.

(10 min. Average / Layer: 35-60m)

3.6 Ceilometer observation

(1)   Personnel

Katsuro Katsumata	JAMSTEC: Principal investigator
Masanori Murakami	Nippon Marine Enterprises, Ltd（NME）
Fumine Okada	NME
Haruna Yamanaka	NME
Yoichi Inoue	MIRAI crew

(2)   Objectives

The information of cloud base height and the liquid water amount around cloud base is important to understand a process on formation of the cloud. As one of the methods to measure them, the ceilometer observation was carried out.

(3)   Parameters

1. Cloud base height [m].
2. Backscatter profile, sensitivity and range normalized at 10 m resolution.
3. Estimated cloud amount [oktas] and height [m]; Sky Condition Algorithm.

(4)   Methods

Cloud base height and backscatter profile were observed by ceilometer (CL51, VAISALA, Finland). The measurement configurations are shown in Table 3.6-1. On the archive dataset, cloud base height and backscatter profile are recorded with the resolution of 10 m.

Table 3.6-1 The measurement configurations

Property	Description	
Laser source	Indium Gallium Arsenide (InGaAs) Diode	
Transmitting center wavelength	910±10 nm at 25 degC	
Transmitting average power	19.5 mW	
Repetition rate	6.5 kHz	
Detector	Silicon avalanche photodiode (APD)	
Responsibility at 905 nm	65 A/W	
Cloud detection range	0 ~ 13 km	
Measurement range	0 ~ 15 km	
Resolution	10 m in full range	
Sampling rate	36 sec.	
	Cloudiness in octas (0 ~ 9)	
	0	Sky Clear
	1	Few
Sky Condition	3	Scattered
	5-7	Broken
	8	Overcast
	9	Vertical Visibility

(5)   Preliminary results

Fig.3.6-1 shows the time series of 1st, 2nd and 3rd cloud base height during the cruise.

(6)   Data archives

These data obtained in this cruise will be submitted to the Data Management Group of JAMSTEC and will be opened to the public via "Data Research System for Whole Cruise Information in JAMSTEC (DARWIN)" in JAMSTEC web site.

http://www.godac.jamstec.go.jp/darwin/e

(7) **Remarks (Times in UTC)**

i)   The following time, the window was cleaned.
20:52, 11 Oct. 2023
01:45, 17 Oct. 2023
04:21, 26 Oct. 2023
02:12, 03 Nov. 2023
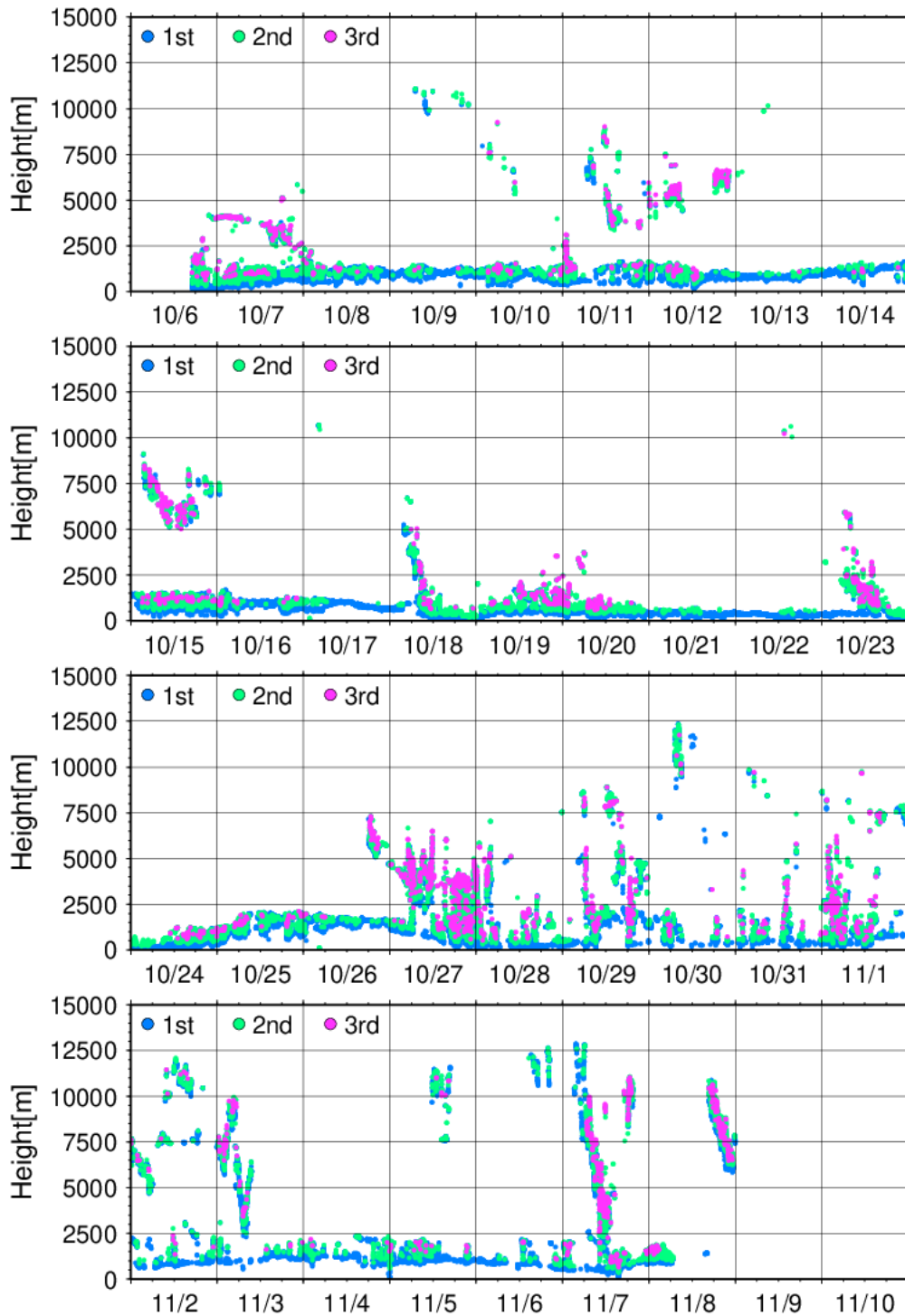
Fig. 3.6-1 1st, 2nd and 3rd cloud base height during this cruise.

33

3.7 C-band weather radar

(1) Personnel

Masaki KATSUMATA	(JAMSTEC)	Principal Investigator (not on board)
Biao GENG	(JAMSTEC)	(not on board)
Masanori MURAKAMI	(NME)	Operation Leader
Fumine OKADA	(NME)	
Haruna YAMANAKA	(NME)	

(2) Objective

Weather radar observations in this cruise aim to investigate the structure and evolution of precipitating systems over the tropical ocean.

(3) Radar specifications

The C-band weather radar on board the R/V Mirai is used. The basic specifications of the radar are as follows:

Frequency:	5370 MHz (C-band)
Polarimetry:	Horizontal and vertical (simultaneously transmitted and received)
Transmitter:	Solid-state transmitter
Pulse Configuration:	Using pulse-compression
Output Power:	6 kW (H) + 6 kW (V)
Antenna Diameter:	4 meter
Beam Width:	1.0 degrees
Inertial Navigation Unit:	PHINS (IXBLUE SAS France)

(4) Available radar variables

Radar variables, which are converted from the power and phase of the backscattered signal at vertically- and horizontally-polarized channels, are as follows:

Radar reflectivity:	Z
Doppler velocity:	V_r
Spectrum width of Doppler velocity:	SW
Differential reflectivity:	ZDR
Differential propagation phase:	Φ_{DP}
Specific differential phase:	KDP
Co-polar correlation coefficients:	ρ_{HV}

(5) Operational methodology

The antenna is controlled to point the commanded ground-relative direction, by controlling the azimuth and elevation to cancel the ship attitude (roll, pitch, and yaw) detected by the navigation unit. The Doppler velocity is also corrected by subtracting the ship movement in the beam direction.

For maintenance, internal signals of the radar are checked and calibrated at the beginning and the end of the cruise. Meanwhile, the peak output power and the radar's pulse width are checked

daily.

During the cruise, the radar is operated in modes shown in Table 3.7-1. A dual PRF mode is used for volume scans. For RHI and surveillance PPI scans, a single PRF mode is used.

(6) Data

The C-band weather radar observations were conducted continuously over the high seas and Japanese EEZ except nearby the main islands of Japan. The observation periods were as follows:

0000UTC on October 19 – 1700UTC on November 7

An example of the obtained snapshots is shown in Fig. 3.7-1. The data in the upper panels were obtained in the midlatitude climate (at around 40 N when the surface air temperature was about 15 degrees C), while the data in the lower panels were obtained in the subtropical climate (at around 29 N when the surface air temperature was about 26 degrees C). The appearance of the convective cells as seen in ZH panels (left) differ in horizontal scale, morphology, etc. Very high ZDR signals (colored by red to orange) were frequently found in the lower right panel for the subtropical case (which implies exitance of large raindrops), while such signals are had to find in the midlatitude case. As in the example, the radar observation in the present cruise was successful in capturing wide variety of the convections in various climatological conditions.

Detailed analyses of the data observed by the radar will be performed after the cruise.

(7) Data archive

The obtained data will be submitted to the Data Management Group of JAMSTEC.

Table 3.7-1 Scan modes of C-band weather radar

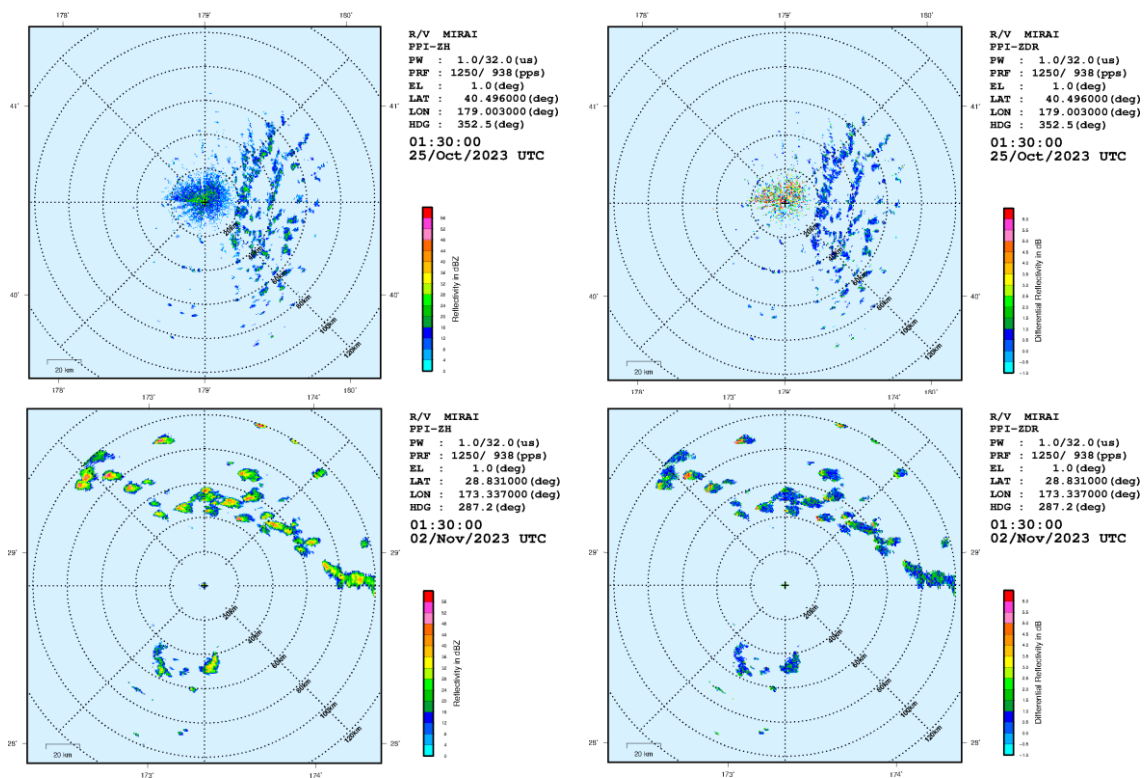|	Surveillance PPI Scan	Volume Scan						RHI Scan
Repeated Cycle (min.)	30	6						6
Times in One Cycle	1	1						3
PRF(s) (Hz)	400	dual PRF (ray alternative)						1250
		667	833	938	1250	1333	2000	
Azimuth (deg)	Full Circle							Option
Bin Spacing (m)	150							
Max. Range (km)	300	150		100		60		100
Elevation Angle(s) (deg.)	0.5	0.5		1.0, 1.8, 2.6, 3.4, 4.2, 5.1, 6.2, 7.6, 9.7, 12.2, 15.2		18.7, 23.0, 27.9, 33.5, 40.0		0.0~ 60.0

Fig. 3.7-1: Examples of the obtained data by the PPI scans (at the elevation of 1.0 degrees) at two scenes, on Oct. 25 (upper panels) and Nov. 02 (lower panels). Right panels are for the reflectivity (ZH), while the right panels are for the differential reflectivity (ZDR).

3.8   Lidar observation

(1) Personnel
 Masaki KATSUMATA (JAMSTEC) Principle Investigator (not on board)
 Kyoko TANIGUCHI (JAMSTEC) (not on board)
 Masanori MURAKAMI (NME)
 Fumine OKADA   (NME)
 Haruna YAMANAKA (NME)

(2) Objective
The objective of this observation is to capture the vertical distribution of clouds, aerosols, and water vapor in high spatio-temporal resolution.

(3) Parameters
 355nm Mie scattering signal
 532nm Mie scattering signal
 1064nm Mie scattering signal
 387nm Raman nitrogen scattering signal (nighttime only)
 408nm Raman water vapor scattering signal (nighttime only)
 607nm Raman nitrogen scattering signal (nighttime only)
 660nm Raman water vapor scattering signal (nighttime only)

(4) Instruments and methods
The Mirai Lidar system transmits a 10-Hz pulse laser in three wavelengths: 1064nm, 532nm, 355nm. For cloud and aerosol observation, the system detects Mie scattering at these wavelengths. The separate detections of polarization components at 532 nm and 355 nm obtain additional characteristics of the targets. The system also detects Raman water vapor signals at 660 nm and 408nm, Raman nitrogen signals at 607 nm and 387nm at nighttime. Based on the signal ratio of Raman water vapor to Raman nitrogen, the system offers water vapor mixing ratio profiles.

(5) Preliminary Results
The lidar system observed the lower atmosphere continuously from 18 October to 8 November, 2023, over the high sea and the EEZ and the territorial water of Japan. All data will be reviewed after the cruise to maintain data quality.

(6) Data Archive
The obtained data will be submitted to the Data Management Group of JAMSTEC.

3.9   Microwave Radiometer

(1) Personnel
Masaki KATSUMATA   (JAMSTEC)   Principle Investigator (not on board)
Kazutoshi SATO   (NIPR)   (not on board)
Akira KUWANO-YOSHIDA   (Kyoto Univ.)   (not on board)
Masahiro MINOWA   (Furuno Electric Co., Ltd.)   (not on board)

(2) Objective

To retrieve the total column integrated water vapor, and the vertical profiles of water vapor and temperature, in the atmosphere

(3) Method

Two microwave radiometers (hereafter MWR; manufactured by Furuno Electric Co., Ltd.) are used. The MWRs received natural microwave within the angle of 20 deg. from zenith. One of the MWRs for the water vapor observes at the frequencies around 22 GHz, to retrieve the column integrated water vapor (or precipitable water), and the vertical profile of the water vapor. The other MWR measures at the frequencies around 55 GHz to retrieve vertical profile of the air temperature. The observation was made approximately every 20 seconds except when periodic auto-calibration was on-going (once in several minutes). The rain sensor is equipped to identify the period of rainfall.

In addition to the MWRs, the whole sky camera was installed beside the MWRs. This is to monitor cloud cover, which also affects the microwave signals. The camera obtained the whole-sky image every 2 minutes.

All instruments were installed at the top of the roof of aft wheelhouse, as in Fig. 3.9-1.

(4) Results

The data have been obtained continuously from 18 October to 8 November, 2023, over the high sea and the EEZ and the territorial water of Japan. The further analyses for the water vapor (column-integrated amount and vertical profile), the air temperature (vertical profile), etc., will be carried out after the cruise.

(5) Data archive

The data will be submitted to the JAMSTEC Data Management Group (DMG).

(6) Acknowledgment

Fig. 3.9-1: Outlook of the instruments installed at the roof of the aft wheelhouse; the microwave radiometer for the air temperature (right), microwave radiometer for the water vapor (middle), and the whole-sky camera (left).

3.10 Atmospheric and surface seawater pCO$_2$

(1) Personnel
>*Akihiko Murata (JAMSTEC)*
>*Masahito Orui （MWJ）*
>*Nagisa Fujiki (MWJ)*

(2) Objective

Concentrations of CO_2 in the atmosphere are now increasing at a rate of about 2.0 ppmv y^{-1} owing to human activities such as burning of fossil fuels, deforestation, and cement production. It is an urgent task to estimate as accurately as possible the absorption capacity of the oceans against the increased atmospheric CO_2, and to clarify the mechanism of the CO_2 absorption, because the magnitude of the anticipated global warming depends on the levels of CO_2 in the atmosphere, and because the ocean currently absorbs 1/3 of the 6 Gt of carbon emitted into the atmosphere each year by human activities.

In this cruise, we measured pCO$_2$ (partial pressure of CO_2) in the atmosphere and surface seawater continuously along cruise tracks in the Pacific in order to quantify how much CO_2 is absorbed in the region. Although the main purpose of the measurement was to collect pCO$_2$ data, we also measured atmospheric and surface seawater pCH$_4$.

(3) Apparatus

Atmospheric and surface seawater pCO$_2$ and pCH$_4$ were measured with a system having the off-axis integrated-cavity output spectroscopy gas analyzer (Off-Axis ICOS; 911-0011, Los Gatos Research). Standard gases were measured every about 12 hours, and atmospheric air taken from the bow of the ship (approx.13 m above the sea level) were measured every about 3 hours. Seawater was taken from an intake placed at the approximately 4.5 m below the sea surface and introduced into the equilibrator at the flow rate of (4 - 5) L min^{-1} by a pump. The equilibrated air was circulated in a closed loop by a pump at flow rate of (0.6 - 0.7) L min^{-1} through two electric cooling units, a starling cooler, and the Off-Axis ICOS.

(4) Preliminary result

Distributions of atmospheric and surface seawater CO_2 were shown in Figure 3.10.1, along with those of sea surface temperature (SST). Distributions of atmospheric and surface seawater CH_4 were displayed in Figure 3.10.2, along with those SST.
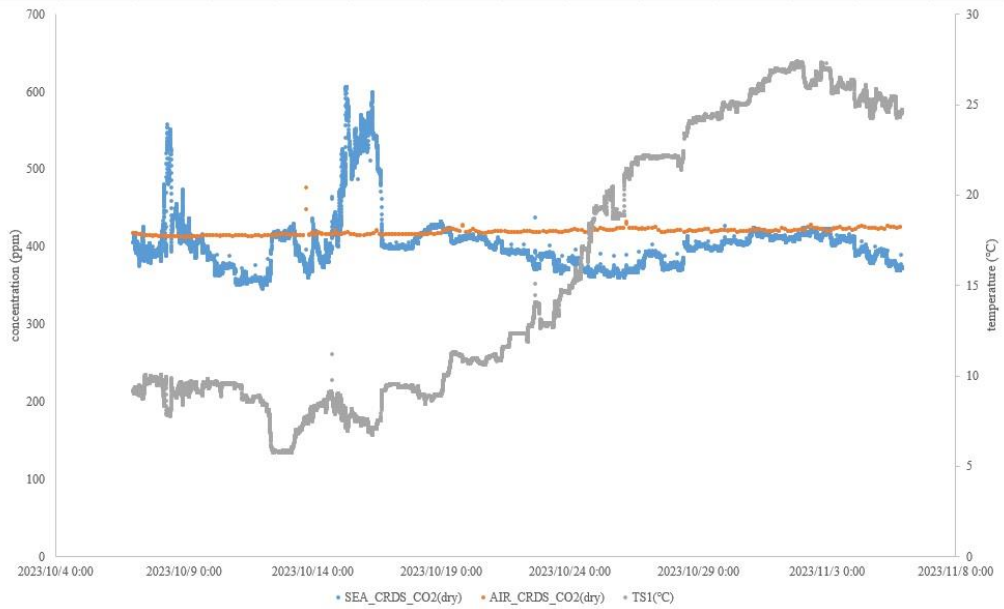

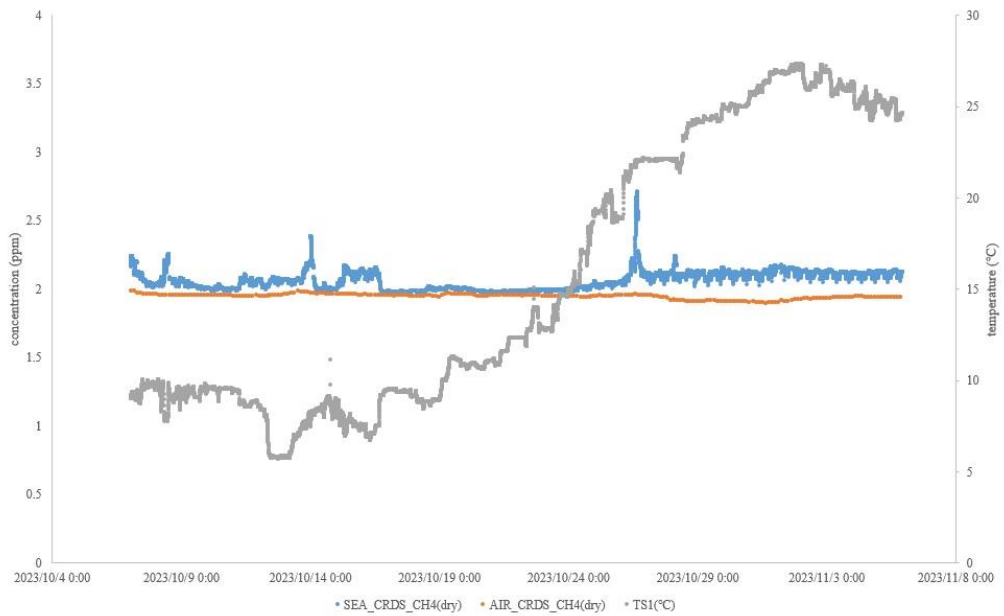Fig. 3.10-1 Distributions of atmospheric and surface seawater CO_2 along the observation line as a function of time.

Fig. 3.10-2 Distributions of atmospheric and surface seawater CH_4 along the observation line as a function of time.

41

3.11   Satellite image acquisition

(1)   Personnel
Katsuro Katsumata   JAMSTEC: Principal investigator
Masanori Murakami   Nippon Marine Enterprises, Ltd.（NME）
Fumine Okada   NME
Haruna Yamanaka   NME
Yoichi Inoue   MIRAI crew

(2)   Objectives
    The objective is to collect cloud data in a high spatial resolution mode from the Advance Very High-Resolution Radiometer (AVHRR) on the NOAA and MetOp polar orbiting satellites.

(3)   Methods
    We received the down link High Resolution Picture Transmission (HRPT) signal from satellites, which passed over the area around the R/V MIRAI. We processed the HRPT signal with the in-flight calibration and computed the brightness temperature. A cloud image map around the R/V MIRAI was made from the data for each pass of satellites. We received and processed polar orbiting satellites data throughout this cruise.

(4)   Data archives
    These data obtained in this cruise will be submitted to the Data Management Group of JAMSTEC and will be opened to the public via "Data Research System for Whole Cruise Information in JAMSTEC (DARWIN)" in JAMSTEC web site.
    http://www.godac.jamstec.go.jp/darwin/e

3.12 Sea Surface Gravity

(1)   Personnel
Katsuro Katsumata	JAMSTEC: Principal investigator
Masanori Murakami	Nippon Marine Enterprises, Ltd.（NME）
Fumine Okada	NME
Haruna Yamanaka	NME
Yoichi Inoue	MIRAI crew

(2)   Introduction
    The local gravity is an important parameter in geophysics and geodesy. The gravity data were collected during this cruise.

(3)   Parameters
Relative Gravity [CU: Counter Unit]
[mGal] = (coef1: 0.9946) * [CU]

(4)   Data Acquisition
    The relative gravity using LaCoste and Romberg air-sea gravity meter S-116 (Micro-g LaCoste, LLC) was measured during this cruise. To convert from the relative gravity to absolute one, we measured gravity, using portable gravity meter (Scintrex gravity meter CG-5), at Shimizu port as the reference points.

(5)   Preliminary Results
    Absolute gravity table is shown in Table 3.12-1.

Table 3.12-1. Absolute gravity table of the MR23-07 cruise

No.	Date mm/dd	UTC	Port	Absolute Gravity [mGal]	Sea Level [cm]	Ship Draft [cm]	Gravity at Sensor * [mGal]	S-116 Gravity [mGal]
#1	08/24	07:05	Shimizu	979,729.49	201	658	979730.39	12001.74
#2	11/09	07:59	Shimizu	979,728.98	187	603	979729.72	11999.90

*:   Gravity at Sensor = Absolute Gravity + Sea Level*0.3086/100 + (Draft-530)/100*0.2222

(6)   Data archives
    These data obtained in this cruise will be submitted to the Data Management Group of JAMSTEC and will be opened to the public via "Data Research System for Whole Cruise Information in JAMSTEC (DARWIN)" in JAMSTEC web site.
    http://www.godac.jamstec.go.jp/darwin/e

3.13 Sea Surface Magnetic Field

(1)   Personnel

Katsuro Katsumata	JAMSTEC: Principal investigator
Masanori Murakami	Nippon Marine Enterprises, Ltd. (NME)
Fumine Okada	NME
Haruna Yamanaka	NME
Yoichi Inoue	MIRAI crew

(2)   Introduction

Measurement of magnetic force on the sea is required for the geophysical investigations of marine magnetic anomaly caused by magnetization in upper crustal structure. We measured geomagnetic field using a three-component magnetometer during this cruise.

(3)   Principle of ship-board geomagnetic vector measurement

The relation between a magnetic-field vector observed on-board, $\mathbf{H}_{ob}$, (in the ship's fixed coordinate system) and the geomagnetic field vector, $\mathbf{F}$, (in the Earth's fixed coordinate system) is expressed as:

$$\mathbf{H}_{ob} = \widetilde{\mathbf{A}}\ \widetilde{\mathbf{R}}\ \widetilde{\mathbf{P}}\ \widetilde{\mathbf{Y}}\ \mathbf{F} + \mathbf{H}_p \qquad (3.13.1)$$

where $\widetilde{\mathbf{R}}$, $\widetilde{\mathbf{P}}$ and $\widetilde{\mathbf{Y}}$ are the matrices of rotation due to roll, pitch and heading of the ship, respectively. $\widetilde{\mathbf{A}}$ is a 3 x 3 matrix which represents magnetic susceptibility of the ship, and $\mathbf{H}_p$ is a magnetic field vector produced by a permanent magnetic moment of the ship's body. Rearrangement of Eq. (3.13.1) makes

$$\widetilde{\mathbf{B}}\ \mathbf{H}_{ob} + \mathbf{H}_{bp} = \widetilde{\mathbf{R}}\ \widetilde{\mathbf{P}}\ \widetilde{\mathbf{Y}}\ \mathbf{F} \qquad (3.13.2)$$

where $\widetilde{\mathbf{B}} = \widetilde{\mathbf{A}}^{-1}$, and $\mathbf{H}_{bp} = -\widetilde{\mathbf{B}}\ \mathbf{H}_p$. The magnetic field, $\mathbf{F}$, can be obtained by measuring, $\widetilde{\mathbf{R}}$, $\widetilde{\mathbf{P}}$, $\widetilde{\mathbf{Y}}$ and $\mathbf{H}_{ob}$, if $\widetilde{\mathbf{B}}$ and $\mathbf{H}_{bp}$ are known. Twelve constants in $\widetilde{\mathbf{B}}$ and $\mathbf{H}_{bp}$ can be determined by measuring variation of $\mathbf{H}_{ob}$ with $\widetilde{\mathbf{R}}$, $\widetilde{\mathbf{P}}$, and, $\widetilde{\mathbf{Y}}$ at a place where the geomagnetic field, $\mathbf{F}$, is known.

(4)   Instruments on R/V MIRAI

A shipboard three-component magnetometer system (Tierra Tecnica SFG2018) is equipped on-board R/V MIRAI. Three-axes flux-gate sensors with ring-cored coils are fixed on the fore mast. Outputs from the sensors are digitized by a 20-bit A/D converter (1 nT/LSB), and sampled at 8 times per second. Ship's heading, pitch, and roll are measured by the Inertial Navigation System (INS) for controlling attitude of a Doppler radar. Ship's position and speed data are taken from LAN every second.

(5)   Data archives

These data obtained in this cruise will be submitted to the Data Management Group of JAMSTEC and will be opened to the public via "Data Research System for Whole Cruise Information in JAMSTEC (DARWIN)" in JAMSTEC web site.

http://www.godac.jamstec.go.jp/darwin/e

(6) Remarks (Times in UTC)

i) The following periods, we made a "figure-eight" turn (a pair of clockwise and anti-clockwise rotation) for calibration of the ship's magnetic effect.
16:41 - 17:05 10 Oct. 2023 around 56-00N, 176-30W
21:30 - 21:51 21 Oct. 2023 around 45-30N, 179-02E
17:44 - 18:07 30 Oct. 2023 around 30-00N, 178-00E
04:59 - 05:22 06 Nov. 2023 around 33-11N, 150-09E

ii) The following periods, navigation data (speed over ground, gyro, longitude, latitude, and sea depth) were invalid.
21:14:24 – 21:14:29 26 Oct. 2023
21:14:36 – 21:14:45 28 Oct. 2023

3.14 Evaluation of performance of the DFMC SBAS from QZSS

(1) Personnel

Toru Takahashi (ENRI)

Amane Fujiwara (JAMSTEC)

(2) Objectives

The aviation and maritime activities in the Arctic are growing with the recession of the Arctic sea ice. A model study suggested that the Global Navigation Satellite System (GNSS), which operates with the augmentation system such as the Satellite-based augmentation systems (SBAS) and Advanced Receiver Autonomous Integrity Monitoring (ARAIM), is effective for the navigation of aviation and maritime in the Arctic because of poor infrastructures (Reid et al., 2016). However, the current L1 SBAS broadcasts augmentation messages from geostationary (GEO) satellites, which are not available practically in the polar region at a latitude of 72 degrees or higher.

The Dual Frequency Multi Constellation Satellite Based Augmentation System (DFMC SBAS) has been standardization by the International Civil Aviation Organization (ICAO). Broadcasting augmentation messages from the Inclined Geosynchronous Orbit (IGSO) satellite is considered to be included in the future updates. The Electronic Navigation Research Institute (ENRI) developed the DFMC SBAS prototype based on the draft standards (Kitamura et al., 2018), and test messages are broadcasted from the Japanese Quasi-Zenith Satellite System (QZSS).

In the polar region, an auroral activity often generates the irregularity ionospheric plasma density and the ionospheric electric filed is intensified simultaneously. The carrier phase of the GNSS signal is fluctuated by the auroral activity. Since the fluctuation sometimes causes the loss of lock on GNSS signals, the impact the auroral activity on the GNSS carrier phase should be investigated.

The main objective of this study is to evaluate the performance DFMC SBAS broadcasted from Japanese QZSS in the Arctic and mid-high latitude regions. To test the DFMC SBAS in the Arctic, we installed the GNSS antenna, GNSS receivers, and DFMC SBAS receivers to oceanographic research vessel MIRAI.

(3) Apparatus

i. GNSS Receiver

A JAVAD DELTA receiver recorded signals from GPS, Galileo, GLONASS, BeiDou, and QZSS at the frequency of L1, L2, and L5 bands. The receiver recorded the observation message, including the pseudorange and carrier phase, with a sampling rate of 1 Hz. The navigation message, including the satellite obit information

ii. DFMC SBAS Message receivers

To obtain DFMC SBAS messages, a Furuno prototype DFMC SBAS receiver and CORE Cohac receivers were installed. The DFMC SBAS messages were generated by Electronic Navigation Research Institute (ENRI) and broadcasted from QZS02 and OZS04 satellites with a frequency of 1 Hz.

iii. Scintillation receiver

The GNSS signals are sometimes fluctuated by a combination of the ionospheric irregularity and electric field. The fluctuation is called scintillation and becomes a cause of the loss-of-lock GNSS signal. Since we need to receive the carrier phase with high and precise sampling to observe the scintillation, the Septentrio PolaRx5S, which records the GNSS signals with a sampling rate of 50

iv. GNSS Antenna

The GNSS Antenna used was a Trimble GA830 capable of receiving L1, L2, and L5 bands. The antenna was designed for maritime and cold weather specification.

(4) Results

The GNSS signals successfully received by JAVAD DELTA and Septentrio PolaRx5S. The DFMC

SBAS message was also recorded by the Furuno prototype receiver and CORE Cohac, but the messages were not sometime recorded. This was likely to be caused by the ionospheric scintillation or visibility of the satellite.

References
Kitamura, M., Aso, T., & Sakai, T. (2018) Wide Area Augmentation Performance of DFMC SBAS Using Global Monitoring Stations, The 16th IAIN World Congress 2018.
Reid, T., Walter, T., Blanch, J., & Enge, P. (2016) GNSS Integrity in The Arctic. NAVIGATION, 63: 469– 492. doi: 10.1002/navi.169.

4. Hydrographic Measurements

4.1 CTDO$_2$
December 8, 2023

(1) Personnel
Hiroshi UCHIDA (JAMSTEC RIGC) (Principal investigator)
Shinya KOUKETSU (JAMSTEC RIGC)
Ryohei YAMAGUCHI (JAMSTEC RIGC)
Rei ITO (MWJ) (Operation leader)
Nobuhiro FUJII (MWJ)
Tun Htet Aung (MWJ)
Riho FUJIOKA (MWJ)
Shinsuke TOYODA (MWJ)
Hiroyuki NAKAJIMA (MWJ) (not onboard)

(2) Objective
The CTDO$_2$/water sampling measurements were conducted to obtain vertical profiles of seawater properties by sensors and water sampling.

(3) Instruments and method
Instruments used in this cruise are as follows:
Winch and cable
Traction winch system (3.0 ton) (Dynacon, Inc., Bryan, Texas, USA) (Fukasawa et al. 2004)
Armored cable (φ = 9.53 mm) (Rochester Wire & Cable, LLC, Culpeper, Virginia, USA)
Compact underwater slip ring swivel (Hanayuu Co., Ltd., Shizuoka, Japan) (Uchida et al. 2018)
Frame
592 kg stainless steel frame for 36-position 12-L water sample bottles
Aluminum rectangular fin (54 × 90 cm) to resist frame's rotation
Water sampler and sampling bottle
36-position carousel water sampler, SBE 32 (Sea-Bird Scientific, Washington, USA)
        Serial no. 3221746-0278
12-L sample bottle, model OTE 110 (OceanTest Equipment, Inc., Fort Lauderdale, Florida, USA)
        (No TEFLON coating, with Viton O-rings)
Deck unit
SBE11plus (Sea-Bird Scientific, Washington, USA)
        Serial no. 11P54451-0872
Underwater unit
Pressure sensor, SBE 9plus (Sea-Bird Scientific, Washington, USA)
        Serial no. 09P54451-1027 (117457) (calibration date: June 9, 2022)
Deep ocean standard thermometer, SBE 35 (Sea-Bird Scientific, Washington, USA)
        Serial no. 22 (calibration date: July 14, 2022)
Temperature sensor, SBE 3Plus (Sea-Bird Scientific, Washington, USA)
        Primary, Serial no. 03P2730 (calibration date: April 11, 2023)
        Secondary, Serial no. 035737 (calibration date: November 05, 2022)
Conductivity sensor, SBE 4C (Sea-Bird Scientific, Washington, USA)
        Primary, Serial no. 042435 (calibration date: September 2, 2022)
        Secondary, Serial no. 043036 (calibration date: March 24, 2023)
Dissolved oxygen sensor, Primary, RINKO III (JFE Advantech Co., Ltd., Hyogo, Japan)
        Serial no. 0287, Sensing foil no. 163011(in situ calibrated on MR23-05 cruise)
Dissolved oxygen sensor, Secondary, SBE 43 (Sea-Bird Scientific, Washington, USA)
        Serial no. 432211 (calibration date: December 20, 2022)
Transmissometer, C-Star, (WET Labs, Inc., Philomath, Oregon, USA)
        Serial no. 1363DR (in situ calibrated on MR23-06C cruise)
Deep ocean turbidity meter, ATUD-CAV-S50 (JFE Advantech Co., Ltd., Hyogo, Japan)

Serial no. 0002 (calibration date: June 14, 2023)
Chlorophyll fluorometer (Seapoint Sensors Inc., New Hampshire, USA)
      Serial no. 3618, Gain: 10X (0-15 ug/L) for stations 1-67
      Serial no. 3700, Gain: 10X (0-15 ug/L) for stations 68-70
Ultraviolet fluorometer (Seapoint Sensors Inc., New Hampshire, USA)
      Serial no. 6246, Gain setting: 30X (0-50 QSU) (calibration date: June 15, 2023)
PAR sensor, PAR-Log ICSW (Sea-Bird Scientific, Washington, USA)
      Serial no. 2201 (calibration date: December 16, 2021)
Altimeter, PSA-916T (Teledyne Benthos, Inc.)
      Serial no. 1100
Pump, SBE 5T (Sea-Bird Scientific, Washington, USA)
      Primary, Serial no. 055816
      Secondary, Serial no. 054598
Bottom contact switch (Sea-Bird Scientific, Washington, USA)

Other additional sensors
Upward and downward looking lowered acoustic Doppler current profilers
AFP07 (micro temperature and conductivity sensors or two micro temperature sensors)
Refractive Index Sensor (Uchida et al. 2019)

Software
Data acquisition software, SEASAVE-Win32, version 7.26.7.121
Data processing software, SBEDataProcessing-Win32, version 7.26.7.129 and some original modules

(4) Pre-cruise calibration

(4.1) Pressure

Pre-cruise sensor calibration for linearization was performed at Sea-Bird Scientific. The time drift of the pressure sensor was adjusted by periodic recertification corrections by using electric dead-weight testers (model E-DWT-H A70M and A200M, Fluke Co., Phoenix, Arizona, USA) and a barometer (model RPM4 BA100Ks, Fluke Co.):

      Serial no. 181 (A70M) (for 10-70 MPa) (calibration date: December 7, 2020)
      Serial no. 1305 (A200M) (for 90 to 100 MPa) (calibration date: December 7, 2020)
      Serial no. 1453 (BA100Ks) (for 0 MPa) (calibration date: November 26, 2020)

These reference pressure sensors were calibrated by Ohte Giken, Inc. (Ibaraki, Japan) traceable to National Institute of Standards and Technology (NIST) pressure standards. The pre-cruise correction was performed at JAMSTEC (Kanagawa, Japan) by Marine Works Japan Ltd. (MWJ) (Kanagawa, Japan).
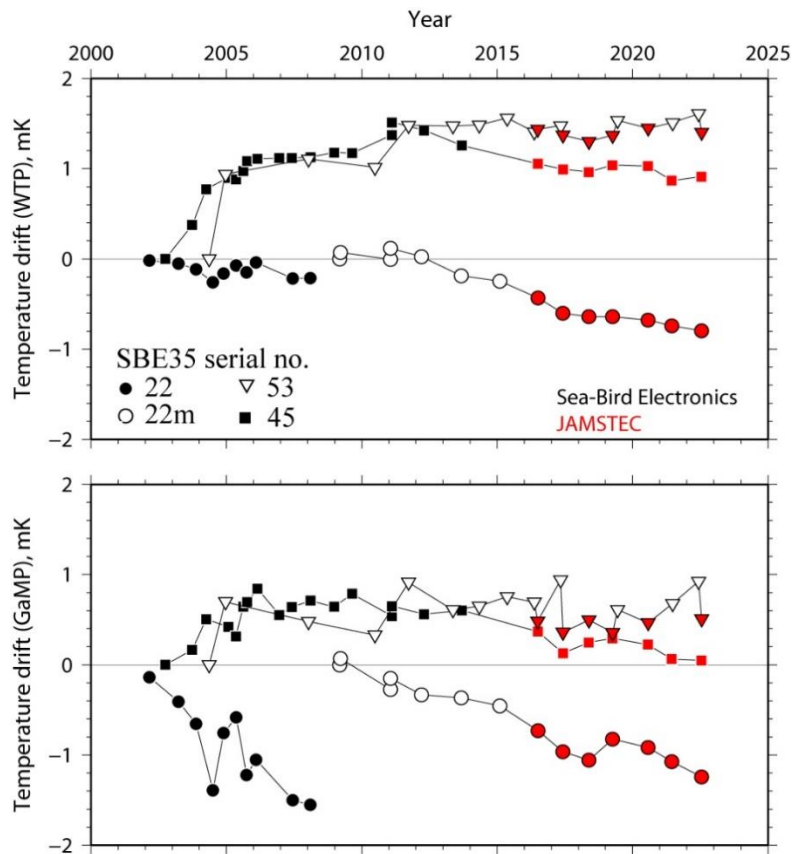
Fig. 4.1-1. Time drifts (temperature offsets relative to the first calibration) of four SBE 35s based on laboratory calibrations in fixed-point cells (water triple point: WTP, gallium melt point: GaMP).

(4.2) Temperature sensors

Pre-cruise sensor calibrations of the SBE 3s were performed at Sea-Bird Scientific. Pre-cruise sensor calibration of the SBE 35s for linearization were also performed at Sea-Bird Scientific. The slow time drift of the SBE 35 was adjusted by periodic recertification corrections by measurements in thermodynamic fixed-point cells (water triple point [0.01 °C] and gallium melt point [29.7646b °C]) (Uchida et al., 2015). Since 2016, pre-cruise calibration was performed at JAMSTEC by using fixed-point cells traceable to National Metrology Institute of Japan (NMIJ) temperature standards (Fig. 4.1-1).

Temperature dependency of the SBE 3 was corrected as follows.

$$Tcor = T + c0 \, P$$

where T is raw data, Tcor is corrected temperature, P is pressure in dbar, and c0 is the correction coefficient.

$$c0 = 2.11007877e\text{-}08 \text{ (for primary temperature sensor)}$$

The correction coefficient for the secondary temperature sensor was not determined yet since the secondary sensor was new.

(4.3) Conductivity sensors

Pre-cruise sensor calibrations were performed at Sea-Bird Scientific.

(4.4) Dissolved oxygen sensors

Pre-cruise sensor in-situ calibration of RINKO sensor was performed on the R/V Mirai MR23-05 cruise. Pre-cruise sensor calibration of SBE 43 was performed at Sea-Bird Scientific.

(4.5) Transmissometer

Light transmission (T_r in %) is calibrated as

$$T_r = (V-V_d) / (V_r-V_d) \times 100$$

wehre V is the measured signal (voltage), V_d is the dark offset for the instrument, and V_r is the signal for

clear water. V_d can be obtained by blocking the light path. The calibration coefficients (V_d and V_r) estimated from the R/V Mirai MR23-06C cruise were used.

(4.6) Deep ocean turbidity meter

Pre-cruise laboratory calibration of the deep ocean turbidity meter (ATUD-CAV-S50) was performed at JAMSTEC on June 14, 2023 by using Formazine standard solution (400 FTU, 500 ml, Kishida Chemical Co. Ltd., Japan) diluted with ultrapure water. However, these sensor data indicated a value of -0.01 FTU at deep ocean. The pre-cruise calibration was performed relative to ultra-pure water measurement, and the difference between the sensor output when the light-receiving face was shielded with a rubber plate and the ultra-pure water measurement was about 0.03 FTU. The sensor output measured at the deep ocean was smaller than the ultra-pure water measurement and larger than the rubber plate shielded sensor output. Therefore, we judged that our laboratory calibration system has systematic bias about 0.01 FTU probably due to slight reflection of light from wall surface of the calibration bucket, and the bias (0.01 FTU) was subtracted from the measured data for JFE turbidity sensors.

The deep ocean turbidity meter was calibrated as

$$\text{Turbidity (FTU)} = c_0 + c_1 V$$

where V is the sensor output (V), and c_0 and c_1 are the calibration coefficients. The calibration coefficients were determined as a line passing through the origin.

$$c_0 = -0.47168998$$
$$c_1 = 1.09839463$$

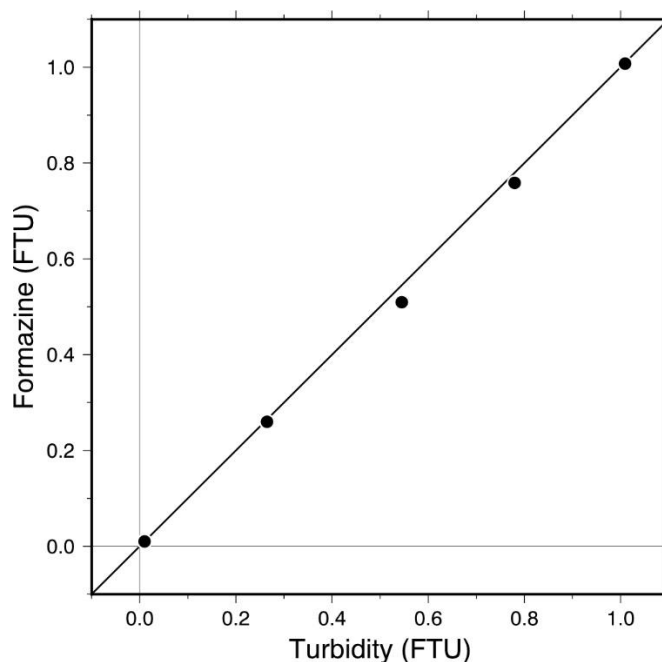Result of the pre-cruise laboratory calibration is shown in Fig. 4.1-2.

Fig. 4.1-2. Result of the pre-cruise laboratory calibration of the deep ocean turbidity meter.

(4.7) Ultraviolet fluorometer

Pre-cruise laboratory calibration of the ultraviolet fluorometer (FDOM sensor) was performed at JAMSTEC on June 15, 2023 by using deep sea water and ultrapure water.

$$\text{CTDUVFLUORcorr [in RU]} = c_0 \times \{(\text{CTDUVFLUOR} - \text{Voffset})/(1.0 + \rho \times [T - Tr])\}$$
$$\rho = -0.0053, \text{Voffset} = 0.0812, c_0 = 0.11629027$$

where CTDUVFLUOR is the raw sensor data (in volt), T is temperature (in °C) and Tr is reference temperature (20 °C). The ρ and Voffset were determined from Fig. 4.1-3. The c_0 was determined from fdom measurement for the seawater by using a benchtop FDOM meter.
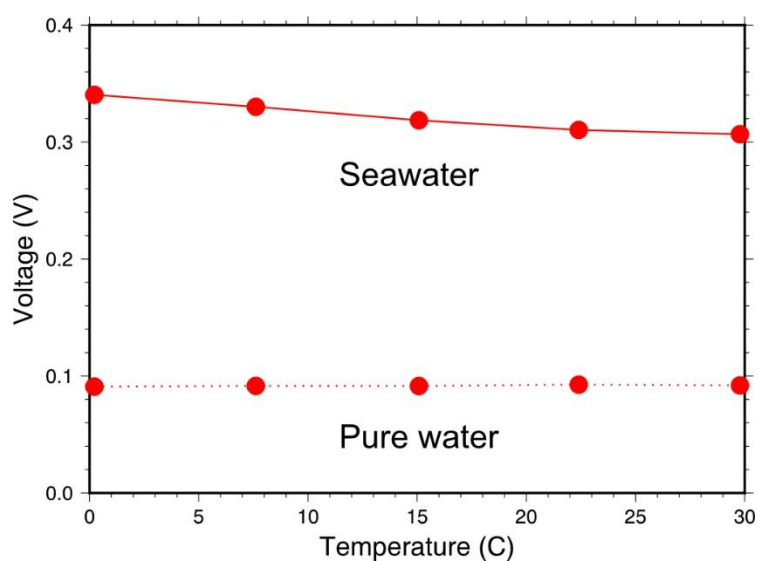
Fig. 4.1-3. Temperature dependency of the ultraviolet fluorometer for seawater and pure water.

(4.8) Chlorophyll fluorometer, PAR, altimeter
　　Periodic recertification was not performed by the manufacturer for these sensors.

(5) Data Collection and processing
(5.1) Data collection
　　The CTD system was powered on at least 15 minutes in advance of the data acquisition to stabilize the pressure sensor. The data was acquired at least two minutes before and after the CTD cast to collect atmospheric pressure data on the ship's deck.
　　The CTD package was lowered into the water from the starboard side and held 10 m beneath the surface to activate the pump. After the pump was activated, the package was lifted to the surface and lowered at a rate of 1.0 m/s to 200 m (or 300m when significant wave height was high) then the package was stopped to operate the heave compensator of the crane. The package was lowered again and at 1.0m/s and after passing the depths where vertical gradient of water properties was large, it was lowered at a rate of 1.2m/s to the bottom. For the up cast, the package was lifted at a rate of 1.2 m/s except for bottle firing stops. As a rule, the bottle was fired after waiting from the stop for more than 30 seconds and the package was stayed at least 5 seconds for measurement of the SBE 35 at each bottle firing stops. For depths where vertical gradient of water properties was expected to be large, the bottle was fired after waiting from the stop for 60 seconds to enhance changing the water between inside and outside of the bottle. At 200m (or 300m) from the surface, the package was stopped to stop the heave compensator of the crane.
　　The water sample bottles and the stainless-steel frame of the CTD package were wiped with acetone before a cast taken for CFCs.

(5.2) Data collection problems
　　At station 23 cast 3, the primary temperature and conductivity data shifted from 1243 dbar of down-cast.
　　At station 27, after the cast was done and CTD package was brought back on deck, modulo error occurred one time (Modulo Error Count, MEC=1), which meant there was a skipped scan in CTD data stream.
　　At station 28, during down cast between 1924 db and 2173 db, modulo error occurred 3 times. CTD package was stopped at 2190 db and brought back to deck. The CTD cast was cancelled to save ship's time. Slip ring swivel was changed after that.
　　At station 29, during down cast between 2365 db and 5183 db modulo error occurred again (total MEC=12). After the cast was done, seacable was re-terminated.
　　At station 34, during up cast between 2154 db and 2079 db, modulo error occurred again (total MEC=7), and CTD data acquisition was lost soon after. CTD package was brought up and seacable was re-terminated.

At station 37, during down cast at 250 dbar, CTD data acquisition was lost suddenly. The cast was aborted and CTD package was brought back to deck. About 14m length of armored cable from evergrip was cut, and seacable was re-terminated.

The fluorometer showed shift at several casts at shallow depths about 10m and above during up cast or during down cast at depths where chlorophyll *a* is high. The shift in fluorescence data appeared even after changing the sensor cable. The fluorometer was changed from serial no.3618 to 3700 after station 67. But the shift appeared again so, the auxiliary sensor ports of flurometer and altimeter were swapped after station 69. At station 70, the shift in data didn't appear again but that was the last cast so, it was difficult to make a conclusion about the reason behind those shifts in data, but it was probably due to the problem with Y-cable of auxiliary sensor port which was connected to flurometer cable.

For the transmissometer, there were shifts and noises in downcast data at stations 15, 7, 40, 55 and 70. The bad data were replaced with good up cast data of the same depth range.

For the deep sea turbidity meter, at station 51 during down cast between 3db and 33db, there was a shift in data, due to ambient light interference. The bad data were replaced with good up cast data of the same depth range.

(5.3) Data Processing

The following are the data processing software (SBEDataProcessing-Win32) and original software data processing module sequence and specifications used in reduction of CTD data in this cruise.

(The process in order)

DATCNV converted the raw data to engineering unit data. DATCNV also extracts bottle information where scans were marked with the bottle confirm bit during acquisition. The scan duration to be included in bottle file was set to 4.4 seconds, and the offset was set to 0.0 seconds. The hysteresis correction for the SBE 43 data (voltage) was applied for both profile and bottle information data.

TCORP (original module, version 1.1) corrected the pressure sensitivity of the temperature (SBE3) sensor for both profile and bottle information data.

RINKOCOR (original module, 1.0) corrected the time-dependent, pressure-induced effect (hysteresis) of the RINKOIII profile data.

RINKOCORROS (original module) corrected the time-dependent, pressure-induced effect (hysteresis) of the RINKOIII bottle information data by using the hysteresis-corrected profile data.

BOTTLESUM created a summary of the bottle data. The data were averaged over 4.4 seconds.

ALIGNCTD converted the time-sequence of sensor outputs into the pressure sequence to ensure that all calculations were made using measurements from the same parcel of water. For a SBE 9plus CTD with the ducted temperature and conductivity sensors and a 3000-rpm pump, the typical net advance of the conductivity relative to the temperature is 0.073 seconds. So, the SBE 11plus deck unit was set to advance the primary and the secondary conductivity for 1.73 scans (1.75/24 = 0.073 seconds). Oxygen data are also systematically delayed with respect to depth mainly because of the long time constant of the oxygen sensor and of an additional delay from the transit time of water in the pumped plumbing line. This delay was compensated by 6 seconds advancing the SBE 43 oxygen sensor output (voltage) relative to the temperature data. Delay of the RINKOIII data was also compensated by 1 second advancing sensor output (voltage) relative to the temperature data. Delay of the transmissometer data was also compensated by 2 seconds advancing sensor output (voltage) relative to the temperature data.

WILDEDIT marked extreme outliers in the data files. The first pass of WILDEDIT obtained the accurate estimate of the true standard deviation of the data. The data were read in blocks of 1000 scans. Data greater than 10 standard deviations were flagged. The second pass computed a standard deviation over the same 1000 scans excluding the flagged values. Values greater than 20 standard deviations were marked bad. This process was applied to pressure, depth, temperature, conductivity, and SBE 43 output.

CELLTM used a recursive filter to remove conductivity cell thermal mass effects from the measured conductivity. Typical values for SBE 9plus with TC duct and 3000 rpm pump which were 0.03 for thermal anomaly amplitude alpha and 7.0 for the time constant 1/beta were used.

FILTER performed a low-pass filter on pressure and depth with a time constant of 0.15 second. In order to produce zero phase lag (no time shift) the filter runs forward first then backward.

WFILTER performed as a median filter to remove spikes in transmissometer data, fluorometer data, turbidity meter data, deep ocean turbidity meter data, and ultraviolet fluorometer data. A median value was determined by 49 scans of the window.

SECTIONU (original module, version 1.1) selected a time span of data based on scan number in

order to reduce a file size. The minimum number was set to be the starting time when the CTD package was beneath the sea-surface after activation of the pump. The maximum number was set to be the end time when the depth of the package was 1 dbar below the surface. The minimum and maximum numbers were automatically calculated in the module.

LOOPEDIT marked scans where the CTD was moving less than the minimum velocity of 0.0 m/s (traveling backwards due to ship roll).

DESPIKE (original module, version 1.0) removed spikes of the data. A median and mean absolute deviation was calculated in 1-dbar pressure bins for both down and up cast, excluding the flagged values. Values greater than 4 mean absolute deviations from the median were marked bad for each bin. This process was performed twice for temperature, conductivity and RINKOIII output.

DERIVE was used to compute dissolved oxygen (SBE43), salinity, potential temperature, and sigma-theta.

BINAVG averaged the data into 1-decibar pressure bins and 1-sec time bins. The center value of the first bin was set equal to the bin size. The bin minimum and maximum values are the center values plus and minus half the bin size. Scans with pressures greater than the minimum and less than or equal to the maximum were averaged. Scans were interpolated so that a data recorded exist every dbar.

BOTTOMCUT (original module, version 0.1) deleted the deepest pressure bin when the averaged scan number of the deepest bin was smaller than the average scan number of the bin just above.

SPLIT was used to split data into down cast and up cast.

Remaining spikes in the CTD data were manually eliminated from the 1-dbar-averaged data. And the data gaps resulting from the elimination were linearly interpolated with a quality flag of 6. The detailed information above these irregularities is recorded in remarks sheet of data submission.

(6) Post-cruise calibration
(6.1) Pressure
The CTD pressure sensor offset in the period of the cruise was estimated from the pressure readings on the ship's deck at the pre- and post-cast by subtracting the atmospheric pressure deviation from a standard atmospheric pressure (1013.25 hPa) (Fig. 4.1-4). The post-cruise correction of the pressure data is not deemed necessary for the pressure sensor.
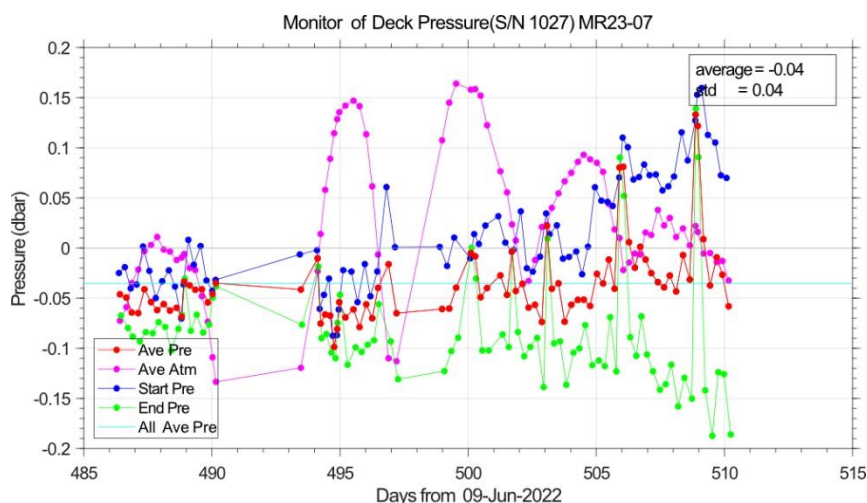

Fig. 4.1-4. Time series of the CTD deck pressure. Atmospheric pressure deviation (magenta dots) from a standard atmospheric pressure was subtracted from the CTD deck pressure. Blue and green dots indicate pre- and post-cast deck pressures, respectively. Red dots indicate averages of the pre- and the post-cast deck pressures.

(6.2) Temperature
The CTD temperature sensors (SBE 3) were calibrated with the SBE 35 under the assumption that discrepancies between SBE 3 and SBE 35 data were due to pressure sensitivity, the viscous heating effect, and time drift of the SBE 3 (Uchida et al., 2015). The CTD temperature was calibrated as

Calibrated temperature = $T - (c_0 \times P + c_1 \times t + c_2)$

where T is CTD temperature in °C, P is pressure in dbar, t is time in days from pre-cruise calibration date

54

of the CTD temperature and c_0, c_1, and c_2 are calibration coefficients. The coefficients for the primary temperature sensor were determined using the data for the depths deeper than 1100 dbar.

$c_0 = 6.42691338e-08$, $c_1 = -1.09559e-05$, $c_2 = 2.0248e-03$ (for primary sensor)

$c_0 = -5.18432632e-09$, $c_1 = 5.29267e-06$, $c_2 = -1.2949e-03$ (for secondary sensor)

The results of the post-cruise calibration for the CTD temperature are shown in Figs 4.1-5 and 4.1-6.

The secondary temperature and conductivity data were calibrated to use for station 23 cast 3.
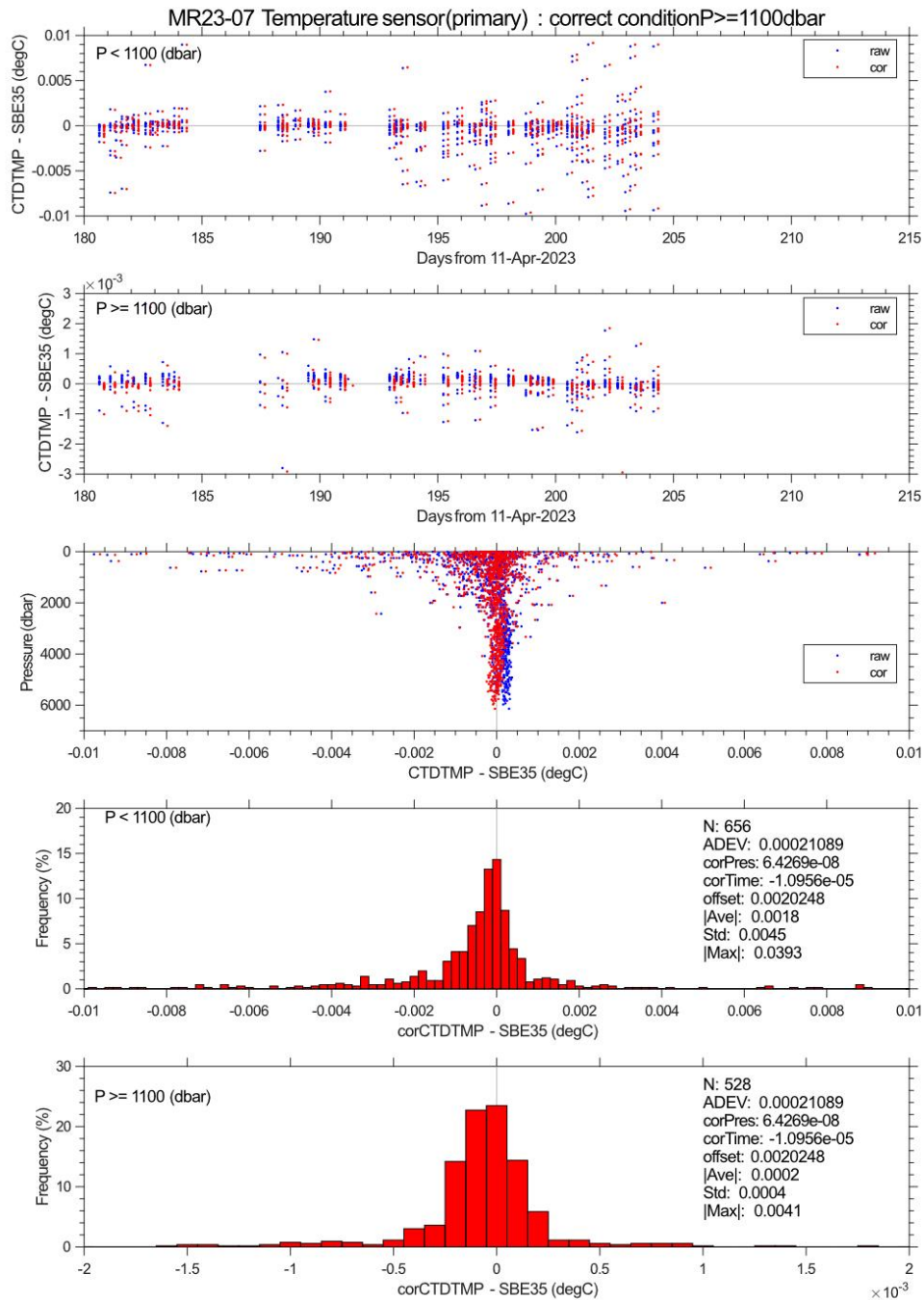

Fig. 4.1-5. Difference between the CTD temperature (primary) and the SBE 35. Blue and red dots indicate before and after the post-cruise calibration using the SBE 35 data, respectively.
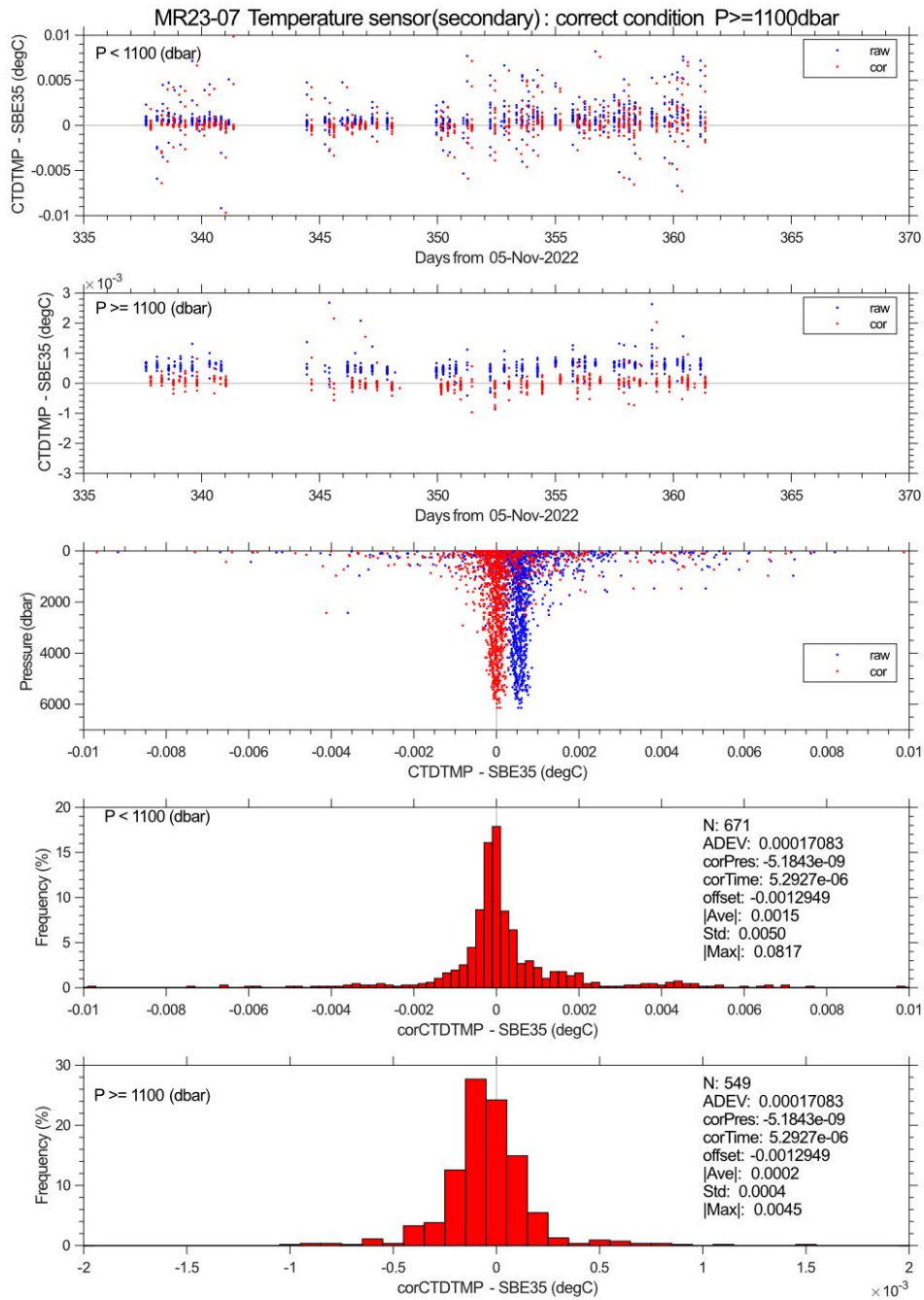
Fig. 4.1-6. Same as Fig. 4.1-5, but for secondary temperature sensor.

(6.3) Conductivity

The discrepancy between the CTD conductivity and the conductivity calculated from the bottle sampled salinity data with the CTD temperature and pressure data is considered to be a function of conductivity, pressure and time. The CTD conductivity was calibrated as

Calibrated conductivity $= C - (c_0 \times C + c_1 \times P + c_2 \times t + c_3)$

where C is CTD conductivity in S/m, P is pressure in dbar, t is time in days and $c_0 - c_3$ are calibration coefficients. The coefficients for the primary conductivity sensor were determined.

$c_0 = 1.6956918331e\text{-}04$, $c_1 = 2.3419645689e\text{-}08$, $c_2 = 7.9176951720e\text{-}06$,

$c_3 = -3.2787907013e\text{-}04$ (for primary conductivity sensor)

56

c0 = 1.5652171794e-04, c1 = 1.9207298465e-08, c2 = 1.0536765377e-05,
c3 = -2.1962084768e-04 (for secondary conductivity sensor)
The results of the post-cruise calibration for the CTD salinity are shown in Figs. 4.1-7 and 4.1-8.
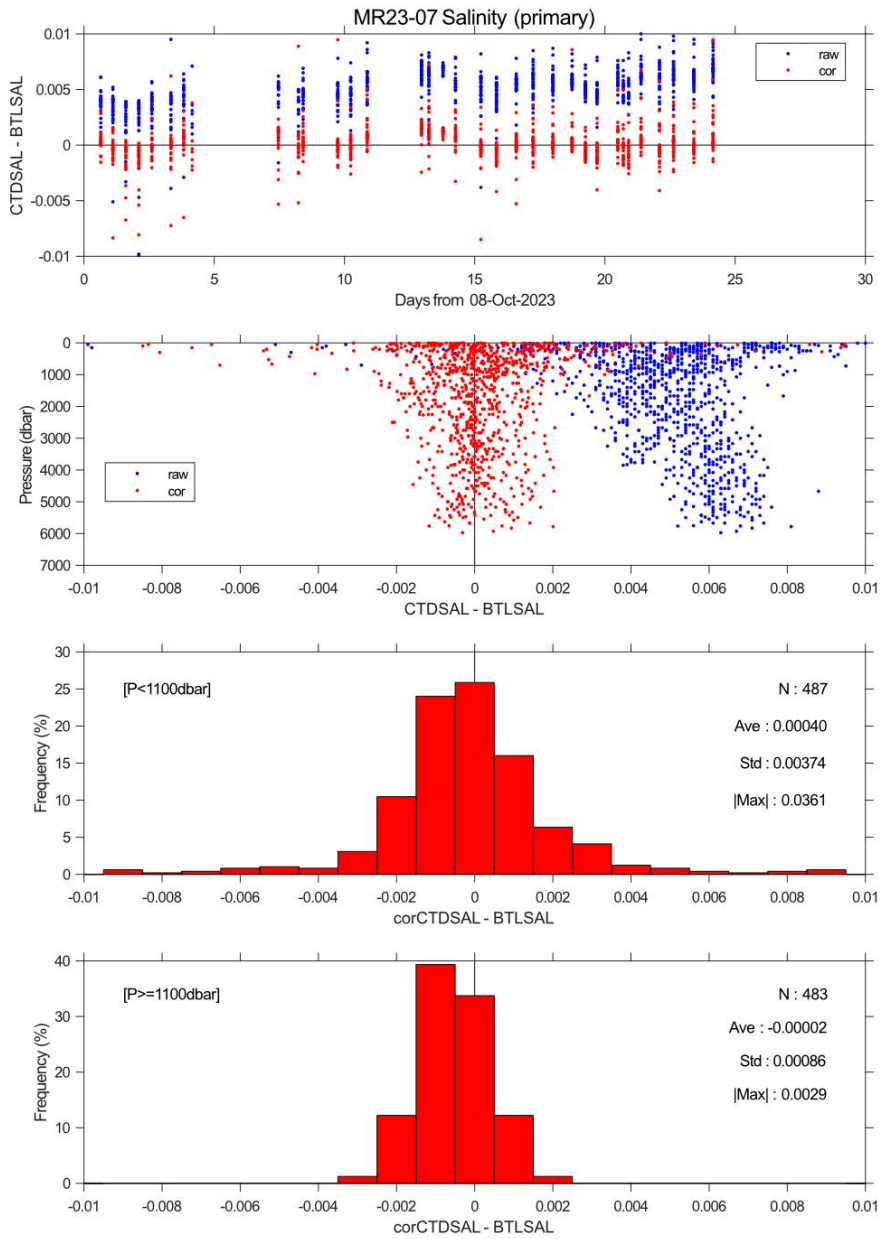

Fig. 4.1-7. Difference between the CTD salinity (primary) and the bottle salinity. Blue and red dots indicate before and after the post-cruise calibration, respectively.
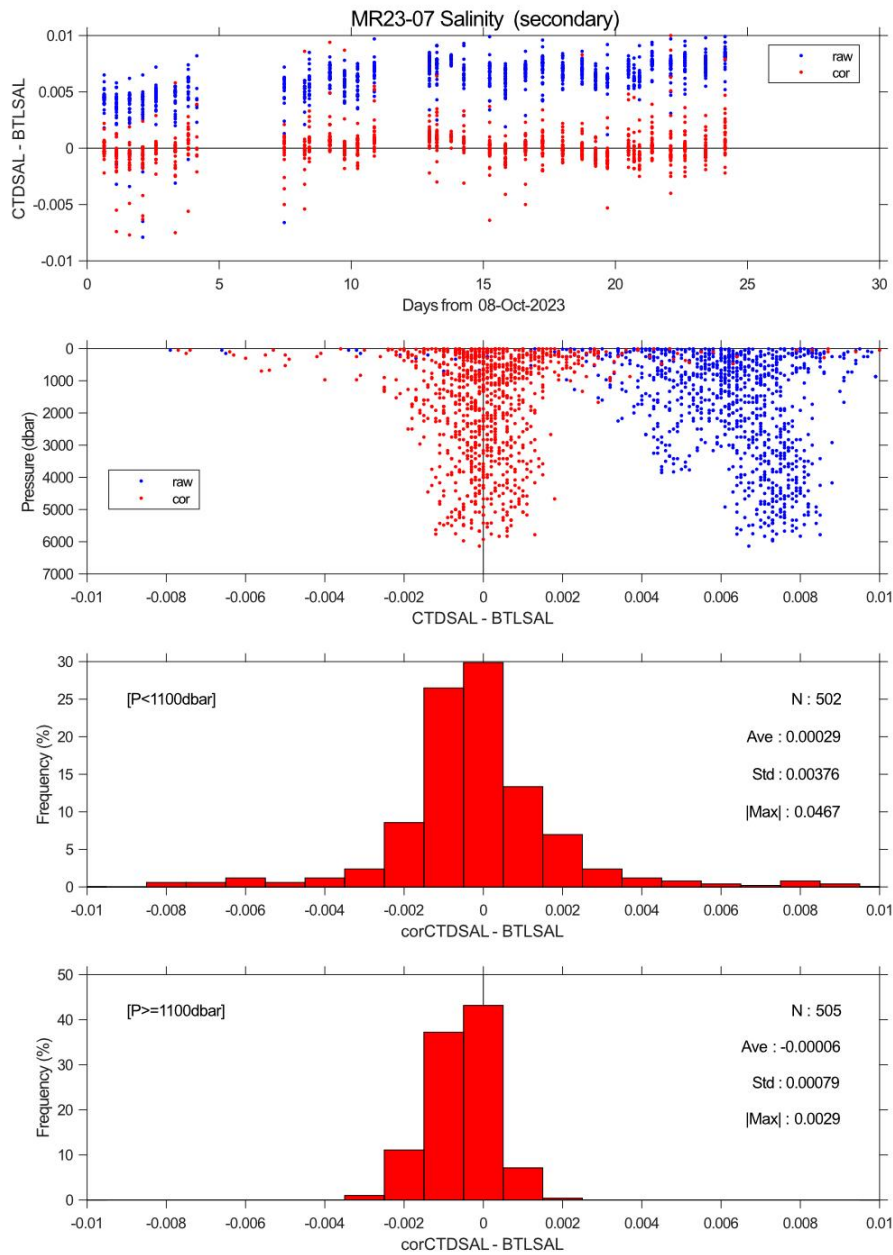
Fig. 4.1-8. Same as Fig. 4.1-7, but for the CTD salinity (secondary).

(6.4) Dissolved oxygen

Data from the RINKO can be corrected for the time-dependent, pressure-induced effect by means of the same method as that developed for the SBE 43 (Edwards et al., 2010). The calibration coefficients, H1 (amplitude of hysteresis correction), H2 (curvature function for hysteresis), and H3 (time constant for hysteresis) were determined to minimize the down-cast and up-cast data.

H1 = 0.005, H2 = 5000.0, H3 = 2000.0

Outputs from RINKO are the raw phase shift data. The RINKO can be calibrated by the modified Stern-Volmer equation slightly modified from a method by Uchida et al. (2010):

$$O_2 \ (\mu mol/l) = [(V0 \ / \ V)^E - 1] \ / \ Ksv$$

where V is voltage, V0 is voltage in the absence of oxygen, Ksv is Stern-Volmer constant. The coefficient E corrects nonlinearity of the Stern-Volmer equation. The V0 and the Ksv are assumed to be functions of temperature as follows.

$$Ksv = c0 + c1 \times T + c2 \times T^2$$
$$V0 = 1 + d0 \times T$$
$$V = d1 + d2 \times Vb + d3 \times t + d4 \times t \times Vb + d5 \times t2 \times Vb$$

where T is CTD temperature (°C) and Vb is raw output (volts). V0 and V are normalized by the output in the absence of oxygen at 0°C, and t is working time (days) integrated from the fist CTD cast. The oxygen concentration is calculated using accurate temperature data from the CTD temperature sensor instead of temperature data from the RINKO. The pressure-compensated oxygen concentration O2c can be calculated as follows.

$$O2c = O2 \ (1 + cp \times P \ / \ 1000)$$

where P is CTD pressure (dbar) and cp is the compensation coefficient. Since the sensing foil of the optode is permeable only to gas and not to water, the optode oxygen must be corrected for salinity. The salinity-compensated oxygen can be calculated by multiplying the factor of the effect of salt on the oxygen solubility (Garcia and Gordon, 1992).

c0 = 4.264864612555792e-03, c1 = 1.781165985250666e-04, c2 = 3.001238109771612e-06,
d0 = -8.906537811077197e-04, d1 = -9.283118618201369e-02, d2 = 3.205690226762825e-01,
d3 = 9.201477981421092e-04, d4 = -1.686076053441669e-04,
E = 1.2, cp = 0.025

The results of the post-cruise calibration for the RINKO oxygen are shown in Figs. 4.1-9.
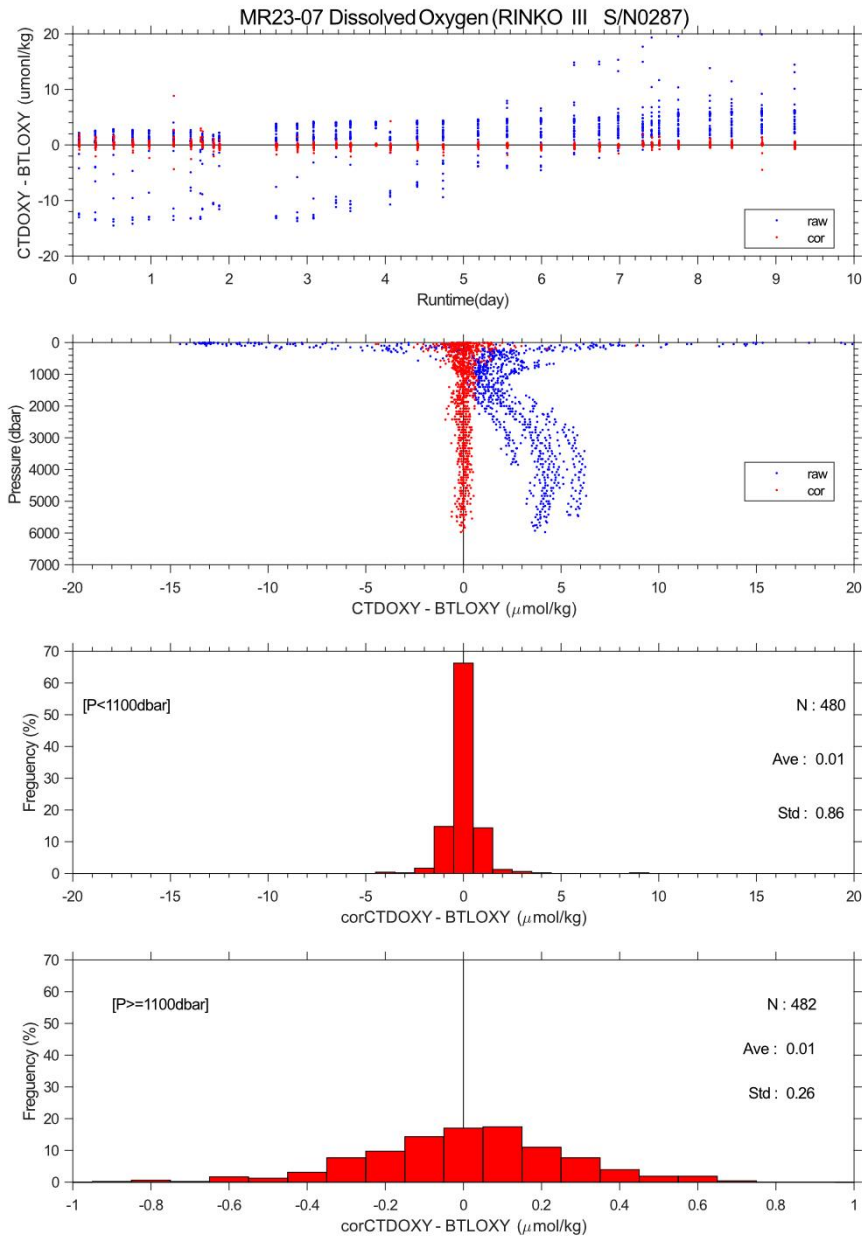
Fig. 4.1-9. Difference between the CTD oxygen and the bottle oxygen. Blue and red dots indicate before and after the post-cruise calibration, respectively.

**(6.5) Transmissometer**

Light transmission Tr (in %) and beam attenuation coefficient cp are calculated from the sensor output V (in volt) as follows:

$$Tr = (V–Vd) / (Vr–Vd) \times 100$$
$$cp = – (1 / 0.25) \ln(Tr / 100)$$

wehre Vd is the dark offset for the instrument, and Vr is the signal for clear water. Vd can be obtained by blocking the light path. Vd was measured on deck before each cast. Vr is estimated from the measured maximum signal in the deep ocean at each cast. The sensor output in the air (Vair) was also measured on deck before each cast to monitor the sensor drift. Since the transmissometer drifted in time (Fig. 3.1.11), Vr is expressed as

$$Vr = c0 + c1 \times t$$

where t is working time (in days) of the transmissometer integrated from the first CTD cast, and c0 and c1 are calibration coefficients. Maximum signal was extracted for each cast and appropriate data detected deep ocean maximum were selected to estimate Vr.

Vd = 0.0028, c0 = 4.269044780489677, c1 = -0.001525088664515
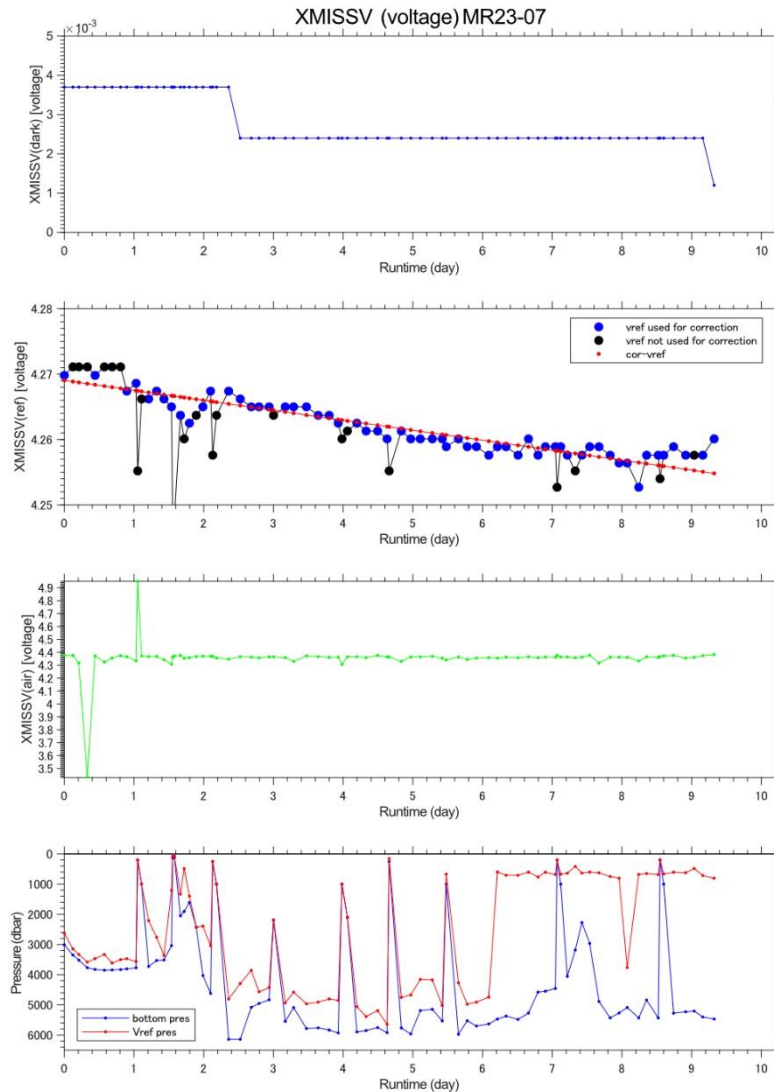
Fig. 4.1-10. Time series of V_d, the maximum value of the transmissometer output, V_{air}, and maximum pressure and pressure measured at the maximum value at each cast. Red dots in the second panel show the estimated V_r.

(6.6) Ultraviolet fluorometer

First of all, the ultraviolet fluorometer data for station 70 showed large shift and large difference between down and up cast. Therefore, the down cast data (CTDUVFLUOR70) was corrected as follows.

CTDUVFLUOR70corr = (CTDUVFLUOR70 + c0) × c1

c0 = 0.0004, c1 = 1.01

The ultraviolet fluorometer data at the bottle firing stops of the up-cast were replaced with the corrected down-cast data.

The ultraviolet fluorometer data was calibrated in situ to match with the bottle sampled FDOM data at wavelength of 370 nm taking time drift into account as follows.

CTDUVFLUORcorr = (c0 + c1 × CTDUVFLUOR) × (1 + c2 × t)

c0 = 7.357443161523909e-04, c1 = 0.8233468576921239, c2 = 1.330006933272535e-02

61

where t is working time (in days) integrated from the first CTD cast, and c0-c2 are calibration coefficients. The results of the post-cruise calibration for the CTD ultraviolet fluorometer are shown in Fig. 4.1-11.
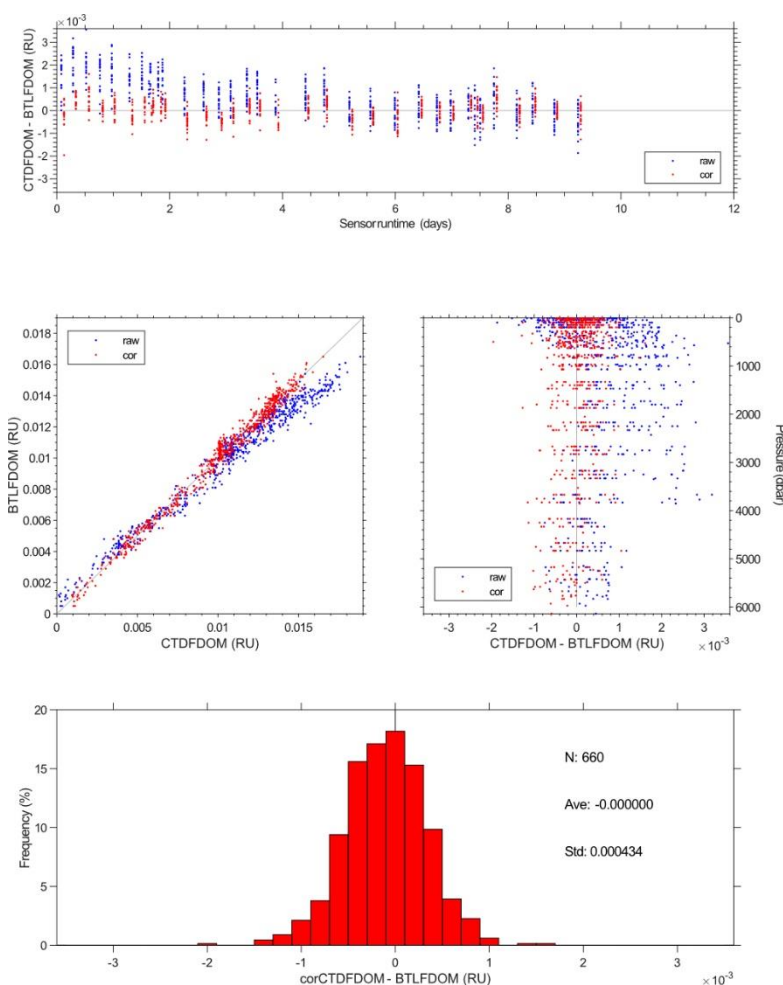
Fig. 4.1-11. Difference between the CTD ultraviolet fluorometer and the bottle sampled FDOM data at wavelength of 370 nm. Blue and red dots indicate before and after the post-cruise calibration, respectively.

(6.7) Chlorophyll fluorometer

The chlorophyll fluorometer showed erroneous shift at many casts after station 19. Therefore, the down-cast profile data were corrected based on visual inspection as follows.

Data replaced with the up-cast data

Station 22 cast 1 90–170 dbar, Station 33 cast 1 112–158 dbar,
Station 34 cast 2 92–136 dbar, Station 34 cast 3, 88–147 dbar,
Station 35 cast 1 74–140 dbar, Station 36 cast 1 75–130 dbar,
Station 37 cast 1 40–142 dbar, Station 38 cast 1 40–130 dbar,
Station 39 cast 1 23–129 dbar, Station 39 cast 2 3–129 dbar,
Station 40 cast 1 84–123 dbar, Station 41 cast 1 4–141 dbar,
Station 42 cast 1 5–145 dbar, Station 50 cast 1 66–82 dbar,
Station 65 cast 1 93–141 dbar, Station 66 cast 1 94–143 dbar,
Station 67 cast 1 93–110 dbar

Data removed and linearly interpolated

Station 20 92–95 dbar, Station 21 cast 1 90–101 dbar,
Station 32 cast 1 140–144 dbar, Station 34 cast 1 88–128 dbar,
Station 39 cast 1 19–22 dbar, Station 40 cast 1 83 dbar,
Station 41 cast 1 10–15 dbar, Station 43 cast 1 97–101 dbar,
Station 59 cast 1 92–96 dbar, Station 61 cast 1 92–110 dbar,

Station 62 cast 1 85–120 dbar, Station 69 cast 1 98–104 dbar and 111–122 dbar

The chlorophyll fluorometer data show positive biases in the deep ocean because of the interference by FDOM (Xing et al., 2017). Therefore, the effect of the interference by FDOM was corrected by using the ultraviolet fluorometer data.

$$CTDFLUORfdom\_corr = CTDFLUOR - (c_0 + c_1 \times CTDUVFLUORcorr)$$

$c_0 = 1.47967472e\text{-}03, c_1 = 2.59733835e\text{+}00$ (for stations $1 - 67$)

$c_0 = 0.014, c_1 = 0.0$ (for CTDUVFLUORcorr > 0.014 of stations $1 - 17$)

$c_0 = 8.13494913e\text{-}03, c_1 = 4.38496972e\text{+}00$ (for stations 68 and 69)

$c_0 = 3.32501056e\text{-}02, c_1 = 3.82230586e\text{+}00$ (for station 70)

where CTDUVFLUORcorr is the in situ calibrated ultraviolet fluorometer data (in RU), and c_0 and c_1 are the correction coefficients. The calibration coefficients were determined by using the data for pressure large than 400 dbar (Fig. 4.1-12).
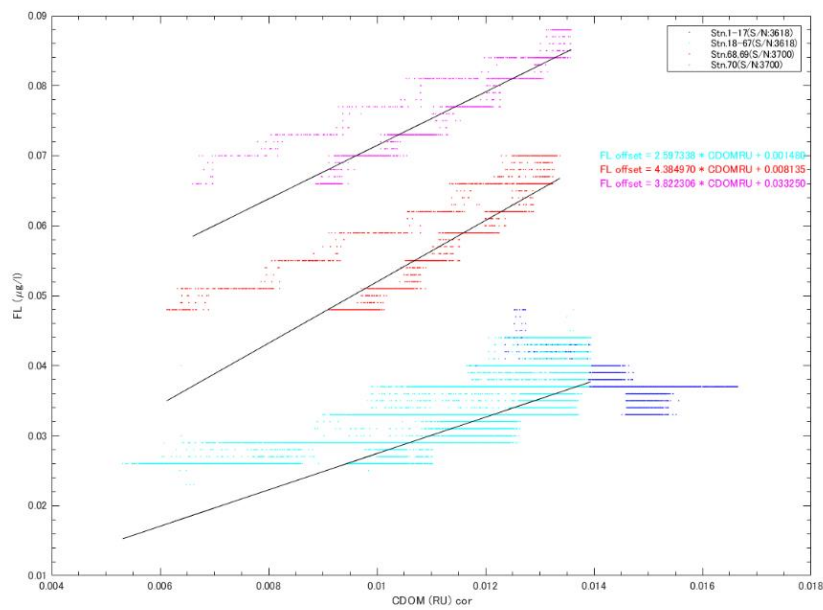
Fig. 4.1-12. Comparisons of chlorophyll fluorometer and ultraviolet fluorometer data for depths deeper than 400 dbar.

The chlorophyll fluorometer data thus corrected was calibrated in situ by using the bottle sampled chlorophyll-a data. The calibration equation is as follows:

$$CTDFLUORcorr = c_0 \times CTDFLUORfdom\_corr + c_1 \times CTDFLUORfdom\_corr^{0.5}$$

$c_0 = 0.8825526137128532, c_1 = 0.0$ (for T $< 8°C$ [stations $16 - 21$])

$c_0 = 0.6870636550281233, c_1 = 0.0$ (for $8°C <=$ T $< 8.5°C$ [stations $1 - 5, 15$])

$c_0 = 0.3648486654523743, c_1 = 0.1299358531494460$
    (for T $>= 8.5°C$ of the Bering Sea [stations $6 - 14$])

$c_0 = 0.2856530337411427, c_1 = 0.1310144567881625$
    (for T $< 21°C$ of the subarctic [stations $22 - 48$])

$c_0 = 0.6798905608802999, c_1 = 0.0$ (for T $>= 21°C$ of the subtropical [stations $49 - 70$])

where c_0 and c_1 are the calibration coefficients (Fig. 4.1-13). The results of the post-cruise calibration for the CTD fluorometer are shown in Fig. 4.1-14.
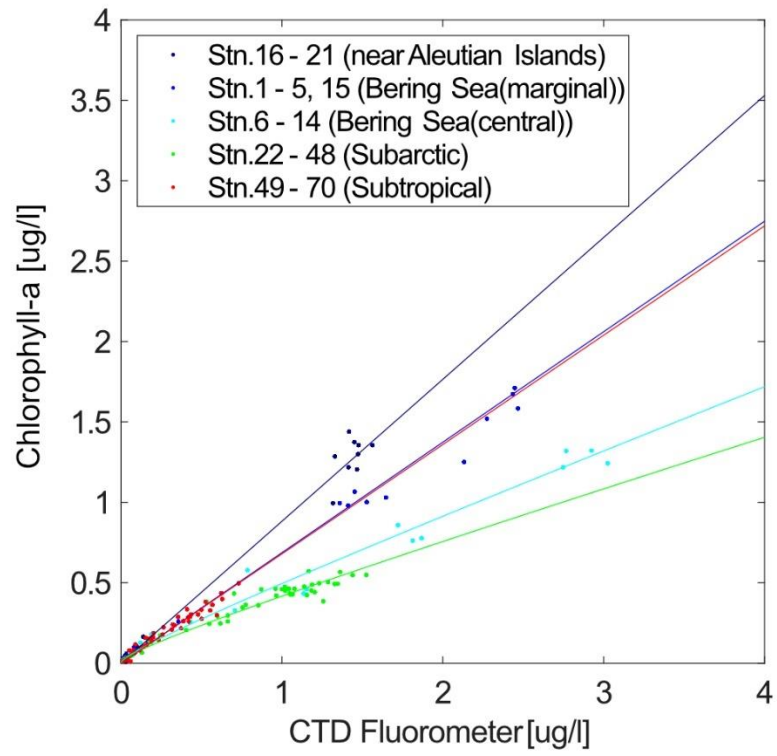
Fig. 4.1-13. Comparisons of CTD chlorophyll fluorometer data and bottle sampled chlorophyll-a data. Lines indicate the calibration equations.
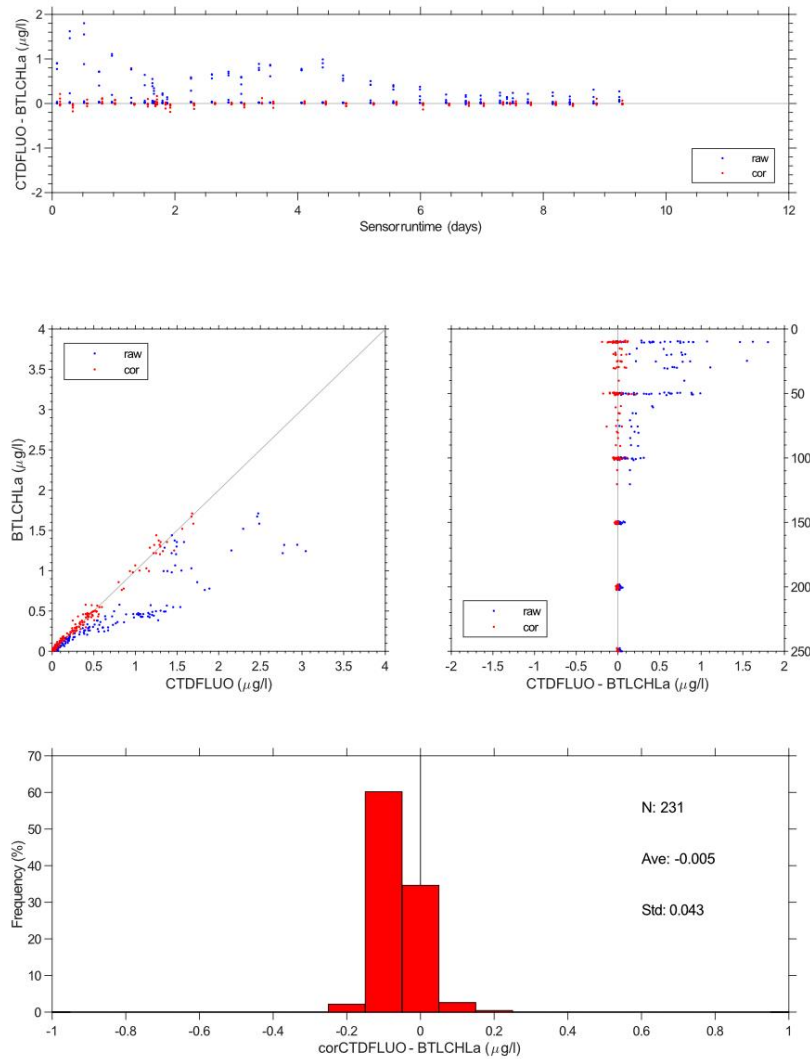
Fig. 4.1-14. Difference between the CTD chlorophyll-a and the bottle sampled chlorophyll-a. Blue and red dots indicate before and after the post-cruise calibration, respectively.

(6.8) PAR

PAR is expected to be zero in the deep ocean. Therefore, the offset measured in the deep ocean was corrected. The corrected data (PARc) is calculated from the raw data (PAR) as follows:

$$PARc \ [\mu E \ m^{-2} \ s^{-1}] = PAR - 0.091.$$

(7) References

Edwards, B., D. Murphy, C. Janzen and N. Larson (2010): Calibration, response, and hysteresis in deep-sea dissolved oxygen measurements, *J. Atmos. Oceanic Technol.*, 27, 920–931.

Fukasawa, M., T. Kawano and H. Uchida (2004): Blue Earth Global Expedition collects CTD data aboard Mirai, BEAGLE 2003 conducted using a Dynacon CTD traction winch and motion-compensated crane, *Sea Technology*, 45, 14–18.

García, H. E. and L. I. Gordon (1992): Oxygen solubility in seawater: Better fitting equations. *Limnol. Oceanogr.*, 37 (6), 1307–1312.

Uchida, H., G. C. Johnson, and K. E. McTaggart (2010): CTD oxygen sensor calibration procedures, The

GO-SHIP Repeat Hydrography Manual: A collection of expert reports and guidelines, IOCCP Rep., No. 14, ICPO Pub. Ser. No. 134.

Uchida, H., Y. Kayukawa, and Y. Maeda (2019): Ultra high-resolution seawater density sensor based on a refractive index measurement using the spectroscopic interference method. Sci. Rep., 9:15482, doi:10.1038/s41598-019-52020-z.

Uchida, H., Y. Maeda and S. Kawamata (2018): Compact underwater slip ring swivel: Minimizing effect of CTD package rotation on data quality, Sea Technology, 11, 30–32.

Uchida, H., T. Nakano, J. Tamba, J. V. Widiatmo, K. Yamazawa, S. Ozawa and T. Kawano (2015): Deep ocean temperature measurement with an uncertainty of 0.7 mK, J. Atmos. Oceanic Technol., 32, 2199–2210.

Xing, X., H. Claustre, E. Boss, C. Roesler, E. Organelli, A. Poteau, M. Barbieux and F. D'Ortenzio (2017): Correction of profiles of in-situ chlorophyll fluoremetry for the contribution of fluorescence originating from non-algal matter, Limnol. Oceanogr.: Methods, 15, 80–93.

(8) Data archive

These data obtained in this cruise will be submitted to the Data Management Group of JAMSTEC, and will be opened to the public via "Data Research System for Whole Cruise Information in JAMSTEC (DARWIN)" in JAMSTEC web site.

4.2 Salinity
November 6, 2023

(1) Personnel
Hiroshi UCHIDA (JAMSTEC RIGC)

(2) Objective
The objective of this study is to collect bottle sampled salinity data to calibrate the CTD and thermo-salinograph salinity data. Seawater samples collected on the R/V Mirai MR23-06C cruise were also measured.

(3) Instruments and method
Salinity measurement was conducted basically based on the method by Kawano (2010) with modification of the time drift correction method (Uchida et al., 2020). Materials used in this cruise are as follows:

Standard Seawater: IAPSO Standard Seawater, Ocean Scientific International Ltd., Hampshire, UK
    Batch P166
Salinometer: Autosal model 8400B; Guildline Instruments, Ltd., Ontario, Canada
    Serial no. 62556
A peristaltic-type sample intake pump: Ocean Scientific International Ltd.
Thermometers: PRT model 1502A, Fluke Co., Everett, Washington, USA
    Serial no. B81549 (for monitoring the bath temperature)
    Serial no. B78466 (for monitoring the room temperature)
Stabilized power supply: model PCR1000LE, Kikusui Electronics Co., Japan
    Serial no. XH004198
Data acquisition software: Vs8400B, Virtual Systems Co., Japan
    Version 1.05T, Rev.02
Sample bottles: 250 mL brown borosilicate glass bottles with translucent screw caps (PTFE packing)
Secondary Standard Seawater: Multiparametric Standard Seawater, KANSO TECHNOS Co., Ltd.
    Lot PRE20
Ultra-pure water: Milli-Q water, Millipore, Billerica, Masachusetts, USA
Sub-standard seawater: Surface seawater collected in the cruise MR19-04 by filtering with a 0.20 μm
    pore capsule cartridge filter, ADVANTEC, Toyo Roshi Kaisha Ltd., Japan
Detergent: 2% neutral detergent, SCAT 20X-N, Dai-ichi Kogyo Seiyaku Co., Ltd., Japan

The bath temperature of the salinometer was set to 24 °C. The salinometer was standardized only at the previous cruise (MR23-05 Leg 1) by using the IAPSO Standard Seawater (SSW). The standardization dial was set to 600 for serial no. 62556 and never changed during the cruise. The mean ± SD of the STANDBY and ZERO was 5126.5 ± 0.7 and 0.00000 ± 0.00000, respectively. The mean ± SD of the ambient room temperature was 23.4±0.5 °C, while that of the bath temperature was 23.9994±0.0007 °C.

The double conductivity ratios measured by the salinometer were used to calculate Practical Salinity using the algorithm for Practical Salinity Scale 1978 (IOC et al., 2010). A constant temperature of 24 °C was used in the calculation instead of using the measured bath temperature.

The measurement cell of the salinometer was rinsed with ultra-pure water and 2% neutral detergent after each day of measurement, and the electrode in the cell was soaked in the neutral detergent until next day of measurement.

Ultra-pure water and the IAPSO SSW were measured at the beginning and the end of each day of measurement (for samples of 1 to 3 stations). Sub-standard seawater was measured every about 10 samples to monitor stability of the salinometer during each day of measurement.

The results of the ultra-pure water and the IAPSO SSW measurement (Fig 4.2-1) suggest that the salinometer drifted in time by changing the span of the slope. Therefore, correction factors of the salinometer were estimated from the mean Practical Salinity value of the SSW measurements and the certified Practical Salinity value for each day (Uchida et al., 2020). The measured Practical Salinities for the water samples were corrected by using the correction factors. For serial no. of day of 27 (November 2, 2023), the IAPSO SSW was also measured at middle of the day of measurement, and slight linear time

drift of the salinometer was estimated from the IAPSO SSW measurements and corrected for the samples of the day. The standard deviation of the IAPSO SSW measurements was 0.0002 in Practical Salinity after the time drift correction. The mean ± SD of the ultra-pure water measurements was – 0.00006±0.00012.

(4) Results

A total of 54 pairs of replicate samples was collected and the SD of the replicate samples was 0.00022 in Practical Salinity.

A total of 3 bottles of MSSW PRE20 was measured and the mean ± SD was 34.2771 ± 0.0000 in Practical Salinity.

(5) References

IOC, SCOR and IAPSO (2010): The international thermodynamic equation of seawater – 2010: Calculation and use of thermodynamic properties. Intergovernmental Oceanographic Commission, Manuals and Guides No. 56, UNESCO (English), 196 pp.

Kawano, T. (2010): Salinity. The GO-SHIP Repeat Hydrography Manual: A collection of Expert Reports and Guidelines, IOCCP Report No. 14, ICPO Publication Series No. 134, Version 1.

Uchida, H., T. Kawano, T. Nakano, M. Wakita, T. Tanaka and S. Tanihara (2020): An updated batch-to-batch correction for IAPSO standard seawater. J. Atmos. Oceanic Technol., 37, 1507-1520, doi:10.1175/JTECH-D-19-0184.1.

(6) Data archive

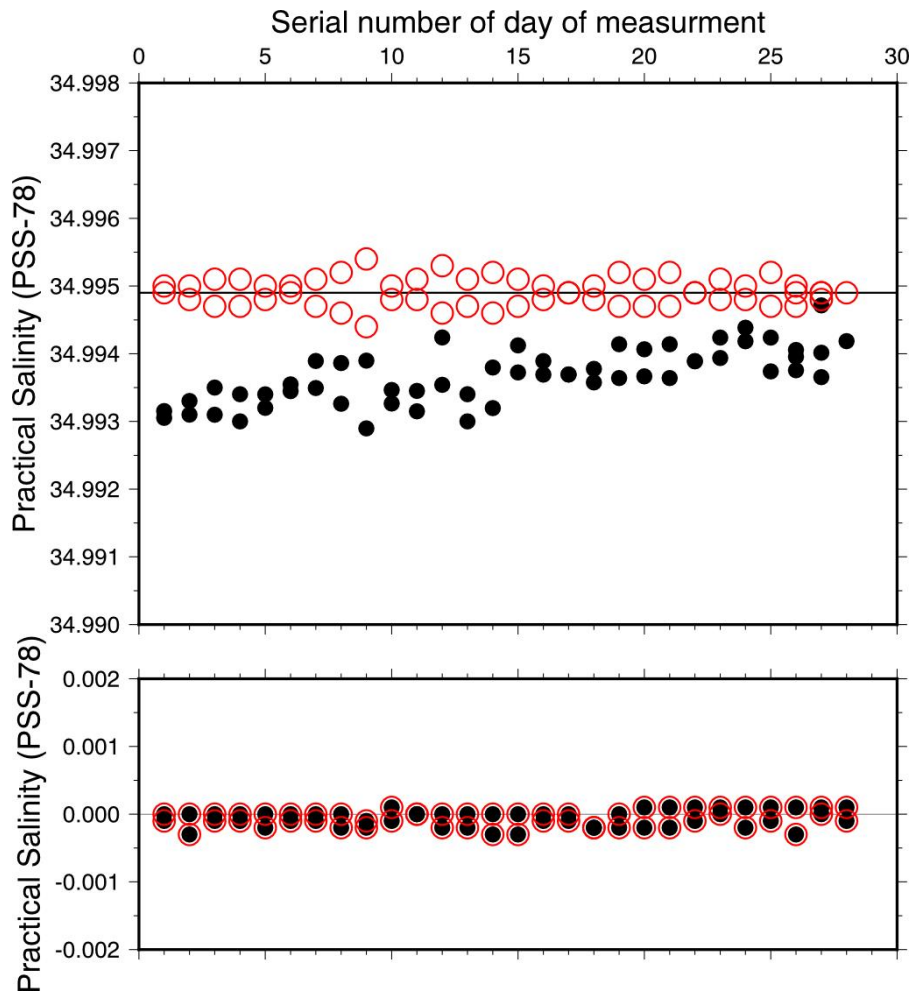These obtained data will be submitted to JAMSTEC Data Management Group (DMG).

Figure 4.2-1. Time-series of the measured Practical Salinities for the ultra-pure water (lower panel) and the IAPSO SSW (upper panel) (black circles). The time-drift corrected Practical Salinities were also shown (red circles).

4.3 Seawater density
November 6, 2023

(1) Personnel
Hiroshi UCHIDA (JAMSTEC RIGC)
Ryohei YAMAGUCHI (JAMSTEC RIGC)

(2) Objective
The objective of this study is to collect Absolute Salinity (also called "density salinity") data and to evaluate the algorithm to estimate Absolute Salinity anomaly provided along with TEOS-10 (the International Thermodynamic Equation of Seawater 2010) (IOC et al., 2010). Seawater samples collected on the R/V Mirai MR23-06C cruise were also measured.

(3) Instruments and method
(3.1) Seawater density for water samples
Seawater density for water samples was measured with a vibrating-tube density meter (DMA 5000M [serial no. 80570578], Anton-Paar GmbH, Graz, Austria) with a sample changer (Xsample 122 [serial no. 8548492], Anton-Paar GmbH). The sample changer was used to load samples automatically from up to forty-eight 12-mL glass vials.

The water samples collected in 250 mL brown borosilicate glass bottles with translucent screw caps (PTFE packing) for Practical Salinity measurement were measured by taking the water sample into a 12-mL glass vial for each bottle just before Practical Salinity measurement. The glass vial was sealed with Parafilm M (Pechiney Plastic Packaging, Inc., Menasha, Wisconsin, USA) immediately after filling. Densities of the samples were measured at 20 °C by the density meter.

The density meter was initially calibrated on the previous cruise (MR23-05 leg 2) by measuring air and pure water according to the instrument manual. However, measured density for the IAPSO Standard Seawater deviates from density of TEOS-10 calculated from practical salinity and composition of seawater, probably due to non-linearity of the density meter (Uchida et al., 2011). The non-linearity can be corrected by measuring a reference sample simultaneously as:

$$\rho_{corr} = \rho - (\rho_{ref} - \rho_{ref\_true}) + c\,(\rho - \rho_{ref\_true}),$$

where ρ_{corr} is the corrected density of the sample, ρ is measured density of the sample, ρ_{ref} is measured density of the reference, ρ_{ref_true} is true density of the reference, and c is non-linearity correction factor.

Time drift of the density meter was monitored by periodically measuring the density of ultra-pure water (Milli-Q water, Millipore, Billerica, Massachusetts, USA) produced on the R/V Mirai and pure water (Pure Water [water hardness 0], Ako Kasei Co. Ltd., Ako Hygo, Japan) made from seawater collected from a depth of 344 m off Muroto, Kochi, Japan, by filtering twice with a reverse osmosis membrane. In addition, Pure Water was deionized using ion exchange resin (Pure Maker, Sanei Corp., Arao, Kumamoto, Japan) conducted on 6 October 2019 and stored in a 2-L PET bottle at room temperature. Practical Salinity measured in this cruise ranged from –0.0003 to 0.0001 for the Milli-Q water and was 0.0002 for the Pure Water. The true density at 20 ºC of the Pure Water was estimated to be 998.2074 kg m^{-3} from the isotopic composition (δD = –3.4 ‰, δ^{18}O = –1.3 ‰) and International Association for the Properties of Water and Steam (IAPWS)-95 standard. An offset correction was applied to the measured density by using the Pure Water measurements ($\rho_{PureWater}$) with a slight modification of the density dependency (Uchida et al., 2011).

The non-linearity factor is estimated to be 0.000411 for the density meter (serial no. 80570578). In this cruise, the non-linearity and time drift of the density meter was monitored by periodically measuring the density of the IAPSO Standard Seawater (batch P166). True density at 20 °C for the batch P166 is estimated to be 1024.7638 kg/m^3 from Practical Salinity and composition changes of Standard Seawater using TEOS-10 (see Uchida et al., 2023). Average with standard deviation for the 104 measurements of the batch P166 was 1024.7639±0.0016 kg/m^3.

A total of 3 bottles of Multiparametric Standard Seawater (MSSW, KANSO TECHNOS Co., Ltd.) was also measured and the mean ± SD was 1024.2202 ± 0.0004 kg/m^3.

(3.2) Seawater density measured in situ
Seawater density was also measured with a refractive index density sensor (serial no. 2) attached to the CTD system (Uchida et al., 2019). The power was supplied from the external battery pack. The data

were sampled at 32 Hz and stored in the internal memory with temperature measured inside the spectroscope sampled at 1 Hz to correct the temperature dependency of the spectroscope.

Data logging was stopped while the station 21_1 and 41_1 due to low batteries. Also, no data was available for the stations 22_1, 23_1, and 23_2 due to low batteries.

The density sensor data will be merged with the CTD data to estimate in situ density by calibrating with the bottle sampled density data after the cruise. Continuous vertical profiles of Absolute Salinity will be determined from thus estimated in situ density and the CTD temperature and pressure using TEOS-10.

(4) Results

Absolute Salinity (also called density salinity, "DNSSAL") can be back calculated from the measured density and temperature (20 °C) with TEOS-10. A total of 50 pairs of replicate samples was measured and the standard deviation of the replicate samples was 0.0014 g/kg. The measured Absolute Salinity anomalies (δS_A) are shown in Fig. 4.3-1. For the Pacific Ocean and the surface water of the Bering Sea, the measured δS_A were well agree with the δS_A estimated from Pawlowicz et al. (2011) which exploits the correlation between δS_A and nutrient concentrations and carbonate system parameters based on mathematical investigation using a model relating composition, conductivity and density of arbitrary seawaters. However, for the deep water of the Bering Sea, the measured δS_A were larger than the δS_A estimated from Pawlowicz et al. (2011).
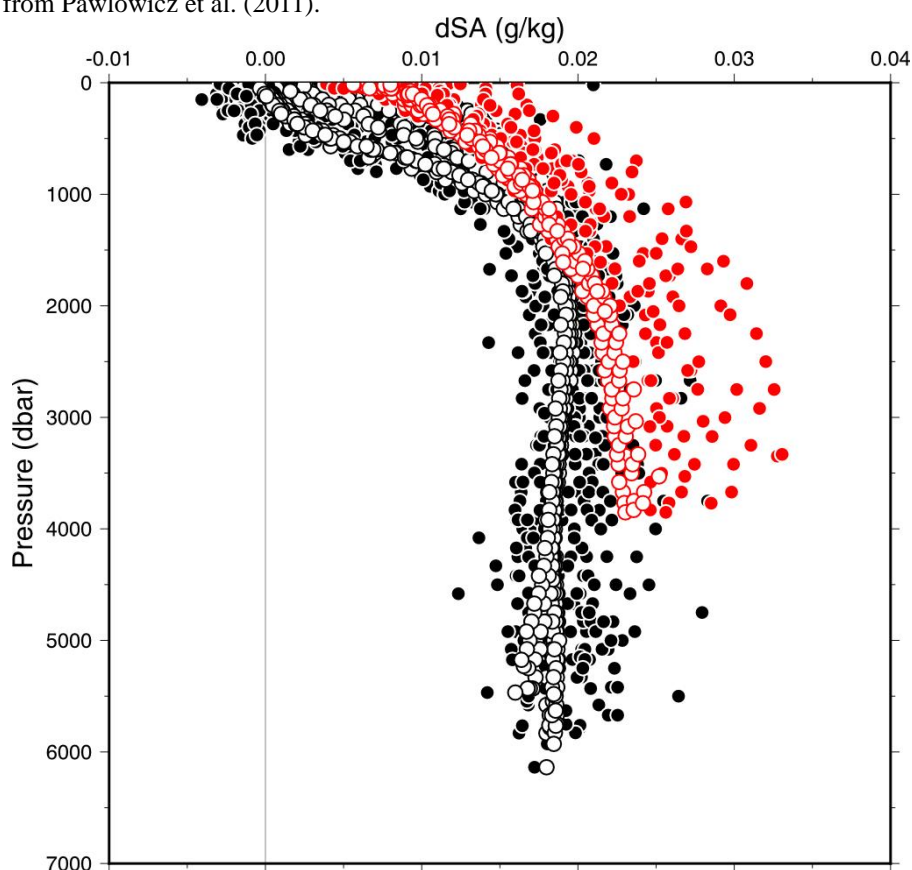
Figure 4.3-1. Vertical distribution of Absolute Salinity anomaly measured by the density meter (closed circles). Absolute Salinity anomaly estimated from nutrients and carbonate system parameters (Pawlowicz et al., 2011) are also shown (open circles). Data shown in red are for the Bering Sea and data shown in black are for the Pacific Ocean.

(5) References

IOC, SCOR and IAPSO (2010): The international thermodynamic equation of seawater – 2010: Calculation and use of thermodynamic properties. Intergovernmental Oceanographic Commission, Manuals and Guides No. 56, UNESCO (English), 196 pp.

Pawlowicz, R., D.G. Wright and F. J. Millero (2011): The effects of biogeochemical processes on ocean

conductivity/salinity/density relationships and the characterization of real seawater. Ocean Science, 7, 363-387.

Uchida, H., T. Kawano, M. Aoyama and A. Murata (2011): Absolute salinity measurements of standard seawaters for conductivity and nutrients. La mer, 49, 237-244.

Uchida, H., Y. Kayukawa, and Y. Maeda (2019): Ultra high-resolution seawater density sensor based on a refractive index measurement using the spectroscopic interference method. Sci. Rep., 9:15482, doi:10.1038/s41598-019-52020-z.

Uchida, H., M. Wakita, A. Makabe, and A. Murata (2023): Changes of the composition of International Association for the Physical and Sciences of the Ocean standard seawater. In: Murata A. Cheong C., editors. Chemical reference materials of ocean science: history, production, certification and current status.

(6) Data archive

These obtained data will be submitted to JAMSTEC Data Management Group (DMG).

4.4 Lowered Acoustic Doppler Current Profiler

(1) Personnel
Shinya Kouketsu   JAMSTEC (principal investigator)
Ryohei Yamaguchi   JAMSTEC

(2) Overview of the equipment
Two acoustic Doppler current profilers (ADCP) were integrated with the CTD/RMS package. The lowered ADCP (LADCP)s, Workhorse Monitor WHM300 (Teledyne RD Instruments, San Diego, California, USA), which has 4 facing transducers with 20-degree beam angles, rated to 6000 m, make direct current measurements at the depth of the CTD, thus providing a full profile of velocity. The LADCPs were powered during the CTD casts by a 48 volts battery pack. The LADCP unit was set for recording internally prior to each cast. After each cast the internally stored observed data were downloaded to the computer in the onboard laboratory. After the cruise, by combining the measured velocity of the sea water and ocean bottom relative to the instrument, shipboard navigation data, and pressure time series from the CTD, the absolute velocity profiles will be obtained with the software implemented by A.Thunherr. The software is based on the method of Visbeck (2002) and available online at ftp://ftp.ldeo.columbia.edu/pub/LADCP;.

The instruments used in this cruise were as follows.
St. 1-23: WHM300(S/N 24545; downward), WHM300(S/N 20754; upward)
St. 24-27: WHM300(S/N 15550; downward), WHM300(S/N 20754; upward)
St 28-70: WHM300(S/N 22902, downward), WHM300(S/N 20754; upward)

(3) Data collection
In this cruise, data were collected with the following configuration.
WHM300: Bin size: 8.0 m, Number of bins: 12
As, at St. 27, a beam intensity of the down-looking instrument (S/N 15550) got weak, 3-beam solution will be used for data processing after the cruise.

Reference
Visbeck, M. (2002): Deep velocity profiling using Lowered Acoustic Doppler Current Profilers: Bottom track and inverse solutions. *J. Atmos. Oceanic Technol.*, **19**, 794-807.

4.5 Microstructure in Temperature and Conductivity

(1) Personnel

Ichiro Yasuda   AORI (Principal investigator)
Yusuke Sasaki   AORI
Shinya Kouketsu   JAMSTEC
Ryohei Yamaguchi   JAMSTEC

(2) Objective

The objective is to measure microstructure in temperature and conductivity to evaluate vertical mixing.

(3) Instruments and method

Microstructure observations were carried out by AFP07 (Rockland Scientific International Inc.), which were mounted on the CTD rosette and were powered from the CTD (SBE 9plus). We installed two fast response thermistors (FP07) on AFP07s to measure microstructure in temperature. We had to replace probes, as some of the probes failed during the cruise. Low-frequency profiles of temperature and conductivity were recorded in the AFP07 with the input from the SBE-3 sensors on the CTD system. We downloaded the raw data from the instruments after each cast. We plan to examine methods for calibration and quality check of the data after the cruise.

(4) Measurements

i) Microstructure measurement

For two casts (the 2nd casts at St. 28 at St. 34), the data file did not exist due to operation problems. We sometimes replaced FP07s due to measurement problems as below:

- Sensor socket 1 (SN286):

St. 1-14: T1320
St. 15-16: T2448
St. 23-25: T2120
St. 26: T2081
St. 27-46: T1975
St. 47-57: T1320
St. 58-70: T1320

- Sensor socket 2 (SN190):

St. 1-26: T1975
St. 27: T2081
St. 28-39(1st cast): T2125
St. 39(2nd cast)-46: T1341
St. 47-57: T1975
St. 58: T2448
St. 59-70: T1341

■

4.6 Oxygen

December 6, 2023
Yuichiro Kumamoto
Japan Agency for Marine-Earth Science and Technology

(1) Personnel
Yuichiro Kumamoto [1], *Katsunori Sagishima* [2], *Misato Kuwahara* [2], *Tomokazu Chiba* [2]
1) Japan Agency for Marine-Earth Science and Technology
2) Marine Works Japan Co. Ltd

(2) Objectives
Dissolved oxygen is one of chemical tracers for the ocean circulation. Climate models predict a decline in dissolved oxygen concentration and a consequent expansion of oxygen minimum layer due to global warming, which results mainly from decreased interior advection and ongoing oxygen consumption by remineralization. In order to discuss the temporal change in oxygen concentration in the water column, we measured dissolved oxygen concentration from surface to bottom layer at all the water sampling stations in the North Pacific Ocean during this cruise.

(3) Reagents
Pickling Reagent I: Manganous chloride solution (3M) Lot: 1-23A02, A03
Pickling Reagent II: Sodium hydroxide (8M) / sodium iodide solution (4M) Lot: 2-23A01, A02, A03
Sulfuric acid solution (5M) Lot: S-23A01, A02, A03
Sodium thiosulfate (0.025M) Lot: T-23D, -23E, -21J
Potassium iodate (0.001667M): Lot KCN5512, FUJIFILM Wako Pure Chemical Industries Ltd, Mass fraction: 99.98 ± 0.04 % (expanded uncertainty) Lot of solution: K-23B

(4) Instruments
Detector: Automatic photometric titrator, DOT-15X manufactured by Kimoto Electronic Co. Ltd. Lot: DOT-09, -10
Burette: APB-620 and APB-510 manufactured by Kyoto Electronic Co. Ltd. / 10 cm^3 of titration piston Lot: DOT-09, MB-10/MY10-10; DOT-10, MB-12/MY10-12; KIO$_3$, MB-06/MY10-06
Dispenser: FORTUNA Optifix 1 cm^3 Lot: Pickling Reagent I, MO-30; Pickling Reagent II, MO-43

(5) Seawater sampling
Seawater samples were collected using 12-liter sample bottles attached to the CTD-system. The seawater was transferred to a volume-calibrated glass flask (ca. 100 cm^3) through a plastic tube. Three times volume of the flask of seawater was overflowed. Sample temperature was measured during the water sampling using a thermometer. Then two reagent solutions (Reagent I, II) of 1.0 cm^3 each were added immediately into the sample flask and the stopper was inserted carefully into the flask. The sample flask was then shaken to mix the contents and to disperse the precipitate finely throughout. After the precipitate has settled at least halfway down the flask, the flask was shaken again to disperse the precipitate. The sample flasks containing pickled samples were stored in an air-conditioned laboratory until they were measured.

(6) Sample measurement
At least two hours after the re-shaking, the pickled samples were measured on board. A magnetic stirrer bar and 1 cm^3 sulfuric acid solution were added into the sample flask and stirring began. Samples were titrated by sodium thiosulfate solution whose molarity was determined by potassium iodate solution. Temperature of sodium thiosulfate during titration was recorded by a thermometer. We measured dissolved oxygen concentration using two sets of the titration apparatus system, named DOT-09 and DOT-10. Molal concentration of dissolved oxygen (μmol kg^{-1}) was calculated by the sample temperature during the water sampling, salinity, flask volume, and concentration and titrated volume of the sodium thiosulfate solution (titrant).

(7) Standardization
Concentration of the sodium thiosulfate titrant (0.025M) was determined by the potassium iodate

standard solution. The potassium iodate was dried in an oven at 130°C. 1.78 g potassium iodate weighed out accurately was dissolved in deionized water and diluted to final volume of 5 dm³ in a calibrated volumetric flask (0.001667M). Then the aliquot (about 400 ml) of the solution was stored in a brown glass bottle (500 ml). 10 cm³ of the potassium iodate solution was added to a flask using a volume-calibrated dispenser. Then 90 cm³ of deionized water, 1 cm³ of sulfuric acid solution, and 1.0 cm³ of pickling reagent solution II and I were added into the flask in order. Amount of titrated volume of sodium thiosulfate (usually 5 times measurements average) gave the molarity of the sodium thiosulfate titrant. Table 4.6.1 show results of the standardization during this cruise. The averaged coefficient of variation (C.V.) for the standardizations was 0.019 ± 0.009 % (standard deviation, n = 10).

(8) Blank determination

The oxygen in the pickling reagents I (1.0 cm³) and II (1.0 cm³) was assumed to be 7.6×10^{-8} mol (Murray *et al.*, 1968). The redox species apart from oxygen in the reagents (the pickling reagents I, II, and the sulfuric acid solution) also affect the titration, which is called the reagent blank. The reagent blank was determined as follows. 1 and 2 cm³ of the standard potassium iodate solution were added to two flasks respectively. Then 100 cm³ of deionized water, 1 cm³ of sulfuric acid solution, and 1.0 cm³ of pickling reagent II and I each were added into the two flasks in order. The reagent blank was determined by difference between the two times of the first (1 cm³ of KIO_3) titrated volume of the sodium thiosulfate and the second (2 cm³ of KIO_3) one. The three results of the blank determination were averaged (Table 4.6.1). The averaged coefficient of variation (C.V.) for the reagent blank determination against the titration volume of the potassium iodate standard (about 4 ml) or 250 µmol kg⁻¹ of dissolved oxygen concentration was 0.022 ± 0.006 % (standard deviation, n = 10). The redox species in seawater sample itself are measured as "dissolved oxygen", which is called as the seawater blank, unless they are corrected. Because we did not measure the seawater blank in this cruise, the dissolved oxygen concentration reported here includes the seawater blank concentration that is less than 1 µmol kg⁻¹ in the open ocean except those in suboxic and anoxic waters (Kumamoto *et al.*, 2015).

(9) Instrumental error

The difference in the concentrations of sodium thiosulfate solution determined by the standardization and blank determination using DOT-09 and DOT-10 were less than 0.2% (Table 4.6.1). The T-test at 95% confidence level suggests that there is no reason to believe that the two concentrations are different. Thus, we concluded that there was no instrumental error in measurements using DOT-09 and DOT-10.

Table 4.6.1 Results of standardization (End Point, cm³) and reagent blank determination (cm³).

No	Date (UTC)	KIO₃ Lot	Na₂S₂O₃ Lot	DOT-09 E.P.	DOT-09 blank	DOT-10 E.P.	DOT-10 blank	Δ (%)*	Remarks
1	2023/Oct/08	Reference 23-01	T-22J	3.931	-	3.936	-	0.20	
2	2023/Oct/08	K23B01	T-22J	3.932	-0.001	3.935	-0.003	0.16	Stn.015-005
3	2023/Oct/11	K23B02	T-22J	3.932	0.000	3.935	-0.003	0.18	Stn.003-017
4	2023/Oct/16	K23B03	T-22J	3.933	-	3.936	-	0.17	Na₂S₂O₃ changed
5	2023/Oct/16	K23B03	T-22D	3.933	0.000	3.935	-0.003	0.14	Stn.019-029
6	2023/Oct/19	K23B04	T-22D	3.932	-0.002	3.936	-0.004	0.16	Stn.031-039
7	2023/Oct/23	K23B05	T-22D	3.933	-0.002	3.938	-0.005	0.21	Stn.042-056
8	2023/Oct/28	K23B06	T-22D	3.932	0.000	3.936	-0.003	0.19	Stn.056-070
9	2023/Nov/02	K-23B07	T-22D	3.933	0.000	3.937	0.000	0.12	Na₂S₂O₃ changed
10	2023/Nov/02	K-23B07	T-22E	3.962	0.000	3.968	0.000	0.16	Final standardization

*Difference between DOT-09 and DOT-10 (DOT-10 minus DOT-09) in sodium thiosulfate concentration determined by the standardization and blank determination.

(10) Replicate sample measurement

At all the water sampling stations, a pair of replicate samples was collected at one or two depths. The standard deviations from the difference of pairs of replicate measurements was estimated to be 0.11 µmol

kg^{-1} (n = 56), which corresponds to 0.044% of the relative standard deviation against 250 μmol kg^{-1}, using the standard operating procedure 23 in Dickson *et al.* (2007). The standard deviations of the difference between the pair of replicate measurement for the samples whose oxygen concentration is higher and lower than 100 μmol kg^{-1} are 0.14 (n = 22) and 0.08 μmol kg^{-1} (n = 34), respectively (Fig. 4.6.1). The difference between the two standard deviations is not significant (F-test at 95% confidence level) and there is no reason to believe contamination of atmospheric O$_2$ during the water sampling for the lower concentration samples.
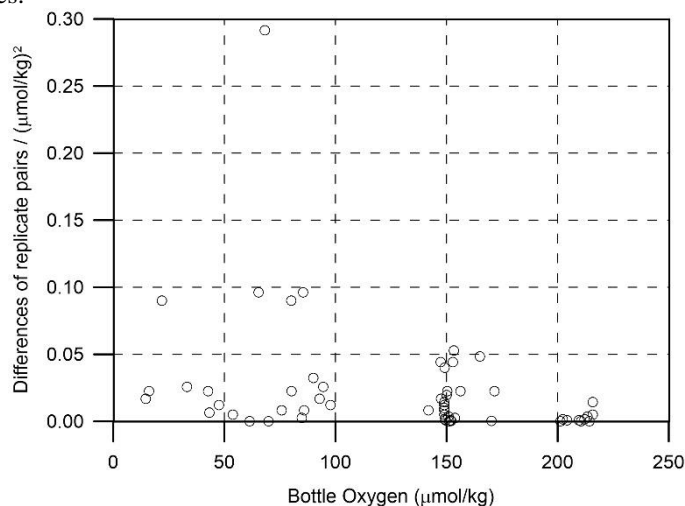
Figure 4.6.1 Oxygen difference between measurements of a replicate pair against oxygen concentration.

(11) Quality control flag assignment

   Quality flag values for oxygen data from sample bottles were assigned according to the code defined in Table 4.9 of WHP Office Report WHPO 90-1 Rev.2 section 4.5.2 (Joyce *et al.*, 1994). Measurement flags of 2 (good), 3 (questionable), 4 (bad), and 5 (missing) have been assigned (Table 4.6.3). For the choice between 2, 3, or 4, we basically followed a flagging procedure as listed below:

   a. If there was a glaring problem or error in the measurement, the datum was flagged 4.
   b. Bottle oxygen concentration at the sampling layer was plotted against sampling pressure and potential density. Any points not lying on a generally smooth trend were noted.
   c. Difference between bottle oxygen concentration and oxygen sensor output was then plotted against sampling pressure. If the noted datum deviated from a group of plots, it was flagged 3 or 4.
   d. If the bottle flag was 4 (did not trip correctly), a datum was flagged 4 (bad). In case of the bottle flag 3 (leaking) or 5 (unknown problem), a datum was flagged based on steps a, b, and c.

Table 4.6.3 Summary of assigned quality control flags.

Flag	Definition	Number*
2	Good	999
3	Questionable	6
4	Bad	2
5	Not report (missing)	0
	Total	1007

*The replicate samples (n = 56) were not included.

(12) Uncertainty

   We assume that the uncertainty of dissolved oxygen determination is derived from those of items listed in Table 4.6.4. Because we did not measure the seawater blank, the dissolved oxygen concentration reported here does include the seawater blank concentration (Section 8). Without the correction by the seawater blank, the combined uncertainty (k = 1) and the expanded combined uncertainty (k = 2) were calculated to be 0.07% and 0.14%, respectively. Note that this combined uncertainty does not include that derived from temporal change in temperature of sodium thiosulfate solution. However, that was negligible because the its variation was small (20.7-22.0 ºC) When we subtract the seawater blank from the oxygen concentration, the uncertainty due to the seawater blank should be added. If it is assumed that

the seawater blank concentration is 0.50 ± 0.50 μmol kg^{-1} and the distribution of the possible values is uniform or rectangular, its standard uncertainty is calculated to be 0.29 μmol kg^{-1} (= 0.50/√3). This value corresponds to the standard uncertainty of 0.116% relative to 250 μmol kg^{-1} of dissolved oxygen concentration. The combined standard uncertainty, which includes the uncertainty of the seawater blank concentration, is calculated to be 0.14% (the extended combined uncertainty is 0.28%). These combined uncertainties, however, are applicable only for the dissolved oxygen concentration corrected by the seawater blank concentration (0.50 μmol kg^{-1}).

Table 4.6.4 Uncertainties of estimated items for the oxygen determination.

#	Estimated items	Relative uncertainty to 250 μmol kg^{-1} (%)	References
1	Sodium thiosulfate concentration	0.056	#2, 3, 4
2	Potassium iodate concentration	0.030	Kumamoto *et al.* (2015)
3	Titration of potassium iodate	0.021	Section 7
4	Reagent blank determination	0.042	Section 8
5	Titration of seawater sample	0.044	Section 10
6	Volume of sample flask	0.015	Kumamoto *et al.* (2015)
	Combined uncertainty (k=1)	0.07	#1, 5, 6
	Expanded combined uncertainty (k=2)	0.14	
7	Seawater blank	0.116	Kumamoto *et al.* (2015)
	Combined uncertainty (k=1)	0.14	#1, 5, 6, 7
	Expanded combined uncertainty (k=2)	0.28	

(13) Problems

The differences between the replicate pair measurements using oxygen bottle 529 were anomalously large. After the cruise, we re-calibrated the volume of bottle 529 and re-calculated the concentrations that were measured using bottle 529.

(14) Data archives

The data obtained in the cruises will be submitted to the Data Management Group of JAMSTEC and will be opened to the public via "Data Research System for Whole Cruise Information in JAMSTEC (DARWIN)" in the JAMSTEC web site.

References

Dickson, A. G., C.L. Sabine, and J.R. Christian (Eds.) (2007) Guide to best practices for ocean CO_2 measurements, PICES Special Publication 3, 191 pp.

Joyce, T., and C. Corry, eds., C. Corry, A. Dessier, A. Dickson, T. Joyce, M. Kenny, R. Key, D. Legler, R. Millard, R. Onken, P. Saunders, M. Stalcup (1994) Requirements for WOCE Hydrographic Programme Data Reporting, WHPO Pub. 90-1 Rev. 2, May 1994 Woods Hole, Mass., USA.

Kumamoto, Y., Y. Takatani, T. Miyao, H. Sato, and K. Matsumoto (2015) Dissolved oxygen, Guideline of Ocean Observations, vol. 3, chap. 1, G301JP:001−029 (in Japanese).

Murray, C.N., J.P. Riley, and T.R.S. Wilson (1968) The solubility of oxygen in Winkler reagents used for determination of dissolved oxygen, Deep-Sea Res., 15, 237-238.

4.7 Nutrients

December 07, 2023
Yuichiro Kumamoto
Japan Agency for Marine-Earth Science and Technology

(1) Personnel
   Yuichiro KUMAMOTO [1]: Principal Investigator
   Yuko MIYOSHI [2]: Operation Leader
   Shiori ARIGA [2]
   Nahoko ADACHI [2]
   1) Japan Agency for Marine-Earth Science and Technology
   2) Marine Works Japan Ltd.

(2) Objectives
   The objective of this document is to show the present status of the nutrient measurement during the R/V MIRAI MR23-07 cruise (EXPOCODE: 49NZ20231006) in the North Pacific Ocean and Bering Sea.

(3) Parameters
   The parameters are nitrate, nitrite, silicate, phosphate, and ammonia in seawater.

(4) Instruments and methods
   The analytical platform was replaced from QuAAtro 2-HR to QuAAtro 39 in March 2021. However, since this replacement, several issues for the QuAAtro 39 system have been reported (see the cruise report of MR21-05C). In July 2022, to improve those issues and the analytical precisions, (1) their pumps were replaced from the 13-tube pump (model number: 166+B214-01, BL TEC K.K.) to the 14-tube pump (model number: TRA+B014-02, BL TEC K.K.), (2) their motor brackets were replaced to the new type that is a stainless model (model number: Motor-Braket-01-Rev-1 and Motor-Braket-02-Rev-1, BL TEC K.K.), and (3) their light source units were fixed firmly to reduce vibration. The modified platform is called "QuAAtro 39-J" and was employed in this cruise.
   The modification of analytical methods for four parameters, nitrate, nitrite, silicate, and phosphate, which were employed in this cruise, are compatible with the methods described in the GO-SHIP repeat hydrography nutrients manual (Hydes et al., 2010; Becker et al., 2019). The analytical method of ammonium is compatible with the method using a vaporization membrane permeability method (Kimura, 2000).

(4.1) Nitrate + nitrite and nitrite
   Nitrate + nitrite and nitrite were analyzed by the following methodology that was modified from the original method of Grasshoff (1976). The flow diagrams are shown in Fig. 4.7.1 for nitrate + nitrite and Fig. 4.7.2 for nitrite. For the nitrate + nitrite analysis, the samples were mixed with the alkaline buffer (Imidazole) and then the mixture was pushed through a cadmium coil which was coated with a metallic copper. This step was conducted due to the reduction from nitrate to nitrite in the sample, which allowed us to determine nitrate + nitrite in the seawater sample. For the nitrite analysis, the sample was mixed with reagents without this reduction step. In the flow system, the seawater sample with or without the reduction step was mixed with an acidic sulfanilamide reagent through a mixing coil to produce a diazonium ion. And then, the mixture was mixed with the N-1-naphthylethylenediamine dihydrochloride (NED) to produce a red azo dye. The azo dye compound was injected into the spectrophotometric detection to monitor the signal at 545 nm. Thus, for the nitrite analysis, the sample was determined without passing through the Cd coil. Nitrate was computed by the difference in concentrations between nitrate + nitrite and nitrite.
Reagents
a) 50 % Triton solution: 50 mL of Triton® X-100 (CAS No. 9002-93-1) was mixed with 50 mL of ethanol (99.5 %).
b) Imidazole (buffer), 0.06 M (0.4 % w/v): Dissolved 4 g of the imidazole (CAS No. 288-32-4) in 1000 mL ultra-pure water, and then added 2 mL of the hydrogen chloride (CAS No. 7647-01-0). After mixing, 1 mL of the 50 % triton solution was added.

c) Sulfanilamide, 0.06 M (1 % w/v) in 1.2 M HCl: Dissolved 10 g of 4-aminobenzenesulfonamide (CAS No. 63-74-1) in 900 mL of ultra-pure water, and then add 100 mL of the hydrogen chloride (CAS No. 7647-01-0). After mixing, 2 mL of the 50 % triton solution was added.

d) NED, 0.004 M (0.1 % w/v): Dissolved 1 g of N-(1-naphthalenyl)-1,2-ethanediamine dihydrochloride (CAS No. 1465-25-4) in 1000 mL of ultra-pure water and then added 10 mL of hydrogen chloride (CAS No. 7647-01-0). After mixing, 1 mL of the 50 % triton solution was added. This reagent was stored in a dark bottle.
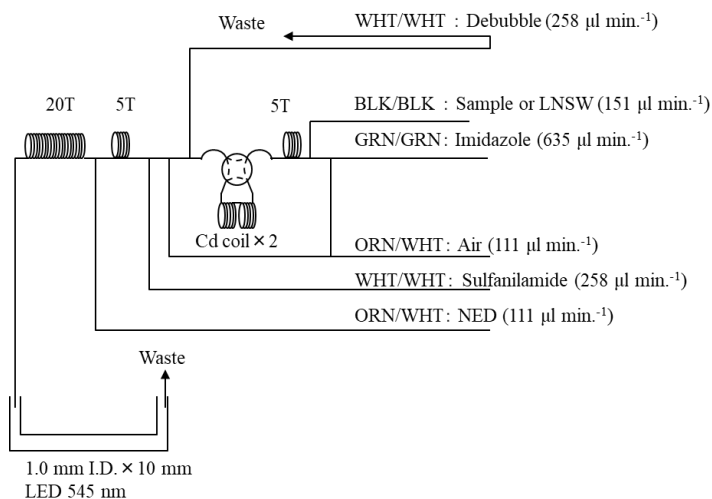
Figure 4.7.1 NO_3+NO_2 (1ch.) flow diagram.
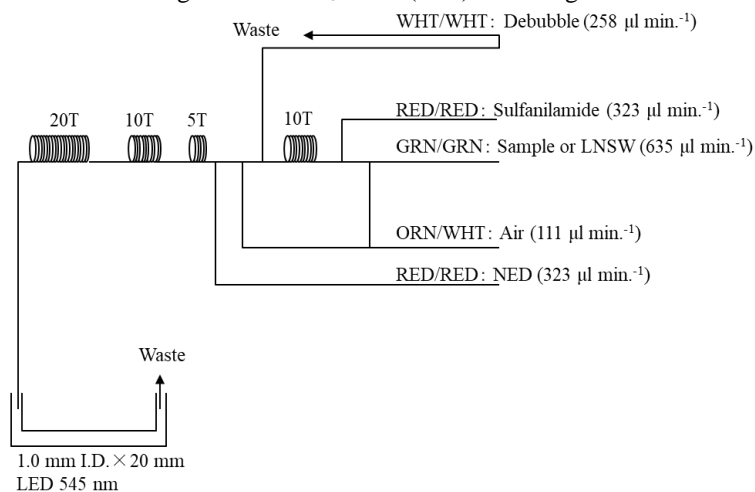
Figure 4.7.2 NO_2 (2ch.) flow diagram.

(4.2) Silicate

The method for silicate is analogous to that described for phosphate (4.3). The method is essentially that of Grasshoff et al. (1999). The flow diagrams are shown in Fig. 4.7.3. Silicomolybdic acid compound was first formed by mixing silicate in the sample with the molybdic acid. The silicomolybdic acid compound was then reduced to silicomolybdous acid, "molybdenum blue," using L-ascorbic acid as the reductant. And then the signal was monitored at 630 nm.
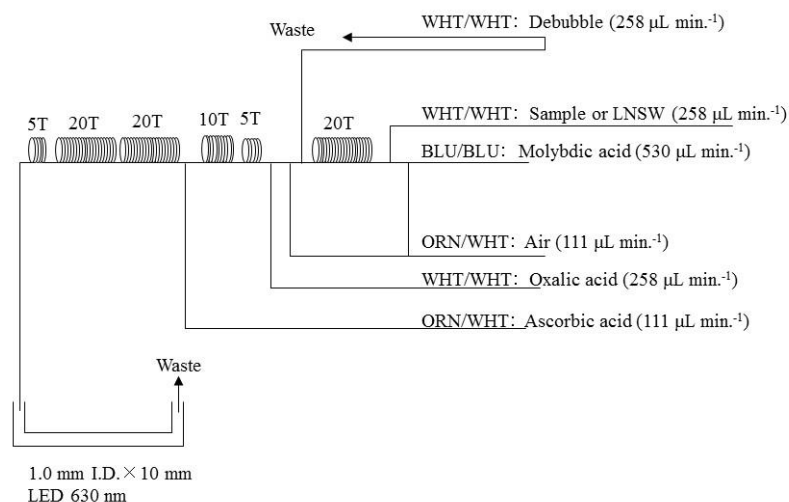
Figure 4.7.3 SiO$_2$ (3ch.) flow diagram.

Reagents

a) 15 % Sodium dodecyl sulfate solution: 75 g of sodium dodecyl sulfate (CAS No. 151-21-3) was mixed with 425 mL ultra-pure water.

b) Molybdic acid, 0.03 M (1 % w/v): Dissolved 7.5 g of sodium molybdate dihydrate (CAS No. 10102-40-6) in 980 mL ultra-pure water, and then added 12 mL of 4.5M sulfuric acid. After mixing, 20 mL of the 15 % sodium dodecyl sulfate solution was added. Note that the amount of sulfuric acid was reduced from the previous report (MR19-03C) since we have modified the method of Grasshoff et al. (1999).

c) Oxalic acid, 0.6 M (5 % w/v): Dissolved 50 g of oxalic acid (CAS No. 144-62-7) in 950 mL of ultra-pure water.

d) Ascorbic acid, 0.01 M (3 % w/v): Dissolved 2.5 g of L-ascorbic acid (CAS No. 50-81-7) in 100 mL of ultra-pure water. This reagent was freshly prepared every day.

(4.3) Phosphate

    The methodology for the phosphate analysis is a modified procedure of Murphy and Riley (1962). The flow diagrams are shown in Fig. 4.7.4. Molybdic acid was added to the seawater sample to form the phosphomolybdic acid compound, and then it was reduced to phosphomolybdous acid compound using L-ascorbic acid as the reductant. And then the signal was monitored at 880 nm.

Reagents

a) 15 % Sodium dodecyl sulfate solution: 75 g of sodium dodecyl sulfate (CAS No. 151-21-3) was mixed with 425 mL of ultra-pure water.

b) Stock molybdate solution, 0.03 M (0.8 % w/v): Dissolved 8 g of sodium molybdate dihydrate (CAS No. 10102-40-6) and 0.17 g of antimony potassium tartrate trihydrate (CAS No. 28300-74-5) in 950 mL of ultra-pure water, and then added 50 mL of sulfuric acid (CAS No. 7664-93-9).

c) PO$_4$ color reagent: Dissolved 1.2 g of L-ascorbic acid (CAS No. 50-81-7) in 150 mL of the stock molybdate solution. After mixing, 3 mL of the 15 % sodium dodecyl sulfate solution was added. This reagent was freshly prepared before every measurement.

81
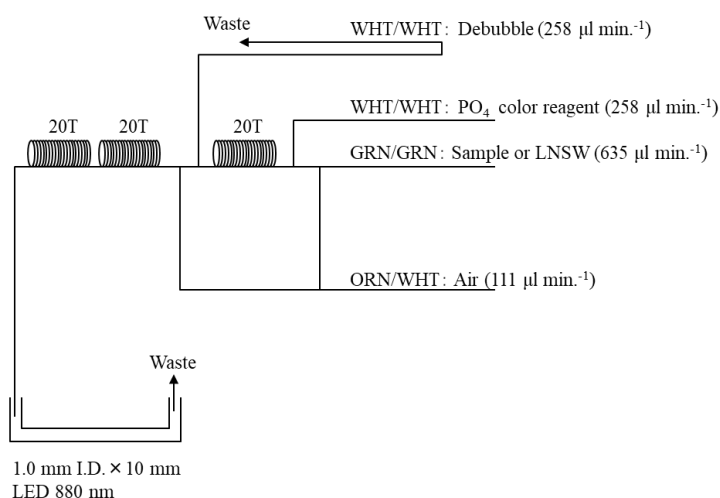
Figure 4.7.4 PO$_4$ (4ch.) flow diagram.

(4.4) Ammonia

The ammonia in seawater was determined using the flow diagrams shown in Fig. 4.7.5. The sample was mixed with an alkaline solution containing EDTA, which ammonia as a gas state was formed from seawater. The ammonia (gas) is absorbed in a sulfuric acid by way of a 0.5 μm pore-size membrane filter (ADVANTEC PTFE) at the dialyzer attached to the analytical system. And then the ammonia absorbed in sulfuric acid was determined by coupling with phenol and hypochlorite to form indophenols blue, and the signal was determined at 630 nm.
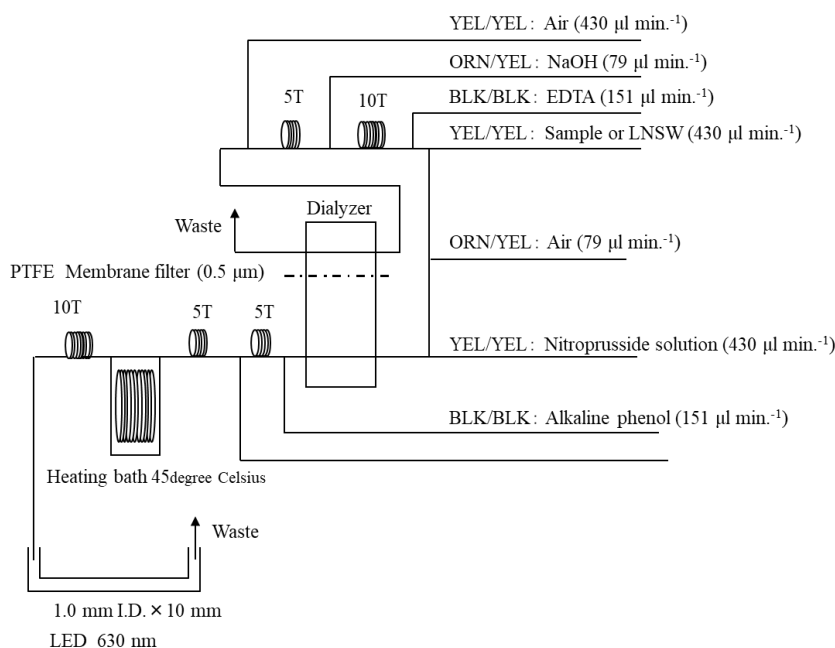
Figure 4.7.5 NH$_4$ (5ch.) flow diagram.

Reagents

a) 30 % Triton solution: 30 mL of the Triton® X-100 (CAS No. 9002-93-1) was mixed with 70 mL ultra-pure water.

b) EDTA: Dissolved 41 g of tetrasodium;2-[2-[bis(carboxylatomethyl)amino]ethyl-(carboxylatemethyl)amino]acetate;tetrahydrate (CAS No. 13235-36-4) and 2 g of boric acid (CAS No. 10043-35-3) in 200 mL of ultra-pure water. After mixing, 1 mL of the 30 % triton solution was added. This reagent is prepared every week.

c) NaOH liquid: Dissolved 1.5 g of sodium hydroxide (CAS No. 1310-73-2) and 16 g of tetrasodium;2-[2-[bis(carboxylatomethyl)amino]ethyl-(carboxylatemethyl)amino]acetate;tetrahydrate (CAS No.

13235-36-4) in 100 mL of ultra-pure water. This reagent was prepared every week. Note that we reduced the amount of sodium hydroxide from 5 g to 1.5 g because pH of C standard solutions has been lowered 1 pH unit due to the change of recipe of B standards solution (the details of those standard solutions, see 6.2.4).

d) Stock nitroprusside: Dissolved 0.25 g of sodium nitroferricyanide dihydrate (CAS No. 13755-38-9) in 100 mL of ultra-pure water, and then added 0.2 mL of 1M sulfuric acid. Stored in a dark bottle and prepared every month.

e) Nitroprusside solution: Added 4 mL of the stock nitroprusside and 4 mL of 1M sulfuric acid in 500 mL of ultra-pure water. After mixing, 2 mL of the 30 % triton solution was added. This reagent was stored in a dark bottle and prepared every 2 or 3 days.

f) Alkaline phenol: Dissolved 10 g of phenol (CAS No. 108-95-2), 5 g of sodium hydroxide (CAS No. 1310-73-2) and 2 g of sodium citrate dihydrate (CAS No. 6132-04-3) in 200 mL of ultra-pure water. Stored in a dark bottle and prepared every week.

g) NaClO solution: Mixed 3 mL of sodium hypochlorite (CAS No. 7681-52-9) in 47 mL of ultra-pure water. Stored in a dark bottle and fleshly prepared before every measurement. This reagent needs to be 0.3 % available chlorine.

(4.5) Sampling procedures

Sampling for the nutrient samples was conducted after the sampling for other gas parameters. The seawater samples were collected into two bottles of new polyacrylate vials (10 mL) without any sample drawing tube that is usually used for the oxygen samples. Each vial was rinsed three times before filling and then was sealed without any head space immediately after the collection. The vials were put into a water bath at 22.1 ± 0.4 degree Celsius for more than 30 minutes before measuring. The seawater sample in the vial was not transferred to another container and the vial was placed on an autosampler (AIM 4000, BL TEC K.K.) tray directly. The seawater samples were analyzed within 24 hours after collection.

(4.6) Data processing

Raw data from QuAAtro 39-J were processed as follows:

a) Checked if there were any baseline shifts.

b) Checked the shape of each peak and positions of peak values. If necessary, a change was made for the positions of peak values.

c) Conducted carry-over correction and baseline drift correction followed by sensitivity correction to apply to the peak height of each sample.

d) Conducted baseline correction and sensitivity correction using linear regression. Conducted baseline correction and sensitivity correction using linear regression.

e) Using the salinity (CTD data* or determined in bottle sampling on board) and the laboratory room temperature (20 degree Celsius), the density of each sample was calculated. The obtained density was used to calculate the final nutrient concentration with the unit of μmol kg^{-1}.

f) Calibration curves to obtain the nutrient concentrations were assumed second-order equations.

* Raw CTD pre-calibrated data have been used.

(5) Certified Reference Material of nutrients in seawater

Certified reference materials produced by KANSO Co., Ltd. were used to ensure the comparability and traceability of nutrient measurements during this cruise. The KANSO CRMs are for inorganic nutrients (nitrate, nitrite, silicate, phosphate, and ammonia) in seawater and have been produced using autoclaved natural seawater based on the quality control system under ISO Guide 34 (JIS Q 0034). KANSO Co., Ltd. has been accredited under the accreditation System of the National Institute of Technology and Evaluation (ASNITE) as a CRM producer since 2011. (ASNITE 0052 R)

The certified values were the arithmetic means of the results of 30 bottles from each batch (measured in duplicates) analyzed by both KANSO Co., Ltd. and Japan Agency for Marine-Earth Science and Technology (JAMSTEC) using the colorimetric method (continuous flow analysis, CFA, method). The salinity of the calibration standards solution to obtain each calibration curve was adjusted to the salinity of the used CRMs within ± 0.5.

Each certified value of nitrate, nitrite, and phosphate of KANSO CRMs was calibrated using one of the Japan Calibration Service System (JCSS) standard solutions for each nitrate ion, nitrite ion, and phosphate ion. JCSS standard solutions were calibrated using the secondary solution of JCSS for each of

these ions. The secondary solution of JCSS was calibrated using the specified primary solution produced by the Chemicals Evaluation and Research Institute (CERI), Japan. CERI-specified primary solutions were calibrated using the National Metrology Institute of Japan (NMIJ) primary standards solution of nitrate ions, nitrite ions, and phosphate ions, respectively. The certified value of silicate of KANSO CRM was calibrated using a newly established silicon standards solution named "exp31", "exp32", and "exp64" produced by JAMSTEC and KANSO and Lot. AA produced by KANSO. This silicon standard solution was produced by a dissolution technique with an alkaline solution. The mass fraction of Si in the produced solution was calibrated based on NMIJ CRM 3645-a Si standard solution by a technology consulting system of the National Institute of Advanced Industrial Science and Technology (AIST), and this value is traceable to the International System of Units (SI).

23 sets of CRM lots CQ, CR, CO, CP, CM, and CN were used in this cruise (Table 4.7.1). Each CRM's serial number was randomly selected. The CRM bottles were stored in a room named "BIOCHEMICAL LABORATORY" on the ship, where the temperature was maintained around 20.11 degree Celsius – 23.65 degree Celsius.

Table 4.7.1 Certified concentration and the uncertainty (k=2) of CRMs (μmol kg^{-1}).

Lot	Nitrate	Nitrite*	Silicate	Phosphate	Ammonia**
CQ	0.06 ± 0.03	0.074 ± 0.07	2.20 ± 0.07	0.030 ± 0.009	1.76 ± 0.07
CR	5.46 ± 0.16	0.975 ± 0.07	14.0 ± 0.3	0.394 ± 0.014	0.95 ± 0.15
CO	15.86 ± 0.15	0.056 ± 0.04	34.72 ± 0.16	1.177 ± 0.014	0.54
CP	24.8 ± 0.3	0.318 ± 0.07	61.1 ± 0.3	1.753 ± 0.018	0.87
CM	33.2 ± 0.3	0.028 ± 0.006	100.5 ± 0.5	2.38 ± 0.03	0.59
CN	43.6 ± 0.4	0.020 ± 0.004	152.7 ± 0.8	2.94 ± 0.03	0.46

* For Nitrite concentration, there is a trend that the value has been increased 0.004 ± 0.002 μmol kg^{-1} per year. Nitrite concentration values were determined by JAMSTEC in June 2023.

** Ammonia values are all reference value. The value of CQ and CR were reported by KANSO. The other values were determined by JAMSTEC.

(6) Standards

To obtain the calibration curves, we prepared in-house standard solutions because (1) the concentrations nitrate, phosphate, and silicate of CRM lot CN were lower than the maximum concentrations in sweater samples, (2) the concentration range of nitrite of the CRMs is not available for the calibration curves, and (3) the concentrations of ammonia of the CRMs are not certified values.

(6.1) Volumetric laboratory-ware of in-house standards

All volumetric glassware and polymethylpentene (PMP)-ware used were gravimetrically calibrated. Plastic volumetric flasks were gravimetrically calibrated at the water temperature of use within 0.9 K at around 20.6 degree Celsius. Volumetric flasks of "Class A" quality are used because their nominal tolerances are 0.05 % or less over the size ranges likely to be used in this work. Since Class A flasks are made of borosilicate glass, the standard solutions were transferred to plastic bottles as quickly as possible after the solutions were made up to volume and well mixed to prevent the excessive dissolution of silicate from the glass. PMP volumetric flasks were gravimetrically calibrated and used only within 2.7 K of the calibration temperature. The computation of volume contained by the glass flasks at various temperatures other than the calibration temperatures was conducted by using the coefficient of linear expansion of borosilicate crown glass. The coefficients of cubical expansion of each glass and PMP volumetric flask were determined by the measurements in 2023. The coefficient of cubical expansion of the glass volumetric flask (SHIBATA HARIO) was 0.00000975 to 0.0000110 K^{-1} and that of the PMP volumetric flask (NALGEN PMP) was 0.00039 to 0.00042 K^{-1}. The weights obtained in the calibration weightings were corrected for the density of water and air buoyancy. All glass pipettes have nominal calibration tolerances of 0.1 % or better. These were gravimetrically calibrated to verify and improve upon this nominal tolerance.

(6.2) Reagents

For nitrate standard, "potassium nitrate 99.995 suprapur$^{®}$" provided by Merck, Batch

B1983565, CAS No. 7757-79-1, was used. For nitrite standard solution, we used nitrite ion standard solutions (NO$_2^-$ 1000) provided by Wako Chemicals, Lot TPH2043, Code. No. 146-06453. These standard solutions were certified by Wako Chemicals. The calibration result is 1004 mg L^{-1} at 20 degree Celsius. Expanded uncertainty of calibration (k=2) is 0.8 % for the calibration result. For the silicate standard solution, we used Si standard solutions Lot. AA produced by KANSO. The mass fraction of Si in the Lot. AA solution was calibrated based on NMIJ CRM 3645-a Si standard solution. For the phosphate standard, we used potassium dihydrogen phosphate anhydrous 99.995 suprapur$^{®}$" provided by Merck, Batch B2015508, CAS No.: 7778-77-0. For the ammonia standard, ammonium chloride (CRM 3011-a) provided by NMIJ, CAS No. 12125-02-9 was used. The purity of this standard was reported as >99.9 % by the manufacturer. Expanded uncertainty of calibration (k=2) was 0.026 %.

(6.3) Low nutrients seawater (LNSW)

Surface water with low nutrient concentrations was taken and filtered using a 0.20 μm pore capsule cartridge filter around 13ºN and 136ºE during the MR21-03 cruise in June 2021. Obtained seawater was drained into multiple 20 L Cubitainer (flexible containers) and stored in a cardboard box. These have been used as the low nutrients seawater (LNSW) for nutrients measurement. The concentrations of each LNSW were measured in June 2022. The averaged nutrient values in the LNSW were 0.01, 0.003,1.08, 0.075, and 0.01 μmol L^{-1} for nitrate, nitrite, silicate, phosphate, and ammonia, respectively. The concentrations of nitrate, nitrite, and ammonia were lower than the detection limit.

(6.4) Standard solutions and calibration curves

Concentrations of nutrients for standard solutions A, B, C, and D are shown in Table 4.7.2. We used the KANSO Si standard solution for A standard of silicate, which doesn't need to be neutralized by the hydrochloric acid. B standard was diluted from A standard with the following recipes shown in Table 4.7.3. To match the salinity and the density of the B standard solution to those of the LNSW, 15.00 g of sodium chloride powder was dissolved in the B standard solution, and then the final volume was adjusted to 500 mL. The C standard solution was prepared in the LNSW following the recipes shown in Table 4.7.4. Then the actual concentrations of nutrients in each standard solution were calculated based on the solution temperature, together with the determined factors of volumetric laboratory wares. The calibration curves for each run for nitrate, nitrite, silicate, and phosphate were obtained using 6 levels, C-2, C-3, C-4, C-5, C-7, and C-8. For ammonia, that was obtained using 3 levels, C-1, C-6, C-8. C-1 was LNSW, C-2, C-3, C-4, C-5, and C-7 were the CRM of nutrients in seawater, and C-6 and C-8 were diluted using the B standard solution. The D standard solutions, which were for calculating the reduction rate of the Cd coil, The was diluted from the A standard solution into the pure water. The in-house standard solutions were remade by each "renewal time" shown in Table 4.7.5.

Table 4.7.2 Nominal concentrations of nutrients for A, D, B and C standards (μmol kg^{-1}).

	A	B	D	C-1	C-2	C-3	C-4	C-5	C-6	C-7*	C-8
NO$_3$	45000	900	900	-	CQ	CR	CO	CP	-	CN	53.9
NO$_2$	21800	17	870	-	CQ	CR	CO	CP	-	CN	1.04
SiO$_2$	35500	3550		-	CQ	CR	CO	CP	-	CN	213.6
PO$_4$	6000	60		-	CQ	CR	CO	CP	-	CN	3.66
NH$_4$	2000	100	LNSW	-	-	-	-	-	3.0	-	6.0

*For samples from stations 01-15 in the Bering Sea, CRM lot CM was employed.

Table 4.7.3 B standard recipes. Final volume was 500 mL.

	A Std.
NO$_3$	10 mL
NO$_2$*	10 mL
SiO$_2$	50 mL
PO$_4$	5 mL
NH$_4$	25 mL

*NO$_2$ was D standard solution which was diluted from A standard.

Table 4.7.4 Working calibration standard recipes. Final volume was 500 mL.

C Std.	B Std.
C-6	15 mL
C-8	30 mL

Table 4.7.5 Renewal times of in-house standards.

Standard	Renewal time
A-1 Std. (NO_3)	maximum a month
A-2 Std. (NO_2)	commercial prepared solution
A-3 Std. (SiO_2)	commercial prepared solution
A-4 Std. (PO_4)	maximum a month
A-5 Std. (NH_4)	maximum a month
D-1 Std.	maximum 8 days
D-2 Std.	maximum 8 days
B Std. (mixture of A-1, D-2, A-3, A-4 and A-5 Std.)	maximum 8 days
C Std.	every 24 hours
36 µM NO_3 (diluted D-1 Std. for reduction estimate)	when C Std. renewed
35 µM NO_3 (diluted D-1 Std. for reduction estimate)	when C Std. renewed

(7) Data quality

During this cruise, a total of the 36 runs were conducted to measure the samples collected by 41 casts at 34 stations. The total number of seawater samples was 1096. The samples were collected into two vials and measured independently (replicate measurement).

(7.1) Precision

The highest-concentration standard solution (C-8) was repeatedly determined every 4 to 12 samples to obtain the analytical precision of the nutrient analyses during this cruise. During each run, the total number of the C-8 determinations was 9-15 times depending on the run. We obtained the analytical precision based on these C-8 results for each run. The overall precisions throughout this cruise were calculated based on the analytical precisions obtained from all of the runs (Table 4.7.6). During this cruise, overall median precisions were 0.13, 0.23, 0.12, 0.15, and 0.38 % for nitrate, nitrite, silicate, phosphate, and ammonia, respectively. These were comparable to those obtained during the past cruises conducted in 2009 - 2022.

(7.2) Comparability

CRM lots CN or CM was measured every run to evaluate the comparability throughout the measurement in this cruise. All of the measured concentrations of CRM lot CN for stations 01-15 (Table 4.7.7) or CM for stations 17-70 (Table 4.7.8) were within the uncertainty of certified values for nitrate, nitrite, silicate, and phosphate.

Table 4.7.6 Overall precisions based on the replicate analyses ($k=1$)

	Nitrate CV %	Nitrite CV %	Silicate CV %	Phosphate CV %	Ammonia CV %
Median	0.13	0.23	0.12	0.15	0.38
Mean	0.13	0.24	0.12	0.15	0.40
Maximum	0.20	0.53	0.19	0.24	0.78
Minimum	0.05	0.12	0.05	0.05	0.11
N	36	36	36	36	36

Table 4.7.7 CRM lot CN measurements for stations 01-15 (μmol kg^{-1}).

	Nitrate	Nitrite	Silicate	Phosphate	Ammonia
Median	43.63	0.021	153.18	2.937	0.88
Mean	43.64	0.020	153.20	2.939	0.85
STDEV	0.06	0.003	0.18	0.008	0.17
N	8	8	8	8	8

Table 4.7.8 CRM lot CM measurements for stations 17-70 (μmol kg^{-1}).

	Nitrate	Nitrite	Silicate	Phosphate	Ammonia
Median	33.25	0.027	100.54	2.389	1.13
Mean	33.23	0.027	100.50	2.389	1.10
STDEV	0.08	0.003	0.18	0.006	0.23
N	28	28	28	28	28

(7.3) Carryover

We also summarized the magnitudes of carry over, which is a sample-to-sample contamination during the flow analysis. To evaluate carryover in each run, we measured the C-8 standard solution and consecutively the LNSW solution two times. The difference from LNSW-1 to LNSW-2 was used to estimate the Carryover (%) by the following equation where [ ] means concentration.

$$\text{Carryover (\%)} = ([\text{LNSW-1}] – [\text{LNSW-2}]) / ([\text{C-8}] – [\text{LNSW-2}]) * 100 \qquad (1)$$

The carryover (%) is shown in Table 4.7.9. Overall results were low % of carryover (<0.3 % for nitrite, nitrate, silicate, and phosphate; <1 % for ammonia). The low % indicates that there is no significant issue during this cruise.

(7.4) Uncertainty (Repeatability)

Empirical equations of (2), (3) and (4) were obtained based on 36 measurements of 23 sets of CRMs (Table 4.7.1) to estimate the uncertainty (repeatability) of measurements of nitrate, silicate, and phosphate, respectively (Figs. 4.7.6-8).

Table 4.7.9 Carryovers (%)

	Nitrate	Nitrite	Silicate	Phosphate	Ammonia
Median	0.24	0.13	0.23	0.19	0.92
Mean	0.24	0.13	0.22	0.19	0.87
Maximum	0.29	0.27	0.31	0.33	1.12
Minimum	0.17	0.00	0.17	0.04	0.37
N	36	36	36	36	36

$$\text{Uncertainty of measurement of nitrate (\%)} = 0.17329 + 1.3088 * (1 / C_{NO3}) \qquad (2)$$

$$\text{Uncertainty of measurement of silicate (\%)} = 0.12886 + 3.9044 * (1 / C_{SiO2}) \qquad (3)$$

$$\text{Uncertainty of measurement of phosphate (\%)} = 0.12254 + 0.32523 * (1 / C_{PO4}) \qquad (4)$$

where C_{NO3}, C_{SiO2}, and C_{PO4} are nitrate, silicate, and phosphate concentrations of sample (μmol kg^{-1}), respectively.

Empirical equations, eq. (5) and (6) were obtained based on duplicate measurements of the samples to estimate the uncertainty (repeatability) of measurements of nitrite and ammonia (Figs. 4.7.9,10).

$$\text{Uncertainty of measurement of nitrite (\%)} =$$
$$2.2674 + 0.16483 * (1 / C_{NO2}) - 0.0000044636 * (1 / C_{NO2}) * (1 / C_{NO2}) \qquad (5)$$

87

$$\text{Uncertainty of measurement of ammonia (\%)} = 0.54051 + 1.0128 * (1 / C_{NH4}) \qquad (6)$$

where C_{NO2} and C_{NH4} are nitrite and ammonia concentrations of sample (μmol kg^{-1}), respectively.

(7.5) Detection limit and quantitative determination

The LNSW was measured every 4 to 12 samples to estimate the detection limit of the nutrient analyses during this cruise. During each run, the total number of the LNSW determination was 8-14 times depending on the run. The detection limit was calculated based on the LNSW results from all the runs by the following equation.

$$\text{Detection limit} = 3 * \text{standard deviation of repeated measurement of LNSW} \qquad (7)$$

The estimated detection limit is shown in Table 4.7.10. The quantitative determination of nutrient analyses is the concentration of which uncertainty is 33 % in the empirical equations, eq. (2) to (6). The estimated quantitative determination is also shown in Table 4.7.10.
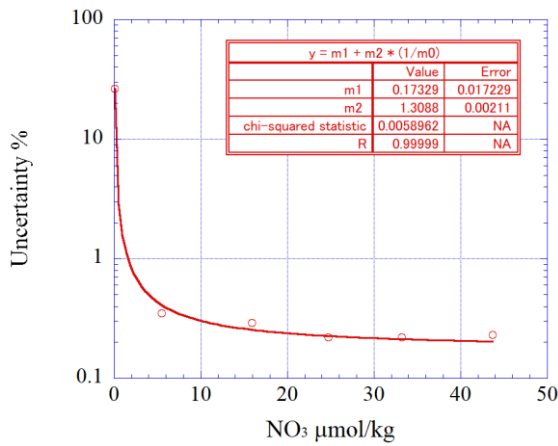
Figure 4.7.6 Uncertainty for NO$_3$.
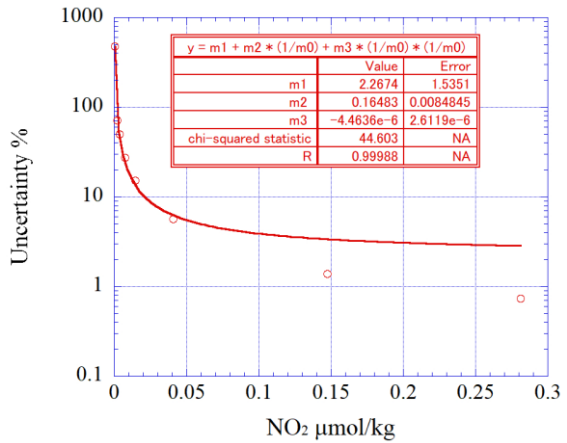
Figure 4.7.9 Uncertainty for NO$_2$.
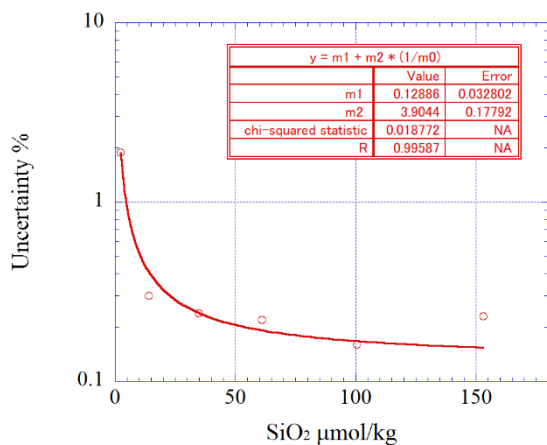
Figure 4.7.7 Uncertainty for SiO$_2$.
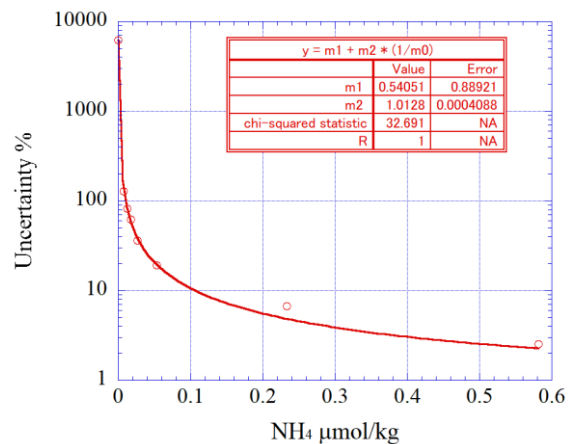
Figure 4.7.10 Uncertainty for NH$_4$.
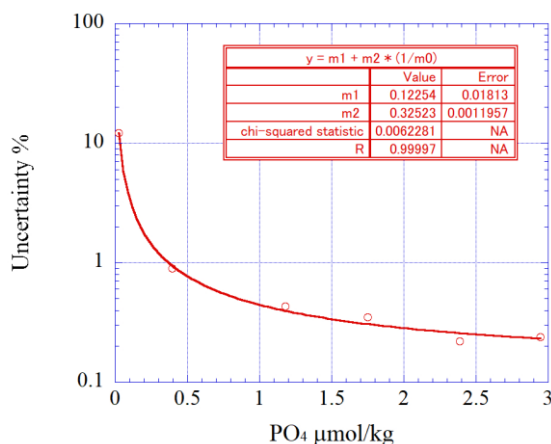
Figure 4.7.8 Uncertainty for PO4.

Table 4.7.10 Detection limit and quantitative determination.

	Nitrate $\mu mol\ kg^{-1}$	Nitrite $\mu mol\ kg^{-1}$	Silicate $\mu mol\ kg^{-1}$	Phosphate $\mu mol\ kg^{-1}$	Ammonia $\mu mol\ kg^{-1}$
Detection limit	0.02	0.004	0.09	0.007	0.02
Quantitative determination	0.04	0.005	0.12	0.010	0.03

Replicate samples were taken at most of the layers. The summary of average and standard deviation of the difference between each replicate pair of analysis was shown in Table 4.7.11.

Table 4.7.11 Average and standard deviation of the difference between each replicate pair of analysis.

	Nitrate $\mu mol\ kg^{-1}$	Nitrite $\mu mol\ kg^{-1}$	Silicate $\mu mol\ kg^{-1}$	Phosphate $\mu mol\ kg^{-1}$	Ammonia $\mu mol\ kg^{-1}$
Average	0.06	0.003	0.19	0.005	0.02
Standard deviation	0.05	0.002	0.18	0.005	0.02
N	1082	1082	1082	1082	1077

(8) Problems
a) During the measurements of samples from stations 7, 13, and 15, a wrong pump tube (WHT/WHT) was employed instead of a designated tube (BLK/BLK) for the nitrate sample line by mistake. However, there was no significant effect on the measurement results.
b) During the measurements of samples from stations 7, 13, and 15, a wrong pump tube (WHT/WHT) was employed instead of a designated tube (BLK/BLK) for ammonia (EDTA and alkaline phenol lines) by mistake. However, there was no significant effect on the measurement results.
c) We employed a N_2 gas generator for purging inside of the two autosamplers. However, the capacity of the generator is not enough for the two autosamplers. As a result, the generator supplied N_2 gas to only one autosampler.

(9) List of reagents
List of reagents used in this cruise is shown in Table 4.7.12.

(10) Data archives
These data obtained in this cruise will be submitted to the Data Management Group of JAMSTEC, and will be opened to the public via "Data Research System for Whole Cruise Information in JAMSTEC (DARWIN)" in JAMSTEC web site. <http://www.godac.jamstec.go.jp/darwin/e>

Table 4.7.12 List of reagents used in this cruise.

IUPAC name	CAS Number	Formula	Compound Name	Manufacture	Grade
4-Aminobenzenesulfonamide	63-74-1	$C_6H_8N_2O_2S$	Sulfanilamide	FUJIFILM Wako Pure Chemical Corporation	JIS Special Grade
Ammonium chloride	12125-02-9	NH_4Cl	Ammonium Chloride	FUJIFILM Wako Pure Chemical Corporation	JIS Special Grade
Antimony potassium tartrate trihydrate	28300-74-5	$K_2(SbC_4H_2O_6)_2 \cdot 3H_2O$	Bis[(+)-tartrato]diantimonate(III) Dipotassium Trihydrate	FUJIFILM Wako Pure Chemical Corporation	JIS Special Grade
Boric acid	10043-35-3	H_3BO_3	Boric Acid	FUJIFILM Wako Pure Chemical Corporation	JIS Special Grade
Hydrogen chloride	7647-01-0	HCl	Hydrochloric Acid	FUJIFILM Wako Pure Chemical Corporation	JIS Special Grade
Imidazole	288-32-4	$C_3H_4N_2$	Imidazole	FUJIFILM Wako Pure Chemical Corporation	JIS Special Grade
L-Ascorbic acid	50-81-7	$C_6H_8O_6$	L-Ascorbic Acid	FUJIFILM Wako Pure Chemical Corporation	JIS Special Grade
N-(1-Naphthalenyl)-1,2-ethanediamine, dihydrochloride	1465-25-4	$C_{12}H_{16}Cl_2N_2$	N-1-Naphthylethylenediamine Dihydrochloride	FUJIFILM Wako Pure Chemical Corporation	for Nitrogen Oxides Analysis
Oxalic acid	144-62-7	$C_2H_2O_4$	Oxalic Acid	FUJIFILM Wako Pure Chemical Corporation	Wako Special Grade
Phenol	108-95-2	C_6H_6O	Phenol	FUJIFILM Wako Pure Chemical Corporation	JIS Special Grade
Potassium nitrate	7757-79-1	KNO_3	Potassium Nitrate	Merck KGaA	Suprapur®
Potassium dihydrogen phosphate	7778-77-0	KH_2PO_4	Potassium dihydrogen phosphate anhydrous	Merck KGaA	Suprapur®
Sodium chloride	7647-14-5	NaCl	Sodium Chloride	FUJIFILM Wako Pure Chemical Corporation	TraceSure®
Sodium citrate dihydrate	6132-04-3	$Na_3C_6H_5O_7 \cdot 2H_2O$	Trisodium Citrate Dihydrate	FUJIFILM Wako Pure Chemical Corporation	JIS Special Grade
Sodium dodecyl sulfate	151-21-3	$C_{12}H_{25}NaO_4S$	Sodium Dodecyl Sulfate	FUJIFILM Wako Pure Chemical Corporation	for Biochemistry
Sodium hydroxide	1310-73-2	NaOH	Sodium Hydroxide for Nitrogen Compounds Analysis	FUJIFILM Wako Pure Chemical Corporation	for Nitrogen Analysis
Sodium hypochlorite	7681-52-9	NaClO	Sodium Hypochlorite Solution	Kanto Chemical co., Inc.	Extra pure
Sodium molybdate dihydrate	10102-40-6	$Na_2MoO_4 \cdot 2H_2O$	Disodium Molybdate(VI) Dihydrate	FUJIFILM Wako Pure Chemical Corporation	JIS Special Grade
Sodium nitroferricyanide dihydrate	13755-38-9	$Na_2[Fe(CN)_5NO] \cdot 2H_2O$	Sodium Pentacyanonitrosylferrate(III) Dihydrate	FUJIFILM Wako Pure Chemical Corporation	JIS Special Grade
Sulfuric acid	7664-93-9	H_2SO_4	Sulfuric Acid	FUJIFILM Wako Pure Chemical Corporation	JIS Special Grade
tetrasodium;2-[2-[bis(carboxylatomethyl)amino]ethyl-(carboxylatomethyl)amino]acetate;tetrahydrate	13235-36-4	$C_{10}H_{12}N_2Na_4O_8 \cdot 4H_2O$	Ethylenediamine-N,N,N',N'-tetraacetic Acid Tetrasodium Salt Tetrahydrate (4NA)	Dojindo Molecular Technologies, Inc.	-
Synonyms: t-Octylphenoxypolyethoxyethanol 4-(1,1,3,3-Tetramethylbutyl)phenyl-polyethylene glycol Polyethylene glycol tert-octylphenyl ether	9002-93-1	$(C_2H_4O)_nC_{14}H_{22}O$	Triton®X-100	MP Biomedicals, Inc.	-

(11) References

Becker, S., Aoyama, M., Malcolm E., Woodward, S., Bakker, K., Coverly, S., Mahaffey, C., Tanhua, T., (2019) The precise and accurate determination of dissolved inorganic nutrients in seawater, using Continuous Flow Analysis methods, n: The GO-SHIP Repeat Hydrography Manual: A Collection of Expert Reports and Guidelines. Available online at: http://www.go-ship.org/HydroMan.html. DOI: http://dx.doi.org/10.25607/OBP-555

Grasshoff, K. (1976). Automated chemical analysis (Chapter 13) in Methods of Seawater Analysis. With contribution by Almgreen T., Dawson R., Ehrhardt M., Fonselius S. H., Josefsson B., Koroleff F., Kremling K. Weinheim, New York: Verlag Chemie.

Grasshoff, K., Kremling K., Ehrhardt, M. et al. (1999). Methods of Seawater Analysis. Third, Completely Revised and Extended Edition. WILEY-VCH Verlag GmbH, D-69469 Weinheim (Federal Republic of

Germany).

Hydes, D.J., Aoyama, M., Aminot, A., Bakker, K., Becker, S., Coverly, S., Daniel, A., Dickson, A.G., Grosso, O., Kerouel, R., Ooijen, J. van, Sato, K., Tanhua, T., Woodward, E.M.S., Zhang, J.Z., (2010). Determination of Dissolved Nutrients (N, P, Si) in Seawater with High Precision and Inter-Comparability Using Gas-Segmented Continuous Flow Analysers, In: GO-SHIP Repeat Hydrography Manual: A Collection of Expert Reports and Guidelines. IOCCP Report No. 14, ICPO Publication Series No 134.

Kimura (2000). Determination of ammonia in seawater using a vaporization membrane permeability method. 7th auto analyzer Study Group, 39-41.

Murphy, J., and Riley, J.P. (1962). Analytica Chimica Acta 27, 31-36.

4.8 Chlorofluorocarbons and Sulfur hexafluoride

December 06, 2023
Yuichiro Kumamoto
Japan Agency for Marine-Earth Science and Technology

(1) Personnel

Yuichiro Kumamoto [1], Masahito Shigemitsu [1]
1) Japan Agency for Marine-Earth Science and Technology

(2) Objectives

Chlorofluorocarbons (CFCs) and sulfur hexafluoride (SF_6) are anthropogenic stable gases. These atmospheric gases can slightly dissolve in sea surface water by air-sea gas exchange and then spread into the ocean interior. Thus, these gases could be used as chemical tracers for ocean circulation and ventilation. To discuss the ventilation rates and pathways of the North Pacific water, we collected seawater samples at every water sampling station (a total of 33 stations, except station 1), and measured concentrations of CFCs, namely CFC-11 (CCl_3F), CFC-12 (CCl_2F_2), CFC-113 ($C_2Cl_3F_3$), and SF_6 in the seawater samples on board.

(3) Instruments

Two sets (A and B) of the analyzing system, each of which consists of seawater stripping, gas traps, standard gas loops, and gas chromatograph, were used (Fig. 4.8.1). The system was driven by pure N_2 gas. We employed the first-grade N_2 gas (Purity > 99.99995%) supplied by Taiyo Nippon Sanso Corporation. The N_2 gas passed through the purifier column with Molecular Sieve 13X before it was introduced into the system (CFCs/SF_6-free N_2 gas). A volume of seawater sample (about 200 ml) was transported into a stripping chamber. Dissolved SF_6 and CFCs in the seawater were extracted by the CFCs/SF_6-free N_2 gas purging for 8 minutes at 220 ml min^{-1}. The gases were dried in the desiccant tube (magnesium perchlorate), and trapped in the main trap at −80 °C. The main trap was a 30-cm length of 1/8-inch stainless steel tube with 80/100 mesh Porapak Q (5 cm) and 60/80 mesh Carboxen 1000 (5cm). Stripping efficiency was estimated from repeat stripping (three times) of surface seawater for every station. More than 99 % of dissolved SF_6 and CFCs were extracted in the first stripping. The trapped gases in the main trap were released by heating at 180 °C. After one minute of heating, the released gases were transferred into the focus trap, which is the same as the main trap but with 1/16-inch tube, at −80 °C for 30 seconds.

The gases trapped in the focus trap were released by heating at 180 °C and then the first carrier N_2 gas transferred the gases into the pre-column 1 (PC 1, ~6 m of Silica Plot capillary column with 0.53 mm i.d. and 6 μm film thickness) in the oven of the gas chromatograph (Shimadzu GC-2014) at 95 °C. The injected gases were roughly separated in the PC 1, and the SF_6 and CFCs were eluted into the pre-column 2 (PC 2, ~5 m of Molsieve 5A Plot capillary column with 0.53 mm i.d. of and 15 μm film thickness). Then, the PC 1 was connected to a cleaning (back flush) line, and the remained gases in the PC 1, which have high boiling points, were flushed out by a counter flow of the back-flush N_2 gas. SF_6 and CFCs were eluted from the PC 2 into the main column 1 (MC 1, ~9 m of Pola Bond-Q capillary column with 0.53 mm i.d. and 6 μm film thickness, and ~18 m of Silica Plot capillary column) but N_2O was retained in the PC 2. The PC 2 was then connected to the second carrier N_2 gas and N_2O was transported into the main column 2 (MC 2, ~3 m of Molsieve 5A Plot connected to ~9 m of Pola Bond-Q capillary column). SF_6 and CFCs were further separated in the MC 1 and detected separately in the first Electron Capture Detector (ECD) at 300 °C. N_2O eluted from the MC 2 was detected in the second ECD. Although the chromatogram of N_2O was obtained, the concentration of N_2O was not calculated in this cruise for some reasons. The mass flow rates of the carrier/back-flush and detector make-up N_2 gases are about 10 ml min^{-1} and 27 ml min^{-1}, respectively.
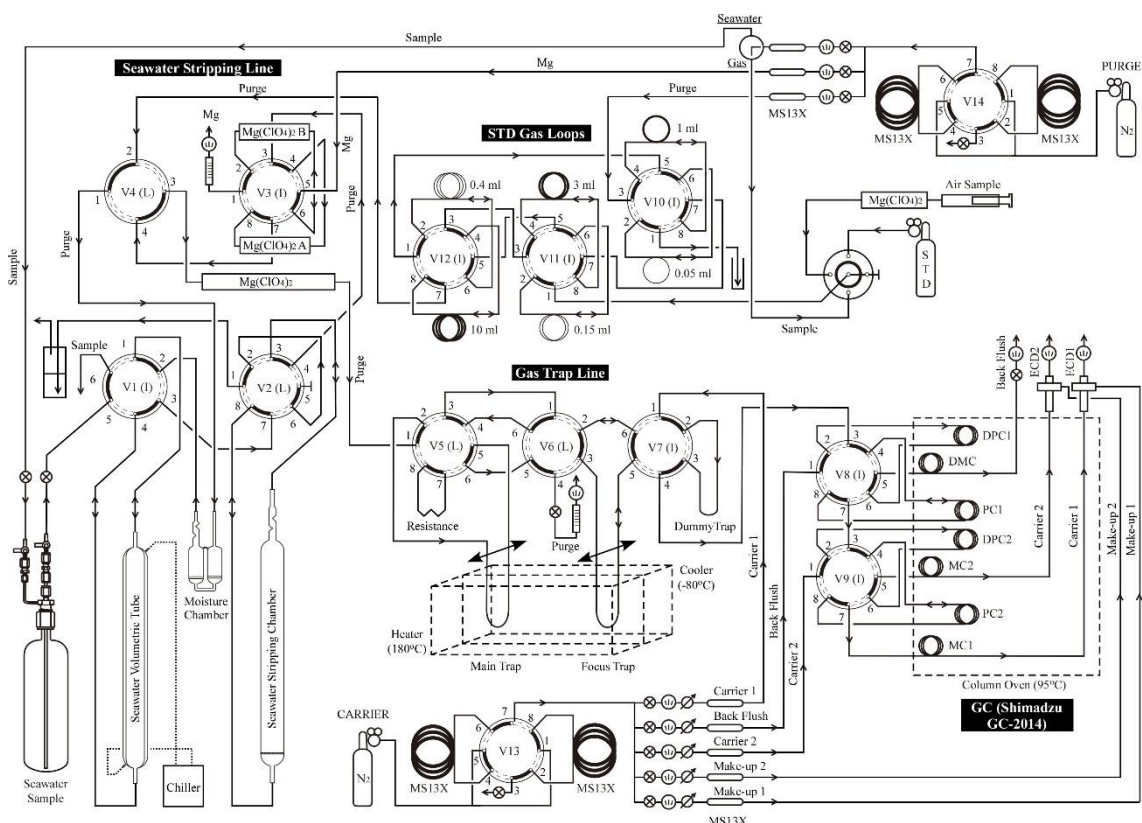
Figure 4.8.1 Outline of the analyzing system for measurements of CFC-11, CFC-12, CFC-113, SF_6, and N_2O.

(4) Standard gases

Two high-pressure gas cylinders of the standard gas for CFCs/SF_6 (Taiyo Nippon Sanso Corporation) were employed during this cruise (Table 4.8.1). To confirm the comparability of measurements of CFCs/SF_6 in our laboratory, we compared the concentrations of standard gas cylinders used in this cruise (MR23-07) with those in the past cruise (MR21-04), and a good agreement between them was obtained. We got the calibration curve (cubic curve) by combining of the standard gas loops (Table 4.8.2) after corrections for the temperature of the gas loops and atmospheric pressure. We also measured the standard gas every 10-15 sample measurements for sensitivity correction.

Table 4.8.1 Concentration of the standard gases.

System	Cylinder Lot	SF_6 (ppt)	CFC-11 (ppt)	CFC-12 (ppt)	CFC-113 (ppt)	(N_2O) (ppm)
A	CPB-20771	9.98	919	489	77.8	15.1
B	CPB-26801	10.4	893	486	80.1	14.8

Table 4.8.2 Volumes of the standard gas loops (ml).

System	L (large)	l (small)	M (large)	m (small)	S (large)	s (small)
A	9.985	0.244	3.291	0.117	1.130	0.055
B	9.965	0.416	3.107	0.156	1.005	0.078

(5) Air sampling and measurement

During the cruise, we measured concentrations of CFCs/SF_6 in the atmosphere to confirm the concentrations of the standard gases and to check saturation levels in the sea surface water. The air sample was continuously introduced into a laboratory using an air pump. The other end of 10 mm OD

Dekaron tube was put on the head of the compass deck. The tube was relayed by a three-way stopcock. An air sample was collected from the flowing air into a 200 ml glass cylinder by attaching the cylinder to the cock. A volume of air sample (about 10 ml) was introduced into the system using the L-loop (Table. 4.8.2).

(6) Seawater sampling

Discrete water samples from each station were collected using 12-liter sampling bottles mounted on the CTD system. Each sample was collected into a glass bottle of 450 ml from a spigot of the sampling bottle through a Tygon tube after water sampling for dissolved oxygen measurement. Before water sampling, the glass bottle was purged with the CFCs/SF_6-free N_2. The seawater was overflowed by twice the bottle volume. The samples were stored in a water bath at about 7°C immediately after the water sampling and then were measured usually within 18 hours after the sampling.

(7) Replicate measurement of seawater sample

We collected seawater samples in two glass bottles from the same sampling bottle collected at about 250 and 900 dbar (replicate sampling). We estimated the analytical precision (repeatability) of the seawater measurement from the results of the replicate pair samples. The standard deviations of the replicate pair measurements of CFC-11, CFC-12, CFC-113, and SF_6 were 0.008 pmol kg^{-1} (n=64), 0.010 pmol kg^{-1} (n=64), 0.004 pmol kg^{-1} (n=64), and 0.038 fmol kg^{-1} (n=64), respectively.

(8) Blank determination

During the sampling and measurement, contamination of the water sample from CFCs/SF_6 in the atmosphere should be avoided as much as possible. In this cruise, we tested the contamination from the Tygon tube (about 30 cm in length) used in the water sampling. We collected seawater in the glass bottles from 2000 dbar at station 68 (28.5ºN/177.8ºE). A glass bubbler tube (sintered glass) was attached to the glass bottle. Then the seawater in the glass bottle was stripped with the CFCs/SF_6-free N_2 at a flow rate of 100-150 ml min^{-1} for more than 10 hours (Fig. 4.8.2). Just after the stripping, we measured CFC-11, CFC-12, CFC-113, and SF_6 in the stripped deep water and found that the concentrations of all the gasses were below the detection limit. Next, we introduced the CFCs/SF_6-free seawater into the analyzing system through the Tygon tube (Fig. 4.8.3), which was used in the water sampling from the 12-liter sampling bottle. And we found small but significant peaks of CFC-11, CFC-12, and CFC-113 on the chromatogram, which correspond to those observed on the chromatograms for measurements of deep water (< 2000 dbar) in the North Pacific Ocean. These results indicated that (1) the contamination in the analyzing system was negligible and (2) the Tygon tube used in the water sampling is one of the significant sources of the contamination (blank).

Figure 4.8.2   Figure 4.8.3

(9) Quality control flag assignment

The quality of the concentration reported has not been controlled yet. And the concentrations have not been corrected for the tripping efficiency (section 3), temporal change in the sensitivity (section 4), and the blank determination (section 8).

(10) Problems

a) October 10 The flow rate of the standard gas in the system B was reduced. Although we cleaned the switching valve connected to the standard gas cylinder, the flow rate was still slow. We replaced the narrow stainless-steel tube for the standard gas drain with a Teflon tube whose I.D. was wider than 1 mm, and then enough flow rate was restored. We also replaced the narrow stainless-steel tube of the system A with a wider Teflon tube.

b) October 27 During the measurements of seawater samples from station 50, CFCs and SF_6 peaks on the chromatogram reduced and disappeared. We found that the stainless-steel tube connected to the main trap was broken (Fig. 4.8.4). We replaced the broken tube and ordinary peaks of the standard gases were restored. The breaking was probably derived from metallic fatigue during the movement of the trap. The quality flags for #1, #5-12 of station 50 were assigned to be "4 (bad)".

Figure 4.8.4

c) October 28 Valve #2 of the system A did not work correctly because of the disconnection of its signal wire. The defect was fixed by the position readjustment of a bundle of signal wires behind the relay box. But it disconnected again on November 6 and has not been restored.

d) The reserve switch of valve #11 for the standard gas loops (loops M/m) in the system B did not work correctly. This should be repaired.

(11) Data archives

The data obtained in this cruise will be submitted to the Data Management Group of JAMSTEC, and will be open to the public via "Data Research System for Whole Cruise Information in JAMSTEC (DARWIN)" in the JAMSTEC web site.

4.9 Dissolved inorganic carbon (C_T) and total alkalinity (A_T)

(1) Personnel

> *Akihiko Murata (JAMSTEC)*
> *Nagisa Fujiki (MWJ)*
> *Masahiro Orui (MWJ)*
> *Yasuhiro Arii (MWJ)*
> *Takuya Izutsu (MWJ)*

(2) Objectives

Concentrations of CO_2 in the atmosphere are now increasing at a rate of about 2.0 ppmv year^{-1} owing to human activities such as burning of fossil fuels, deforestation, and cement production. It is an urgent task to estimate as accurately as possible the absorption capacity of the oceans against the increased atmospheric CO_2, and to clarify the mechanism of the CO_2 absorption, because the magnitude of the anticipated global warming depends on the levels of CO_2 in the atmosphere, and because the ocean currently absorbs 1/3 of the 6 Gt of carbon emitted into the atmosphere each year by human activities.

The Pacific Ocean has been known as a significant uptake region of anthropogenic CO_2. However, it is unclear that the ocean can continue to absorb anthropogenic CO_2 into the future. We intended to quantify how much anthropogenic CO_2 was absorbed in the ocean interior of the Pacific Ocean by comparing the data obtained in this cruise with those collected in 2007. For the purpose, we measured CO_2-system properties such as dissolved inorganic carbon (C_T), and total alkalinity (A_T) in the oceans.

(3) Apparatus
i. C_T

Measurement of C_T was made with automated TCO$_2$ analyzer (Nippon ANS, Inc., Japan). The system comprises of a seawater dispensing system, a CO_2 extraction system and a coulometer (Model 3000, Nippon ANS, Inc., Japan). Specification of the system is as follows:

The seawater dispensing system has an auto-sampler (6 ports), which dispenses seawater from a 250 ml borosilicate glass bottle (DURAN® glass bottle, 250ml) into a pipette of about 15 ml volume by PC control. The pipette is kept at 20 °C by a water jacket, in which water from a water bath set at 20 °C is circulated. CO_2 dissolved in a seawater sample is extracted in a stripping chamber of the CO_2 extraction system by adding phosphoric acid (~ 10 % v/v) of about 2 ml. The stripping chamber is approx. 25 cm long and has a fine frit at the bottom. The acid is added to the stripping chamber from the bottom of the chamber by pressurizing an acid bottle for a given time to push out the right amount of acid. The pressurizing is made with nitrogen gas (99.9999 %). After the acid is transferred to the stripping chamber, a seawater sample kept in a pipette is introduced to the stripping chamber by the same method as in adding an acid. The seawater reacted with phosphoric acid is stripped of CO_2 by bubbling the nitrogen gas through a fine frit at the bottom of the stripping chamber. The CO_2 stripped in the chamber is carried by the nitrogen gas (flow rates is 140 ml min^{-1}) to the coulometer through a dehydrating module. The module consists of two electric dehumidifiers (kept at ~4 °C) and a chemical desiccant (Mg(ClO$_4$)$_2$).

The measurement sequence such as system blank (phosphoric acid blank), 1.5 % CO_2 gas (nitrogen-base) in a nitrogen base, sea water samples (6) is programmed to repeat. The measurement of 1.5 % CO_2 gas is made to monitor response of coulometer solutions purchased from UIC, Inc.

The repeatability calculated from replicate seawater samples was 0.7 ± 0.6 μmol kg^{-1} (n = 78).

ii. A_T

Measurement of A_T was made based on spectrophotometry with a single acid addition procedure using a custom-made system (Nippon ANS, Inc., Japan). The system comprises of a water dispensing unit, an auto-syringe (Hamilton) for hydrochloric acid, a spectrophotometer (TM-UV/VIS C10082CAH, Hamamatsu Photonics, Japan), and a light source (Mikropack, Germany), which are automatically controlled by a PC. The water dispensing unit has a water-jacketed pipette (~40 mL at 25°C) and a titration cell, which is also controlled at 25°C.

A seawater of approx. 40 ml is transferred from a sample bottle (DURAN® glass bottle, 100 ml) into the pipette by pressurizing the sample bottle (nitrogen gas), and is introduced into the titration cell. The seawater is used to rinse the titration cell. Then, Milli-Q water is introduced into the titration cell, also for rinse. A seawater of approx. 40 ml is weighted again by the pipette, and is transferred into the titration cell. Then, for seawater blank, absorbances are measured at three wavelengths (730, 616 and 444

nm). After the measurement, an acid titrant, which is a mixture of approx. 0.05 M HCl at 25°C in 0.65 M NaCl and ~40 μM bromocresol green (BCG) is added into the titration cell. The volume of the acid titrant is changed between ~1.9 mL and ~2.1 mL according to estimated values of A_T. The seawater + acid titrant solution is stirred for over 9 minutes with bubbling by nitrogen gas in the titration cell. Then, absorbances at the three wavelengths are measured.

Calculation of A_T is made by the following equation:

$$A_T = (-[H^+]_T V_{SA} + M_A V_A)/V_S,$$

where M_A is the molarity of the acid titrant added to the seawater sample, $[H^+]_T$ is the total excess hydrogen ion concentration in the seawater, and V_S, V_A and V_{SA} are the initial seawater volume, the added acid titrant volume, and the combined seawater plus acid titrant volume, respectively. $[H^+]_T$ is calculated from the measured absorbances based on the following equation (Yao and Byrne, 1998):

$$pH_T = -\log[H^+]_T = 4.2699 + 0.002578(35 - S) + \log((R - 0.00131)/(2.3148 - 0.1299R))$$
$$- \log(1 - 0.001005S),$$

where S is the sample salinity, and R is the absorbance ratio calculated as:

$$R = (A_{616} - A_{730})/(A_{444} - A_{730}),$$

where A_i is the absorbance at wavelength i nm.

The repeatability calculated from replicate seawater samples was 0.7 ± 0.6 μmol kg^{-1} (n = 76).

(4) Results

Cross sections of C_T, and A_T (uncorrected data) during the cruise are illustrated in Figs. 4.9.1 – 4.9.2.
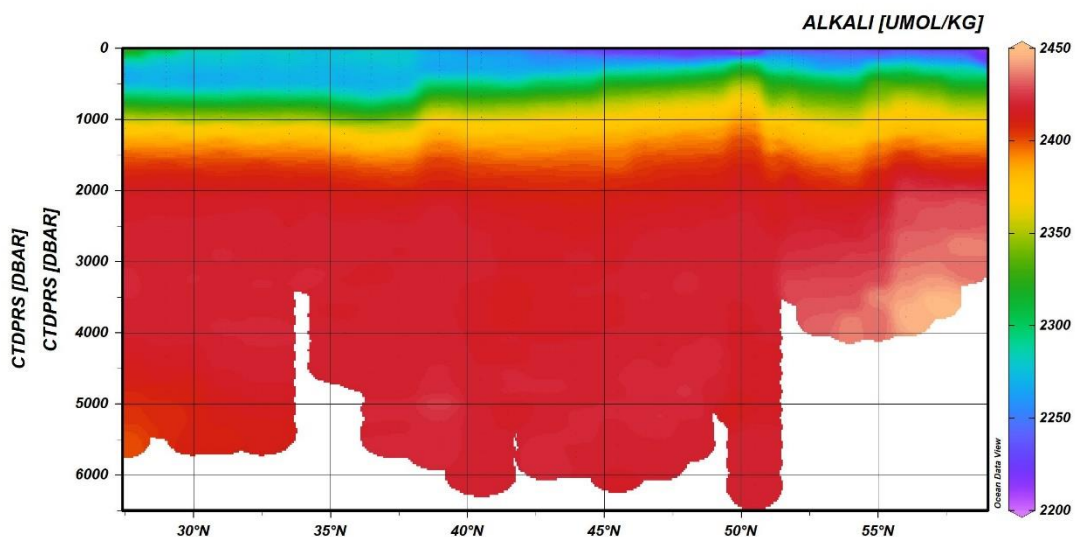
Fig. 4.9.1 Distributions of C_T along the section in MR23-07.

References

Yao W. and R. H. Byrne (1998), Simplified seawater alkalinity analysis: Use of linear array spectrophotometers. *Deep-sea Research Part I*, **45**, 1383-1392.

4.10 Chlorophyll *a*

(1) Personnel

Kosei Sasaoka (JAMSTEC)
Misato Kuwahara (MWJ)
Katsunori Sagishima (MWJ)
Tomokazu Chiba (MWJ)

(2) Objectives

Chlorophyll *a* is one of the most convenient indicators of phytoplankton biomass, and has been used extensively for the estimation of phytoplankton abundance in various aquatic environments. In this study, we investigated meridional distribution of phytoplankton biomass along the P14N section, including the Bering Sea and North Pacific. The chlorophyll *a* data is also utilized for calibration of fluorometers, which were installed in the surface water monitoring and CTD profiler system.

(3) Instrument and Method

Seawater samples were collected in 250 mL brown Nalgene bottles without head-space, by using the Niskin bottles and a bucket at the surface. All samples were gently filtrated by low vacuum pressure (<0.02 MPa) through Whatman GF/F filter (diameter 25 mm) in the dark room. Whole volume of each sampling bottle was precisely measured in advance. After filtration, phytoplankton pigments were immediately extracted in 7 ml of N,N-dimethylformamide (DMF), and samples were stored at -20°C under the dark condition to extract chlorophyll *a* more than 24 hours. Chlorophyll *a* concentrations were measured by the Turner fluorometer (10-AU-005, TURNER DESIGNS), which was previously calibrated against a pure chlorophyll *a* (Sigma-Aldrich Co., LLC) (Figure 4.10.1). To estimate the chlorophyll *a* concentrations, we applied to the fluorometric "Non-acidification method" (Welschmeyer, 1994).

(4) Preliminary results

Vertical distributions of chlorophyll *a* concentration at each station (n=34) along the P14N line during the cruise were shown in Figure 4.10.2. Cross section of chlorophyll *a* concentration along the P14N line was shown in Figure 4.10.3. Particularly, high chlorophyll *a* concentrations (over 1.0 mgm^{-3}) were clearly seen in the surface layer (0-50m) at northward stations from Stn.20 (51N) of the Bering Sea. On the other hand, the chlorophyll *a* concentrations were relatively low (less than 0.5 mgm^{-3}) in all sampling depths at southward stations from Stn.23 (50N) of the North Pacific, and the weak subsurface chlorophyll *a* maximum (about 0.2-0.5 mgm^{-3}) were captured between 50-110m depth in the southern part of the section (39-27.5N; Stn.47-70).

To examine the measurement precision, 68-pairs of replicate samples were obtained from hydrographic casts at the chlorophyll *a* maximum and 10m depth. The absolute values of the difference between replicate samples were 0-0.08 mgm^{-3}, and the precision estimated from the standard deviation of them were approximately 0.01.

(5) Reference

Welschmeyer, N. A. (1994): Fluorometric analysis of chlorophyll a in the presence of chlorophyll b and pheopigments. Limnor. Oceanogr., 39, 1985-1992.
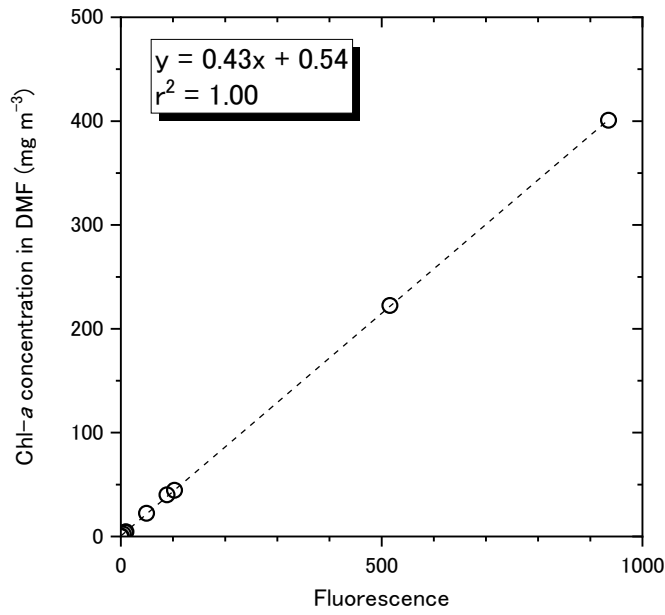
Figure 4.10.1 Relationships between pure chlorophyll *a* concentrations and fluorescence light intensity (n=10).
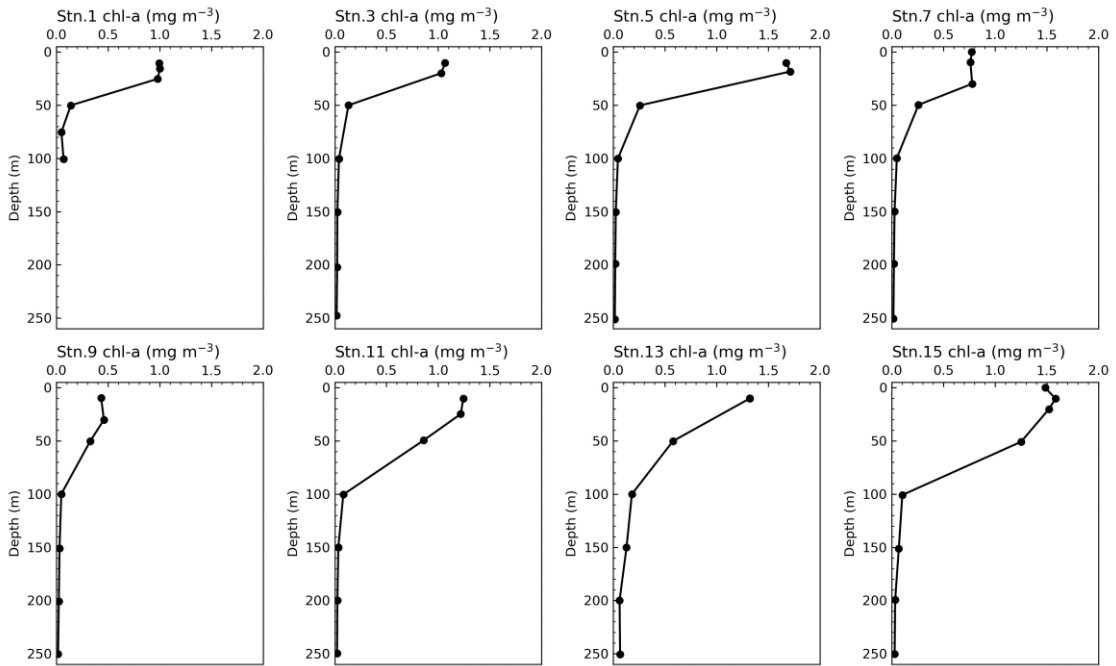
Figure 4.10.2 Vertical profiles of chlorophyll *a* concentration at each station (n=34) along the P14N section obtained from hydrographic casts.

Figure 4.10.2 (Continued)

100
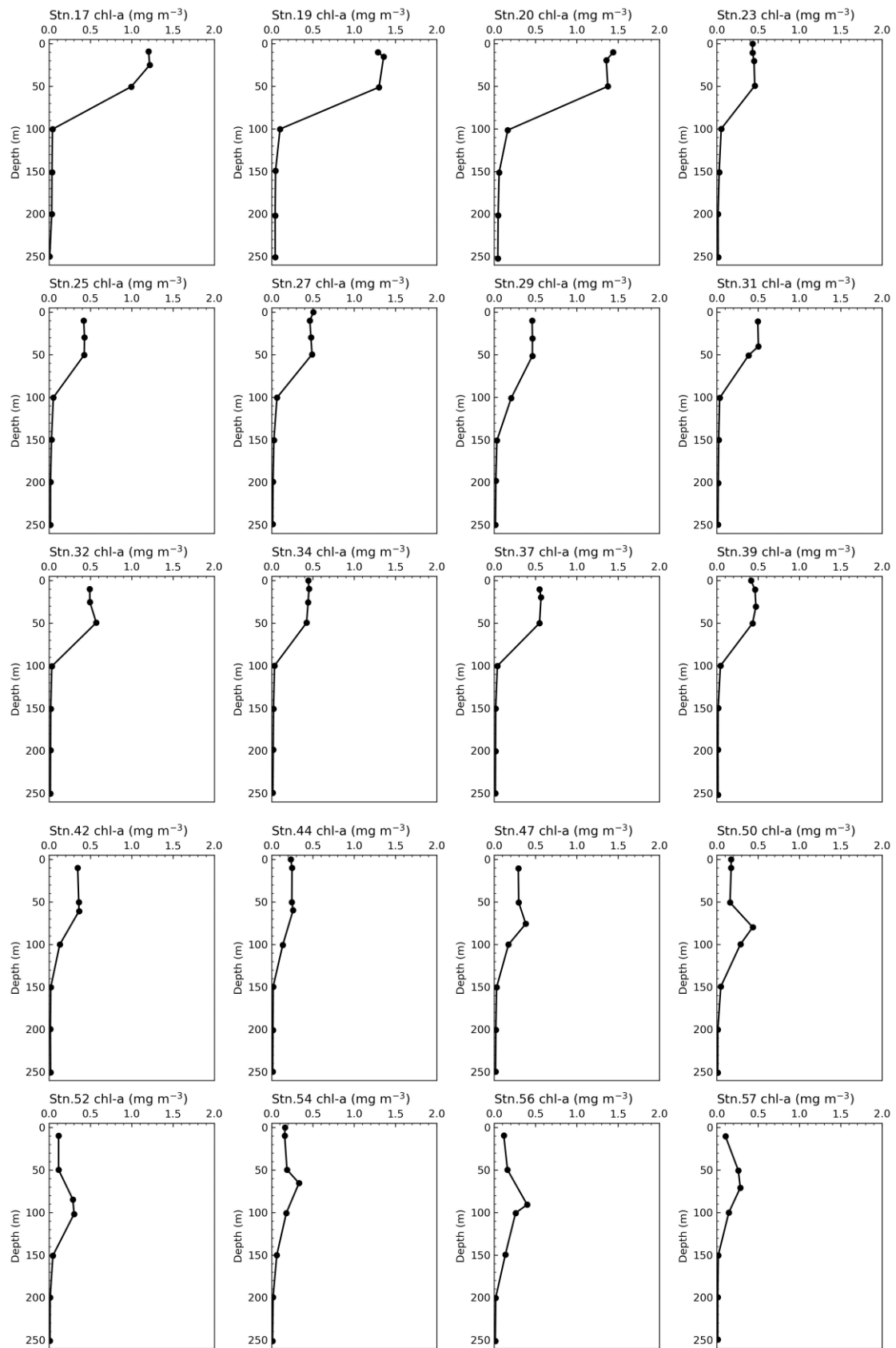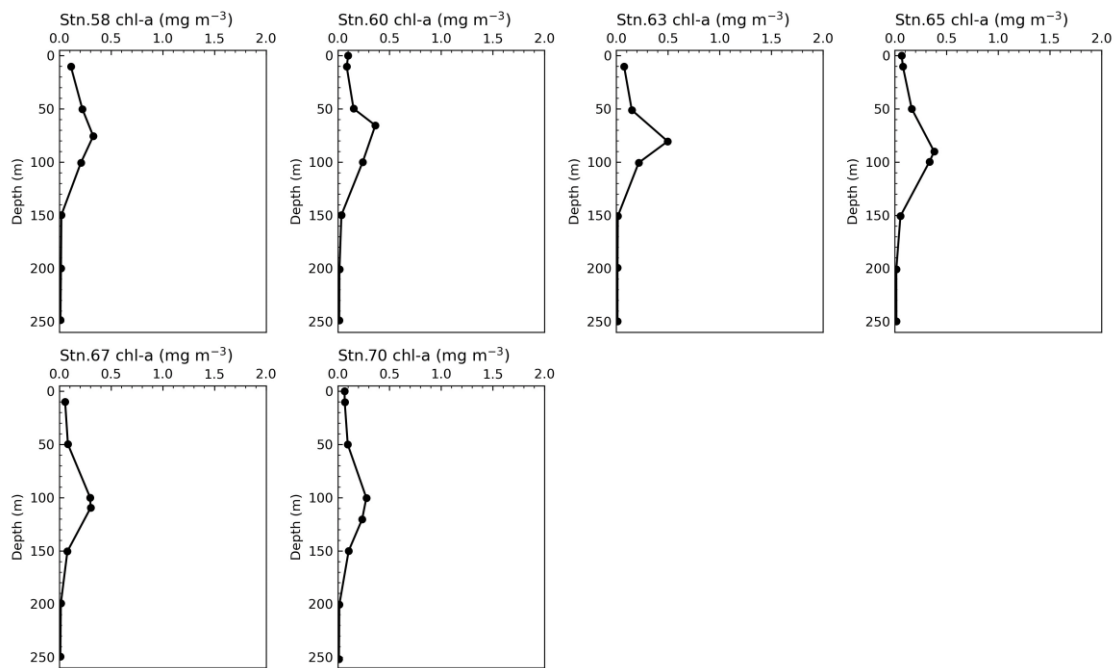
Figure 4.10.2 (Continued)
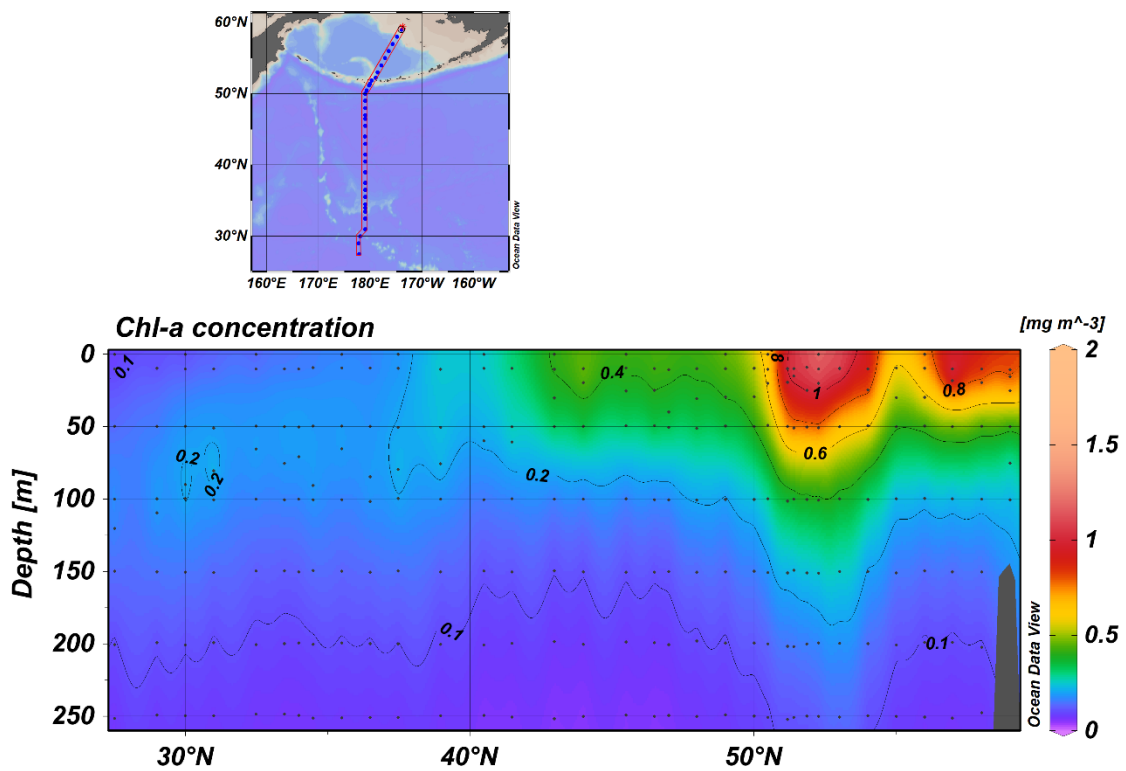
Figure 4.10.3 Cross section of chlorophyll *a* concentrations along the P14 section (upper map) obtained from hydrographic casts.

4.11 Carbon isotopes

November 06, 2023

Yuichiro Kumamoto

Japan Agency for Marine-Earth Science and Technology (JAMSTEC)

(1) Personnel

Yuichiro Kumamoto

Japan Agency for Marine-Earth Science and Technology

(2) Objective

In order to investigate the water circulation and carbon cycle in the North Pacific Ocean and Bering Sea, seawaters for measurements of carbon-14 (radiocarbon) and carbon-13 (stable carbon) ratios of dissolved inorganic carbon were collected by the hydrocasts from surface to near bottom.

(3) Sample collection

The sampling stations and number of samples are summarized in Table 4.11.1. All samples for carbon isotope ratios (total 178 samples) were collected at 8 stations using the 12-liter bottles. The seawater sample was siphoned into a 250 cm^3 glass bottle with enough seawater to fill the glass bottle 2 times. Within a few hours after sampling, 10 cm^3 of seawater was removed from the bottle and poisoned by 0.1 cm^3 μl of saturated $HgCl_2$ solution. Then the bottle was sealed by a glass stopper with Apiezon grease M and stored in a dark space on board.

Table 4.11.1 Sampling stations and number of samples for carbon isotopic ratios.

Station	Lat. (N)	Long. (E)	Sampling Date (UTC)	Number of samples	Max. Pressure (dbar)
005	56.98	-175.68	2023/10/11	20	3528.8
011	54.00	-177.89	2023/10/09	21	3851.1
025	50.01	178.99	2023/10/17	24	5080.0
032	46.49	179.01	2023/10/21	24	5761.0
042	41.49	179.00	2023/10/24	24	5146.9
052	36.49	179.01	2023/10/27	23	4574.4
058	33.48	178.99	2023/10/28	19	2963.3
067	29.00	177.75	2023/10/31	23	5229.2
			Total	178	

(4) Sample preparation and measurements

In our laboratory, dissolved inorganic carbon in the seawater samples will be stripped as CO_2 gas cryogenically and split into three aliquots: radiocarbon measurement (about 200 μmol), carbon-13 measurement (about 100 μmol), and archive (about 200 μmol). The extracted CO_2 gas for radiocarbon will be then converted to graphite catalytically on iron powder with pure hydrogen gas. The carbon-13 ratio ($^{13}C/^{12}C$) of the extracted CO_2 gas will be measured using a mass spectrometer (Finnigan MAT253). The carbon-14 ratio ($^{14}C/^{12}C$) in the graphite sample will be measured by Accelerator Mass Spectrometry.

(5) Data archives

The data obtained in this cruise will be submitted to the Data Management Group of JAMSTEC and will be opened to the public via "Data Research System for Whole Cruise Information in JAMSTEC (DARWIN)" in the JAMSTEC web site.

4.12 Particulate and dissolved organic matter in the surface waters
(1) Personnel
   Masahito Shigemitsu, Kosei Sasaoka, and Masahide Wakita (JAMSTEC)

(2) Introduction
   Redfield ratio in the ocean has been used to quantify carbon fluxes there by relating cycles of nitrogen and phosphorus to carbon. However, several lines of evidence have recently shown that particulate organic matter in the surface ocean has variable C:P, N:P, and C:N ratios among oceanic regions. So far, there have not been studies that measure particulate organic carbon (POC), nitrogen (PON), and phosphorus (POP) as well as dissolved organic carbon (DOC), nitrogen (DON), and phosphorus (DOP) in the surface ocean, and compare the spatial patterns of POC, PON, and POP with those of dissolved correspondents.

   In this cruise, we try to clarify the latitudinal patterns in the elemental ratios of particulate and dissolved organic matter in the North Pacific.

(3) Methods
Bucket sampling
   Water samples for organic matter were collected by using a ~20L bucket at the stations, 7, 15, 23, 27, 34, 39, 44, 50, 54, 60, 65, and 70. Water sample at each station was divided into duplicates for POC/PON/DOC/DON and POP/DOP, respectively, and then those were treated using pre-combusted glass fiber filters (GF/F, Whatman). Particulate matters on the filters, for the measurements of POC/PON/POP, were wrapped in combusted aluminum foil and were immediately stored at -20 °C until analysis on land. The filtrates, for the DOC/DON/DOP measurements, were also frozen at -20 °C until analysis immediately after the filtration.

DOC/DON measurement
The samples will be thawed at room temperature and the DOC concentrations will be measured by a Shimadzu TOC-L system coupled with a Shimadzu Total N analyzer in JAMSTEC.

DOP measurement
DOP will be estimated as the difference between total dissolved phosphorus (TDP) and phosphate. As for TDP measurements, the samples will be autoclaved in acid potassium persulfate solution at 123 °C for 120 min (Hansen and Koroleff, 1999; Ridal and Moore, 1990), and then the concentrations will be determined by a colorimetric method.

POC/PON measurement
POC/PON will be measured by an elemental analyzer in JAMSTEC after particulate inorganic carbon is removed by HCl.

POP measurement
POP will be measured by the same colorimetric method as that used in the TDP analysis after high temperature combustion and acid hydrolysis of the filters as described by Solórzano and Sharp (1980).

(5) References
Hansen, H.P., Koroleff, F. (1999). Determination of nutrients. In: Grasshoff, K., Kremling, K., Ehrhardt, M. (Eds.), Methods of Seawater Analysis. Willey-VCH, Weinheim, Germany, pp. 159–228.
Ridal, J.J., Moore, R.M. (1990). A re-examination of the measurement of dissolved organic phosphorus in seawater. Marine Chemistry 29, 19–31.
Solórzano, L., Sharp, J.H., 1980. Determination of total dissolved phosphorus and particulate phosphorus in natural waters. Limnology and Oceanography 25, 754–758.

4.13 Dissolved organic carbon and fluorescent dissolved organic matter (FDOM)
(1) Personnel
Masahito Shigemitsu, Kosei Sasaoka, Yugo Nishimura, Mone Ozawa and Masahide Wakita (JAMSTEC)

(2) Introduction
Marine dissolved organic matter (DOM) is known to be the largest ocean reservoir of reduced carbon, and a large fraction of the carbon exists as refractory DOM (RDOM) (Hansell et al., 2009). RDOM is considered to be generated during microbial degradation of organic matter produced in the sunlit surface ocean, and is hypothesized to play an important role in the atmospheric CO_2 sequestration (Jiao et al., 2010). A fraction of the RDOM can be detected as fluorescent DOM (FDOM). In the intermediate waters of the North Pacific, allochthonous RDOM is introduced from the surrounding marginal seas and is mixed into the above-mentioned autochthonous RDOM (Yamashita et al., 2021).

In this cruise, we try to gain insights into the relative proportion of allochthonous and autochthonous RDOM in the intermediate waters of the North Pacific.

(3) Instruments and methods
Bottle sampling
Discrete water samples for each station were collected using 12L Niskin bottles mounted on a CTD system. Each sample taken in the upper 250 m was filtered using a pre-combusted glass fiber filter (GF/F, Whatman). The filtration was carried out by connecting a spigot of Niskin bottle through silicone tube to an inline plastic filter holder.

Filtrates were collected for DOC and FDOM measurements in acid-washed 60 mL High Density Polyethylene (HDPE) bottles and pre-combusted glass vials with acid-washed teflon-lined caps after triple rinsing, respectively. Other samples taken below 250 m were unfiltered. The samples for DOC and FDOM were collected at the stations 1, 3, 5, 7, 9, 11, 13, 15, 17, 19, 20, 23, 25, 27, 29, 31, 32, 34, 37, 39, 42, 44, 47, 50, 52, 54, 56, 57, 58, 60, 63, 65, 67, and 70.

DOC measurement
The samples for DOC were immediately stored frozen onboard until analysis on land. The samples will be thawed at room temperature and measured by a Shimadzu TOC-L system coupled with a Shimadzu Total N analyzer in JAMSTEC. The standardization will be achieved using glucose, and the analyses will be referenced against reference material provided by Hansell Laboratory, University of Miami.

FDOM measurement
Fluorescence excitation-emission matrices (EEMs) were measured onboard using the Horiba Scientific Aqualog after the samples were allowed to stand until reaching near room temperature. Emission scans from 248 to 829 nm taken at 2.33-nm intervals were obtained for the excitation wavelengths between 240 and 560 nm at 5-nm intervals. The fluorescence spectra were scanned with a 12-s integration time and acquired in the high CCD gain mode. The fluorescence intensities were converted to Raman Units (R.U.) (Lawaetz and Stedmon, 2009) using the water Raman peak of Milli-Q water (excitation = 350 nm) analyzed daily.

(4) Preliminary results of FDOM
We measured all samples of FDOM onboard, but all data are still preliminary. Here, we show the results of FDOM (FDOM370/440) for the single pair of excitation and emission wavelengths (370/440 nm) which are considered to be humic-like FDOM (Coble, 2007) (Figures 4.13). The FDOM370/440 results are similar to the apparent oxygen utilization profiles detailed elsewhere in this cruise report and indicate that this type of FDOM is produced in the

ocean interior during mineralization of organic matter.
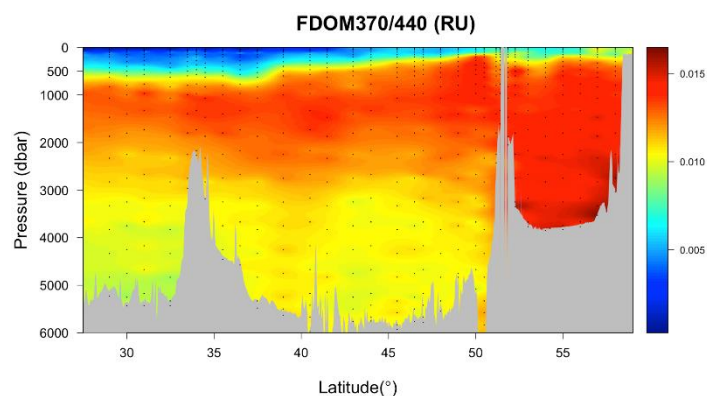
Figure 4.13 Vertical section of FDOM370/440 (RU)

(5) References

Coble, P.G. (2007). Marine optical biogeochemistry: the chemistry of ocean color. Chem. Rev. 107, 402–418.

Hansell, D.A., C.A. Carlson, D.J. Repeta, and R. Schlitzer (2009). Dissolved organic matter in the ocean: New insights stimulated by a controversy. Oceanography 22, 52-61.

Jiao, N., G. Herndl, D.A. Hansell, R. Benner, G. Kattner, S. Wilhelm, et al. (2010). Microbial production of recalcitrant dissolved organic matter: long-term carbon storage in the global ocean. Nat. Rev. Microbiol. 8, 593–599. doi:10.1038/nrmicro2386

Lawaetz, A.J., and C.A. Stedmon (2009). Fluorescence intensity calibration using the Raman scatter peak of water. Appl. Spectrosc. 63(8), 936-940.

Yamashita, Y., T. Tosaka, R. Bamba, R. Kamezaki, S. Goto, J. Nishioka, et al. (2021). Widespread distribution of allochthonous fluorescent dissolved organic matter in the intermediate water of the North Pacific. Prog. Oceanogr. 191, 102510.

4.14 Absorption coefficients of Chromophoric Dissolved Organic Matter (CDOM)

(1) Personnel

Kosei Sasaoka (JAMSTEC)

Masahito Shigemitsu (JAMSTEC)

(2) Objectives

Oceanic dissolved organic matter (DOM) is the largest pool of reduced carbon, and its inventory in the ocean is approximately 660 Pg C (Hansell et al., 2009). Thus, investigating the behavior of oceanic DOM is important to exactly evaluate the carbon cycle in the ocean. As the part of the DOM, Chromophoric Dissolved Organic Matter (CDOM) play an important role in determining the optical properties of seawater, and the global CDOM distribution appears regulated by a coupling of biological, photochemical, and physical oceanographic processes all acting on a local scale, and greater than 50% of blue light absorption is controlled by CDOM (Siegel et al., 2002). Additionally, some investigators have reported that CDOM emerges as useful tracers for diagnosing changes in the overturning circulation and evaluating DOC quality, similar to dissolved oxygen (e.g., Nelson et al., 2010; Catala et al., 2015). The objectives of this study are to clarify the meridional distributions of light absorption by CDOM along P14N section in the Bering Sea and North Pacific.

(3) Methods

Seawater samples for determination of the absorption coefficient of CDOM ($a_{cdom}(\lambda)$) were taken from a spigot of Niskin bottles directly at 300m-bottom depths (non-filtration), and through silicone tube to an inline plastic filter holder with a pre-combusted 47mm Whatman GF/F filter (450℃ for 4 hours) at the shallow depths above 200m (filtration). According to the method of Catala et al. (2015) and Shigemitsu et al. (2021), CDOM samples were not filtered to remove particles in the seawater except for 6-samples of shallow depth, using the same way as DOC and FDOM. All samples were collected in 60 ml pre-combusted glass vials with acid-washed Teflon-lined caps after triple rinsing. We stored the samples in the dark in refrigerator until analysis. After the samples were acclimated to laboratory temperature in the dark, optical absorbance of CDOM ($Abs(\lambda)$) in seawaters between 190 and 750 nm were measured at 0.5 nm intervals by an UV-VIS recording spectrophotometer (UV-2600, Shimadzu Co.) onboard, using 10-cm pathlength quartz cells. We measured Milli-Q water as a blank every 5-8 samples to correct linearly any instruments drift. To correct baseline offsets in the measurements, we subtracted average values ranging from 590 to 600 nm from the entire absorbance spectrum of each sample (Yamashita and Tanoue, 2009). The absorption coefficient of CDOM ($a_{cdom}(\lambda)$ (m^{-1})) was calculated from the absorbance at wavelength ($Abs(\lambda)$) as follows (Green and Blough, 1994):

$$a_{cdom}(\lambda) = 2.303 \times [\ Abs(\lambda) - Abs_{590-600}]\ /\ 1$$

where $Abs_{590-600}$ is the average absorbance between 590 and 600 nm, l is the path length of quartz cell (0.1 m), and 2.303 is the factor that converts from decadic to natural logarithms.

(4) Preliminary results

Vertical profiles of $a_{cdom}(\lambda=325)$ (as absorption coefficient at 325nm, unit = m^{-1}) at each station (n=34) were shown in Fig. 4.14.1. Cross sections of $a_{cdom}(\lambda=325)$ along P14N section was shown in Fig. 4.14.2. The difference between the $a_{cdom}(\lambda=325)$ in the Bering Sea (high) and North Pacific (low) was clearly seen. Furthermore, $a_{cdom}(\lambda=325)$ near the bottom in the Bering Sea were relatively high.

A total of 22-bottles of PRE20 (Multiparametric Standard Seawater: MSSW, lot PRE20, KANSO TECHNOS Co., Ltd.) (see 4.24) was used as reference. The mean ± SD of $a_{cdom}(\lambda=325)$ of all PRE20 bottles was 0.247 ± 0.008. 127-pairs of replicate CDOM samples were obtained from hydrographic casts. The absolute values of the difference between replicate samples of $a_{cdom}(\lambda=325nm)$ were 0-0.069 m^{-1}, and the precision estimated from SD of them were approximately 0.011. This variability (0.011) was not significantly different from that of the PRE20 (0.008).

(5) References

Catala, T. S., et al., 2015, Turnover time of fluorescent dissolved organic matter in the dark global ocean, *Nat. Com., 6*, 1-8, doi:10.1038/ncomms6986.

Green, S. A. and N. V. Blough, 1994, Optical absorption and fluorescence properties of chromophoric dissolved organic matter in natural waters. *Limnol. Oceanogr. 39*, 1903–1916.

Hansell, D. A., C. A. Carlson, D. J. Repeta, and R. Shlitzer, 2009, Dissolved organic matter in the ocean: A controversy stimulates new insight, *Oceangr., 22*, 202-211

Nelson, N. B., D. A. Siegel, C. A. Carlson, and C. M. Swan, 2010, Tracing global biogeochemical cycles and meridional overturning circulation using chromophoric dissolved organic matter, *Geophys. Res. Lett., 37*, L03610, doi:10.1029/2009GL042325.

Shigemitsu, M., T. Yokokawa, H. Uchida, S. Kawagucci, and A. Murata. 2021. Sedimentary supply of humic-like fluorescent dissolved organic matter and its implication for chemoautotrophic microbial activity in the Izu-Ogasawara trench. *Sci. Rep. 11*: 19006, doi:10.1038/s41598-021-97774-7

Siegel, D.A., Maritorena, S., Nelson, N.B., Hansell, D.A., Lorenzi-Kayser, M., 2002, Global distribution and dynamics of colored dissolved and detrital organic materials. *J. Geophys. Res., 107*, C12, 3228, doi:10.1029/2001JC000965.

Yamashita, Y. and E. Tanoue, 2009, Basin scale distribution of chromophoric dissolved organic matter in the Pacific Ocean, *Limnol. Oceanogr., 54*, 598–609.
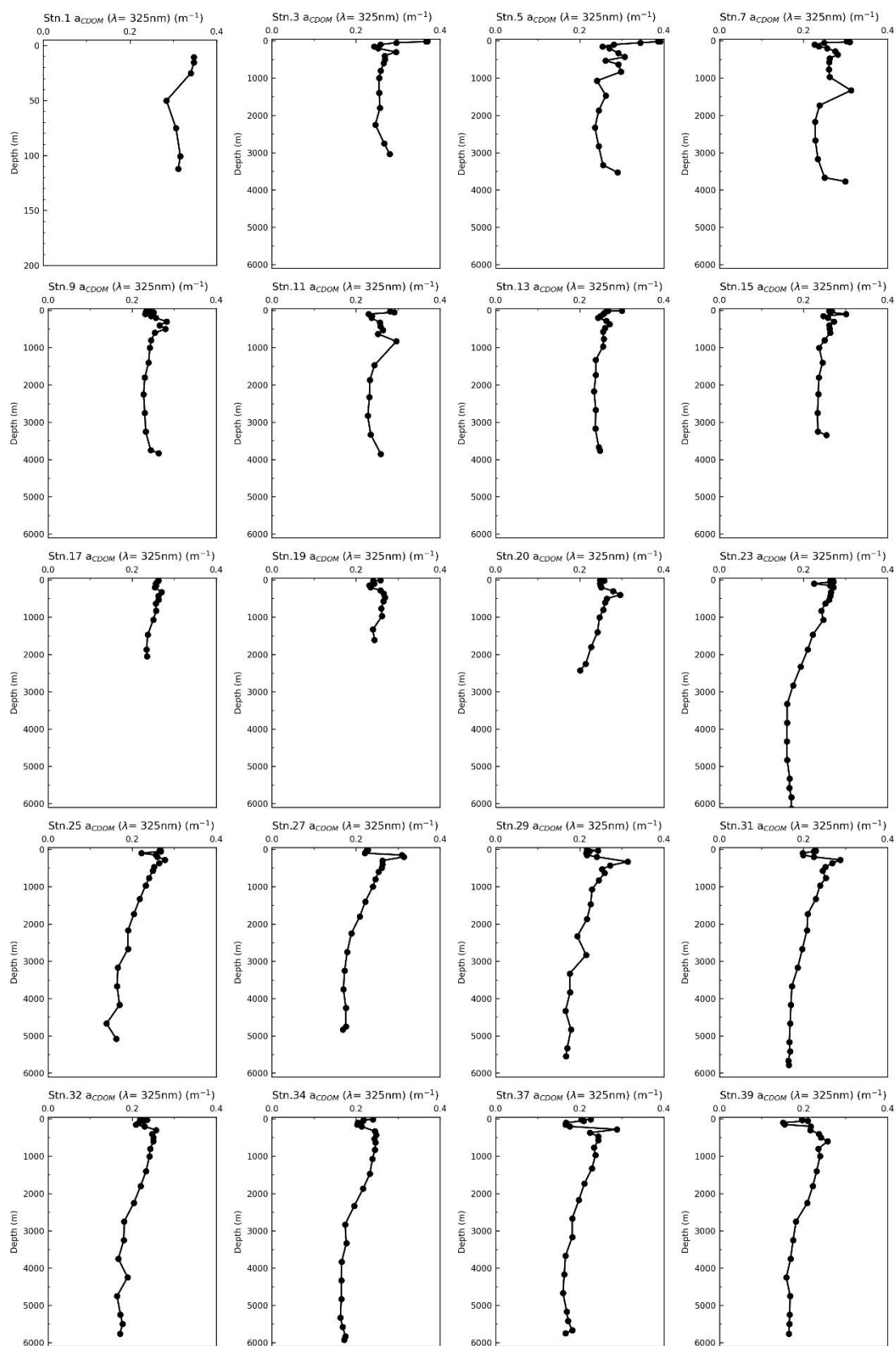
Fig.4.14.1 Vertical profiles of CDOM (as absorption coefficient at 325 nm, unit = m^{-1}) at 34 stations.
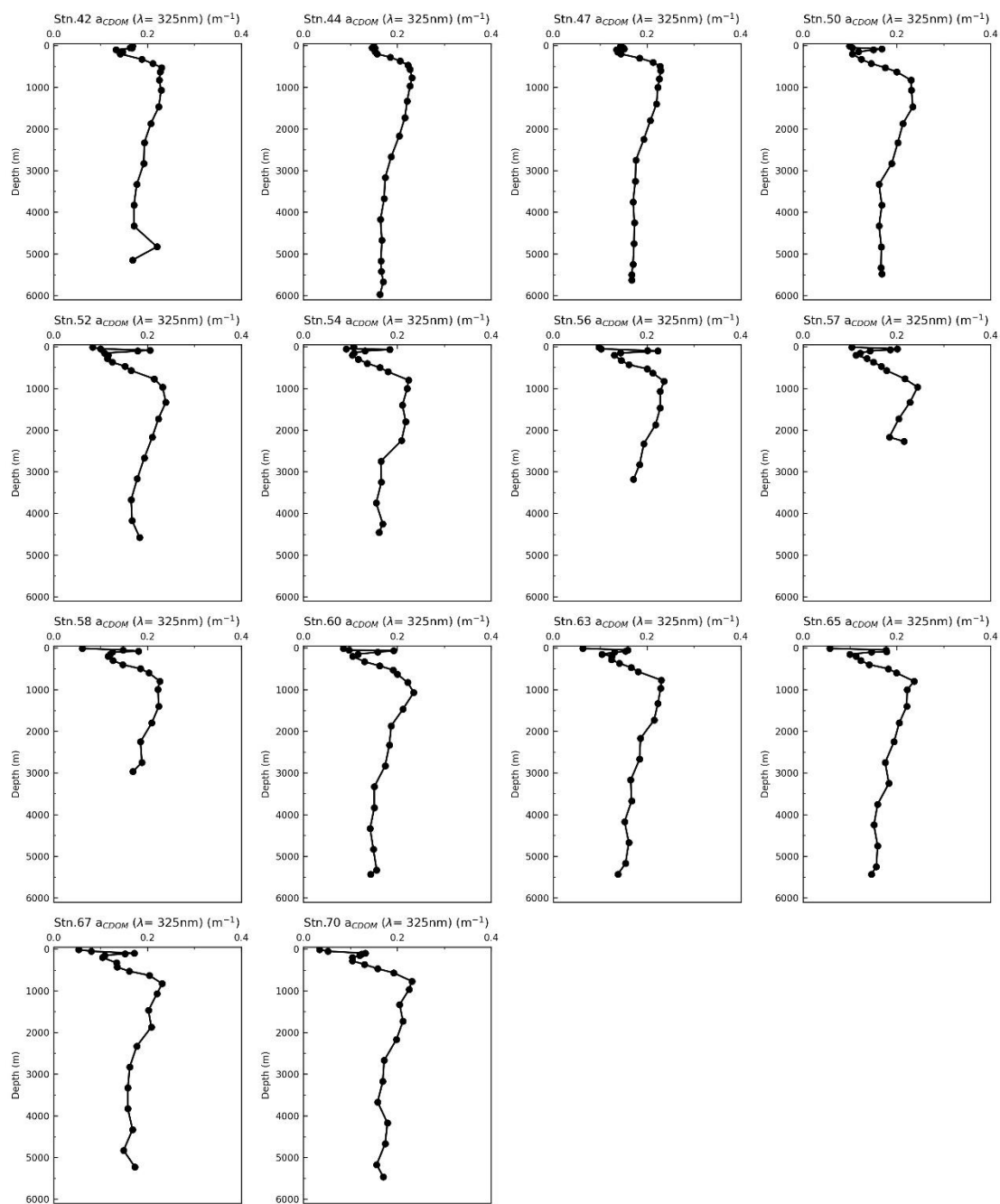
Fig.4.16.1 (Continued).
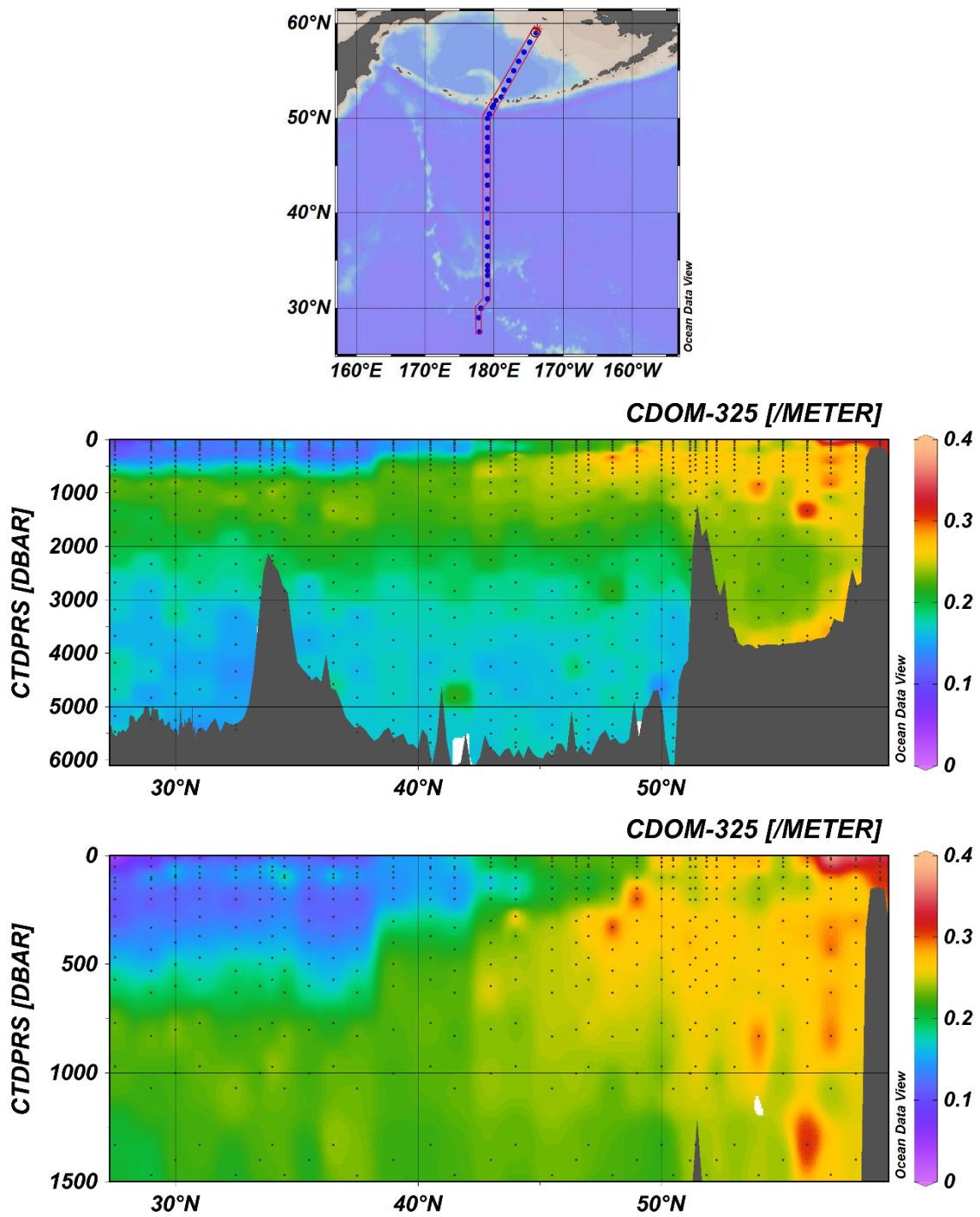
Fig.4.14.2 Sections of CDOM (as absorption coefficient at 325 nm, unit = m^{-1}) along P14N section obtained from hydrographic casts. The top section covers surface to the bottom and the lower section covers the upper 1,500 m.

4.15 Radiocesium and tritium

November 06, 2023　Yuichiro Kumamoto

Japan Agency for Marine-Earth Science and Technology (JAMSTEC)

(1) Personnel

Yuichiro Kumamoto
　　Japan Agency for Marine-Earth Science and Technology

Mutsuo Inoue
　　Kanazawa University

(2) Objective

In order to investigate the water circulation and ventilation process in the North Pacific Ocean and Bering Sea, seawater samples were collected for measurements of radiocesium (^{137}Cs) and tritium (^{3}H), which were mainly released from the global fallout in the 1950s and 1960s and the Fukushima accident in 2011.

(3) Sample collection

The sampling stations and number of samples are summarized in Table 4.15.1 and Table 4.15.2. Seawater samples for radiocesium measurement were collected at 11 stations from surface water that pumped up from about 4 m depth from the sea surface. We also collected seawater at 8 stations using the 12-liter Niskin-type bottles at 9 depths between surface to 1000 m depth. Seawater for tritium measurement was also collected vertically at 5 stations using Niskin-type bottles. The seawater sample was collected into a 20-L plastic containers and 1-L glass bottle after two time washing for radiocesium and tritium, respectively. The total number of seawater samples for radiocesium and tritium are 83 and 45, respectively.

(4) Sample preparation and measurements

In our laboratory on shore, radiocesium in the seawater samples will be concentrated using ammonium phosphomolybdate (AMP) that forms insoluble compound with cesium. The radiocesium in AMP will be measured using Ge γ-ray spectrometers. Tritium in the seawater samples will be concentrated electrochemically and measured using liquid scintillation spectrometry.

(5) Data archives

The data obtained in this cruise will be submitted to the Data Management Group of JAMSTEC and will be opened to the public via "Data Research System for Whole Cruise Information in JAMSTEC (DARWIN)" in the JAMSTEC web site.

Table 4.15.1 Sampling stations of surface seawater for radiocesium using the pumping-up system

	Station	Latitude End time	Longitude End time	Sampling Date (UTC)	Sampling Time (UTC)	Sampling Lab.
1	006	56-29.77N	176-05.72W	2023/10/11	04:06-04:14	Wet Lab. 2
2	012	53-29.63N	178-14.17W	2023/10/09	07:52-08:01	Wet Lab. 2
3	025	50-00.38N	178-59.69E	2023/10/17	17:27-17:36	Wet Lab. 2
4	029	47-59.19N	179-01.01E	2023/10/18	20:44-20:52	Wet Lab. 2
5	034	45-29.95N	179-01.61E	2023/10/21	18:35-18:42	Wet Lab. 2
6	039	42-57.99N	179-00.08E	2023/10/23	18:26-18:33	Wet Lab. 2
7	043	40-58.50N	178-59.81E	2023/10/24	20:43-20:53	Wet Lab. 2
8	051	36-59.48N	179-00.52E	2023/10/26	23:01-23:11	Wet Lab. 2
9	061	31-59.73N	178-59.03E	2023/10/29	16:05-16:11	Wet Lab. 2
10	066	29-29.95N	177-52.52E	2023/10/31	02:15-02:23	Wet Lab. 2
11	070	27-30.01N	177-52.43E	2023/11/01	03:20-03:27	Wet Lab. 2

Table 4.15.2 Vertical sampling stations and number of samples for radiocesium and tritium.

Station	Lat.	Long.	Sampling Date (UTC)	Number of samples for radiocesim	Number of samples for tritium	Max. Pressure (dbar)
006	56-29.77N	176-05.76W	2023/10/11	9	-	1069.9
012	53-29.66N	178-14.16W	2023/10/09	9	-	1058.0
024	50-14.65N	179-09.05E	2023/10/17	9	9	970.1
033	45-59.54N	179-01.09E	2023/10/21	9	9	1000.2
043	40-58.49N	178-59.81E	2023/10/24	9	-	1070.4
051	36-59.50N	179-00.59E	2023/10/27	9	9	968.9
059	32-58.74N	178-58.96E	2023/10/29	9	9	1069.9
066	29-29.96N	177-52.51E	2023/10/31	9	9	1071.0
			Total	72	45	

4.16 Radium isotopes

November 06, 2023
Yuichiro Kumamoto
Japan Agency for Marine-Earth Science and Technology (JAMSTEC)

(1) Personnel

Mutsuo Inoue
Kanazawa University

(2) Objectives

In order to investigate the water circulation and ventilation process in the North Pacific Ocean and the Bering Sea, seawater samples were collected for measurements of radium isotopes (^{226}Ra and ^{228}Ra).

(3) Sample collection

The sampling stations and number of samples are summarized in Table 4.16.1 and Table 4.16.2. Seawater samples for radium isotopes measurement were collected at 11 stations from surface water that pumped up from about 4 m depth from the sea surface. We also collected seawater at 3 stations using the 12-liter Niskin-type bottles at 6 depths between surface to 300 m depth. The seawater sample was collected into a 20-L plastic container after two time washing. The total number of seawater samples is 29.

(4) Sample preparation and measurements

In our laboratory on shore, Ra-free Barium carrier and SO_4^{2-} are added to the seawater sample to coprecipitate radium with $BaSO_4$. After evaporating to dryness, the $BaSO_4$ fractions are compressed to disc as a mixture of $Fe(OH)_3$ and NaCl for gamma-ray spectrometry using Ge-detectors.

(5) Data archives

These data obtained in this cruise will be submitted to the Data Management Group of JAMSTEC, and will be opened to the public via "Data Research System for Whole Cruise Information in JAMSTEC (DARWIN)" in JAMSTEC web site.

Table 4.16.1 Sampling stations of surface seawater for radium isotopes using the pumping-up system.

	Station	Latitude End time	Longitude End time	Sampling Date (UTC)	Sampling Time (UTC)	Sampling Lab.
1	006	56-29.77N	176-05.72W	2023/10/11	04:06-04:14	Wet Lab. 2
2	012	53-29.63N	178-14.17W	2023/10/09	07:52-08:01	Wet Lab. 2
3	025	50-00.38N	178-59.69E	2023/10/17	17:27-17:36	Wet Lab. 2
4	029	47-59.19N	179-01.01E	2023/10/18	20:44-20:52	Wet Lab. 2
5	034	45-29.95N	179-01.61E	2023/10/21	18:35-18:42	Wet Lab. 2
6	039	42-57.99N	179-00.08E	2023/10/23	18:26-18:33	Wet Lab. 2
7	043	40-58.50N	178-59.81E	2023/10/24	20:43-20:53	Wet Lab. 2
8	051	36-59.48N	179-00.52E	2023/10/26	23:01-23:11	Wet Lab. 2
9	061	31-59.73N	178-59.03E	2023/10/29	16:05-16:11	Wet Lab. 2
10	066	29-29.95N	177-52.52E	2023/10/31	02:15-02:23	Wet Lab. 2
11	070	27-30.01N	177-52.43E	2023/11/01	03:20-03:27	Wet Lab. 2

Table 4.16.2 Vertical sampling stations and number of samples for radium isotopes.

Station	Lat.	Long.	Sampling Date (UTC)	Number of samples	Max. Pressure (dbar)
006	56-29.77N	176-05.76W	2023/10/11	6	330.6
012	53-29.66N	178-14.16W	2023/10/09	6	325.6
043	40-58.49N	178-59.81E	2023/10/24	6	330.3
			Total	18	

4.17 Nitrogen Cycles
(1) Personnel
Akiko Makabe (JAMSTEC)
Chisato Yoshikawa (JAMSTEC)

(2) Objectives
The marine nitrogen cycle in surface waters is known to control biological activity in the ocean, because inorganic forms of nitrogen such as ammonium and nitrate are indispensable nutrients for phytoplankton. Following the primary production, organic nitrogen compounds are metabolized into ammonium and low molecular organic nitrogen compounds that are substrates for nitrification and/or nitrogen source of microbes. Ammonium is oxidized to nitrate via nitrite by nitrification. In low-nutrient region, nitrogen fixation is important source of nitrogen. Nitrous oxide (N_2O), a significant anthropogenic greenhouse gas and a stratospheric ozone destroyer, is known to be produced by microbial activity such as nitrification.

To understand transformation of nitrogen compounds by (microbial) organisms and production processes of greenhouse gasses (N_2O and CH_4), both natural abundance and tracer stable isotope technique are useful. We collected water samples to analyze natural abundance stable isotope ratio of dominant nitrogen species such as nitrate, nitrite, ammonium, organic nitrogen, and nitrous oxide, which would have records of biological processes. On the other hand, we conducted on-board incubation experiments with tracer compounds to analyze nitrification activities.

(3) Apparatus
i. Nitrate isotope ratio
Full-depth samples for nitrate stable isotope analysis were collected into a 30mL plastic syringe with a filter (pore size: 0.45μm) and filtered immediately after sampling at the routine cast, while samples for surface water (~ 200m) at the biocast were collected directly from a niskin sampler to a 25mL PP bottle through a 0.2μm filter. The filtrates were frozen until analysis at JAMSTEC. We will measure both nitrogen and oxygen stable isotope ratio of nitrate by a GC-IRMS after conversion to N_2O using the bacterial method.

Samples for nitrate stable isotope ratio were collected at Station#: 1, 7, 15, 23, 34, 44, 54, and 65.

ii. Nitrite isotope ratio
Samples for nitrite stable isotope analysis were collected directly from a niskin sampler to a 100mL PE bottle through a 0.2μm filter. The filtrates were frozen until analysis at JAMSTEC. We will measure both nitrogen and oxygen stable isotope ratio of nitrite by a GC-IRMS after conversion to N_2O using the azide method.

Samples for nitrate stable isotope ratio were collected at Station#: 7, 23, 34, 44, 54, and 65.

iii. Ammonium isotope ratio
Samples for ammonium stable isotope analysis were collected directly from a niskin sampler to a 50mL PE bottle through a 0.2μm filter. A glass fiber filter (GF/D) with sulfuric acid solution and MgO were added to subsamples of 50 ml filtrate. The glass fiber filters trapped with ammonia after shaken for 6days were taken from the subsamples to glass bottles with silica gel desiccant until analysis at JAMSTEC. We will measure nitrogen stable isotope ratio of ammonium by a GC-IRMS after conversion to N_2O using wet oxidation and the bacterial method.

Samples for nitrate stable isotope ratio were collected at Station#: 7, 23, 34, 44, 54, and 65.

iv. Particulate organic nitrogen (PON) isotope ratio
Samples for nitrogen stable analysis of PON were collected into a 500mL PC bottle. The seawater samples were filtered by a 0.3μm glass fiber filter (GF-75) on board. The GF-75 was wrapped by aluminum foil and frozen until analysis at JAMSTEC. We will measure nitrogen stable isotope ratio of PON by a GC-IRMS after conversion to N_2O using wet oxidation and the bacterial method.

Samples for nitrate stable isotope ratio were collected at Station#: 7, 23, 34, 44, 54, and 65.

v. Dissolved organic nitrogen (DON) isotope ratio
Samples for nitrogen stable analysis of DON were collected directly from a niskin sampler to a

25mL PP bottle through a 0.2µm filter. The filtrates were frozen until analysis at JAMSTEC. We will measure nitrogen stable isotope ratio of DON by a GC-IRMS after conversion to N_2O using wet oxidation and the bacterial method.

Samples for nitrate stable isotope ratio were collected at Station#: 7, 23, 34, 44, 54, and 65.

vi. Nitrous oxide (N_2O) and Methane (CH_4) isotope ratio

Samples for N_2O and CH_4 stable isotope analysis were collected into 100 mL glass vials and added with $HgCl_2$ solution immediately after sampling. Nitrogen and oxygen stable isotope ratio of N_2O and carbon stable isotope ratio of CH_4 will be measured by GC-IRMS.

Samples for nitrate stable isotope ratio were collected at Station#: 7, 15, 23, 34, 44, 54, and 65.

vii. Nitrification activity

Samples for nitrification activity measurement were collected into 100 mL amber glass vials without head space. Substrates of nitrification, ammonium or urea (^{15}N 99 atom %), were added to the vials and incubated in dark at near in situ temperature on board. At the end of incubation period, water samples were filtrated by a glass fiber filter (pore size: 0.3µm) and frozen until analysis at JAMSTEC. The transfer rate from substrates to nitrite and nitrate is determined by enrichment of ^{15}N in nitrite and nitrate.

Samples for nitrate stable isotope ratio were collected at Station#: 7, 23, 34, 44, 54, and 65.

4.18 Spatial patterns of prokaryotic abundance and community composition in relation to the water masses in the central Pacific

(1) Personnel

Taichi Yokokawa (JAMSTEC)

(2) Introduction

Prokaryotes (bacteria and archaea) play an important role in marine biogeochemical fluxes. Biogeochemical transformations and functional diversity of microbes are representative major topics in marine microbial ecology. However, the relationship between prokaryotic properties and biogeochemistry in the mesopelagic and bathypelagic layers has not been systematically elucidated, despite recent studies highlighting the role of microbes in the cycling of organic and inorganic matter. In addition, the composition and biogeography of microbial communities in the meso- and bathypelagic ocean and their relationship with the upper layers and deep-water circulation have not been well studied.

The objectives of this study, which analyzed the water columns from the sea surface to 10 m above the bottom of the central Pacific, were 1) to determine the abundance of microbes; 2) to assess the community composition of prokaryotes; 3) to know the microbial diversity through the water columns along the latitudinal transect.

(3) Methods

Microbial abundance

Samples for microbial abundances (prokaryotes, eukaryotes and viruses) were collected in Station#: 1, 7, 15, 23, 27, 34, 39, 44, 50, 54, 60, 65 and 70. Samples were fixed with glutaraldehyde (final concentration 1%) and frozen at -80°C. The abundance and relative size of microbes and viruses will be measured by a flow cytometry in JAMSTEC after nucleic acid staining with SYBR-Green I.

Microbial diversity

Microbial cells in water samples were filtrated on cellulose acetate filter (0.2μm) and stored at -80˚C. Environmental DNA or RNA will be extracted from the filtrated cells and used for 16S rRNA gene tag sequencing, quantitative PCR for genes for 16S rRNA, shotgun sequencing and metatranscriptomics. Samples for microbial diversity were taken at stations 1, 7, 15, 23, 27, 34, 39, 44, 50, 54, 60, 65 and 70 in the routine casts and at stations 7, 23, 34, 44, 54 and 65 of the biological cast.

4.19 Spatial patterns of phototrophic organisms and their pigments

(1) Personnel
  Yusuke Tsukatani and Shigeru Kawai (JAMSTEC, MRU)

(2) Introduction

Photosynthesis is the fundamental process that converts light energy into biologically available chemical energy. Planktonic phototrophic microorganisms consisting of algae, cyanobacteria, and aerobic anoxygenic phototrophic bacteria (AAPB) are ecologically important groups for geobiological cycling in aquatic environments especially in the ocean. AAPB, which belong to the phylum *Proteobacteria* (recently renamed as *Pseudomonadota*), constitute up to 20% of marine microbial communities, although it depends on the area and season. Until 21st century, the marine euphotic microbial community was considered to be dominated by oxygenic phototrophs. It could partly be because planktonic algae and cyanobacteria having chlorophyll-based proteins and phycobilisomes can be easily detected using fluorescence microscopy and flow cytometry due to strong fluorescence emission from chlorophylls and bilins. However, through developing technologies for sequencing environmental DNA, bacteriochlorophyll (BChl)-containing anoxygenic phototrophs — mostly AAPB— began to be widely detected in marine environments. In this study, our objective is to understand the distribution and spatial patterns of BChl-based phototrophy along a longitude. Another objective is to try to isolate a new BChl-based phototrophic bacterium having an unusual light and carbon metabolism, which would be anticipated and verified by the metagenomic analysis (section 4.18) and also by the BChl pigment analysis.

(3) Methods
Pigment analysis

  Water samples for pigment composition analysis were collected from Station #7, 23, 34, 44, 54, and 65. Microorganisms in the samples were concentrated on filters (0.2 μm, Omnipore hydrophilic PTFE membrane, Merck) by vacuum filtration and the filters were stored at -20℃. Pigments will be extracted and measured by a HPLC system in

JAMSTEC.

Microbial cultivation

Water samples were collected from the same station as pigment analysis. The samples were diluted with inorganic and organic medium and incubated at 15°C with LED and incandescent light. The samples were also spread on agar plates and incubated at the same condition as liquid cultivation.

4.20 Organic alkalinity

(1) Personnel

Ryan Woosley (MIT)
Jiyoung Moon (MIT)
Zhaohui Alex Wang (WHOI)
Akihiko Murata (JAMSTEC)
Hiroyuki Fujiwara (JAMSTEC)
Nagisa Fujiki (MWJ)

(2) Objectives

There is increasing evidence of non-negligible amounts of organic alkalinity being present in open ocean waters. Quantifying the presence of any organic alkalinity is important for accurately calculating carbon system parameters such as carbonate ion concentrations and calcium carbonate saturation states. We take two approaches to quantify organic alkalinity. First, we compare the total alkalinity measured from the same Niskin bottle but using two different methods for endpoint detection. Differences in total alkalinity made by the different groups would suggest the presence of organic alkalinity with an acid dissociation constant near the end point of the titration. The second method involves direct detection of organic alkalinity using a back titration technique in which all of the carbon dioxide is driven off in the first titration, the sample is then returned to its initial pH using sodium hydroxide and titrated again to quantify the non-volatile components of total alkalinity.

(3) Sampling

Seawater samples were collected at given layers of 12 CTD stations (Table 4.20-1). The seawater samples were taken from the Niskin bottle with a plastic drawing tube (PFA tubing connected to silicone rubber tubing) connected from the Niskin drain into the 250 ml borosilicate glass bottle. The glass bottle was filled with seawater smoothly from the bottom following a rinse with a seawater of 2 full, bottle volumes. The glass bottle was closed by a stopper, which was fitted to the bottle mouth gravimetrically without additional force. At the chemical laboratory on the R/V Mirai, a headspace of approx. 1% of the bottle volume was made by removing seawater using a plastic pipette. A saturated mercuric chloride of 100 μl was added to poison seawater samples. The glass bottle was sealed with a greased ground glass stopper and the clip was secured.

Table 4.20-1 List of sampling layers for organic alkalinity

Station	Cast	LATITUDE	LONGITUDE	Niskin Bottle No.	WHOI bottle No.	MIT bottle No.	sampling layer
9	1	54.9974	-177.1813	36	52		
9	1	54.9974	-177.1813	27	51		just below thermocline
9	1	54.9974	-177.1813	24	50		O2 min.
9	1	54.9974	-177.1813	2	49		Chla max
9	1	54.9974	-177.1813	1	47		bottom
3	1	58.0001	-174.8726	36	68	85	
3	1	58.0001	-174.8726	35		84	
3	1	58.0001	-174.8726	34		83	

3	1	58.0001	-174.8726	33		82	
3	1	58.0001	-174.8726	32		80	
3	1	58.0001	-174.8726	31	69	120	just below thermocline
3	1	58.0001	-174.8726	30		119	
3	1	58.0001	-174.8726	29		118	
3	1	58.0001	-174.8726	28		117	
3	1	58.0001	-174.8726	27		116	
3	1	58.0001	-174.8726	26		115	
3	1	58.0001	-174.8726	25		114	
3	1	58.0001	-174.8726	24		113	
3	1	58.0001	-174.8726	23	63	112	O2 min.
3	1	58.0001	-174.8726	22		111	
3	1	58.0001	-174.8726	21		110	
3	1	58.0001	-174.8726	20		109	
3	1	58.0001	-174.8726	19		108	
3	1	58.0001	-174.8726	18		107	
3	1	58.0001	-174.8726	17		106	
3	1	58.0001	-174.8726	16		105	
3	1	58.0001	-174.8726	15		104	
3	1	58.0001	-174.8726	2	58	102	Chla max
3	1	58.0001	-174.8726	1	53	101	bottom
17	1	51.8517	-179.7835	36	59		
17	1	51.8517	-179.7835	28	57		just below thermocline
17	1	51.8517	-179.7835	23	56		O2 min.
17	1	51.8517	-179.7835	2	55		Chla max
17	1	51.8517	-179.7835	1	54		bottom
23	3	50.4835	179.2754	36	65	123	
23	3	50.4835	179.2754	34		122	
23	3	50.4835	179.2754	32		121	
23	3	50.4835	179.2754	30		103	
23	3	50.4835	179.2754	29	64		just below thermocline
23	3	50.4835	179.2754	28		100	
23	3	50.4835	179.2754	27	62		O2 min.
23	3	50.4835	179.2754	26		99	

23	3	50.4835	179.2754	24		98	
23	3	50.4835	179.2754	22		97	
23	3	50.4835	179.2754	20		96	
23	3	50.4835	179.2754	18		95	
23	3	50.4835	179.2754	16		94	
23	3	50.4835	179.2754	14		93	
23	3	50.4835	179.2754	12		92	
23	3	50.4835	179.2754	10		91	
23	3	50.4835	179.2754	8		90	
23	3	50.4835	179.2754	6		89	
23	3	50.4835	179.2754	4		88	
23	3	50.4835	179.2754	2	61	87	Chla max
23	3	50.4835	179.2754	1	60	86	bottom
29	1	47.986	179.0171	36	67		
29	1	47.986	179.0171	31	66		just below thermocline
29	1	47.986	179.0171	26	72		O2 min.
29	1	47.986	179.0171	2	70		
29	1	47.986	179.0171	1	71		Chla max
31	1	47.0003	178.9945	36	77	147	
31	1	47.0003	178.9945	34		148	
31	1	47.0003	178.9945	32		151	
31	1	47.0003	178.9945	31	76		just below thermocline
31	1	47.0003	178.9945	30		154	
31	1	47.0003	178.9945	28		150	
31	1	47.0003	178.9945	26		149	
31	1	47.0003	178.9945	25	73		O2 min.
31	1	47.0003	178.9945	24		146	
31	1	47.0003	178.9945	23		145	
31	1	47.0003	178.9945	22		144	
31	1	47.0003	178.9945	21		139	
31	1	47.0003	178.9945	20		140	
31	1	47.0003	178.9945	19		141	
31	1	47.0003	178.9945	18		142	
31	1	47.0003	178.9945	17		143	

31	1	47.0003	178.9945	16		134	
31	1	47.0003	178.9945	15		135	
31	1	47.0003	178.9945	14		136	
31	1	47.0003	178.9945	13		137	
31	1	47.0003	178.9945	12		138	
31	1	47.0003	178.9945	11		129	
31	1	47.0003	178.9945	10		130	
31	1	47.0003	178.9945	9		133	
31	1	47.0003	178.9945	8		132	
31	1	47.0003	178.9945	7		131	
31	1	47.0003	178.9945	6		128	
31	1	47.0003	178.9945	5		127	
31	1	47.0003	178.9945	4		126	
31	1	47.0003	178.9945	2	74	125	Chla max
31	1	47.0003	178.9945	1	75	124	bottom
34	1	45.4993	179.027	surface	78		
34	1	45.4993	179.027	1	79		bottom
34	3	45.4982	179.0282	31	82		just below thermocline
34	3	45.4982	179.0282	23	81		O2 min.
34	3	45.4982	179.0282	2	80		Chla max
39	2	42.9684	179.0073	31	87		just below thermocline
39	2	42.9684	179.0073	22	86		O2 min.
39	2	42.9684	179.0073	3	85		
39	2	42.9684	179.0073	2	84		Chla max
39	2	42.9684	179.0073	1	83		bottom
44	2	40.4998	179.0144	surface	92	169	
44	2	40.4998	179.0144	30	91	168	just below thermocline
44	2	40.4998	179.0144	28		167	
44	2	40.4998	179.0144	26		166	
44	2	40.4998	179.0144	24		165	
44	2	40.4998	179.0144	22	90	164	O2 min.
44	2	40.4998	179.0144	20		163	
44	2	40.4998	179.0144	18		162	
44	2	40.4998	179.0144	16		161	

44	2	40.4998	179.0144	14		160	
44	2	40.4998	179.0144	12		159	
44	2	40.4998	179.0144	10		158	
44	2	40.4998	179.0144	8		157	
44	2	40.4998	179.0144	6		156	
44	2	40.4998	179.0144	4		155	
44	2	40.4998	179.0144	2	89	153	Chla max
44	2	40.4998	179.0144	1	88	152	bottom
56	1	34.49	178.9926	36	97		
56	1	34.49	178.9926	28	96		just below thermocline
56	1	34.49	178.9926	22	98		O2 min.
56	1	34.49	178.9926	2	94		Chla max
56	1	34.49	178.9926	1	93		bottom
65	1	29.9994	178.0169	31	102		just below thermocline
65	1	29.9994	178.0169	30		186	
65	1	29.9994	178.0169	28		185	
65	1	29.9994	178.0169	26		184	
65	1	29.9994	178.0169	24		183	
65	1	29.9994	178.0169	22	101	182	O2 min.
65	1	29.9994	178.0169	20		181	
65	1	29.9994	178.0169	18		180	
65	1	29.9994	178.0169	16		179	
65	1	29.9994	178.0169	14		178	
65	1	29.9994	178.0169	12		177	
65	1	29.9994	178.0169	10		176	
65	1	29.9994	178.0169	8		175	
65	1	29.9994	178.0169	6		174	
65	1	29.9994	178.0169	4	100	173	
65	1	29.9994	178.0169	3		172	
65	1	29.9994	178.0169	2	99	171	Chla max
65	1	29.9994	178.0169	1	95	170	bottom
70	1	27.5003	177.874	36	107	414	
70	1	27.5003	177.874	34		413	
70	1	27.5003	177.874	32		412	

70	1	27.5003	177.874	30		411	
70	1	27.5003	177.874	28		410	
70	1	27.5003	177.874	26		409	
70	1	27.5003	177.874	24		408	
70	1	27.5003	177.874	23	106		just below thermocline
70	1	27.5003	177.874	22	105	407	O2 min.
70	1	27.5003	177.874	20		406	
70	1	27.5003	177.874	18		405	
70	1	27.5003	177.874	16		404	
70	1	27.5003	177.874	14		403	
70	1	27.5003	177.874	12		402	
70	1	27.5003	177.874	10		401	
70	1	27.5003	177.874	9		400	
70	1	27.5003	177.874	8		192	
70	1	27.5003	177.874	7		191	
70	1	27.5003	177.874	6		190	
70	1	27.5003	177.874	5		189	
70	1	27.5003	177.874	2	104	188	Chla max
70	1	27.5003	177.874	1	103	187	bottom

4.21 Polycyclic Aromatic Hydrocarbons (PAHs)

November 06, 2023

Yuichiro Kumamoto

Japan Agency for Marine-Earth Science and Technology (JAMSTEC)

(1) Personnel

Tetsuya Matsunaka
   Kanazawa University

(2) Objectives

Determination of polycyclic aromatic hydrocarbons (PAHs) concentration in surface seawater in the North Pacific Ocean and Bering Sea.

(3) Sample collection

The sampling stations and number of samples are summarized in Table 4.21.1 and Table 4.21.2. Seawater samples for PAHs measurement were collected at 11 stations from surface water that pumped up from about 4 m depth from the sea surface. We also collected seawater at 3 stations using the 12-liter Niskin-type bottles at 6 depths between surface to 300 m depth. The seawater sample was collected into a 10-L stainless container after two time washing. The total number of seawater samples is 29.

(4) Sample preparation and measurements

Particulate and dissolved phases of 10 L seawater sample are separated by filtration through 0.5 µm glass-fiber filters. Dissolved organic compounds, including PAHs, are concentrated using C18 solid-phase extraction disks. Particulate and dissolved PAHs are respectively extracted from the glass-fiber filters using an ultrasonic method and eluted from the C18 disks with dichloromethane. Dimethyl sulfoxide is added to both extracted solutions, the dichloromethane is evaporated to dryness, and the residue of dimethyl sulfoxide is dissolved in acetonitrile. PAHs in the samples were quantified using the HPLC system with a fluorescence detector.

(5) Data archives

These data obtained in this cruise will be submitted to the Data Management Group of JAMSTEC, and will be opened to the public via "Data Research System for Whole Cruise Information in JAMSTEC (DARWIN)" in JAMSTEC web site.

Table 4.21.1 Sampling stations of surface seawater for PAHs using the pumping-up system.

	Station	Latitude End time	Longitude End time	Sampling Date (UTC)	Sampling Time (UTC)	Sampling Lab.
1	006	56-29.77N	176-05.72W	2023/10/11	04:06-04:14	Wet Lab. 2
2	012	53-29.63N	178-14.17W	2023/10/09	07:52-08:01	Wet Lab. 2
3	025	50-00.38N	178-59.69E	2023/10/17	17:27-17:36	Wet Lab. 2
4	029	47-59.19N	179-01.01E	2023/10/18	20:44-20:52	Wet Lab. 2
5	034	45-29.95N	179-01.61E	2023/10/21	18:35-18:42	Wet Lab. 2
6	039	42-57.99N	179-00.08E	2023/10/23	18:26-18:33	Wet Lab. 2
7	043	40-58.50N	178-59.81E	2023/10/24	20:43-20:53	Wet Lab. 2
8	051	36-59.48N	179-00.52E	2023/10/26	23:01-23:11	Wet Lab. 2
9	061	31-59.73N	178-59.03E	2023/10/29	16:05-16:11	Wet Lab. 2
10	066	29-29.95N	177-52.52E	2023/10/31	02:15-02:23	Wet Lab. 2
11	070	27-30.01N	177-52.43E	2023/11/01	03:20-03:27	Wet Lab. 2

Table 4.21.2 Vertical sampling stations and number of samples for PAHs.

Station	Lat.	Long.	Sampling Date (UTC)	Number of samples	Max. Pressure (dbar)
006	56-29.77N	176-05.76W	2023/10/11	6	330.6
012	53-29.66N	178-14.16W	2023/10/09	6	325.6
043	40-58.49N	178-59.81E	2023/10/24	6	330.3
			Total	18	

4.22 Coloured Dissolved Organic Matter (CDOM)

(1) Personnel

      Adelaide Wink (University of Galway): Co-investigator (onboard)
      Peter Croot (University of Galway): Principal Investigator

(2) Objective

Overall there is currently a lack of data worldwide for the CDOM (Coloured dissolved organic matter) properties of the different oceanic regions (Nelson and Gauglitz, 2016; Nelson and Siegel, 2013; Röttgers and Doerffer, 2007) including the North Pacific. CDOM can play an important role in many oceanic processes. CDOM strongly absorbs light, most notably in the biologically damaging ultraviolet (UV) B wavelengths (280–320 nm), and thus provides some protection for phytoplankton and other biota. CDOM can also attenuate the photosynthetically active radiation available to phytoplankton, resulting in decreased primary production. Information on the high CDOM absorption in the blue region of the spectrum can also help improve the accuracy of satellite derived phytoplankton chlorophyll estimates (D'Sa et al., 1999). Changes in CDOM properties throughout the water column may indicate phenomena such as photo-bleaching or changes in the sources of the CDOM (Helms et al., 2008). Overall increasing our knowledge of the processes influencing CDOM distributions and its influence on optical properties of oligotrophic waters are important for understanding the role of light in biogeochemical cycles. For MR23-07 CDOM data were collected to examine two main questions:

    (i)   Do CDOM optical parameters have a stoichiometric link to other biogeochemical parameters such as AOU, nitrate, phosphate and silicate reflecting remineralization in the intermediate and deep waters of the North Pacific?

    (ii)   What is the relationship between CDOM optical parameters in the euphotic zone and in situ chlorophyll in the North Pacific?

The shipboard objective to observe colored dissolved organic matter (CDOM) optical properties at all depths for selected stations, differed from that originally proposed (see below for explanation).

(3) Apparatus

Samples were collected at all depths in 125mL brown bottle from stations 3, 7, 11, 15, 17, 25, 29, 31, 34, 37, 42, 44, 47, 50, 56, 63, 67, and 70. There were as an issue with the optical shutter on the light source employed that occurred at stations 31 and 70 and data could not be fully completed for those stations. Station 31, only two samples could be run and for station 70 only 9 samples were run. The first 4 stations' data could not be used due to user error.

Briefly, a liquid waveguide capillary cell (LWCC), with an optical pathlength of 49.5cm (WPI LWCC-3050), was connected between an Ocean Optics DH-mini light source and an Ocean Optics USB2000+ spectrophotometer using 600µm fiber optic cables. The USB2000+ measures over a wavelength range from 300-850 nm.

Water samples were collected from the CTD Niskin bottles directly into 125 mL brown HDPE bottles (Nalge). Subsamples were filtered by hand into 30 ml LDPE (Nalge) bottles using a 20 mL NORM-JECT luer lock syringe and a Filtropur S 0.2µm filter. The first 10mL were discarded to ensure that there was no contamination from the antibacterial residue in the newly opened filters. Fresh ultrapure water (Millipore 18.2MΩ – denoted as MQ) was flushed through the LWCC system at the start of each experiment and used to set the absorbance blank. To clean the system, filtered surface seawater was pulled through the LWCC, immediately followed by MQ water. Filtered seawater samples were run through the spectrophotometer and the absorbance measurements saved using Ocean Optics SpectraSuite software running on a laptop PC. Data was converted to units of m^{-1} by the formula $a_\lambda = 2.303 \times A_\lambda / 1.029$, where A_λ is the wavelength specific absorbance.

(4) Results

The original shipboard objective was to make shipboard measurements of urea and iodate onboard, as had been done previously during MR19-04 in the Indian Ocean. However for MR23-07 the chemicals for these analyses needed to be shipped separately from the equipment, as some were classed as dangerous goods in limited quantities for the air transport to Alaska, unfortunately they did not arrive in time to be loaded onto the ship in Dutch Harbor. This was despite the shipment being originally sent 3 weeks prior to the ship's departure, as the courier DHL returned the box after a week without explanation and then picked it up again two days before the ship sailed, with the original paperwork. All samples were analyzed onboard MR23-07, but the data, as of this report, is still preliminary and post-processing corrections need to be applied. Please enquire about finalized results.

(5) References

D'Sa, E.J., Steward, R.G., Vodacek, A., Blough, N.V., Phinney, D., 1999. Determining optical absorption of colored dissolved organic matter in seawater with a liquid capillary waveguide. Limnol. Oceanogr. 44, 1142-1148.

Helms, J.R., Stubbins, A., Ritchie, J.D., Minor, E.C., Kieber, D.J., Mopper, K., 2008. Absorption spectral slopes and slope ratios as indicators of molecular weight, source, and photobleaching of chromophoric dissolved organic matter. Limnol. Oceanogr. 53, 955-969.

Nelson, N.B., Gauglitz, J.M., 2016. Optical Signatures of Dissolved Organic Matter Transformation in the Global Ocean. Frontiers in Marine Science 2.

Nelson, N.B., Siegel, D.A., 2013. The Global Distribution and Dynamics of Chromophoric Dissolved Organic Matter. Annual Review of Marine Science 5, 447-476.

Röttgers, R., Doerffer, R., 2007. Measurements of optical absorption by chromophoric dissolved organic matter using a point-source integrating-cavity absorption meter. Limnology And Oceanography-Methods 5, 126-135.

4.23 Biogeography of Plankton
(1) Personnel
Siyu Jiang **(AORI, University of Tokyo)**
(2) Objectives
Study 1. Biogeography and diversity of microzooplankton in the North Pacific
Microzooplankton components in oligotrophic ecosystems, are playing crucial roles in food-web dynamics and biogeochemical cycles. Our previous study focusing on composition and diversity of dinoflagellate community around the Kuroshio current showed both the composition and diversity of dinoflagellate community were associated with environmental parameters. The present cruise covering a wide research area from 27.5 to 59 °N in the North Pacific, allows us to study the microzooplankton community along a wide environmental gradient. In this study, I aim to figure out the biogeography and diversity of unicellular microzooplankton including dinoflagellates, foraminifera, radiolarians, ciliates etc., by collecting the environmental DNA along the meridional transect in the North Pacific.
Study 2. Response of phytoplankton to the subsurface seawater enrichment through the North Pacific
It is well known that phytoplankton biomass depends on the available nutrients, the so-called bottom-up control. One common way of nutrient supply in the surface ocean is through vertical mixing, that is, the nutrient replete subsurface water could enrich nutrients to the surface ocean and lead to surface phytoplankton bloom. However, the detailed mechanism of such phytoplankton bloom remains less studied. For instance, is this kind of bloom always occur with vertical mixing? Or, it occurs in certain regions or under certain conditions? If it occurs, how does it initiate, develop and decay? How is the magnitude? What is the dominant phytoplankton? Could the phytoplankton community be different in different regions? If it does not occur, what is the possible reason? Is it possible the phytoplankton growth is limited by other parameters (such as temperature) rather than nutrient availability? To answer these questions, I conducted incubation experiments at five stations along the wide environmental gradient through the North Pacific.
(3) Instrument and Method
Study 1. Biogeography and diversity of microzooplankton in the North Pacific
At each station, water samples were collected from 5 layers (10, 50, 100, 150, 200 m). For each layer, seawater was collected from CTD system to two polycarbonate bottles (2.4 L) as parallel samples. All bottles used are pre-washed with 10% HCl and rinsed with distilled water and seawater 3–4 times to avoid any contamination.
The seawater in each bottle is then filtered on 0.2 μm pore size Supor® PES filter membranes (47 mm, Pall Corp., Port Washington, NY, USA) with gentle vacuum (< 0.013 MPa) as environmental DNA (eDNA) samples (Cheung et al., 2017, 2020). Filters are frozen in cryogenic vials immediately in a deep freezer at -80°C until analysis.
Study 2. Response of phytoplankton to the subsurface seawater enrichment through the North Pacific
The subsurface seawater enrichment experiments were conducted at the 10 m layer at five stations throughout the cruise, by using a refined dilution experiment (Landry and Hassett, 1982). All carboys, tubes and capsule filters were washed with 10% HCl and rinsed with distilled water and then seawater for 3–4 times before use.
At each station, eight pre-washed polycarbonate carboys (13.3 L capacity, labelled with A~H) were use for incubation (Figure 4.22.1). Firstly, four of them (A, B, E, F) were filled with the subsurface seawater (200 m) to 20% of capacity. Then, the carboys labelled with A~D were filled with particle-free seawater (prepared by filtering natural seawater (10 m) through an acid-rinsed 0.2-μm filter capsule (Pall Corporation, New York, NY, USA)) to 80% of capacity. Finally, carboys labelled with A~F were filled with natural seawater (10 m) to the capacity. In addition, two carboys labelled with G and H were filled with 100% natural seawater (10 m) as controls. Samples for analyzing nutrients, chlorophyll *a* (Chl *a*), picophytoplankton community, phytoplankton pigments, DNA and microzooplankton community were collected from natural seawater (from 10 and 200 m for nutrients, Chl *a*, picophytoplankton and microzooplankton analysis, only from 10 m for others) as initial samples.

NSW: natural seawater
FSW: filtered seawater (0.2 μm)
SSW: subsurface seawater (200 m)

| Mixed with SSW | | Control | | Mixed with SSW | | Control | |

A, B, C, D, E, F, G, H

A: 20% 10m NSW / 60% 10m FSW / 20% SSW
B: 20% 10m NSW / 60% 10m FSW / 20% SSW
C: 20% 10 m NSW / 80% 10m FSW
D: 20% 10 m NSW / 80% 10m FSW
E: 80% 10m NSW / 20% SSW
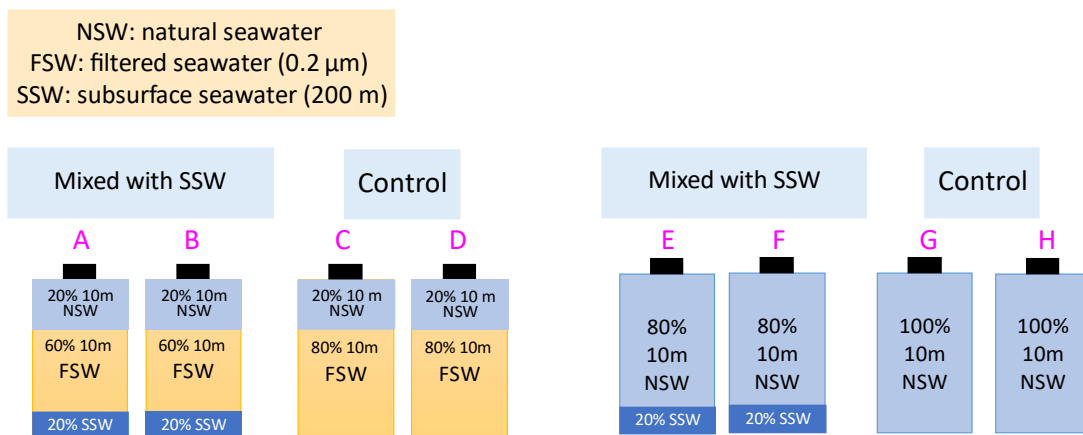F: 80% 10m NSW / 20% SSW
G: 100% 10m NSW
H: 100% 10m NSW

Figure 4.23.1 Schematic diagram of the incubation experiment.

All carboys were gently mixed and those labelled with A~F were sampled for nutrients. Then, these carboys were tightly capped and incubated for totally 72 h in an on-deck incubator with running surface seawater. For simulating the ambient light, the incubator was covered by a neutral-density filter to 50% of the surface light irradiance.

After incubating for 24 h and 48 h, all carboys were gently mixed and sampled for analyzing nutrients, Chl *a*, picophytoplankton, and DNA with a 3-port polypropylene filling/venting closure (Thermo Scientific). One of the ports was used to transfer water for sampling. The other two ports were used for venting and were connected to two 0.2-μm PTFE filters to avoid any contaminations from air. In addition, 0.2 L water was sampled from carboys E~H for examining microzooplankton community. After sampling, all carboys were tightly capped, gently mixed and put back in the incubator. At the end of incubation (72 h), all carboys were gently mixed and sampled for nutrients, Chl *a*, picophytoplankton community, DNA as well as for phytoplankton pigment and microzooplankton community.

The detailed sampling method is described as following:

To examine the concentrations of inorganic nutrients (NO_3^-, NO_2^-, NH_4^+, PO_4^{3-} and $Si(OH)_4$), water samples were collected in 12 mL acrylic tubes and stored in a gas-tight aluminum bag in a deep freezer at -80 °C and analyzed on land using a BL-Tec autoanalyzer (QuAAtro, SEAL Analytical Inc., Mequon, WI, USA).

For measuring Chl *a* concentrations, seawater samples (~0.6 L) were filtered through 25-mm-diameter Whatman GF/F filters (GE Healthcare Life Sciences, Pittsburgh, PA, USA) under low vacuum (< 0.02 MPa). The filters were immediately immersed in 7 mL N,N-dimethylformamide. Chl *a* was extracted at − 20 °C in dark for at least 24 hours and measured onboard by a fluorometer (10-AU-005; Turner Designs, San Jose, CA, USA) following a non-acidification method.

To reveal the picophytoplankton community composition, seawater (4 mL) for flow cytometry (FCM) analysis was fixed immediately with buffered paraformaldehyde (final concentration of 0.5%), placed at room temperature for 15 min, and stored in a -80 °C freezer until analyzed.

For analyzing concentrations of phytoplankton specific pigments, seawater (2~4 L) for high-performance liquid chromatography (HPLC) analysis was filtered on 25-mm- diameter Whatman GF/F filters under low vacuum (< 0.02 MPa). The filters were immediately frozen and stored at − 80 °C.

Seawater for microzooplankton analysis (0.2~0.5 L) was fixed by Lugol's iodine solution (final concentration 3%) in dark polyethylene bottles and preserved at 4~6 °C until analysis.

For collecting DNA samples, seawater (2~4 L) was filtered on 0.2 μm pore size Supor® PES filter membranes (47 mm, Pall Corp., Port Washington, NY, USA) with gentle vacuum (< 0.013 MPa) (Cheung et al., 2017, 2020). Filters are frozen in cryogenic vials immediately in a deep freezer at -80 °C until analysis.

(4) Expected results

Study 1. Biogeography and diversity of microzooplankton in the North Pacific

The biogeography, diversity and nutritional strategy of microzooplankton community obtained by 18S rRNA analysis are expected to be explained by environmental parameters (temperature, salinity, depth, nutrient and Chl *a* concentrations, phytoplankton biomass and productivity) along the meridional transect in the North Pacific.

Study 2. Response of phytoplankton to the subsurface seawater enrichment through the North Pacific
The preliminary results showed the subsurface seawater (nutrient) enrichment induced surface phytoplankton blooms at stations 39, 54 and 65, where the Chl *a* concentration in carboys incubated with subsurface seawater enrichment exceeded that incubated without it during the incubation (Figure 4.23.2). It is also worth noting that the magnitude of blooms was different at these stations. At station 39, the bloom was observed after 48h incubation. At the end of incubation, however, the Chl *a* incubated with the subsurface seawater enrichment was only 1.15 times high than that incubated without it. In contrast, at stations 54 and 65, the bloom occurred after 24h incubation. The Chl *a* concentrations incubated with the subsurface seawater enrichment were 1.93 and 2.18 times high, although the absolute Chl *a* concentration was not so high (~0.2 µg L^{-1}) in these areas where is considered oligotrophic.
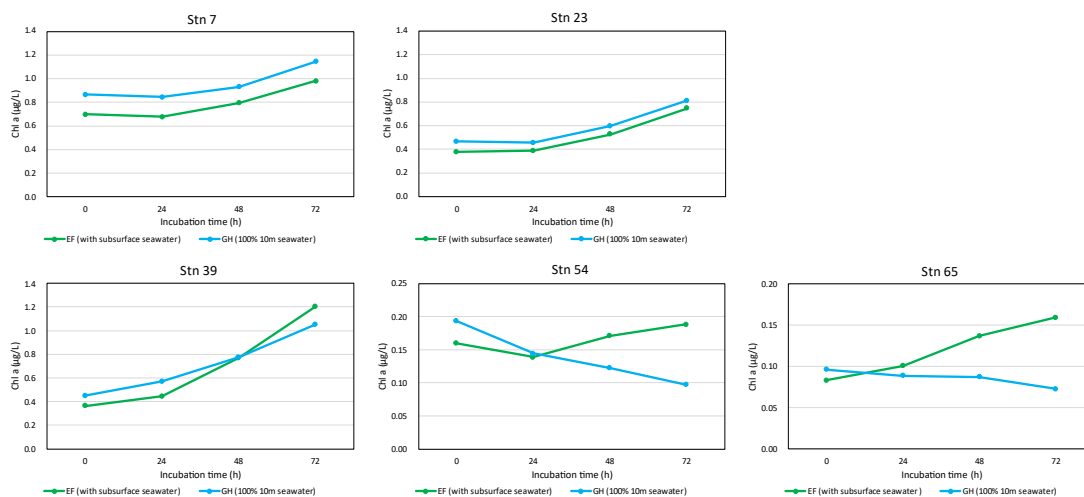

Figure 4.23.2 Chl *a* concentrations incubated with (green) and without subsurface seawater enrichment (blue) at five stations.

In addition, the phytoplankton growth rates incubated with (µ-sub) and without subsurface seawater enrichment (µ0) was calculated by Chl *a* concentrations in carboys A~D (Figure 4.22.3). Similar with Chl *a* concentrations, growth rates showed different patterns at five stations. At stations 7 and 23 where no phytoplankton bloom was observed, both µ0 and µ-sub were very low or negative at T24. After 24h incubation, growth rates turned to positive, and sometimes µ-sub slightly exceeded µ0 (station 7). However, this did not lead to phytoplankton bloom during the 72h incubation. These results might indicate the response of phytoplankton growth was very slow thus was difficult to induce a phytoplankton bloom, at least in 72 hours, which could be attributed to the low temperature that possibly limited the phytoplankton metabolism or activity. The samples collected for further DNA or RNA analysis are expected to provide valuable data to verify this speculation. Station 39 has a special situation in which µ0 and µ-sub were similar through the 72h incubation, which means there might be no nutrient limitation on phytoplankton growth at this station. However, the Chl *a* incubated with subsurface seawater enrichment slightly exceeded that without it, and a bloom with small magnitude was still observed at the end of incubation (Figure 4.23.2). According to the phytoplankton mortality rate (data not shown), the mortality rate with subsurface seawater enrichment was lower than without it from T48, thus the phytoplankton net growth was slightly higher with enrichment. Therefore, the enrichment of subsurface seawater might dilute the surface zooplankton community and further decrease their grazing on phytoplankton. Finally, the pattern at stations 54 and 65 were obviously different with other stations. Although µ-sub was lower than µ0 and T24, µ0 turned to negative at the end of incubation where µ-sub largely exceeded µ0. It is possible that the relatively depleted surface nutrient was exhausted by phytoplankton in carboys without any enrichment from T48. In contrast, phytoplankton in those with enrichments had replete nutrients to utilize for their active growth. The nutrient samples collected during the incubation will provide further information on nutrient utilization of phytoplankton community.
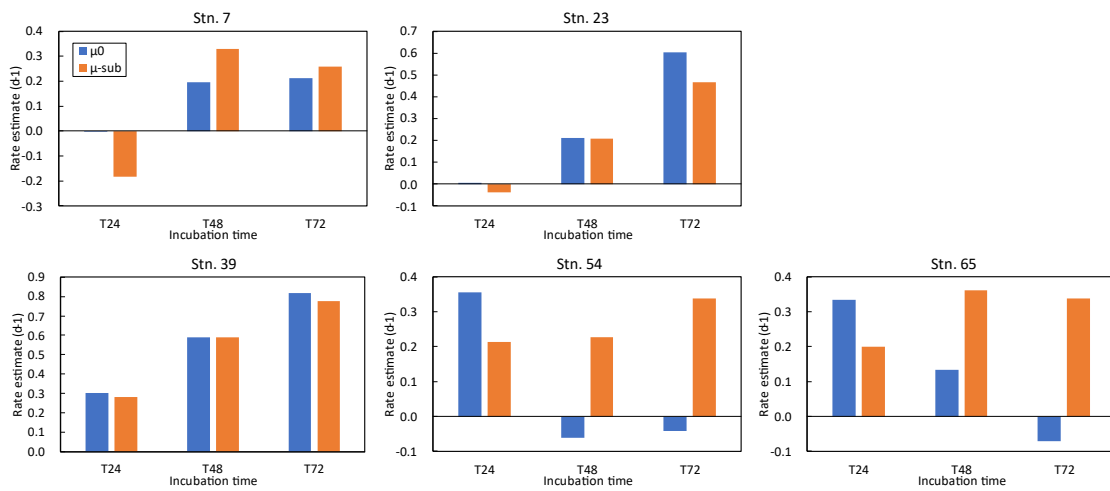
Figure 4.23.3 Phytoplankton growth rates incubated with (μ-sub, orange) and without subsurface seawater enrichment (μ0, blue) at five stations.

*Please note the result shown here is the preliminary result that could be different with the finalized one.

(5) References

Cheung, S., Suzuki, K., Saito, H., Umezawa, Y., Xia, X., & Liu, H. (2017). Highly heterogeneous diazotroph communities in the Kuroshio Current and the Tokara Strait, Japan. *PloS one*, *12*(10), e0186875.

Cheung, S., Nitanai, R., Tsurumoto, C., Endo, H., Nakaoka, S. I., Cheah, W., ... & Suzuki, K. (2020). Physical forcing controls the basin-scale occurrence of nitrogen-fixing organisms in the North Pacific Ocean. *Global Biogeochemical Cycles*, *34*(9), e2019GB006452.

Landry, M. R., & Hassett, R. P. L. (1982). Estimating the grazing impact of marine micro-zooplankton. *Marine biology*, *67*, 283-288.

4.24 pH

November 6, 2023

(1) Personnel

Hiroshi UCHIDA (JAMSTEC RIGC)

(2) Objective

The objective of this study is to understand pH change in the North Pacific and the Bering Sea.

(3) Instruments and method

Seawater pH for water samples was measured with a glass electrode pH meter (F-72 [serial no. A23C0014], Horiba, Japan) with the long glass electrode (9680S [serial no. 9Z3A0104], Horiba).

The water samples were collected in 100-mL aluminum bottles (Mini Bottle Can, Daiwa Can Company, Japan). Each bottle was rinsed three times with sample water and was filled without air space after overflowed the sample water two times of volume of the bottle (about 10 seconds) by using a plastic drawing tube (PFA tubing connected to silicon rubber tubing).

The collected seawater samples were stored in a refrigerated room (about 4 °C) until measurements, and the seawater samples were measured usually within 12 hours after water sampling. Preservability of seawater samples was checked on the R/V Mirai cruise MR23-05 leg 2.

Before measurements, the sample bottles were immersed in a water bath whose temperature was controlled to about 25 °C by a thermostat (HT-90D, AS ONE), whose temperature was set to 26 °C. The pH measurements were conducted at 25 °C in a refrigerated temperature control bath (TRL-108H, THOMAS KAGAKU Co., Ltd.), whose temperature was set to 25.1 °C.

Two buffers (*2-aminophyridine*, AMP [016-28183, lot TPH2930, expiration date: August 2024, Fujifilm Wako Chemicals Co.], and *2-amino-2-hydroxy-1,3-propanediol*, TRIS, [013-28193, lot TPG2979, expiration date: October 2024, Fujifilm Wako Chemicals]) and Multiparametric Standard Seawater (MSSW, lot PRE20, KANSO TECHNOS Co., Ltd.) (see Uchida et al., 2020) were used as references. Certified reference material (CRM) for oceanic CO_2 measurements (batch 209) provided by Prof. A. G. Dickson (Scripps Institution of Oceanography, University of California San Diego) were also measured for comparison.

The pH of seawater samples was calibrated by AMP (6.6866 in pH units of total scale at 25 °C) and PRE20 by considering the results obtained on the R/V Mirai MR23-05 leg 2 cruise. Since the pH value was not certified for PRE20, the calculated pH value (7.6400 in pH units of total scale) estimated from Practical Salinity (34.2768), dissolved inorganic carbon (2191.4 μmol/kg), total alkalinity (2301.3 μmol/kg), phosphate (1.991 μmol/kg), silicate (61.44 μmol/kg), temperature (25 °C), and pressure (0 dbar) by using CO2SYS program developed by Lewis and Wallace (1998) (K1, K2 from Lueker et al., 2000) was used as reference. The voltage values of AMP and TRIS (8.0936 in pH units of total scale at 25 °C) measured at the beginning and the end of the measurements for each day were used to estimate time drift of the pH meter, and the time drift was corrected linearly for each day of measurements.

Actual temperature measured by the glass electrode were sometimes slightly different from 25 °C. It's mean ± SD was 25.02±0.07 °C (minimum of 24.7 °C and maximum of 25.2 °C). Voltage changes due to this slight temperature deviation from 25 °C were corrected by using temperature dependencies of the voltage for AMP, TRIS, and PRE20 measurements (Fig. 4.24-1). The temperature coefficients were 0.68 mV/°C, 1.07 mV/°C, and 0.16 mV/°C for AMP, TRIS, and PRE20, respectively. For seawater samples, the temperature coefficients were assumed to be the same as that of the standard seawater (PRE20). The temperature coefficient of the standard seawater was smaller than that of AMP and TRIS. The magnitude of the correction for seawater samples was within ±0.001 pH units for temperature deviation of ±0.3 °C.
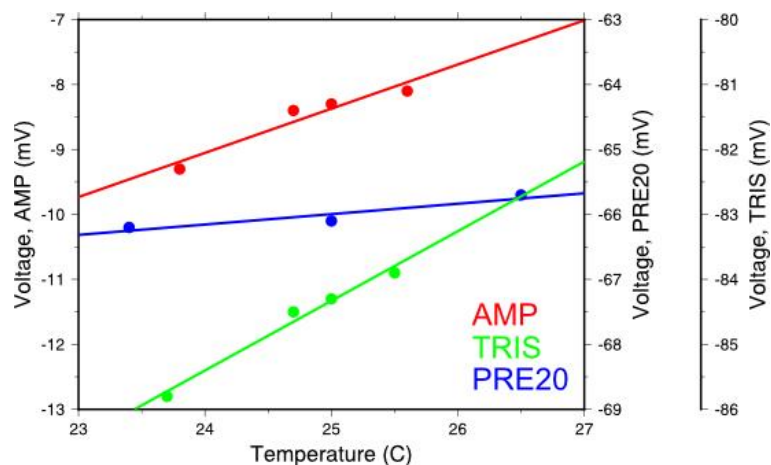
Figure 4.24-1. Temperature dependencies of the voltage for AMP, TRIS, and PRE20 measurements. Data were obtained on the R/V Mirai cruise MR23-05 leg 2.

(4) Results

A total of 22 bottles of PRE20 was used as reference. From the comparison with CRM (Table 4.24-1) and variability of the seawater samples in the deep ocean, one bottle (serial no. 316) of PRE20 was judged to have a bias in pH. The bias of PRE20 serial no. 316 was estimated to be –0.0066 by adjusting the pH value of CRM serial no. 0844 to 7.7623, and the pH measurement for station 44 was conducted by using the bias corrected pH value. The mean ± SD of pH of PRE20 calibrated with AMP and TRIS was 7.6716 ± 0.0028. This variability (0.0028) seems to be resulting from the variability of TRIS buffer measurement.

A total of 66 pairs of replicate samples was measured and SD of the replicate samples was 0.0009 pH unit.

Comparison between the measured pH and the calculated pH from measured dissolved inorganic carbon and total alkalinity with salinity, phosphate, and silicate at temperature of 25 °C and pressure of 0 dbar by using CO2SYS program developed by Lewis and Wallace (1998) (K1, K2 from Lueker et al., 2000) was shown in Fig. 4.24-2. Variability of the measured pH in the deep ocean was smaller than that of the calculated pH.

Table 4.24-1. Results of pH measurements for CRM batch 209. The mean value (7.762) calculated excluding #0844 was smaller than the calculated pH value (7.771) and the measured value (7.798) calibrated with AMP and TRIS.

Serial number of CRM	pH (total scale) calibrated with AMP and PRE20	pH (total scale) calibrated with AMP and TRIS	Stations (Serial no. of PRE20)
0658	7.7624	7.7987	42 (311)
0844	7.7548	7.7969	44 (316)
0594	7.7623	7.7998	47,50 (318)
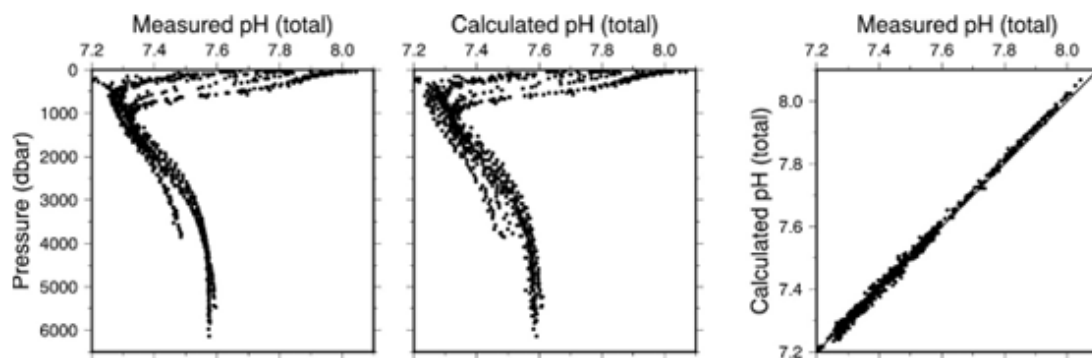
Figure 4.24-2. Vertical profiles of the measured pH (left panel) and the calculated pH (middle panel). Comparison of the measured pH and the calculated pH is also shown (right panel).

(5) References

Dickson, A. G., C. L. Sabine, and J. R. Christian (Eds.) (2007): Determination of the pH of sea water using a glass/reference electrode cell. In Guide to best practices for ocean CO2 measurements. PICES Special Publication 3, IOCCP report no. 8.

Lewis, E., and D. W. R. Wallace (1998): Program developed for CO2 system calculations. Report 105, 33 pp., Oak Ridge, TN: Oak Ridge National Laboratory. Retrieved from https://cdiac.esd.ornl.gov/oceans/co2rprt.html.

Uchida, H., T. Kawano, T. Nakano, M. Wakita, T. Tanaka and S. Tanihara (2020): An updated batch-to-batch correction for IAPSO standard seawater. J. Atmos. Oceanic Technol., 37, 1507-1520, doi:10.1175/JTECH-D-19-0184.1.

(6) Data archive

These obtained data will be submitted to JAMSTEC Data Management Group (DMG).

4.25 Iodine isotopes and uranium isotopes
November 08, 2023

(1) Personnel
    Hiroyuki Matsuzaki (The University of Tokyo)
    Yuanzhi Qi (The University of Tokyo)

(2) Objective
    The objective of this study is to explore the cycling processes of stable iodine (^{127}I), radioiodine (^{129}I), and radio-uranium (^{238}U and ^{236}U) in the North Pacific Ocean and the Bering Sea.

(3) Sample collection
    The sampling stations of iodine and uranium samples are summarized in Table 4.25-1 and Table 4.25-2, respectively. Surface seawater samples were obtained using the sampling pump system installed on the research vessel. Seawater samples from other depths were collected using 12 L Niskin bottles mounted on a CTD/Carousel Water Sampling System (CTD system). Immediately after sampling, iodine samples were filtered through 0.45 μm mixed cellulose ester membrane filters (ADVANTEC). Part of filtered seawater was separated and stored in 50 mL PP bottles for ^{127}I measurement and the remaining seawater for ^{129}I was treated onboard. Uranium samples were directly collected into 5-L plastic containers and stored at room temperature until further analysis.

(4) Instruments and method
    The bulk concentration of ^{127}I and ^{238}U will be measured by Inductively Coupled Plasma Mass Spectrometry (ICP-MS) after 10-time dilution by 0.5% tetramethylammonium hydroxide (TMAH) and 1 M HNO$_3$, respectively. Iodide-127 (^{127}I$^-$) concentration of seawater will be measure by Ion Chromatography (IC) directly. Since the dissolved organic iodine concentration is very low in open ocean, the iodate-127 (^{127}IO$_3^-$) concentration will be calculated by the difference of bulk ^{127}I and ^{127}I$^-$.

    Different ^{129}I species, including bulk ^{129}I, ^{129}I$^-$, and ^{129}IO$_3^-$, have been separated by a onboard coprecipitation method (Qi and Matsuzaki, 2022) and will be measured by ^{129}I-AMS system in MALT (Micro Analysis Laboratory, Tandem accelerator, The University of Tokyo). The uranium in seawater will be absorbed by hydrated titanium oxide (HTO) and then dissolved in 3 M HNO$_3$. The uranium in the above acidic solution will be coprecipitated by Fe(OH)$_3$ and the ^{236}U in the obtained precipitate will be analyzed by ^{236}U-AMS system in MALT.

(5) Data archive

  The data obtained in this cruise will be submitted to the Data Management Group of JAMSTEC and will be opened to the public via "Data Research System for Whole Cruise Information in JAMSTEC (DARWIN)" in the JAMSTEC web site.

Table 4.25-1 Sampling stations of seawater for iodine

Station	Sampling Date (UTC)	Position Latitude	Position Longitude	Depth (m)
005	2023/10/11	56-58.74N	175-40.39W	3482
011	2023/10/09	53-59.67N	177-53.35W	3800
025	2023/10/17	50-00.41N	178-59.61E	4981
032	2023/10/21	46-29.30N	179-00.36E	5636

042	2023/10/24	41-29.30N	179-00.02E	4988
052	2023/10/27	36-29.81N	179-00.54E	4522
058	2023/10/28	33-28.84N	178-59.38E	2938
067	2023/10/31	29-00.00N	177-45.00E	5358

Table 4.25-2 Sampling stations of seawater for uranium

Station	Sampling Date (UTC)	Position		Depth (m)
		Latitude	Longitude	
4	2023/10/11	57-29.69N	175-15.32W	3526
10	2023/10/09	54-29.59N	177-33.34W	3860
24	2023/10/17	50-14.66N	179-09.04E	6138
33	2023/10/21	45-59.53N	179-01.09E	5849
41	2023/10/24	41-58.76N	178-59.62E	5216
51	2023/10/26	36-59.38N	179-00.64E	5282
59	2023/10/29	32-58.75N	178-58.99E	4908
66	2023/10/31	29-30.00N	177-52.50E	5231

(6) Reference

Qi, Y. and Matsuzaki, H. Speciation analysis of both inorganic and organic [129]I in seawater and its application in the study of marine iodine cycle. Analytical Methods, 4., 37, pp.3623-3631, August, 2022.

4.26 XCTD
November 8, 2023

(1) Personnel
Hiroshi UCHIDA (JAMSTEC RIGC)
Masanori MURAKAMI (NME)
Fumine OKADA (NME)
Haruna YAMANAKA (NME)

(2) Objective
The objective of this study is to evaluate XCTDs (eXpendable Conductivity, Temperature and Depth profiler) data by side-by-side comparisons with the shipboard CTD (Conductivity, Temperature and Depth profiler) measurements.

(3) Instruments and method
The probes used were XCTD-4N, XCTD-4A, and XCTP-4 (Tsurumi-Seiki Co., Ltd., Yokohama, Kanagawa, Japan) (Table 4.26-1) with an MK-150N deck unit and a data acquisition software AL12 version 1.8.0 (Tsurumi-Seiki). The XCTD/XCTP probes were deployed during the down cast of the shipboard CTD measurement (Table 4.26-2). The XCTD probes were deployed by using a 12-loading automatic launcher (Tsurumi-Seiki), except for the XCTD-4A at station 070 for test of the operating system. The XCTP probes were deployed by a hand launcher because the automatic launcher was not compatible for the slower fall rate probe (a shutter of the automatic launcher will close before the end of the measurement). At station 011, the XCTP-4 probe was carefully deployed by hand keeping its position vertically.

Table 4.26-1. List of XCTD/XCTP probes prepared for this cruise. The XCTD-4N (board version XCTD R1.5) was prepared for an alternative measurement of the shipboard CTD measurement, but there was no need to deploy it instead of conducting the CTD measurement.

Probe type	Board version Approximate interval	Resolution of A/D converter			
		Temperature (°C)	Conductivity (mS/cm)	Pressure (dbar)	depth (m)
XCTD-4N	XCTD R1.5	0.01 (12 bit)	0.015 (12 bit)	N/A	0.13
XCTD-4N	XCTD R1.6	0.01 (12 bit)	0.015 (12 bit)	N/A	0.13
XCTD-4N	XCTP R1.2	0.01 (12 bit)	0.015 (12 bit)	N/A	0.13
XCTD-4A	XCTP R1.2	0.001 (16 bit)	0.001 (16 bit)	N/A	0.27
XCTP-4	XCTP R1.2	0.002 (15 bit)	0.001 (16 bit)	0.07 (15 bit)	0.2

Table 4.26-2. List of the side-by-side comparisons with the shipboard CTD measurement.

Probe type (board ver.)	Serial no.	CTD depths	Note
Station 011_1, 53° 59.66'N, 177° 53.34'E, 3801 m, SST: 8.726 °C, SSS 32.952			
XCTD-4A	23055501	Down 3-444 m	
XCTD-4N (XCTD R1.6)	23014230	Down 618-1311 m	
XCTD-4N (XCTP R1.2)	23055513	Down 1505-2220 m	
XCTP-4	23030041	Down 2351-3227 m	Hand launcher
Station 028_1, 48° 31.23'N, 178° 59.48'E, 5587 m, SST: 8.489 °C, SSS 32.808			
XCTD-4A	23055502	70 minutes after the CTD cast (just before leaving the station)	
Station 035_1, 45° 03.45'N, 179° 00.92'E, 5788 m, SST: 12.438 °C, SSS 33.090			
XCTD-4A	23055503	Down 1-461 m	
XCTD-4N (XCTD R1.6)	23014231	Down 662-1291 m	
XCTD-4N (XCTP R1.2)	23055514	Down 1538-1730 m	Failed at 575 m
XCTP-4	23030042	Down 2058-2935 m	Hand launcher
Station 044_2, 40° 29.96'N, 179° 00.89'E, 5861 m, SST: 18.959 °C, SSS: 34.108			
XCTD-4A	23055504	Down 0-488 m	
XCTD-4N (XCTD R1.6)	23014233	Down 732-1396 m	
XCTD-4N (XCTP R1.2)	23055516	Down 1645-2357 m	
XCTP-4	23030044	Down 2587-3493 m	Hand launcher
Station 054_1, 35° 30.03'N, 179° 01.09'E, 4396 m, SST: 21.862 °C, SSS: 34.504			
XCTD-4A	23055505	Down 2-451 m	
XCTD-4N (XCTD R1.6)	23014234	Down 665-1264 m	
XCTD-4N (XCTP R1.2)	23055517	Down 1483-2188 m	
XCTP-4	23030045	Down 2322-3199 m	Hand launcher
Station 064_1, 30° 29.96'N, 178° 29.97'E, 4768 m, SST: 24.793 °C, SSS: 34.762			
XCTD-4A	23055506	Down 0-420 m	
XCTD-4N (XCTD R1.6)	23014235	Down 621-1237 m	
XCTD-4N (XCTP R1.2)	23055518	Down 1452-2092 m	Failed at 1823 m
XCTP-4	23030046	Down 2266-3130 m	Hand launcher
Station 066_1, 29° 29.97'N, 177° 52.51'E, 5195 m, SST: 25.508 °C, SSS: 35.092			
XCTD-4A	23055507	Down 1-470 m	
XCTD-4A	23055508	Down 618-1270 m	
Station 067_1, 28° 59.90'N, 177° 45.07'E, 5156 m, SST: 25.874 °C, SSS: 35.207			
XCTD-4A	23055509	Down 0-436 m	
XCTD-4A	23055511	Down 528-1134 m	
Station 070_1, 27° 29.95'N, 177° 52.46'E, 5382 m, SST: 26.655 °C, SSS: 35.454			
XCTD-4A	23055512	Down 200-780 m	Hand launcher

(4) Results

The results of the side-by-side comparisons with the shipboard CTD will be combined with the results of the side-by-side comparisons obtained in the R/V Mirai cruise MR23-05 leg 2 and the results of temperature sensor calibration performed before the cruise (June 12, 2023), and will be used to evaluate performance of these probe types of XCTD/XCTP similarly to Uchida et al. (2011).

Figure 4.26-1 shows an example of obtained temperature-salinity profiles of CTD and XCTD/XCTP. As reported by Uchida et al. (2011), a loop shape and low salinity bias in a region of strong vertical temperature gradient can be seen for the XCTD-4N (board version XCTD R1.6). These errors result from a mismatch of temperature and conductivity data acquisition. For the XCTD/XCTP with the board version XCTP R1.2, such artificial errors resulting from the mismatch of temperature and conductivity data can not be seen. For the XCTD-4N, noise resulting from the low data resolution is noticeable in deeper part. Such noise can not be seen for the XCTD-4A and XCTP-4 because resolutions of temperature and conductivity data are one order higher than the data of XCTD-4N.

(5) Reference

Uchida, H., K. Shimada, and T. Kawano (2011): A method for data processing to obtain high-quality XCTD data. *J. Atmos. Oceanic Technol.*, **28**, 816–826.

(6) Data archive
  These obtained data will be submitted to JAMSTEC Data Management Group (DMG).

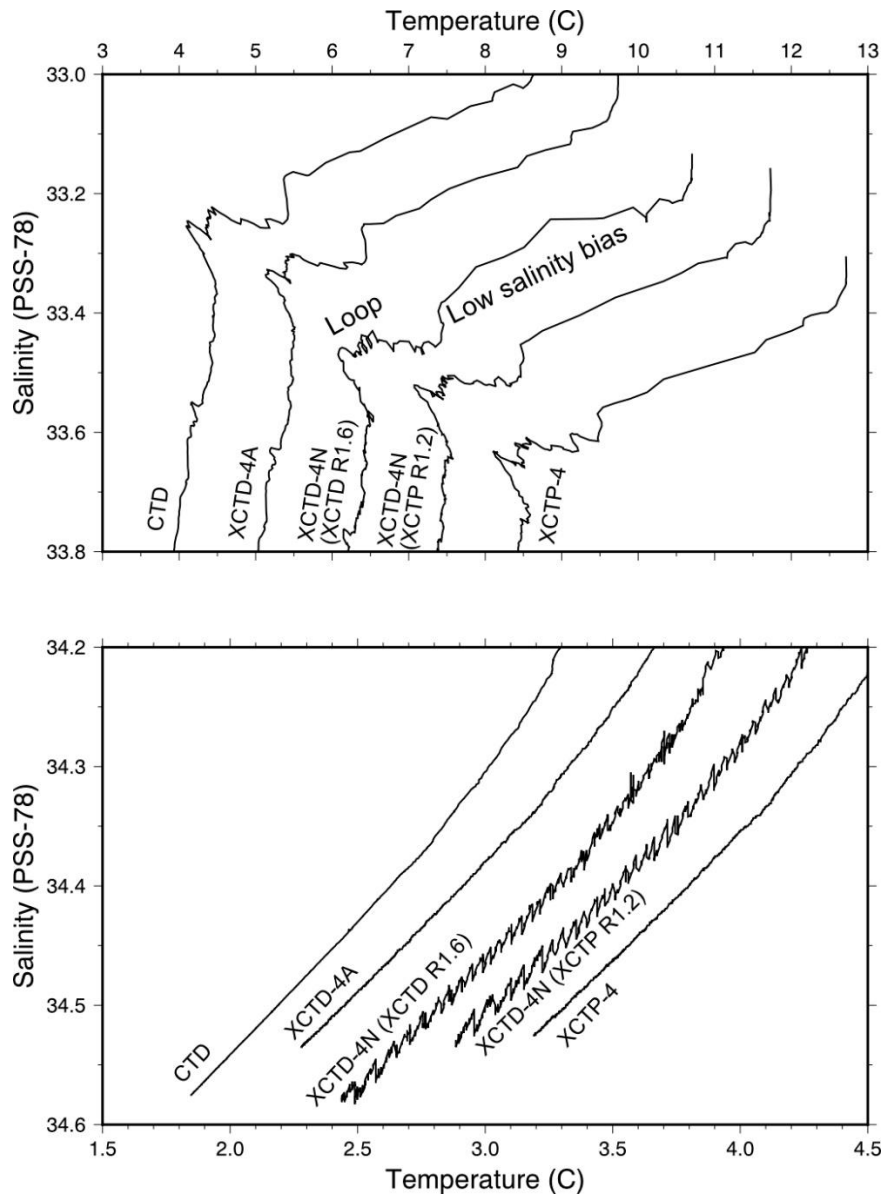Figure 4.26-1. Comparison of temperature-salinity profiles from CTD and XCTD/XCTP data obtained at
  station 011_1. Upper panel shows the shallower part (from surface to about 300 m) and lower panel
  shows the deeper part (depths deeper than about 800 m). The profiles are shown with horizontal and
  vertical offsets to prevent overlap.

5. Float Deployments

5.1 Core and Deep Argo Floats

(1) Personnel
Shigeki Hosoda (JAMSTEC): Principal investigator
Kanako Sato (JAMSTEC)
Mizue Hirano (JAMSTEC)
Nobuhiro Fujii (MWJ)   Technical Staff
Tun Htet Aung (MWJ)   Technical Staff

(2) Objective
The objective of the core and deep Argo float deployments is to clarify interior oceanic changes associated with variations in climate and ocean environment, monitoring physical and biogeochemical parameters within the framework of the Argo programme. To achieve the objective, three core Argo floats and one deep Argo float were deployed to carry out automatic measurements of long-term temperature, salinity, and dissolved oxygen variations in the North Pacific Ocean where the spatial density of the Argo floats is insufficient due to a lack of float deployment opportunities. The data will be validated to meet the target accuracies of core and deep Argo which have been decided by the Argo data management team, using shipboard CTD data in this GO-SHIP cruise. Data accumulated from all deployed Argo floats are submitted to Argo data flow in real-time to contribute to maintaining the Argo observing array, as well as improvement of accuracy on long-term forecasts of climate changes through data assimilation systems.

(3) Parameters
・Core Argo float :Water temperature, salinity and pressure.
・Deep Argo float :Water temperature, salinity, pressure and dissolved oxygen.

(4) Method
We launched APEX floats manufactured by Teledyne and Deep NINJA float manufactured by Tsurumi-Seiki Co., Ltd. Those floats are equipped with a CTD sensor manufactured by Sea-Bird Electronics Inc. or RBR Ltd. RINKO AROD-FT manufactured by JFE-Advantec is mounted on the Deep NINJA. The float drifts at a depth of 1000dbar or 2000dbar (called the parking depth) during waiting measurement, then goes upward from a depth of 2000dbar or 4000dbar to the sea surface every 1-10 days. During the ascent, physical values are measured following the depth table. During surfacing for approximately half an hour, the float sends all measured data to the land via the Iridium RUDICS or SBD telecommunication system. The lifetime of floats is expected to be about four to eight years. The status of floats and its launching information are described in Table 5.1. 1.

Table 5.1. 1 Specifications of floats and their launching positions

Float Type	Core	APEX float manufactured by Teledyne Webb Research.
	Deep	Deep NINJA float manufactured by Tsurumi-Seiki Co., Ltd.
CTD sensor	Core	SBE41 manufactured by Sea-Bird Electronics Inc.
		RBR argo manufactured by RBR Ltd.
	Deep	SBE41 manufactured by Sea-Bird Electronics Inc.
Dissolved oxygen sensor	Deep	AROD-FT manufactured by JFE Advantech Co., Ltd..
Cycle	Core	every 1-10 day (approximately 30minutes at the sea surface)
	Deep	every 2-10 day (approximately 30minutes at the sea surface)
Iridium transmit type	Core	Router-Based Unrestricted Digital Internetworking Connectivity Solutions (RUDICS)
	Deep	

		Iridium Short Burst Data(SBD)
Target Parking Pressure	Core	1000 dbar
	Deep	2000 dbar
Sampling layers	Core	2dbar interval from 2000 dbar to surface (approximately 1000 levels)
	Deep	physical parameters(water temperature, salinity, pressure) 2dbar interval from 2000 dbar to surface (approximately 1000 levels) .
		Biogeochemical parameter(dissolved oxygen) interval 50dbar from 5500 dbar to 2000 dbar interval 20dbar from 1980 dbar to 1000 dbar interval 10dbar from 990 dbar to 400 dbar interval 2dbar from 398 dbar to surface

Table 5.1.2 Floats launching positions

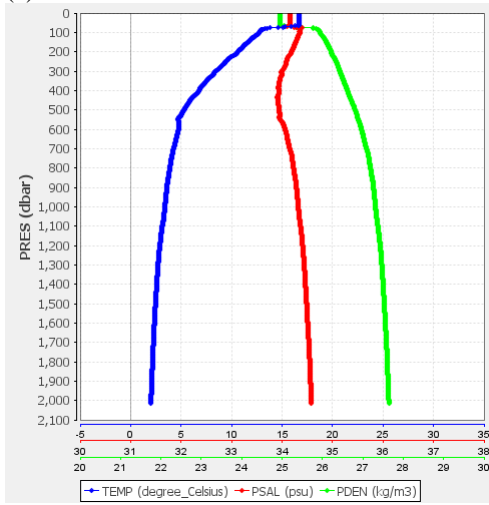| Float S/N	WMO ID	Date and Time of Launch (UTC)		Location of Launch		Station
10056	5906599	2023/10/24	16:45	41° 28.92' N	178° 59.71'E	042
10057	5906600	2023/10/26	02:45	38° 58.01'N	179° 01.48'E	047
35	7900875	2023/10/28	02:01	35° 29.05'N	179° 00.70'E	054-3
9949	5906598	2023/10/30	23:45	29° 59.53'N	178°01.03' E	065

Table 5.1.3 Floats configrations.

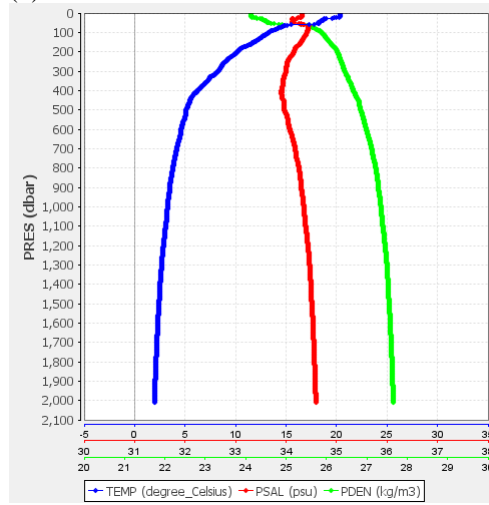| Float S/N	Type of type	Name of product	CTD sensor
10056	Core	APEX	RBR argo
10057	Core	APEX	RBR argo
35	Deep	DeepNINJA	SBE41
9949	Core	APEX	SBE41

(5) Data archive

The Argo float data will be provided conducting the real-time quality control within 24 hours following the procedure decided by Argo data management team. Then the delayed mode quality control will be conducted within 6 months ~ 1 years, to satisfy their data accuracy for climate research use. Those quality-controlled data are freely available via internet and utilized for not only research but also weather forecasts and any other variable use through internet. Global Data Assembly Center (GDAC: https://usgodae.org/argo/argo.html, https://www.coriolis.eu.org/Observing-the-Ocean/ARGO, https://dataselection.euro-argo.eu/), Global Telecommunication System (GTS).
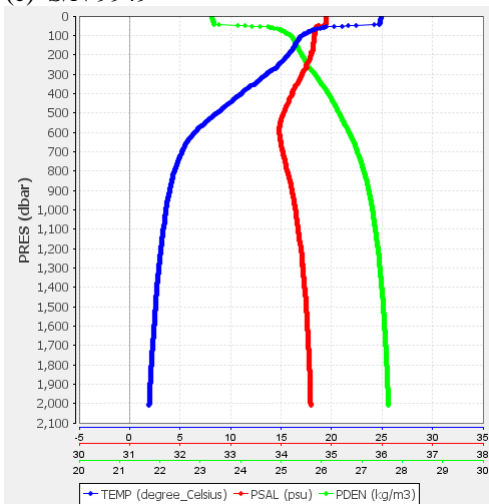
(a) S/N10056

(b) S/N 10057

(c) S/N 9949

Fig. 5.1.1 (a , b and c). Vertical temperature, salinity and density profiles of their first measurements for three Core Argo floats (SN10056, SN10057 and SN 9949). Blue, red and light green lines show temperature, salinity and density profiles.
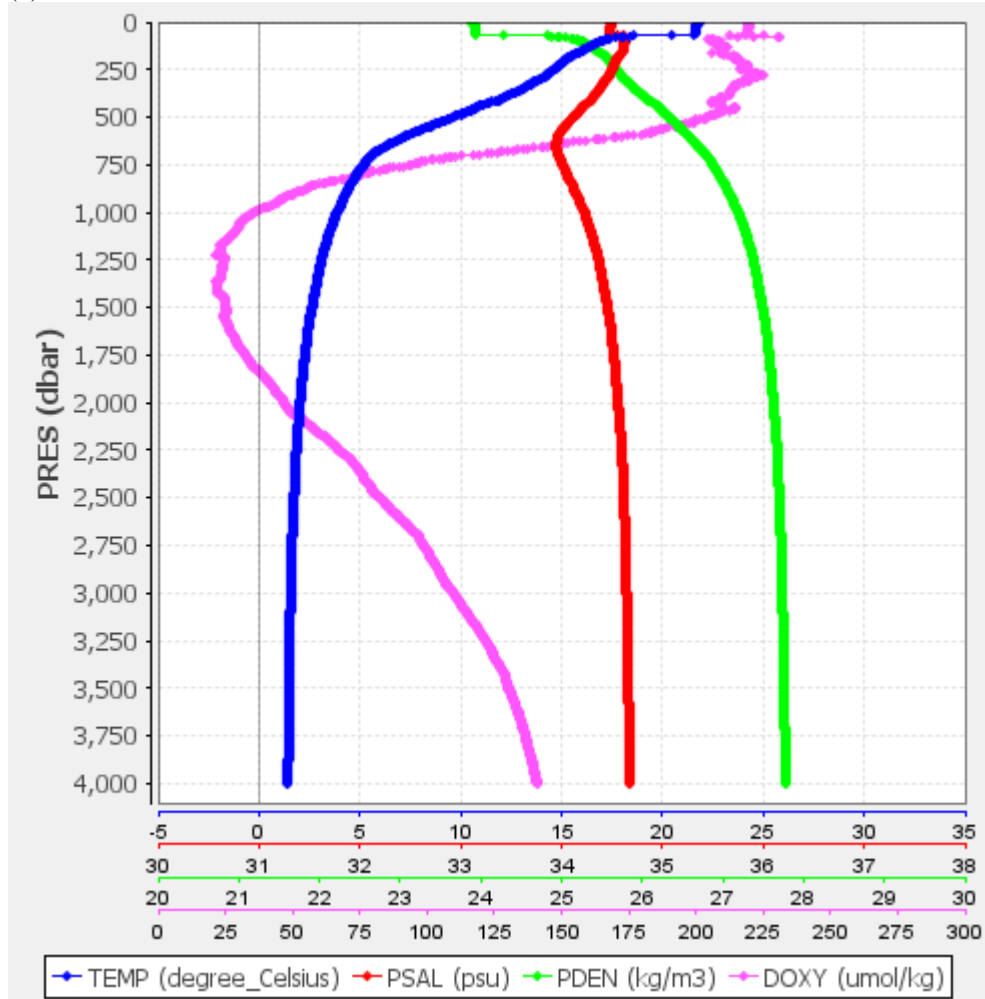
(d) S/N35

Fig. 5.1.2 (c). Vertical temperature, salinity, density and dissolved oxygen profile of third measurements for Deep NINJA float (SN053). Blue and red lines show temperature and salinity profiles. And light green and pink lines show density and dissolved oxygen profiles.

5.2 GO-BGC floats

(1) Personnel

Lynne Talley (UCSD Scripps Institution of Oceanography)	Principal Investigator
Kenneth Johnson (Monterey Bay Aquarium Research Institute)	Principal Investigator
Stephen Riser (University of Washington)	Principal Investigator
Curtis Deutsch (Princeton University)	Principal Investigator
Susan Wijffels (Woods Hole Oceanographic Institution)	Principal Investigator
Andrew Meyer (University of Washington)	Float check in Dutch Harbor
George Matsumoto (Monterey Bay Aquarium Research Institute)	Outreach contact
Jennifer Magnusson (Monterey Bay Aquarium Research Institute)	Outreach contact
Addie Norgaard (UCSD Scripps Institution of Oceanography/University of Alaska Fairbanks)	On board

(2) Objectives

The Global Ocean Biogeochemistry (GO-BGC) Array is a program funded by the U.S. National Science Foundation to build a global network of autonomous biogeochemical profiling floats. This float network collects data on ocean chemistry and biology from the surface to a depth of 2,000 meters to expand our understanding of ocean ecosystems, ocean health and productivity, global chemical cycles, and how they are responding to climate change and increasing atmospheric carbon dioxide.

Each float was adopted and named by classrooms as a part of the "Adopt-a-Float" outreach program. Addie Norgaard decorated floats with each school's theme and wrote blog posts which can be found at https://www.go-bgc.org/expedition-logs/north-pacific-2023.

(3) Methods

Teledyne Webb Apex floats were equipped by the GO-BGC team to measure seven parameters: salinity, temperature, oxygen, pH, nitrate, fluorescence, and optical backscatter. Expected float lifetime is 5 years. The observation cycle is a 9-day drift at 1000 dbar, descending to 2000 dbar and then ascending to the sea surface every 10th day, when data are transmitted via satellite. The data are

processed and streamed to the Argo GDAC where they are publicly available in nearly real time. The windows of the nitrate sensor and fluorescence and optical backscatter sensor were cleaned by Addie Norgaard prior to deployment using lens wipes, ultra-pure water and lens paper. Deployments coincided with CTD sampling casts to provide sensor validation measurements. CTD, oxygen, nitrate and carbon validation measurements were made by JAMSTEC. Optical validation measurements (HPLC and POC) were not made by GO-BGC due to sampling equipment not arriving to Dutch Harbor in time. Float deployments were conducted immediately following each station's final CTD cast. All seven float deployments were observed by Addie Norgaard and were without incident.

(4) Deployment information

Float ID	WMO ID	Adopt-A-Float Name	Date and Time of Launch (UTC)	Location of Launch	CTD Station No.
21818	5907058	Mr. Plank	2023/10/10 22:49	55-0.10 [N] 176-29.05 [W]	7
21839	6990584	The NaviGator	2023/10/18 23:35	47-58.23 [N] 179-00.12 [E]	29
21939	4903748	Doc Bellamy	2023/10/22 07:33	45-29.87 [N] 179-01.88 [E]	34
21792	6990584	Tiger Time	2023/10/23 08:16	43-59.60 [N] 178-58.64 [E]	37
21285	2903862	CCTYMareLA23	2023/10/26 20:20	37-28.86 [N] 179-00.61 [E]	50
21810	1902646	Cougar Courage Climbs High	2023/10/29 11:38	32-29.11 [N] 179-00.48 [E]	60
21861	2903860	The Milford Buc	2023/11/1 06:00	27-29.99 [N] 177-52.27 [E]	70

(5) Data archive

GO-BGC data can be used freely, with no restrictions, as part of the public Argo float data set. It can be accessed in various formats through multiple data portals, both in near-real time with automatic adjustments, and following a delayed-mode quality control. More information about data access can be found here: https://www.go-bgc.org/data/access-and-visualization

6. Postgraduates

A number of postgraduate assistants contributed to the cruise. Here are the voices from some of them. English writing was assisted by Addie Norgaard.
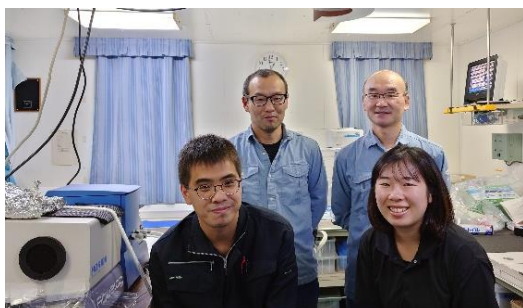
Yugo Nishimura（Okayama University）

I am proud of having participated in this state-of-the-art oceanographic research aboard the research vessel Mirai!

I major in Earth science at university and do not have much to do with oceanography, but I am interested in research cruises because I use marine sediments in my research. So, when my supervisor told me about this opportunity to do laboratory work at sea, I wanted to give it a try. It was a long cruise of about one month duration, so I was worried about many things, such as life on the ship and seasickness, but it turned out to be very fulfilling. I used an Aqualog instrument (HORIBA Scientific) to analyze fluorescent dissolved organic matter (FDOM). I had never seen this analytical instrument before at university, so it has been exciting to perform the analysis. At first, there were many things I did not understand, but it has been a happy experience to learn how to use the instrument and to understand how it works through many questions and investigations. I was also thrilled to be able to see with my own eyes state-of-the-art oceanographic research such as observations using the CTD, water sampling, and the deployment of autonomous profiling floats. This was my first time on a ship for such a long period, and I did not feel well a few times when the ship was rocking hard in rough weather, but with advice from senior colleagues, I managed to get through it. Looking back, the month since we left Japan seems like a day. It was a great experience that I will never forget. If possible, I would like to do more research on R/V Mirai. I would like to thank all the people who took care of me this time.

Aya Takagi

I joined this cruise as a sampling assistant, and it's my first time of boarding R/V MIRAI. Compared to previous voyages I have participated in, the size of the ship and the scale of the observations were much larger. It was the first time for me to see full-scale measurement operations, so it was very intriguing. I am also glad that I had the opportunity to talk with so many researchers and students who participated from various regions and institutions. Although it was a long cruise, I found life onboard exciting and different from my usual research at the university, and because of that, and the delicious meals, the days were fulfilling. Since I am interested in laboratory works and always wanted to experience oceanographic laboratory works at sea, I am very glad that I have participated in this GO-SHIP cruise at the end of my-time as a student. Thank you very much.

Essay about the R/V MIRAI cruise
Mariko Honda
Technical assistant in the Marine Work Japan (assistant water sampler)

Sea water sampling from Niskin bottles was the main and favorite job for me. Before beginning sampling, we checked Niskin bottles for leaks. Then, we opened the nozzle and poured water into various bottles according to various sampling methods. The methods prescribe, for example, how many times we have to rinse, how many seconds of overflow, whether air bubbles are allowed depending on the target substance. It was not easy for me to remember all of the sampling methods even after many sampling stations.

The cruise track is southward in this cruise, from about 58N to 28N. The hydrography dramatically changed, and I recognized the changes from water and air temperature while sampling. My hands were chilled from cold water in the first half of schedule. On the other hand, it was hot enough to make me sweat in the latter half. Thanks to this experience, I reached the northernmost point in my life and crossed the dateline by ship for the first time.

Lastly, I appreciate all the support from kind researchers, skillful technicians, and experienced crew. Thank you very much for the delicious food and clean onboard facilities. I was just one sampler and made only a small contribution to the project, but, to me, all experience on this cruise will definitely be valuable in my life.

Hibiki Otsuka

In March 2023, I contacted Mr. Katsumata, the principal researcher, to apply for an assistant job on R/V Mirai for JAMSTEC observation voyage MR23-07 (10/6~11/9) . At that time, I only thought that I wanted to sail on a big ship! When I was hired for the job, I become more anxious than happy, because I had never traveled abroad before and because I was afraid that my PhD studies would be delayed. However, once CTD observations started, I was fully absorbed in the fun of water sampling. I couldn't set up the CTD with 36 Niskin bottles because my arms are too short to reach out the trigger, but I was OK doing other work. This voyage of more than a month length was a great experience. For example, I realized the changes in ocean color and sea water temperature as I sailed in the Bering Sea and North Pacific Ocean from from 60°N to almost 20°N. In particular, it was my favorite time to see sky, sea, and sea birds with Team P members while waiting for the CTD to come on deck. I was sea sick almost every day, and I couldn't eat much. But I enjoyed the days onboard. This cruise left me with a positive impression. I would like to thank everyone involved in this voyage.

Takumi Iwai

I had never done sea water sampling before in my life. At first, it was very difficult for me because there are many differences among different samples such as dissolved oxygen, carbon, and CDOMs. But Mr. Fujiwara (sampling leader of Team P) was very patient, and he taught me how to sample day by day. Chlorofluorocarbon sampling was the most difficult for me, and I made a large number of mistakes. But he encouraged me, and he said, "take it easy and do it slowly". Ms. Uno and Ms. Otsuka (assistant sampler colleagues) were like older sisters for me. They helped me in many areas.

Bucket sampling required physical strength. I had sore arms because I didn't exercise before the cruise. I look forward to exercising when I get off the ship.

Washing sampling bottles was not difficult for me, I liked it. Ms. Fujiki, Ms. Miyoshi and Mr. Izutsu taught me how to wash sampling bottles thoroughly. They helped me a lot.

Meals of R/V Mirai are very delicious and plenty. I enjoyed it every day. I ate many dishes every day and I put on about 5kg.

Drinking beer after work was the best part of the day. Mr. Izutsu, Mr. Fujii, Mr. Yamaguchi, Mr. Fujiwara, and Mr. Katsumata gave me a lot of beer. I thank them as beer was the savior of my hard days. Mr. Tun gave me a lot of cigarettes. I also thank him.

Mr. Izutsu (my roommate) talked with me about many things, and we would drink beer together after work. I liked this time because it was very relaxing. I thank him.

Finally, I would like to thank the following people as this cruise has been such a precious experience to me: Principal Investigator Mr. Katsumata, my advisor Professor Ohshima who allowed me to have this opportunity, Ms. Uno, Ms. Otsuka, and other assistant samplers, Mr. Arii and other technicians from Marine Works Japan, researchers from JAMSTEC, all cooking staff for such delicious meals, and the crew and officers of R/V Mirai for a safe cruise. Thank you all.

Wakana Sawada

My main job was analysis of CFC samples. The most amazing thing I learned was that the equipment was handmade. The process included extracting CFCs from sea water and detecting target gases without contamination. At first, I was fully occupied just learning the operation. As I got used to the operation, I started understanding the mechanism of the analysis. I found it both interesting to quantify CFCs that cannot be seen with my eyes and dissolved in only a tiny amount in seawater, and also difficult it was to control the quality of analysis. I have seen some of the observation and analysis methods before in my university cruise classes, but it was refreshing to learn the methods again on board. Total Alkalinity, which I had never heard of, is a difficult quantity to understand but it is very interesting because this quantity is important for understanding seawater carbon dioxide chemistry. After observations, I was able to see the results. I felt as if I was looking into the North Pacific with my own eyes. I had a chance to see the engine room, where I was impressed by the power required to move the big ship. As a whole, I found great pleasure in seeing what cannot be directly seen. This realization stretches my imagination even further when I think about the work of nature that is the ocean – my favorite place. Lastly, I thank the researchers, the technicians, the crew members, the officers, and everyone that helped me participation this cruise.

Harua Uno

I was assigned to help with water sampling during this research cruise. I mainly distributed the seawater collected by the CTD system into sampling bottles following the procedures designated by each sample. I had seen a CTD system with 24 Niskin bottles before, so I felt that the CTD system with 36 Niskin bottles that was used for this cruise was very large. There were a large number of not only sampling depths but also substances. I sampled water in sampling bottles that I had never seen nor heard before. In particular, I was surprised to see water sampled in something like a syringe or a dripper in biological water sampling. It was difficult to sample water from Niskin bottles, but it was interesting and fun to sample water with other researchers in a cramped space, shoulder to shoulder.

In the cruise, I was most impressed by the ocean color in the tropical ocean which was very clear and blue. It was completely different from the green ocean which I had seen when swimming at the beach. The further south I went, the brighter blue the ocean became. I learned that the clear and bright blue sea water has fewer nutrients and plankton, which means, in a sense, that it is more "dead". But the blue and shining ocean under the sun was very, very beautiful.

Thank you for this great experience!!

Cruise report

Ozawa Mone

I have been on research vessels several times, but this was my first time onboard R/V Mirai. When I saw the Mirai for the first time, I was surprised at its sheer size and began looking forward to the voyage. During the tour of the ship, I was afraid I would get lost because it was like a labyrinth in the ship. However, as the days went by, I gradually got used to the ship. The weather was not so good for a while after departure. I remember, looking out from the window, the sky was all cloudy.

I worked as an assistant analyst on this voyage. My job was to analyze FDOM. I was nervous because it was my first time using this analytical instrument, and because the data I produced will be used as proper science data in the future. But I got used to operating the instrument and I became able to work smoothly. I sometimes made mistakes. When this

happened, I tried to remember the feeling I had when I started this job and tried to work carefully. In addition to measurements, I prepared bottles for sea water sampling and washed filters used in sampling. I did those tasks while waiting for the samples to be measured in the instrument, so I was not in hurry to get ready for the next observation station.

As we moved south, it got warmer outside. The weather also got better with more sunny days. The sea was so blue. Because of previous weather days, some stations were cancelled, and southern samples were reduced, but we were able to complete the voyage without incident. At the final observation station, I measured FDOM with different temperature settings. After the station sampling was finished, I continued to work and earned extra salary.

It was my first time out at sea for more than one month without port calls. I was, however, able to spend an enjoyable time watching movies and anime and reading books. I have enjoyed meeting people on this voyage and it has been a very valuable experience.

7. Notice on Using

This cruise report is a preliminary documentation as of the end of cruise.

This report is not necessarily corrected even if there is any inaccurate description (i.e. taxonomic classifications). This report is subject to be revised without notice. Some data on this report may be raw or unprocessed. If you are going to use or refer the data on this report, it is recommended to ask the Chief Scientist for latest status.

Users of information on this report are requested to submit Publication Report to JAMSTEC.
http://www.godac.jamstec.go.jp/darwin/explain/1/e#report
E-mail: submit-rv-cruise@jamstec.go.jp